

20-4083 445

FOREIGN TECHNOLOGY DIV WRIGHT-PATTERSON AFB OH  
REMOTE TROPOSPHERIC RADIO COMMUNICATIONS(U)  
MAR 80 I A GUSYATINSKIY, A S NEMIROVSKIY  
FTD-ID(RS)T-0251-80

F/O 17/2.1

**UNCLASSIFIED**

NL

1 of 6  
 10/31/05



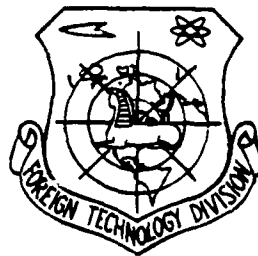
# FOREIGN TECHNOLOGY DIVISION



REMOTE TROPOSPHERIC RADIO COMMUNICATION

By

I. A. Gusyatinskiy, A. S. Nemirovskiy, et al



Approved for public release;  
distribution unlimited.

80 4 17 112

## UNEDITED MACHINE TRANSLATION

FTD-ID(RS)T-0251-80 / 19 March 1980

MICROFICHE NR: FTD-80-C-000394L

REMOTE TROPOSPHERIC RADIO COMMUNICATION,

By: I. A. Gussyatinskiy, A. S. Nemirovskiy, et al

English pages: 521

Source: Dal'nayaya Troposfernaya Radiosvyaz',  
Publishing House "Svyaz'", Moscow,  
1968, pp. 1-247.

Country of Origin: USSR

This document is a machine translation.

Requester: FSTC

THIS TRANSLATION IS A RENDITION OF THE ORIGINAL FOREIGN TEXT WITHOUT ANY ANALYTICAL OR EDITORIAL COMMENT. STATEMENTS OR THEORIES ADVOCATED OR IMPLIED ARE THOSE OF THE SOURCE AND DO NOT NECESSARILY REFLECT THE POSITION OR OPINION OF THE FOREIGN TECHNOLOGY DIVISION.

PREPARED BY:

TRANSLATION DIVISION  
FOREIGN TECHNOLOGY DIVISION  
WP-AFB, OHIO.

## Table of Contents

U. S. Board on Geographic Names Transliteration System.....	11
Preface.....	2
Chapter 1. Features of the Remote Tropospheric Propagation of Ultra Short Waves.....	5
Chapter 2. Diverse Reception on the of Remote Tropospheric Propagation of VHF (DTR).....	111
Chapter 3. Frequency Characteristics of the Section of Radiowave Propagation in a Troposphere.....	162
Chapter 4. Power of Noises in Telephone Channel at the Output of One Section of Line DTR.....	250
Chapter 5. Equipment for Tropospheric Radio Relay Lines.....	312
Chapter 6. Calculation of Lines DTR During the Transmission Multichannel Telephony and Binary Information.....	464
Chapter 7. Prospects for the Development of Tropospheric Radio Relay Lines.....	505

A



# U. S. BOARD ON GEOGRAPHIC NAMES transliteration SYSTEM

Block	Italic	Transliteration	Block	Italic	Transliteration
А а	<i>А а</i>	A, a	Р р	<i>Р р</i>	R, r
Б б	<i>Б б</i>	B, b	С с	<i>С с</i>	S, s
В в	<i>В в</i>	V, v	Т т	<i>Т т</i>	T, t
Г г	<i>Г г</i>	G, g	У у	<i>У у</i>	U, u
Д д	<i>Д д</i>	D, d	Ф ф	<i>Ф ф</i>	F, f
Е е	<i>Е е</i>	Ye, ye; E, e*	Х х	<i>Х х</i>	Kh, kh
Ж ж	<i>Ж ж</i>	Zh, zh	Ц ц	<i>Ц ц</i>	Ts, ts
З з	<i>З з</i>	Z, z	Ч ч	<i>Ч ч</i>	Ch, ch
И и	<i>И и</i>	I, i	Ш ш	<i>Ш ш</i>	Sh, sh
Й й	<i>Й й</i>	Y, y	Щ щ	<i>Щ щ</i>	Shch, shch
К к	<i>К к</i>	K, k	Ъ ъ	<i>Ъ ъ</i>	"
Л л	<i>Л л</i>	L, l	Ы ы	<i>Ы ы</i>	I, i
М м	<i>М м</i>	M, m	Ь ь	<i>Ь ь</i>	'
Н н	<i>Н н</i>	N, n	Э э	<i>Э э</i>	E, e
О о	<i>О о</i>	O, o	Ю ю	<i>Ю ю</i>	Yu, yu
П п	<i>П п</i>	P, p	Я я	<i>Я я</i>	Ya, ya

\*ye initially, after vowels, and after ъ, ѣ; e elsewhere.  
When written as ё in Russian, transliterate as yë or ë.

## RUSSIAN AND ENGLISH TRIGONOMETRIC FUNCTIONS

Russian	English	Russian	English	Russian	English
sin	sin	sh	sinh	arc sn	arcsin
cos	cos	ch	cosh	arc ch	arcosh
tg	tan	th	tanh	arc th	artanh
ctg	cot	cth	coth	arc cth	arcoth
sec	sec	sch	sech	arc sch	sech
cosec	csc	csch	csch	arc csch	arcsch

Russian English

rot curl  
lg log

## REMOTE TROPOSPHERIC RADIC COMMUNICATION.

I. A. Gusyatinskiy, A. S. Nemircvskiy, A. V. Sokolov, V. N. Troitsky.

Page 2.

In the book are presented questions of the transmission multichannel and television signals on radic relay lines, which use an effect of the remote tropospheric propagation of VHF.

Are

examined the mechanisms of remote tropospheric propagation of VHF, special feature/peculiarity of the passage of radiosignals through the troposphere and the different methods of the diverse reception/procedure. Analyzed frequency and phase characteristics of the circuit of propagation in the troposphere and are derived formulas for calculating the thermal and transient interferences with multichannel telephony at the output of one section of tropospheric line. To remaining chapters they are dedicated antenna feeder.

The book is of large interest for the engineers of radio communications.

Illustrations 144.

Tables 3.

Bibliographies 100.

Page 3.

Preface.

Development of contemporary technology led to the need for the rapid and exact solution of the problems of control and coordination taking into account the events, occurring at large distances from the control centers. In this case sharply increased the role of communication not only in the diagram of "man-man", but also for the data transmission in the system, which connects between themselves two electronic computers. The character of the transmitted information in this case causes special requirements for the circuit: first, an increase in the transmission ability of communicating systems, and, in the second place, an increase in the requirements for reliability and quality of transmission.

One of possible technical equipment, which satisfy the stated requirements under conditions of the sparsely populated and almost inaccessible areas of terrestrial globe, is communication equipment with the aid of the lines of remote tropospheric propagation of ultra short waves (DTR).

The wide development of the network of the tropospheric lines of communications (to January 1965 in entire world were counted more than 70 thousand km of lines DTR) confirms their expediently uses, especially in those areas where are hindered/hampered (or they are impossible) construction and operation of usual radio relay lines.

The proposed to the reader book is dedicated to the study of the problem of the transmission of broadband multichannel signals along the radio relay lines, which use an effect of the remote tropospheric propagation VHF.

It rests in the larger part on the original works, carried out by collective writers in the period 1959-1967.

The book assumes knowledge by the readers of the fundamental policies of radio engineering VUZ [BYB] - Institute of Higher

Education]; it is intended to engineers and to scientific workers, who work in the area of exploration, planning and operation of tropospheric communicating systems and can be use books of the students of senior courses at VUZ.

Sections of a book are written; Chapter 2, §§ 4.1, 4.2, 4.3, 4.4, 4.5, 4.6, 4.7, 4.8, 4.9, 4.10, 4.11, 4.12, 4.13, 4.14, 4.15, 4.16, 4.17, 4.18, 4.19, 4.20, 4.21, 4.22, 4.23, 4.24, 4.25, 4.26, 4.27, 4.28, 4.29, 4.30, 4.31, 4.32, 4.33, 4.34, 4.35, 4.36, 4.37, 4.38, 4.39, 4.40, 4.41, 4.42, 4.43, 4.44, 4.45, 4.46, 4.47, 4.48, 4.49, 4.50, 4.51, 4.52, 4.53, 4.54, 4.55, 4.56, 4.57, 4.58, 4.59, 4.60, 4.61, 4.62, 4.63, 4.64, 4.65, 4.66, 4.67, 4.68, 4.69, 4.70, 4.71, 4.72, 4.73, 4.74, 4.75, 4.76, 4.77, 4.78, 4.79, 4.80, 4.81, 4.82, 4.83, 4.84, 4.85, 4.86, 4.87, 4.88, 4.89, 4.90, 4.91, 4.92, 4.93, 4.94, 4.95, 4.96, 4.97, 4.98, 4.99, 4.100, 4.101, 4.102, 4.103, 4.104, 4.105, 4.106, 4.107, 4.108, 4.109, 4.110, 4.111, 4.112, 4.113, 4.114, 4.115, 4.116, 4.117, 4.118, 4.119, 4.120, 4.121, 4.122, 4.123, 4.124, 4.125, 4.126, 4.127, 4.128, 4.129, 4.130, 4.131, 4.132, 4.133, 4.134, 4.135, 4.136, 4.137, 4.138, 4.139, 4.140, 4.141, 4.142, 4.143, 4.144, 4.145, 4.146, 4.147, 4.148, 4.149, 4.150, 4.151, 4.152, 4.153, 4.154, 4.155, 4.156, 4.157, 4.158, 4.159, 4.160, 4.161, 4.162, 4.163, 4.164, 4.165, 4.166, 4.167, 4.168, 4.169, 4.170, 4.171, 4.172, 4.173, 4.174, 4.175, 4.176, 4.177, 4.178, 4.179, 4.180, 4.181, 4.182, 4.183, 4.184, 4.185, 4.186, 4.187, 4.188, 4.189, 4.190, 4.191, 4.192, 4.193, 4.194, 4.195, 4.196, 4.197, 4.198, 4.199, 4.200, 4.201, 4.202, 4.203, 4.204, 4.205, 4.206, 4.207, 4.208, 4.209, 4.210, 4.211, 4.212, 4.213, 4.214, 4.215, 4.216, 4.217, 4.218, 4.219, 4.220, 4.221, 4.222, 4.223, 4.224, 4.225, 4.226, 4.227, 4.228, 4.229, 4.230, 4.231, 4.232, 4.233, 4.234, 4.235, 4.236, 4.237, 4.238, 4.239, 4.240, 4.241, 4.242, 4.243, 4.244, 4.245, 4.246, 4.247, 4.248, 4.249, 4.250, 4.251, 4.252, 4.253, 4.254, 4.255, 4.256, 4.257, 4.258, 4.259, 4.260, 4.261, 4.262, 4.263, 4.264, 4.265, 4.266, 4.267, 4.268, 4.269, 4.270, 4.271, 4.272, 4.273, 4.274, 4.275, 4.276, 4.277, 4.278, 4.279, 4.280, 4.281, 4.282, 4.283, 4.284, 4.285, 4.286, 4.287, 4.288, 4.289, 4.290, 4.291, 4.292, 4.293, 4.294, 4.295, 4.296, 4.297, 4.298, 4.299, 4.300, 4.301, 4.302, 4.303, 4.304, 4.305, 4.306, 4.307, 4.308, 4.309, 4.310, 4.311, 4.312, 4.313, 4.314, 4.315, 4.316, 4.317, 4.318, 4.319, 4.320, 4.321, 4.322, 4.323, 4.324, 4.325, 4.326, 4.327, 4.328, 4.329, 4.330, 4.331, 4.332, 4.333, 4.334, 4.335, 4.336, 4.337, 4.338, 4.339, 4.340, 4.341, 4.342, 4.343, 4.344, 4.345, 4.346, 4.347, 4.348, 4.349, 4.350, 4.351, 4.352, 4.353, 4.354, 4.355, 4.356, 4.357, 4.358, 4.359, 4.360, 4.361, 4.362, 4.363, 4.364, 4.365, 4.366, 4.367, 4.368, 4.369, 4.370, 4.371, 4.372, 4.373, 4.374, 4.375, 4.376, 4.377, 4.378, 4.379, 4.380, 4.381, 4.382, 4.383, 4.384, 4.385, 4.386, 4.387, 4.388, 4.389, 4.390, 4.391, 4.392, 4.393, 4.394, 4.395, 4.396, 4.397, 4.398, 4.399, 4.400, 4.401, 4.402, 4.403, 4.404, 4.405, 4.406, 4.407, 4.408, 4.409, 4.410, 4.411, 4.412, 4.413, 4.414, 4.415, 4.416, 4.417, 4.418, 4.419, 4.420, 4.421, 4.422, 4.423, 4.424, 4.425, 4.426, 4.427, 4.428, 4.429, 4.430, 4.431, 4.432, 4.433, 4.434, 4.435, 4.436, 4.437, 4.438, 4.439, 4.440, 4.441, 4.442, 4.443, 4.444, 4.445, 4.446, 4.447, 4.448, 4.449, 4.450, 4.451, 4.452, 4.453, 4.454, 4.455, 4.456, 4.457, 4.458, 4.459, 4.460, 4.461, 4.462, 4.463, 4.464, 4.465, 4.466, 4.467, 4.468, 4.469, 4.470, 4.471, 4.472, 4.473, 4.474, 4.475, 4.476, 4.477, 4.478, 4.479, 4.480, 4.481, 4.482, 4.483, 4.484, 4.485, 4.486, 4.487, 4.488, 4.489, 4.490, 4.491, 4.492, 4.493, 4.494, 4.495, 4.496, 4.497, 4.498, 4.499, 4.500, 4.501, 4.502, 4.503, 4.504, 4.505, 4.506, 4.507, 4.508, 4.509, 4.510, 4.511, 4.512, 4.513, 4.514, 4.515, 4.516, 4.517, 4.518, 4.519, 4.520, 4.521, 4.522, 4.523, 4.524, 4.525, 4.526, 4.527, 4.528, 4.529, 4.530, 4.531, 4.532, 4.533, 4.534, 4.535, 4.536, 4.537, 4.538, 4.539, 4.540, 4.541, 4.542, 4.543, 4.544, 4.545, 4.546, 4.547, 4.548, 4.549, 4.550, 4.551, 4.552, 4.553, 4.554, 4.555, 4.556, 4.557, 4.558, 4.559, 4.560, 4.561, 4.562, 4.563, 4.564, 4.565, 4.566, 4.567, 4.568, 4.569, 4.570, 4.571, 4.572, 4.573, 4.574, 4.575, 4.576, 4.577, 4.578, 4.579, 4.580, 4.581, 4.582, 4.583, 4.584, 4.585, 4.586, 4.587, 4.588, 4.589, 4.590, 4.591, 4.592, 4.593, 4.594, 4.595, 4.596, 4.597, 4.598, 4.5

The authors are sincerely grateful to the reviewer of the book

V. V. Markov, who gave the number of valuable councils, taken into consideration by the authors during final preparation of the manuscript for the publication.

Responses and observations about the book should be guided into the publishing house ~~"Svyaz"~~ (Moscow-Center, Chistoprudnyy avenue, 2).  
"Svyaz"

Page 4.

Chapter 1.

FEATURES OF THE REMOTE TROPOSPHERIC PROPAGATION OF ULTRA SHORT WAVES.

§ 1.1. On the nature of the phenomenon of the remote tropospheric propagation of ultra short waves.

Heterogeneities of the lower layers of the atmosphere.

The effect of the atmosphere on the propagation of ultra short waves is connected in essence with the fact that the dielectric permeability of air  $\epsilon$  is not a constant value and depends on temperature, pressure and, air humidity

$$(\epsilon - 1) 10^6 = \frac{155}{T} \left( P + \frac{4810e}{T} \right), \quad (1.1)$$

where T - temperature of air in °K;

P - pressure in the millibars;

e - vapor pressure in the millibars.

It is well known that the temperature, pressure and air humidity change in the space and in the time; therefore the same changes according to (1.1) undergoes value  $\epsilon$ . Three-dimensional/space changes  $\epsilon$  have both regular and irregular character. Regular changes  $\epsilon$  with the altitude cause, as is known, the phenomenon of the refraction of radio waves. As subsequently in essence they will interest irregular, random heterogeneities  $\epsilon$  which cause reflection and scattering of ultrashort radio waves. These heterogeneities  $\epsilon$  which have different dimensions and forms, continuously are modified in the time, they disappear and appear again, they move with the flow of air masses, creating the complicated picture of random fluctuations  $\epsilon$  in atmosphere.

Random fluctuations  $\epsilon$  it is possible to divide into two fundamental forms: 1) laminar heterogeneities even 2) the heterogeneities, connected with vortex, turbulent air motion.

The laminar heterogeneities of the atmosphere are encountered they are very frequently and caused by the most diverse reasons. First of all, such heterogeneities include the layers with small or even negative gradients of the temperature (i.e. the layers where  $T \leftarrow$  increases with the altitude).

Such layers, which are stable formation, they usually call

inversions.

Page 5.

Inversions block vertical air motion and therefore are trapping layers, which are accompanied by different divergences in change the air humidity and wind velocity. An abrupt change of the absolute humidity in inversion layer is caused by the fact that the inversion delays the admission of water vapors into the overlying layers where the air proves to be drier. As can be seen from (1.1), the temperature rise and the drop in the humidity with altitude in inversion layer create extremely favorable conditions for forming irregularities of dielectric permeability.

Most essential for us are the inversions of free atmosphere, i.e., inversion, encounter at the altitudes of more than 500 m. They include so-called subsidence temperature inversion which frequently are formed in the anticyclonic conditions when the upper air layers are omitted down due to the spreading of lower layers and in this adiabatically are heated. Such inversions have large extent in the horizontal plane and considerable intensity. Dynamic inversions are developed in the layers with high wind velocities. The rapidly moving flow draw-in air of the layers with the lower speed of the wind. In this case on the upper bound of layer high velocities are created the



descending motions and temperature is raised, and on lower boundary it is reduced.

Inversions appear also due to different transparency of air in the different layers due to the presence in the atmosphere of water vapors, clouds and dust. Layers with the increased content of the droplets of water, water vapors and dust can be warmed thoroughly by solar radiation considerably more strong than surrounding air. The passage of fronts also sometimes causes the appearance of inversion due to the stratification of the warm air above the cold.

One of the important reasons for the appearance of heterogeneities of laminar character is the presence of the cloudiness; on the boundary of cloud occurs a rather sharp drop in the absolute humidity of air and a noticeable change in the temperature, which leads to abrupt change in the air.

The heterogeneities of laminar character appear also as a result of the horizontal movement of air masses which were heated differently above the different parts of the earth's surface, as a result of the convection of warm air, due to the internal gravity waves and many other reasons.

Heterogeneities of laminar character have thickness from the

tenths of meter to several hundred meters. Increment  $\epsilon$  in such layers oscillates from  $10^{-6}$  to  $(5-10) \cdot 10^{-5}$ . The extent of laminar heterogeneities in the horizontal plane is changed also over wide limits: from tens of meters to tens of kilometers.

The heterogeneities of the second form are caused by turbulent air motion as a result of the inequality of the earth's surface, nonuniformity of its heating and other reasons.

Page 6.

The eddy, which was being formed in one region of the atmosphere, is moved into other regions, assuming to known degree the temperature and the humidity of initial region. Therefore this vortex forms the local heterogeneity, which has on the average spherical form. According to the general theory of turbulence, developed by A. N. Kolmogorov and A. M. Obukhov, the turbulent motion begins from the formation of large-size vortices (approximately of the same order as the size of entire flow as a whole). These vortices during their motion gradually are diminished, being converted into the vortices of smaller dimensions. In this case the intensity of turbulent motion falls, since with the decrease of size of vortex increases the role of viscosity. Energy of the smallest vortices is converted into the heat. This leads to the fact that in the atmosphere constantly and

simultaneously there are vortices of different sizes. Therefore it is possible to speak about the continuous spectrum of heterogeneities caused by turbulent motion. In this case, the less the dimension of heterogeneity, the smaller will be the increment  $\epsilon$ , which is noted by the known law of two thirds, according to which

$$\overline{(z_1 - z_2)^2} = B l_{12}^{2/3}, \quad (1.2)$$

where  $z_1$  and  $z_2$  - value at points 1 and 2,  $l_{12}$  - a distance between these two points, and  $B$  - constant. Here line above the bracketed expression indicates average value. Value  $\overline{(z_1 - z_2)^2}$ , which characterizes random heterogeneities  $\epsilon$ , is called of structural function. For the varied conditions the constant  $B$  takes different values.

Thus, in the atmosphere simultaneously there are heterogeneities of different nature and various forms which continuously move and change. The quantitative description of these heterogeneities presents considerable difficulties. Usually they assume

$$z = \overline{z} + \Delta z(t, x),$$

where  $\overline{z}$  - average value  $z$ , and  $\Delta z$  - random variable, which changes in the time and in the space. In this case it is assumed that function  $\Delta z$  is statistically stationary, although the latter position, apparently, is not entirely correct. For the statistical description of fluctuations they use either structural function or three-dimensional/space correlation function,

$$\rho(\vec{l}) = \overline{\Delta z_1 \Delta z_2} \quad (1.3)$$

where  $\vec{l}$  - distance between points 1 and 2. In general  $\rho(\vec{l})$  depends not only on distance  $l$ , but also on direction of the vector  $\vec{l}$ , carried out from point 1 into point 2.

Page 7.

Between structural function (1.1) and correlation function (1.3) there is the single bond

$$\rho(\vec{l}) = \overline{\Delta z^2} - \frac{1}{2} f(\vec{l}).$$

Both the structural function  $f(\vec{l})$  and correlation function  $\rho(\vec{l})$  can be determined experimentally with the aid of the measurement of fluctuation  $z$  in the atmosphere. The experimental data about heterogeneities  $z$  of the atmosphere thus far are very limited and incomplete, first of all, due to the insufficiency of the space of such measurements and, furthermore, due to the insufficient instrument accuracy with aid of which are measured these heterogeneities. In more detail with the experimental data about fluctuations  $z$  in the atmosphere it is possible to be introduced in work [1.1]. Experiments show that the intensity of fluctuations  $z$ , i.e., value  $\overline{\Delta z^2}$ , slowly decreases with the altitude approximately according to the same law, as value  $z_0^2$  which, speaking in general terms, exponentially falls with the altitude. At the altitudes from 1 to 3

km the standard deviation of value  $\Delta\epsilon$  comprises  $(1-3) \cdot 10^{-6}$  with the interval of averaging on the order of 1 km.

Reflection and scattering of ultra short waves by atmospheric irregularities.

Then tropospheric propagation is caused by the re-emission (scattering or reflection) of ultra short waves by heterogeneities which were discussed above. Let us pause in greater detail at the nature of this phenomenon.

As is known, ultra short waves, in particular centimeter and decimeter ranges, possess the comparatively weak ability to go around obstructions due to the phenomenon of diffraction. Therefore for the transmitting station the earth's surface creates the rather sharp boundary between that illuminated and that shaded by regions. The same boundary is formed also from the side flatten stations (Fig. 1.1). The reception of waves proves to be possible only from certain space, horizontal above intersection of tangents to the earth's surface, carried out through the corresponding points. If in this space prove to be heterogeneities  $\epsilon$ , then such heterogeneities will cause reflection and scattering of the incident on them wave. The part of the scattered or reflected energy can achieve receiving point. Because at large distances (it is more than 100-150 km)

diffraction field on VHF proves to be negligibly small, the field, re-emitted with heterogeneities  $\epsilon$ , will be fundamental, although its value also small.

For determining the field, re-emitted with heterogeneities, they use the usually following method.

Page 8.

In view of the fact that  $\Delta\epsilon \ll \epsilon_0$  and  $E \ll E_0$ , where  $E$  - strength of the re-emitted field, and  $E_0$  - strength of the field of the incident wave, in the equations of Maxwell leave only the members where  $\Delta\epsilon$  and  $E$  enter to the first degree (Born approximation). As a result for the re-emitted field is obtained the following expression:

$$E = \frac{\kappa^2}{4\pi} \int_V \frac{\Delta\epsilon}{\epsilon_0} \frac{E_0 e^{-i\kappa r_2}}{r_2} dV, \quad (1.4)$$

where:  $\kappa = \frac{2\pi}{\lambda}$  - wave number,

$E_0$  - strength of the field of the incident wave,

$r_2$  - a distance from the current point to the point of reception,

$a$  - the space in which are located the heterogeneities.

After averaging on the space and passing to the attenuation factor  $\bar{V} = \frac{V}{V_0}$ , is not difficult to obtain

$$\bar{V} = \frac{\lambda^2}{16\pi^2} \operatorname{Re} \int_{\Omega} \frac{\Delta z \Delta z'}{r_1 r_2} \frac{\exp[-i\kappa(r_1 - r_1' + r_2 - r_2')]}{r_1 r_1' r_2 r_2'} dz dz' \quad (1.5)$$

Here  $r_1$  - distance from the transmitter to the current point,  $r_2$  - distance from the current point to the point of reception. Under the integral sign will cost already known from the preceding section correlation function  $\rho(\vec{r}) = \overline{\Delta z \Delta z'}$ .

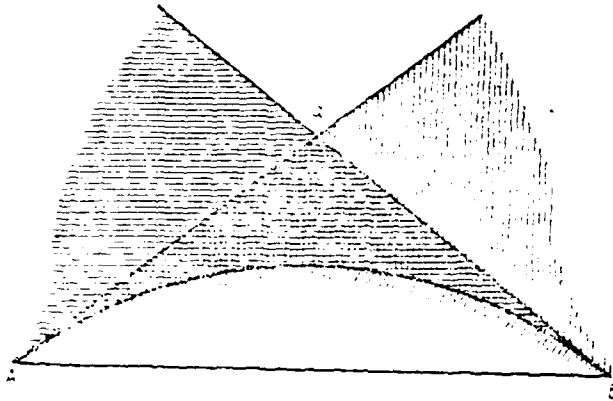


Fig. 1.1. Space of re-emission.

Page 9.

Equality (1.5) can be recorded otherwise

$$\overline{P^2} = \frac{\kappa^2 d \Delta \varepsilon_0}{4\pi \varepsilon_0} \operatorname{Re} \int_{\Delta} F \frac{da'}{r_1 r_2}, \quad (1.6)$$

here  $\Delta = \{ \overline{\Delta \kappa^2}, d = r_1 + r_2 \}$  - the distance between corresponding points, and  $F$  - reflection coefficient from the only heterogeneity, which has the form, depicted as correlation function

$$F = \frac{\kappa^2 d}{4\pi} \frac{\varepsilon_0}{\Delta \varepsilon_0} \int_{\Delta} \rho \frac{\exp[-j\kappa(r_1 + r_2 - r'_1 - r'_2)]}{r_1 r_2} da'. \quad (1.7)$$

Thus, expressions (1.5) and (1.6) make simple sense. The first integration indicates the determination of reflection coefficient from one certain averaged heterogeneity whose form is determined by the form of the function of correlation, and the second integration



indicates the addition of fields from all heterogeneities, located in space  $a'$ .

Let us now examine the behavior of reflection coefficient or, are more accurate, the coefficient of re-emission based on the example of the correlation function of the form

$$\rho = \Delta \varepsilon_0^2 \exp \left[ -\frac{(x-x')^2}{l_1^2} - \frac{(y-y')^2}{l_2^2} - \frac{(z-z')^2}{l_1^2} \right], \quad (1.8)$$

where  $x, y, z$  - rectangular coordinates, and  $l_1, l_2$  - the so-called scales of heterogeneities in the horizontal and vertical planes. If  $l_1 > l_2$ , heterogeneity has the pancake form, elongated in the horizontal plane. The computation of integral (1.7) with the steepest descent method for  $\rho$  from (1.8) leads to the following result:

$$F = \frac{\kappa^2 \Delta \varepsilon_0}{4\pi \epsilon_0} \frac{V(2\pi)^3}{VB} \frac{d}{r_1 r_2} \exp \left\{ -\kappa^2 \left[ \frac{1}{\gamma_1} (\cos \psi_1 - \cos \psi_2)^2 + \frac{1}{\gamma_2} (\sin \psi_1 + \sin \psi_2)^2 \right] \right\}. \quad (1.9)$$

For simplicity it was here assumed that the center of heterogeneity was located in the vertical plane, passing through the corresponding points. Value  $B$  is determined by the expression:

$$B = \gamma_1 \left[ \frac{4}{l_1^2 l_2^2} + j \frac{2}{l_1^2} \frac{1}{D^2} \cos^2 \psi_1 + j \frac{2}{l_2^2} \frac{1}{D^2} \sin^2 \psi_2 \right];$$

$\psi_1$  - this the angle between the direction in the transmitter and the horizontal plane,  $\psi_2$  - an angle between the direction in the receiving point and the same plane (Fig. 1.2);

$$\gamma_1 = \frac{2}{l_1^2} + j \frac{1}{D^2}, \quad \gamma_2 = \frac{2}{l_2^2} + j \frac{1}{D^2},$$

$D = \sqrt{\frac{r_1 r_2}{\kappa}}$  - size of the first Fresnel zone in the plane, perpendicular to direction of propagation.

Page 10.

From (1.9) it follows that the maximum value  $F$  will have in the direction of incident wave  $\psi_1 = -\psi_2$ . This maximum corresponds to re-emission forward. Besides it, is a maximum near the direction of the mirror reflection when  $\psi_1 = \psi_2$ . This maximum is feasible, if  $D \gg l_0$  and  $D < l_0$  it corresponds to the mirror reflected wave. The diagram of the re-emission of energy by irregularity in the vertical plane proves to be by such as it is depicted in Fig. 1.3.

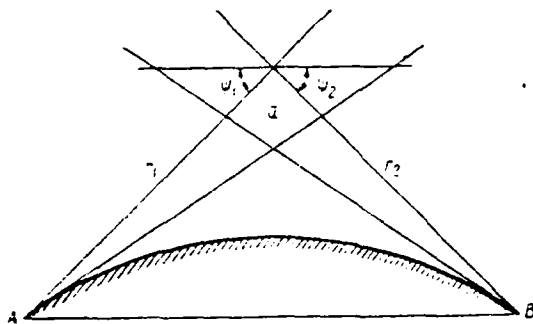


Fig. 1.2.

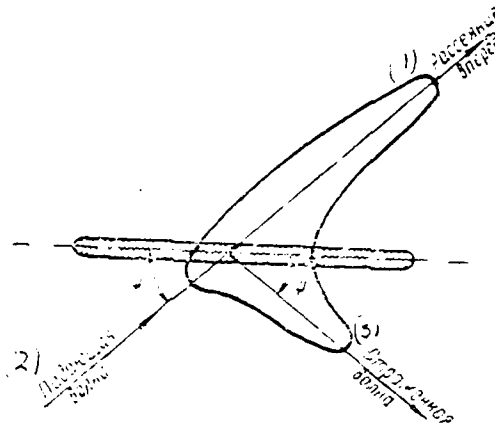


Fig. 1.3.

Fig. 1.2. To computation of field level, re-emitted with heterogeneities of troposphere.

Fig. 1.3. Radiation pattern of re-emission of energy by heterogeneity.

Key: (1). Forward scattering. (2). Incident wave. (3). Wave reflected.

Page 11.

With the decrease of sizes of heterogeneities of less than the Fresnel zone the maximum in the mirror direction disappears and we

come to the case of the usual scattering

$$F = \frac{\sqrt{\pi}}{4} \frac{\Delta \epsilon}{\epsilon_0} l_1^2 l_2 \kappa^2 \exp \left\{ -\frac{\kappa^2}{4} \left[ l_1^2 (\cos \psi_1 - \cos \psi_2)^2 + l_2^2 (\sin \psi_1 + \sin \psi_2)^2 \right] \right\}. \quad (1.10)$$

In the case of recte tropospheric propagation in view of the geometry of route  $\psi_1$  differs little from  $\psi_2$  in the essential part of space  $a'$ ; therefore

$$F = \frac{\sqrt{\pi}}{4} \frac{\Delta \epsilon_0}{\epsilon_0} l_1^2 l_2 \kappa^2 \exp \left[ -\kappa^2 l_2^2 \sin^2 \psi \right], \quad (1.11)$$

where  $\psi = \psi_1 = \psi_2$ .

This is a known expression for relative value of the scattered energy in the case of the correlation function of form (1.8). Another extreme case - reflection from the layer - we will obtain from (1.9), assuming  $l_1 \rightarrow \infty$ ;

$$|F| \approx \frac{\sqrt{\pi}}{2} \frac{\Delta \epsilon_0}{\epsilon_0} \kappa l_2 \frac{\exp \left( -\kappa^2 l_2^2 \sin^2 \psi \right)}{\sin \psi}. \quad (1.12)$$

This expression, naturally, coincides with the known expression for the reflection coefficient from the layer whose form is determined by Gaussian function  $\Delta \epsilon = \Delta \epsilon_0 \exp \left( -\frac{x^2}{l_2^2} \right)$ , obtained by other methods. From equalities (1.11) and (1.12) it is evident that the cases of scattering and reflection differ radically from each other in form of dependence of  $F$  on the wavelength, dimensions of heterogeneities and angle  $\psi$ . With quasi-mirror reflection (1.12) the dependence on angle  $\psi$  is sharper and from the wavelength weaker than

during pure scattering (1.11).

By analogous method it is possible to find value of  $F$  for other forms of the function of correlation. Just as for the case of Gaussian correlation function (1.8), the form of dependence of  $F$  on the wavelength of angle  $\theta$  will be changed with a change in the character of re-emission (quasi-mirror reflection or scattering). The real heterogeneities of the atmosphere have very complicated structure. In the atmosphere there is constantly a whole spectrum of both laminar heterogeneities and heterogeneities of isotropic structure; therefore the computation of attenuation factor in the case of remote tropospheric propagation proves to be sufficiently complex problem. It is further complicated by the fact, that we, until now, do not have available statistically reliable data about heterogeneities of the atmosphere. However, general laws it is not difficult to explain from equalities (1.5), (1.6) and (1.11), (1.12). Based on the example to the correlation function of form (1.8) we note that the re-emitted field possesses large directivity.

Page 12.

Both possible maximum of re-emission (straight line and mirror) are sufficiently acute, since value  $x_{00}^2$  in (1.10) is great in view of the fact that the dimensions of heterogeneities are considerably greater

wavelength.

Therefore space  $a'$ , which we will call the tropospheric space of re-emission, sharply will be restricted on the altitude, since the heterogeneities, located highly, will not participate in the formation of the field in the place of reception in view of the sharp drop  $P$  with increase  $h$  and  $D$ . Then it is possible to speak also about the heterogeneities of the atmosphere, located beside the route. The radiation pattern of re-emission in the horizontal plane is also narrow; therefore the space of re-emission will be limited, also, in the horizontal plane. Let us note that in the case of the scattering when  $h \ll D$ , the directed properties of re-emissions less and the dimensions of the re-emitting space more in comparison with the case of quasi-mirror reflection.

Thus, during the remote tropospheric propagation in the process of the re-emission of energy participates limited region of space - tropospheric space of re-emission  $a'$ . Specifically, by this space actually is conducted integration in (1.6). The angular dimensions of this volume are determined by the properties of heterogeneities, i.e., by their dimensions, wavelength and by angle  $\psi$  or, which is the same, by distance. In the case when are applied the pencil-beam antennas, the space of re-emission can be determined by the antenna radiation pattern, if the angle of antenna directivity becomes less

than angular dimensions tropospheric volume of re-emission  $\alpha'$ .

§ 1.2. Dependence of the average signal level on the distance.

The dependence of the average value of attenuation factor from the distance is connected, in the first place, with the dependence of the coefficient of re-emission  $F$  on angle  $\psi$ . The value of angle  $\psi$  in the space of re-emission is determined by the geometry of route. Roughly it is possible to consider that angle  $\psi$  is equal to the half geocentric angle  $\theta$  (Fig. 1.4). With an increase in the distance, i.e., with an increase  $\theta$ , increases  $\psi$ , and consequently, according to (1.11) and (1.12) or analogous equalities for other forms of the function of correlation falls value  $F$ . If the dimensions of heterogeneities are small ( $L < D$ ), then occurs usual scattering and dependence of  $V$  on angle  $\psi$  is not as acute as with  $L \gg D$ , when is observed quasi-mirror wave reflection from the heterogeneities. Therefore in the first case dependence of  $V$  on the distance proves to be weak in comparison with large-size case of heterogeneities. Great effect on dependence of  $V$  on the distance exerts change with the distance of the dimensions of the space of re-emission. In fact, with increase  $\psi$  and, therefore,  $\theta$  and  $\psi$  according to (1.9) or similar equalities for other forms of the function of correlation the directivity of the characteristic of re-emission increases and therefore decrease the angular dimensions of the space of re-emission.

a'.

Page 13.

Consequently, with the omnidirectional antennas the angular dimensions of the space of re-emission fall. On the other hand, with an increase in the distance with constant quantity of the angular dimension of space  $a'$  its geometric space increases proportionally  $d^3$ . Therefore in depending on the characteristics of heterogeneities and line of wave the value of the space of re-emission will either increase or fall from the distance. With the pencil-beam antennas when space is determined by the intersection of the antenna radiation patterns, the dimensions of the space of re-emission, obviously, increase with the distance proportionally  $d^3$ .

Another factor, which affects the course of the average value of signal level with the distance, is change with the distance of altitude of space of re-emission. It is obvious that with an increase in the distance the altitude of the space of re-emission above the earth's surface increases. Since the average intensity of heterogeneities  $\overline{A_0^2}$  falls from the altitude  $h$ , this phenomenon causes an increase in the rate of the drop in signal with the distance.

FOOTNOTE 1. The intensity of heterogeneities  $\overline{A_0^2}$  falls from the



altitude in view of the fact that falls absolute value  $\epsilon$  and, furthermore, due to the distance from earth's surface, which plays large role in the formation of heterogeneities. ENDFCCTNOTE.

With an increase in altitude, apparently, is changed not only value  $\Delta\epsilon^2$ , but also dimensions of heterogeneities and their form, which also superimposes its impression on dependence of  $V$  on the distance.

Thus, the dependence of attenuation factor  $V$  on distance is caused by a sufficiently large quantity of different factors.

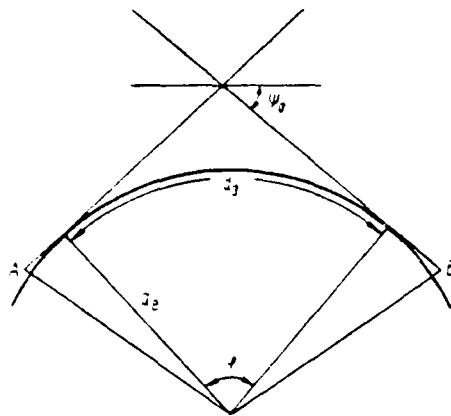


Fig. 1.4. connection of angle  $\psi_0$  with the geocentric angle.

Page 14.

The quantitative account of these all factors represents significant difficulty, in particular, if one considers that the information about the structure of the heterogeneities of the atmosphere are still very limited. Under these conditions are of special interest the experimental data about the average signal levels at different distances. However, the use these data for determining the dependence of  $V$  on the distance meets with the known difficulties at which we will pause below.

The fact is that the attenuation factor in the case of remote tropospheric propagation proves to be such small that even at the

considerable power of transmitter for the reliable reception at large distances is necessary the use of the pencil-beam antennas; however, in this case the space of re-emission will depend on directivity of both antennas, therefore, and attenuation factor  $V$  will also depend on antenna directivity. Experimental data about the average values of factor of weakening at different distances in the majority of the cases are acquired precisely for the pencil-beam antennas, moreover in different experiments were applied different antennas. Therefore in order in some way to order the data about the average signal levels in the case of remote tropospheric propagation, it is necessary to eliminate the effect of antenna directivity. For this has the sense to construct the dependence of attenuation factor on the distance for the omnidirectional antennas, first after converting experimental the data about the average signal levels for the omnidirectional antennas. The effect of antenna directivity in this case is considered separately.

Dependence of  $V$  on the antenna directivity is conventionally designated as losses of antenna gain. On this phenomenon the speech will go in the following paragraphs; therefore here we will be restricted only to confirmation, that this translation to produce is possible. Furthermore, for the characteristic of signal usually utilize not average value and not rms value the  $V$ , but median value of attenuation factor. But, as it will be further shown, this

value is inconvenient for the calculations, it does not reflect the energy characteristic of signal and strongly it depends on the depth of fadings. Therefore as the characteristic of signal level we will apply value  $\overline{V}$  or  $V_{med} = 10 \lg \overline{V}$ . Consequently, is necessary the translation of experimental data from value  $V_{med}$  to value  $V_{opms}$ .

It is known that the attenuation factor continuously is changed in the time, in this case are observed both the rapid fluctuations with the period less than 5 min and slow fluctuations with the period it is more than 5 min (in detail about fluctuations  $V$  it will be described into § 1.4). For determining the rms value of attenuation factor they enter as follows. First is determined the rms value  $V$  in every 5 min. Then finding the statistical distribution of the five minute rms values of the  $V$  during the large period observations. From the same distribution they find  $V_{med}$ . Thus,  $V_{med}$  - this median value of five minute rms values.

Page 15.

Running in forward, let us say that the statistical distribution of the five minute rms values  $V$  is subordinated to logarithmic normal law with the standard deviation  $\sigma$ . In this case is easy to obtain the connection between  $V_{opms}$  and  $V_{med}$ . Let us record  $V_{opms}$  and  $V_{med}$  in the decibels:

$$V_{\text{ср. кв}}(\delta\delta) = 10 \lg \bar{V}^2.$$

In the case of logarithmic normal law the average from  $\lg V$  coincides with the median value  $V$ , since logarithmic normal law - this normal law for  $\lg$  of the  $V$ , while in the case normal law average and median values coincide; therefore

$$V_{\text{мед}}(\delta\delta) = 20 \lg \bar{V} = 10 \lg V^2.$$

Probability density  $V$  in the case of logarithmic normal law  $W(V_{\delta\delta})$  will be

$$W(V_{\delta\delta}) = \frac{1}{\sqrt{2\pi\sigma_{(\delta\delta)}^2}} e^{-\frac{(V_{(\delta\delta)} - V_{\text{мед}}(\delta\delta))^2}{2\sigma_{(\delta\delta)}^2}}.$$

Here  $V$  and  $\sigma$  are expressed in the decibels. We find the rms value of attenuation factor, using the usual method:

$$\begin{aligned} \bar{V}^2 &= \left( \overline{\frac{1}{e^{4,34} V_{(\delta\delta)}}} \right) = \int_{-\infty}^{\infty} \frac{1}{e^{4,34} V_{(\delta\delta)}} W(V_{(\delta\delta)}) dV_{(\delta\delta)} = \frac{1}{\sqrt{2\pi\sigma_{(\delta\delta)}^2}} \times \\ &\times \int_{-\infty}^{\infty} \frac{1}{e^{4,34} V_{(\delta\delta)}} e^{-\frac{(V_{(\delta\delta)} - V_{\text{мед}}(\delta\delta))^2}{2\sigma_{(\delta\delta)}^2}} dV_{(\delta\delta)} = e^{\left( \frac{2^2}{2 \cdot 4,34^2} + \frac{1}{4,34} V_{\text{мед}}(\delta\delta) \right)}. \end{aligned}$$

Expressing  $\bar{V}^2$  in the decibels, we obtain

$$V_{\text{ср. кв}}(\delta\delta) = \frac{2^2}{8,68} + V_{\text{мед}}(\delta\delta)$$

or

$$V_{\text{ср. кв}}(\delta\delta) = V_{\text{мед}}(\delta\delta) + 0,115\sigma_{(\delta\delta)}^2. \quad (1.13)$$

For obtaining dependence  $\bar{V}^2$  on the distance were used the experimental data (1.1-1.10), obtained by winter in essence on the

land routes under conditions of the moderate and subarctic climates. In the winter months are observed the lowest values of the average signal levels; therefore precisely these data about the average levels after unfavorable period are of greatest interest during the design of the tropospheric lines of communications.

Page 16.

Fig. 1.5a gives the dependence of root-mean-square values of attenuation factor  $V_{\text{rms}}$  on the distance for the omnidirectional antennas, obtained in essence from work [1.2] for three lengths of waves, while in Fig. 1.5b - for the directional antennas with the angle of directivity of  $10^\circ$ .

FOOTNOTE 1. At the angle of directivity in the future we will understand the width of the main lobe of radiation of antenna on the points of the half power. ENDFCCTINCTE.

Fig. 1.5a and b gives dependence  $V_{\text{rms}}(d)$  rct on the true distance between points d, but from so-called equivalent distance  $d_0$ . Under  $d_0$ , here is understood the distance between the points of contact of the tangency of the rays of the earth's surface (see Fig. 1.4).

Equivalent distance is determined after the construction of profile, i.e. the section of route in the vertical plane. In this case the construction of profile is conducted taking into account the

refraction, i.e. it is assumed that equivalent radius of the earth  $r_e$  is equal to approximately 8500 km. The introduction of the concept of equivalent distance makes it possible simply to consider the altitude effect of the setting up of antennas. With an increase in altitude of antennas decreases angle  $\phi_0$  and, therefore, rises signal level. The curves of Fig. 1.5b, generally speaking, do not coincide with the analogous curves of works [1.1; 1.2]. This is explained, in the first place, by the fact that Fig. 1.5a and b gives the rms values  $V$ , but not median as in [1.1; 1.2] and, in the second place, fact that the account of losses, amplification [1.1; 1.2] was conducted inaccurately. The dependence Fig. 1.5b was constructed on the base of more precise data about the losses of amplification, checked experimentally. Translation of the median levels, obtained by other authors [1.3-1.10], was also done according to the specified data about the losses of antenna gain. As can be seen from Fig. 1.5, attenuation factor falls from the distance exponentially or, if  $V_{\text{loss}}$  is expressed in the decibels, then it is possible to speak about linear drop  $V_{\text{loss}}(dB)$  with the distance. Linear attenuation depends on wavelength, increasing with the shortening of wave. At the frequency of approximately 1000 Mcz linear weakening is 0.075 dB/km.

Figure 1.5a shows that if we consider corrections for the losses of amplification, then experimental data for the worst season have comparatively small spread, in spite of difference in the



geographical position of the investigated routes. Thus, the curves Fig. 1.5a and b possess sufficiently good statistical authenticity.

For the summer, most favorable time, the dependence on the distance somewhat is changed. Average value  $V_{\text{summer}}$  in this case sufficiently strongly increases in comparison with winter period, moreover this increase is the greater, the less the distance; therefore linear weakening in summer increases.

Fig. 1.6 gives for the comparison of dependence  $V_{\text{winter}}$  on the distance for the winter and summer periods, obtained at the frequency of approximately 1000 MHz under conditions of the middle strip of the European territory of the USSR and those converted for the antennas with the angle of directivity of  $1^\circ$ .

Page 17.

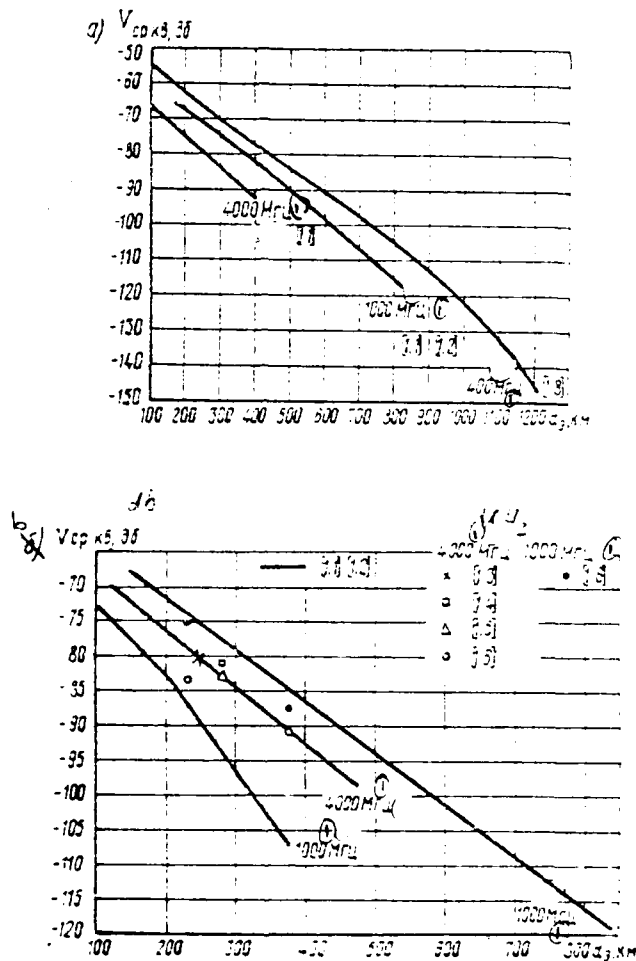


Fig. 1.5. Dependence of rms value of attenuation factor  $V_{cp, \alpha}$  from distance: a) for nondirected antennas,  $\alpha < 2^\circ$ ; b) for directed antennas,  $\alpha = 1^\circ$ .

Key: (1). MHz.

Page 18.

It should be noted that the scatter of the experimental data about the average levels for the summer months proves to be considerably more than for winter period. The average levels in summer sufficiently strongly depend on climatic and geographical conditions.

§ 1.3. Dependence of the average signal level on the wavelength.

Experimental investigations showed [1.1; 1.2] that the dependence of signal level on the frequency carries random character. At different moments of time the relation of signal level on different waves proves to be different. The radiation of the relation of the average values of signal level at different frequencies showed [1.1] that on the routes 100-200 km this relation was proportional  $\lambda^2$ . With an increase in the distance the slope/transconductance of this dependence increases already at the distances of 300-400 km ( $M_{\text{spm}} \sim \lambda$ ). The frequency dependence of the average signal levels and its dependence on the distance it is easy to see in Fig. 1.5a and b.

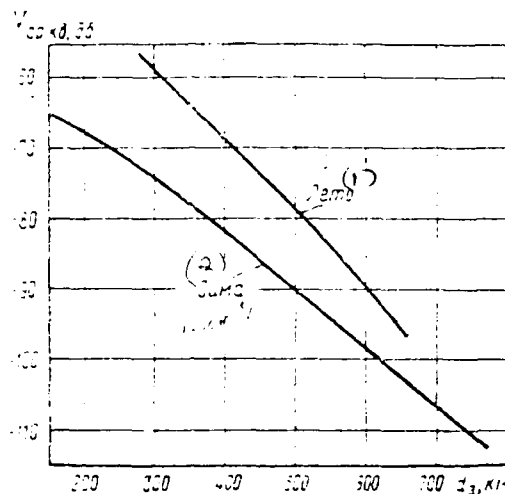


Fig. 1.6. Dependence of the rms value of attenuation factor  $K_{0.35}$  from the distance for the summer and winter seasons of year. (Wave 30 cm, omnidirectional antennas).

Key: (1). Summer. (2). Winter.

Page 19.

#### § 1.4. Signal fading.

In the case of recte tropospheric propagation signal level is subjected to continuous vibrations. Simultaneously are observed the rapid fluctuations of level with the frequency, which reaches ten and even hundreds of the hertz, and the slower changes in the level whose

greatest period is measured by months.

During the remote tropospheric propagation it is accepted to divide fadings into three forms: 1) rapid fadings whose duration is less than 5 min, 2) slow fadings, which are changes in the five minute average values of signal during the period not more than 1-3 months and finally 3) seasonal behavior of the level of the signal, which is a change in the average monthly (or median in the month) values of signal level. Certainly, the boundaries between these forms of fadings to a determined degree are conditional. However, this division has the specific substantiation, since these forms of fadings are caused by different physical causes. Now let us pause in greater detail at each of these forms of fadings.

Rapid fadings. Under these fadings we understand changes in the instantaneous values of level during the period of 5 min. Fig. 1.7a and b shows the example to the recording of the instantaneous values of level it drove off on the route 303 km on the wave 30 cm. In these figures the angle  $\alpha$  indicates the width of the radiation pattern of the antennas ( $\alpha_1$  - transmitting antenna,  $\alpha_2$  - receiving) used. Such fadings are caused by the interference of many waves, re-emitted with individual heterogeneities. Since the heterogeneities continuously move in the space of re-emission, then the phase of each of the incident waves changes sufficiently rapidly in the time. Phase

differences of waves, re-emitted with heterogeneities, rapidly and chaotically fluctuate. All this leads to the rapid interference signal fading. During the period 5 min heterogeneities themselves do not manage substantially to change; therefore fading characteristics are almost wholly connected with the interference of waves, caused by the motion of heterogeneities.

It is known [for 1.1] that during the addition of many waves with different amplitude and the random phase, evenly distributed in the range from 0 to  $2\pi$ , is obtained the wave whose amplitude is the random variable, which obeys the law Rayleigh distribution. Therefore logical to expect that rapid signal fading also must obey the law of rayleigh, since, apparently, the condition of many of the incident waves and randomnesses of a change of the phase difference in this case must be fulfilled. According to the Rayleigh law the probability density  $W(q)$  of value  $q = \frac{E}{E_{cp,ms}}$ , where  $E$  - an instantaneous value of signal amplitude,  $E_{cp,ms}$  - the rms value of amplitude, it is determined by the following equality:

$$W(q) = 2q e^{-q^2}.$$

Pages 20-21.

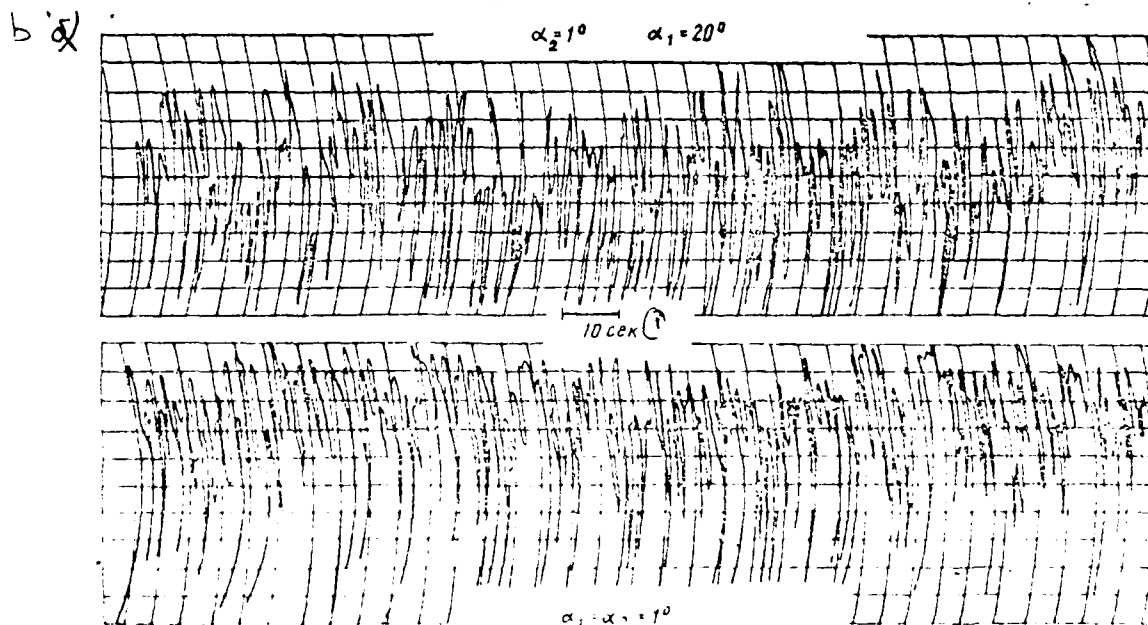
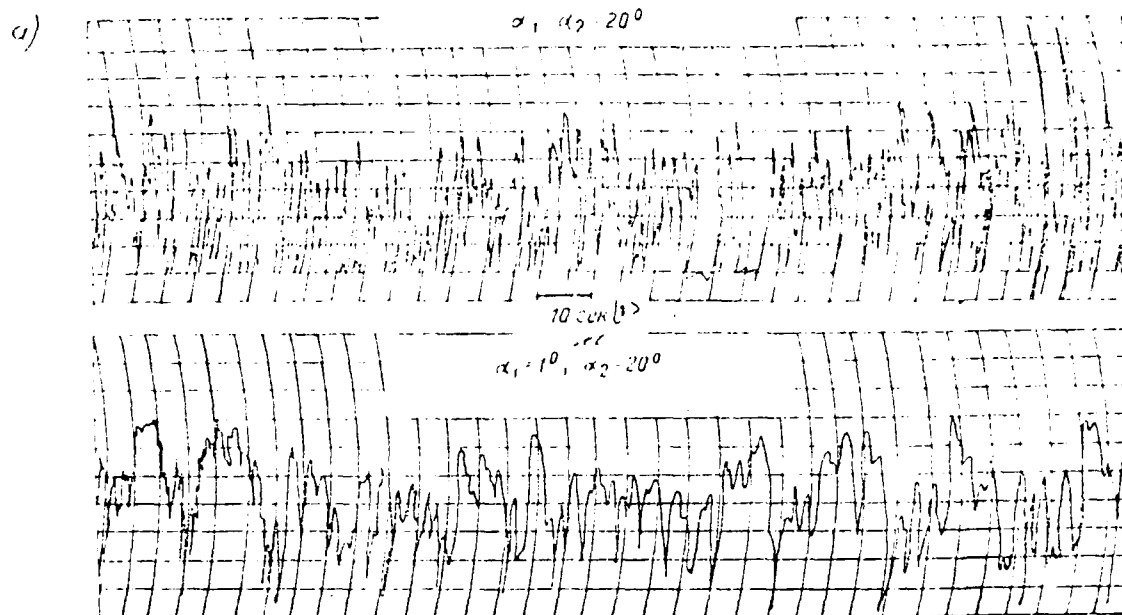


Fig 1.7.

Fig. 1.7. Example to simultaneous recording of signal from receiving antennas of  $\alpha_1=20^\circ$  and  $\alpha_1=1^\circ$ : a) transmitting antenna of  $\alpha_2=20^\circ$ ; b) transmitting antenna of  $\alpha_2=1^\circ$ .

Key: (1). S.

Page 22.

Probability that relation  $q = \frac{E}{E_{cp.ka}}$  will be less than value  $q_1$  it is determined by the integral function of probability  $Q(q_1)$ :

$$Q(q_1) = 2 \int_0^{q_1} q e^{-q^2} dq = 1 - e^{-q_1^2}. \quad (1.14)$$

Plotted function  $Q(q_1)$  is given in Fig. 1.8.

The experiments, which were being carried out on the routes of different extent, on different waves [1.1; 1.2], showed that on the average the law of Rayleigh for the rapid fadings is fulfilled. Fig. 1.9 for an example gives the experimental integral curve for the rapid fadings, obtained on the route with a length of 303 km at the frequency of approximately 1000 MHz. Curve is averaged for 130 five minute performances. Comparison with Rayleigh's curve, given in the same figure, he indicates good coincidence of both dependences.



It should be noted that a good coincidence with the Rayleigh law is obtained with the averaging for a large number of performances, since separate distributions for the five minute performance can sometimes differ from the Rayleigh law.

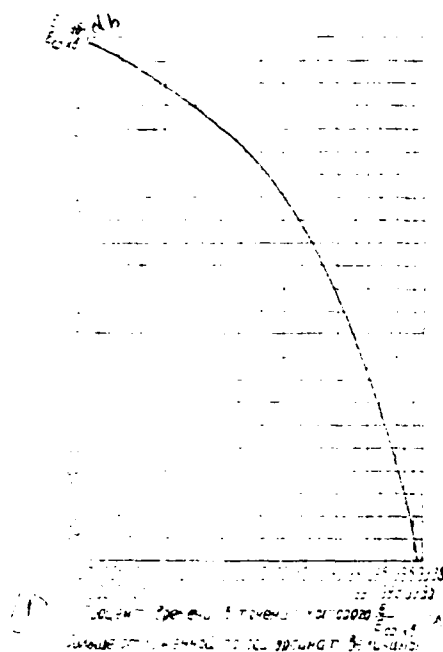


Fig. 1.8.

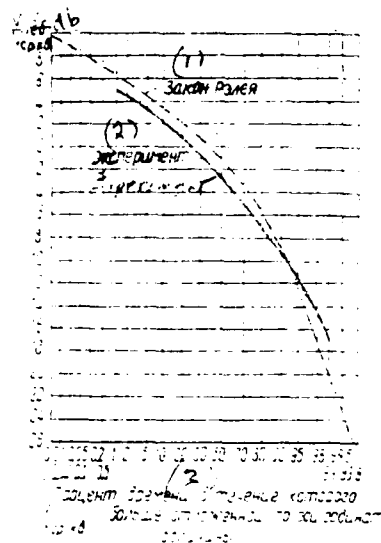


Fig. 1.9.

Fig. 1.8. Depth of rapid fadings (Rayleigh law).

Key: (1). The percentage of time during which  $\frac{E}{E_{avg}}$  is more than the deposited along the axis of ordinates value.

Fig. 1.9. Comparison of experimental dependence of depth of rapid fadings and Rayleigh law.

Key: (1). Rayleigh law. (2). experiment. (3). Percentage of time during which it is more than deposited along the axis of ordinates value.

Page 23.

This is connected, perhaps, with the fact that sometimes five minute interval it is insufficiently for the manifestation of statistical law. This position can be, for example, then when the period of rapid fadings proves to be comparable with the duration of the interval of recording.

Now let us examine how is determined duration or quasi period of rapid fadings. For simplicity let us examine two heterogeneities, one of which is located in the middle of the space of re-emission, and the second in the extreme lateral angle of this space (Fig. 1.10). Let the linear dimension of the space of re-emission be equal to  $L$ , then the distance between two these heterogeneities will be  $L/2$ . A phase difference between the waves, scattered by these heterogeneities,  $\Delta\varphi$  it is easy to determine from the geometric relationships:

$$\Delta\varphi \approx \kappa \frac{L^2}{2d}. \quad (1.15)$$

If the second heterogeneity moves relative to the first heterogeneity with a velocity of  $v$  along direction  $L$ , then

$$\Delta\varphi \approx \kappa \frac{(L + vt)^2}{2d}. \quad (1.16)$$

Now from (1.16) let us determine the time, for which a phase

difference will change to value  $2\pi$ . This will be nothing else but the quasi period of fadings  $\tau$ :

$$\tau = \frac{\lambda d}{\sigma L}. \quad (1.17)$$

Thus, the quasi period of fadings is proportional to wavelength, it is inversely proportional to the relative rate of heterogeneities and to the size of the space of re-emission. Experimental data confirm this dependence. Actually/really, the period of rapid fadings is approximately proportional to wavelength and it is inversely proportional to the space of re-emission. The first fact is widely-known as far as position is concerned second, then it will not be worthwhile to stop in more detail, since usually it is forgotten.

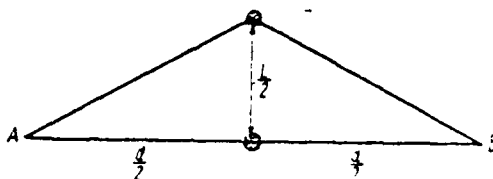


Fig. 1.10. Path difference of rays, re-emitted with two different irregularities.

Page 24.

The effect of the dimensions of the space of re-emission on the period of rapid fadings can be seen with the simultaneous reception of signal on two antennas with the different directivity. Such experiments were done on the route with a length of 303 km on the wave of approximately 30 cm. In this case at the transmitting end was applied the weakly directed antenna with the amplification 22 dB, and at receiving end the recording of signal was conducted from two antennas one of which had amplification 45 dB, and the second of 22 dB. In this case average sizes of the space of re-emission during the use of the pencil-beam antenna were approximately three times less than for the weakly directed antenna. The simultaneous recording of signal showed that if on the weakly directed antenna the quasi period was 1.5 s, then in the case when on the one hand there was the pencil-beam antenna, quasi period increased to 4.8 s. When on the

same route were applied on both points the pencil-beam antennas, quasi period increased to 5.8 s. An increase in the quasi period occurred approximately as much once, in as decreased the linear dimension of the space of re-emission, which corresponds to equality (1.17) <sup>1</sup> (see Fig. 1.7a and b).

FOOTNOTE <sup>1</sup>. This phenomenon was observed also in experiments [1.3], [1.15]. ENDFOOTNOTE.

Experiments show that with an increase in the distance the quasi period of fadings slowly decreases. With an increase in the distance, on one hand, increases  $d$  in (1.17), on the other hand, increases  $L$ . One should, however, consider that if we examine rate of change of a phase difference of heterogeneities, spread in the vertical plane, then we will obtain for the quasi period approximately the same expression as (1.17), only quasi period will be, furthermore, it is inversely proportional to geocentric angle  $\theta$ . By an increase in the geocentric angle is explained decrease  $\tau$  with the distance.

Slow signal fading. As has already been spoken, under the slow fadings usually is understood the change in the time of the five minute average values of signal level. The effect of interference fadings on changes in the five minute average values virtually is absent, since the maximum period of interference fadings is measured

by seconds or by tens of seconds. Therefore slow fadings have other entirely nature <sup>2</sup>.

FOOTNOTE <sup>2</sup>. Sometimes the period of averaging is selected somewhat greater (to 1 hour), which, as it seems to us, is inexpedient, since otherwise it would be necessary to additionally investigate the statistical characteristics of signal in the limits of each hour. The distributions of the instantaneous values of level per hour do not already frequently obey the law of Rayleigh, since for this large interval strongly are changed heterogeneities themselves and, therefore, are changed the amplitudes of the interfering waves.

ENDFOOTNOTE.

As already mentioned above, during the period of time 5 min of the heterogeneities, arranged in the space of re-emission, they do not manage strongly to change; therefore the amplitudes of the interfering waves also change little.

Page 25.

Under such conditions the average value of the square of wave amplitude  $\xi^2 = \bar{E}^2$  during the period 5 min will be equal to the sum of the squares of the amplitudes of interfering waves  $E_n^2$ :

$$\xi^2 = \bar{E}^2 = \sum_n E_n^2, \quad (1.13)$$

where  $E_m$  - amplitude the  $m$ -th components. Changes in values  $\xi$ , which we call slow fadings, are caused, as is evident from (1.18), by change in the time of the amplitudes of interfering waves  $E_m$ .

Amplitude change with the  $m$  heterogeneity of wave  $E_m$  reflected is connected with a change in the dimensions, form and increment  $\Delta\xi$  in this heterogeneity. Let us introduce new random variable  $\delta$ :

$$\delta = \xi^2 - \bar{\xi}^2, \quad (1.19)$$

where  $\bar{\xi}^2$  - an average value of  $\xi^2$  during the large period of observations. Relative value of level changes will be

$$\frac{\xi^2}{\bar{\xi}^2} = 1 + \frac{\delta}{\bar{\xi}^2}.$$

After taking the logarithm this equality, we will obtain

$$\ln \frac{\xi^2}{\bar{\xi}^2} = \ln \left( 1 + \frac{\delta}{\bar{\xi}^2} \right).$$

Expanding in the exponential series/row, we will have

$$\ln \frac{\xi^2}{\bar{\xi}^2} = \frac{\delta}{\bar{\xi}^2} - \left( \frac{\delta}{\bar{\xi}^2} \right)^2 + \left( \frac{\delta}{\bar{\xi}^2} \right)^3 - \left( \frac{\delta}{\bar{\xi}^2} \right)^4 + \dots, \quad (1.20)$$

since

$$\delta = \sum \delta_m,$$

where

$$\delta_m = E_m^2 - \bar{E}_m^2,$$

that series in rightside (1.20) is the sum of many random variables

$$\ln \left( \frac{\xi^2}{\bar{\xi}^2} \right) = \frac{1}{\bar{\xi}^2} \sum \delta_m - \left( \frac{1}{\bar{\xi}^2} \sum \delta_m \right)^2 + \left( \frac{1}{\bar{\xi}^2} \sum \delta_m \right)^3 - \dots \quad (1.21)$$

Values  $\delta_m$  are not depended from each other, since are changes in the wave amplitudes, reflected by the individual heterogeneities, isolated from each other. According to the limit theorem of Lyapunov



the sum of independent random quantities has normal distribution under the condition for existence of mathematical expectation and dispersion of each of the terms.

Page 26.

This condition in our case is observed; therefore random variable  $\ln\left(\frac{P^2}{P_0^2}\right)$  must be subordinated to normal law, and  $\frac{P^2}{P_0^2}$  - to logarithmic normal law. Thus, slow fadings must be subordinated to logarithmic normal law. The dispersion of these fadings

$$\sigma^2 = \left[ \ln\left(\frac{P^2}{P_0^2}\right) \right]^2,$$

as can be seen from (1.21), it is determined by a number of components  $n$  and by a law of amplitude distribution of each of the components.

Experiments show that slow fadings are actually subordinated to logarithmic normal law. Fig. 1.11 for an example gives the integral distributions of the five minute average values of attenuation factor  $V$  for the routes in extent 303, 448 and 630 km [1.2] on the wave of approximately 30 cm, obtained in winter and summer time during the large period of observation. On the axis of the abscissas Fig. 1.11 is used the scale, which corresponds to normal law, and along the axis of ordinates value  $V$  is deposited in the decibels; therefore logarithmic normal law with the selected scales will be represented

in Fig. 1.11 straight inclined line. It is easy to see from the figure that for all distances the integral curves are subordinated to the approximately logarithmic normal law whose dispersion is changed with the distance. Divergences from the logarithmic normal law are observed only in summer for the high levels of the signal when in the small percentage of time integral curve differs from logarithmic normal law toward an increase in the probability of high levels.

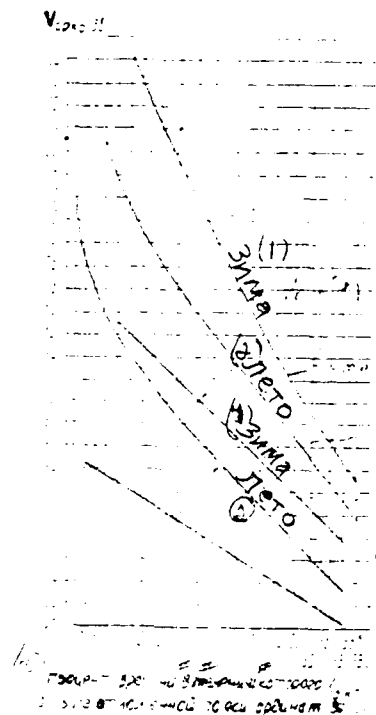


Fig. 1.11. Distribution of the five-minute mean values of attenuation factor on different routes into the different seasons of year on wave of 30 cm for the antennas with the angle of directivity of  $10^\circ$ .

Key: (1). Winter. (2). Summer. (3). Percentage of time during which is more than deposited along the axis of ordinates value.

Page 27.

Thus, for the characteristic of slow fadings it is possible to use only value - standard deviation  $\sigma$ . It is usually accepted to

express value  $\sigma$  in the decibels. Value  $\sigma$  it is easy to determine from the experimental integral distribution curves of the levels (see Fig. 1.11), after taking a difference in values  $V_{(\sigma\delta)}$  for 50o/o and for 84o/o of time:

$$\sigma_{(\delta\delta)} = V_{(\delta\delta) 50\%} - V_{(\delta\delta) 84\%}.$$

FOOTNOTE 1. This equality directly follows from the expression for the normal law of random number distribution in the integral form.  
ENDFOOTNOTE.

If value  $\sigma$  depended only on distance, then for the practical targets would be on the basis of experimental data to sufficiently construct the dependence  $\sigma$  on the distance as this done in works [1.1, 1.2] and use it in all of the case for determining the depth of slow fadings. However, experiments show that  $\sigma$  to a considerable degree depends also on antenna directivity. Therefore during the use of experimental data about the depth of slow fadings it is necessary to consider the directivity of the antennas used.

Let us examine in more detail a question about the effect of antenna directivity on the depth of slow fadings. With an increase in the antenna directivity is decreased the space of re-emission. With the pencil-beam antennas the angular dimensions of the space of re-emission are wholly determined by the angles of antenna directivity.

As we already spoke,  $\sigma$  in the case of slow fadings depends on a number of reemitters, i.e. on Mach number (1.21). But a number of heterogeneities, which participate in the re-emission of energy, i.e. Mach number, depends on the value of the space of re-emission, and also, therefore, on antenna pattern. Thus,  $\sigma$  also must depend on antenna directivity.

Let us mentally break the space of re-emission  $\Omega$  into  $n$  of equal parts  $\Omega_n$ , each of which has dimensions considerably more than the dimensions of individual heterogeneities. Let us change now the order of the addition of the waves, arriving from the space of re-emission, why the result of addition, of course, will not change. We will initially summarize the waves, which arrive from space  $\Omega_n$ , then let us accumulate  $n$  of the signals, which correspond to each of spaces  $\Omega_n$ . As a result of the addition of the waves, arriving from space  $\Omega_n$  and averaging in the five minute interval, we will obtain signal  $\xi_n$  whose random changes are subordinated to logarithmic normal law. Let the standard deviation in this case be  $\sigma_n$ . The signal, arriving from entire space of re-emission  $\Omega$ , also is subordinated, as we already explained, to logarithmic normal law. This signal can be found, by adding  $n$  of random variables  $\xi_n$ :

$$\xi = \sum_{n=1}^n \xi_n.$$

Page 28.

As is known, during the addition of random variables mathematical expectation or average value of sum is equal to the sum of the average values of terms. It relates also to the dispersions. The dispersion of sum is equal to the sum of the dispersions of the terms.

$$\bar{\xi} = n \bar{\xi}_n \quad \text{and} \quad \overline{\xi^2} - \bar{\xi}^2 = n (\bar{\xi}_n^2 - \bar{\xi}_n^2).$$

We assume that all  $n$  components have the identical average values and identical dispersions in view of the equality spaces  $\Omega_n$ . After using these relationships, it is possible to find standard deviation  $\sigma$  for value  $\ln \xi$ :

$$\sigma^2 = \ln \left[ \frac{1}{n} \left( e^{\frac{\sigma_n^2}{\bar{\xi}_n^2}} - n - 1 \right) \right], \quad (1.22)$$

where  $\sigma_n$  - standard deviation for  $\ln \xi_n$ . Expressing  $\sigma$ , as usual, in decibels we will obtain the equality

$$\sigma_{(\text{dB})}^2 = 75 \ln \left[ \frac{1}{n} \left( e^{\frac{\sigma_n^2 (\text{dB})^2}{75}} - n - 1 \right) \right]. \quad (1.23)$$

When  $\sigma_{n(\text{dB})}^2 \ll 75$ , as can be seen from (1.23), expanding exponential and logarithmic functions in series and leaving the first term of expansion, we will obtain

$$\sigma_{(\text{dB})}^2 = \frac{1}{n} \sigma_{n(\text{dB})}^2. \quad (1.24)$$

This is equality correctly approximately as long as value  $\sigma_{n(\text{dB})}^2 \ll 75$  dB. Thus, the dispersion of slow fades are smaller, the greater the space of re-emission (number  $n$ ). The sharper/more acute

the antenna radiation pattern, the less the space of re-emission and the greater  $\sigma$ , i.e. is more the depth of slow fadings. This position was checked experimentally on the route with a length of 303 km at the frequency of approximately 1000 MHz. At the transmitting end was applied the weakly directed antenna with the amplification 22 dB, and reception was conducted from two antennas one of which had amplification 45 dB and width of radiation pattern of approximately  $1^\circ$  (according to the half power), and the second was that weakly directed with the amplification into 22 dB and width of diagram of  $20^\circ$ . The prolonged simultaneous recording of signal level from these antennas showed that the depth of slow fadings on the weakly directed antenna was considerably less than with the reception/procedure from the pencil-beam antenna. Fig. 1.12 gives the integral distribution curves of the value of attenuation factor for the highly directional and weakly directed receiving antennas. As we already spoke, the value of the space of re-emission in this case was changed upon transfer from one antenna to another approximately four times ( $n=4$ ).

Page 29.

It is not difficult to see from Fig. 1.12 that in the case of the directional antenna  $\sigma_1=8$  dB, and in the case of the omnidirectional antenna  $\sigma_2=5$  dB. Thus, the relationship between  $\sigma_1$  and  $\sigma_2$  corresponded approximately to equality (1.23). This equality gives

for  $\sigma_1 = 8$  dB and  $n=4$  the value of  $\sigma_2 = 4.7$  dB.

FOOTNOTE 1. In the work of Crawford [1.3] are also given the experimental data about the effect of antenna directivity on the depth of slow fadings which coincide approximately with data given above. ENDFOOTNOTE.

In summary, knowing, in how often decrease the space of re-emission upon transfer from the less directional antenna toward the antenna that of more directed can be defined along (1.23) and (1.24), as will increase standard deviation  $\sigma$ . Therefore, it is possible to lead the experimental data about the dispersion of slow fadings to the case of the omnidirectional antennas. Fig. 1.13 gives the dependence of standard deviation  $\sigma$  from the distance for the case when on both corresponding points are used these weakly directed antennas with the angle of directivity are more than  $2^\circ$ . This dependence is constructed according to the experimental data of works [1.1; 1.2], corrected taking into account applied in these experiments antennas. In order to obtain data for other antennas, it is necessary to use equality (1.23) or (1.24).

In this case standard deviation for the directional antennas will be  $\sigma_n$ , and as  $\sigma_0$  is understood the value of standard deviation for the omnidirectional antennas.



Determining  $\sigma_n$  from (1.23) and (1.24), we obtain

$$\sigma_n^2(\beta\delta) = 75 \ln \left[ n \left( e^{\frac{\sigma_0^2(\beta\delta)}{75}} + \frac{1}{n} - 1 \right) \right], \quad (1.23a)$$

with  $\frac{1}{n} \ll 1$

$$\sigma_n^2(\beta\delta) = \pi \sigma_0^2(\beta\delta). \quad (1.24a)$$

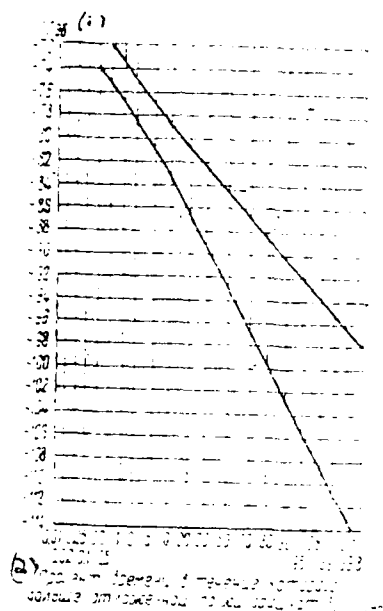


Fig. 1.12. Comparison of the depth of slow fadings in the case of reception to that directed ( $G=45$  dB, curve 1) and not directed of antenna ( $G=22$  dB, curve 2). Wave  $\lambda=30$  cm. Transmitting antenna with the amplification 22 dB. Route - 303 km.

Key: (1). dB. (2). Percentage of time during which  $V$  are more than deposited along the axis of ordinates value.

Page 30.

In this case value  $n$  in that case will be the ratio of the size of the space of re-emission with omnidirectional antennas  $a_2$  to the space of re-emission with directional antennas  $a_1$ .

$$n = \frac{a_2}{a_1}. \quad (1.25)$$

When on both corresponding points are applied identical antennas, which almost always occurs, as it will be shown into § 5, relation  $n$  can be determined, if are known the angles of antenna directivity in horizontal and vertical planes  $\alpha_{10}$  and  $\alpha_{20}$  and the angular dimensions of the space of re-emission in horizontal and vertical planes  $\theta_{10}$  and  $\theta_{20}$ . In the case of use on both points of the identical antennas

$$n = \left[ 1 - \left( \frac{\alpha_{20}}{\alpha_{10}} \right)^2 \right] \sqrt{1 - \left( \frac{\theta_{20}}{\theta_{10}} \right)^2}. \quad (1.26)$$

If are applied different antennas, then

$$n = \sqrt{1 - \left( \frac{\alpha_{20}}{\alpha_{10}} \right)^2} \sqrt{1 - \left( \frac{\alpha_{20}}{\alpha_{10}} \right)^2} \sqrt{1 - \left( \frac{\theta_{20}}{\theta_{10}} \right)^2}. \quad (1.26a)$$

Here:  $\alpha_{10}$  - the angle of directivity in the vertical plane of one antenna,  $\alpha_{20}$  - the same, but for another antenna,  $\theta_{10}$  - the smallest angle of directivity in the horizontal plane of two angles (in the case of use on the route of different antennas).

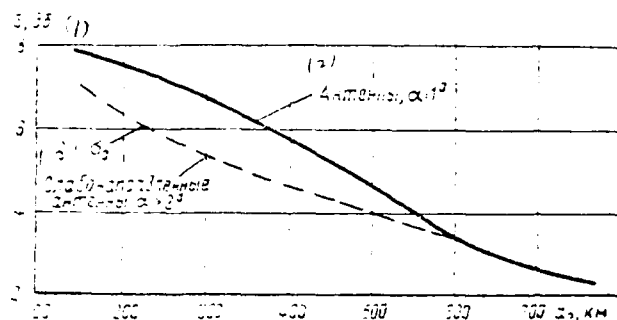


Fig. 1.13. Experimental dependence of the standard deviation  $\sigma$  of slow fadings for the antennas, with  $\alpha=1^\circ$ , and for omnidirectional antennas ( $\alpha>2^\circ$ ).

Key: (1) dB. (2). Antennas. (3). Weakly directed antennas,  $\alpha>2^\circ$ .

Page 31.

According to experiments  $\Theta_{\text{opt}} \approx 1.7^\circ$ , while  $\Theta_{\text{ro}} \approx 1^\circ$  (see § 1.5). Dependence  $\sigma_0$  on the distance for the weakly directed antennas when  $\alpha_{\text{so}}>3^\circ$  and  $\alpha_{\text{ro}}>2^\circ$ , obtained experimentally, is given to Fig. 1.13 together in by dependence of  $\sigma$  for pencil-beam antennas ( $\alpha_{\text{so}}=\alpha_{\text{ro}}=\alpha=1^\circ$ ). Let us note that these dependences are constructed, generally speaking, according to the experimental data, obtained in essence on the waves 30-40 cm. However, judging by the series of other experimental works [1.3-1.10], this dependence, apparently, is justified over a wide range of frequencies.

Until now, the discussion dealt with one fundamental reason for slow fadings, connected with the change in the time of the form of intensity and dimensions of heterogeneities in the space of re-emission. There are other reasons for slow changes in the level, for example, change in the time of refraction, thanks to which must change angle  $\psi_a$  (see Fig. 1.4), which, in turn, leads to a change in the signal level. A change of the refraction in the layer of the atmosphere thickness than 1-2 km is small, yes even the dependence of signal level on the refraction comparatively weak; therefore it is difficult to expect the essential fluctuations of signal level which are small in comparison with the fundamental form of fadings. Experimental data confirm this position. The fact is that the refractive index, which characterizes the degree of wave refraction, has distinct daily variation with the maximum into the evening and night hours. At the same time experiments [1.1; 1.2] do not detect any essential daily variation of signal level during the remote tropospheric propagation. Furthermore, if, refraction fadings played the significant role, then it would not be observed this strong effect of antenna directivity on the depth of fadings, since with the refraction fadings their depth does not depend on antenna directivity.

Another reason for slow fadings are slow changes in the time of the characteristics of heterogeneities simultaneously in entire space of the re-emissions which can occur due to a change in the weather conditions. Such synchronous changes really are observed, for example, with the passage of the fronts of warm or cold air, causing noticeable decrease or raising signal level. These fluctuations of level superimpose the specific impression to the general statistics of slow fadings. Especially large role such fadings play in the favorable months of the year when the average signal level is high. Under the unfavorable conditions when the average signal levels are low, effect of this type of fadings becomes small. As confirmation this serves the fact of the sharp effect of antenna directivity on the depth of slow fadings in particular in the unfavorable period of year. Since greatest interest for us are of the data about the fadings precisely in this season, then fadings of the type examined can be disregarded.

Page 32.

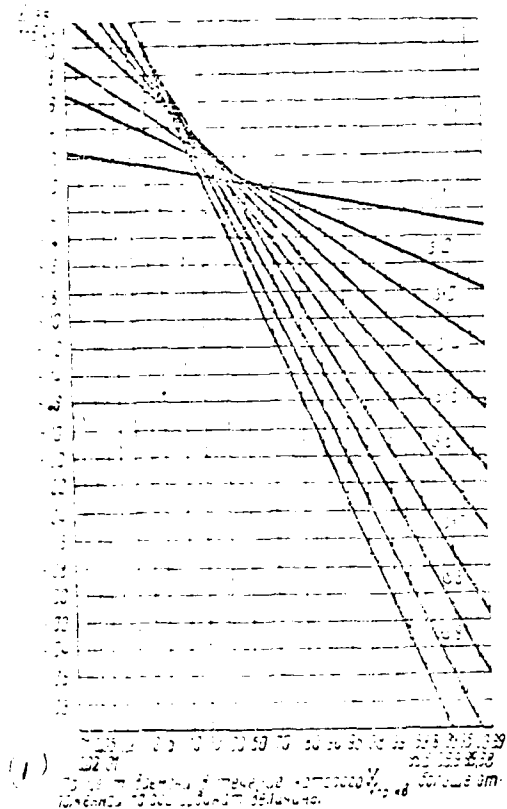
In conclusion let us present the integral distribution curves of slow fadings for different values  $\sigma_{(00)}$ , which can prove useful for the stability analyses of the work of tropospheric lines. On curves of Fig. 1.14 these distributions are constructed for values  $\frac{\gamma}{V_{sp, 0.5}} = 1$ , where  $V_{sp, 0.5}$  - rms value of attenuation factor. We resemble the order

of the determination of the depth of slow fadings.

FOOTNOTE 1. The depth of fadings is determined with respect to rms value  $V_{\text{rms}}$ , therefore the median values  $V$  in Fig. 1.14 do not coincide with zero. ENDFOOTNOTE.

On curve Fig. 1.13 is determined value  $\sigma_0$  for the omnidirectional antennas, then according to formula (1.26) is determined value  $n$ , also, according to formulas [1.23a) or (1.24a) is determined value  $\sigma_n$  for the directional antennas. Finally, on curves of Fig. 1.14 is determined the depth of fadings for the specific percentage of time.

Seasonal behavior of signal level. The average monthly value of the strength of field sufficiently considerably depends on the season of year. The lowest signal levels are observed by winter and most high in summer. On Fig. 1.15 for an example is given seasonal behavior of attenuation factor for the ultrashort waves on the route with the length of 270 km [1.1; 1.2], which passes above Caspian Sea. A maximum change in the average monthly values from the winter to summer composes at the distances of 200-300 km of approximately 12-15 dB. the spread of seasonal changes decreases with an increase in the distance and at a distance of 600-700 km becomes different approximately 7-8 dB. This it is possible to see at least from Fig. 1.11, where are given the integral distributions  $V$  for different distances to summer and winter periods.



Key: (1). Percentage of time during which  $\frac{V}{\sqrt{2}}$  is more than deposited along the axis of ordinates value.

Seasonal changes in the signal level are connected with seasonal changes in the structure of the heterogeneities of the atmosphere. In

summer the intensity of heterogeneities, i.e., value  $\overline{\Delta \varepsilon^2}$ , noticeably increases due to an increase in the temperature gradients and mainly due to an increase of the role of air humidity in the formation of heterogeneities.

#### § 1.5. Losses of antenna gain.

In the first and second paragraphs of this chapter has already been discussed the fact that the average value of attenuation factor  $V_{CP, KR}$  depends on the dimensions of the space of re-emission  $a'$ , which is evident at least from equality (1.6). The greater the dimension of the space of re-emission, the greater the heterogeneities, which participate with the re-emission of energy, the greater the value of attenuation factor

$$V_{CP, KR}^2 \sim a'.$$

But in the case of the pencil-beam antennas the value of the space of re-emission is determined by antenna directivity, so that with an increase in the directivity, i.e., with the decrease of the angle of directivity of antennas  $\alpha$ , the space of re-emission  $a'$  decreases. Thus, from an increase in the antenna directivity attenuation factor falls.



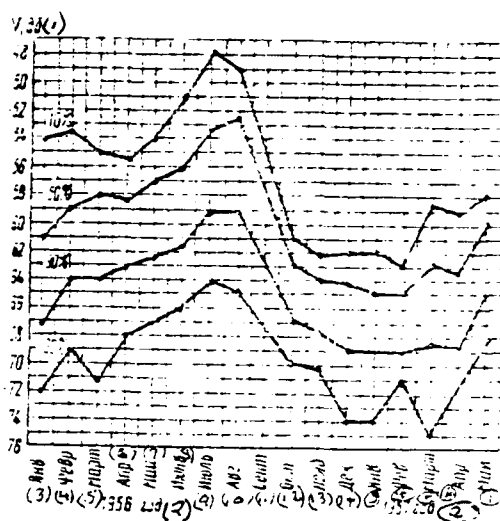


Fig. 1.15. Seasonal behavior  $V$  for sea route with a length of 270 km. In the curves are noted the percentages of time, during which  $V_{(dB)}$  exceeded the level, noted in the curve. Curved 50-percent corresponds to median level.

Key: (1) dB. (2) year. (3). Jan. (4). Feb. (5). March. (6). Apr. (7). May. (8). June. (9). July. (10). Aug. (11). Sept. (12). OCT. (13). Nov. (14). Dec.

Page 34.

Consequently, with an increase of the antenna gain the power of the signal in the place of reception will not increase proportional to an increase in the antenna gain. An increase in the signal will lag

behind an increase in the antenna gain. This phenomenon accepted to call the losses of the amplification of antennas. Although this name and does not reflect the essence of phenomenon itself, we it apply in view of the taking root tradition. In fact, no losses of antenna gain there exists actually, but there is only a dependence of attenuation factor on the directivity of antennas (drop in  $\sqrt{V}$  with an increase in the directivity).

The losses of amplification  $\delta_{yc}$  according to determination are equal to:

$$\delta_{yc} = \frac{V_0}{V_1} \quad (1.27)$$

where  $V_0$  - an attenuation factor for the omnidirectional antennas, and  $V_1$  - attenuation factor for the directional antennas. As has already been spoken,  $V_0^2 = ca_0$  and  $V_1^2 = ca_1$ , where  $c$  - constant,  $a_0$  - the effective space of re-emission in the case of the omnidirectional antennas and  $a_1$  - the effective space of re-emission for the directional antennas; therefore

$$\delta_{yc} = \frac{a_1}{a_0} = \frac{1}{n} \quad (1.28)$$

The geometric dimensions of tropospheric space  $a_1$  can be determined from the experimental data about the angular characteristics of the tropospheric field (see § 16). The comparison of the average signal levels, taken from the spaced on the angle antennas during the large period of observations, makes it possible to obtain the dependence of the level of signal  $V$  on azimuthal angle

$\Theta_r$  and on the angle of elevation  $\Theta_a$ . Such dependences were obtained for the series of the routes (see § 1.6). Dependences  $V(\Theta_r)$  and  $V(\Theta_a)$  can be approximated with the aid of the following functions:

$$\begin{aligned} V(\Theta_a) &= e^{-1.39 \left( \frac{\Theta_a}{\Theta_{a0}} \right)^2} \\ V(\Theta_r) &= e^{-1.39 \left( \frac{\Theta_r}{\Theta_{r0}} \right)^2} \end{aligned} \quad (1.29)$$

When  $\Theta_a = \frac{1}{2} \Theta_{a0}$  and  $\Theta_r = \frac{1}{2} \Theta_{r0}$ ,  $V(\Theta_a) = \frac{1}{2}$ ,  $V(\Theta_r) = \frac{1}{2}$ . Thus,  $\Theta_{a0}$  and  $\Theta_{r0}$  - effective width and altitude of space, determined on the decay power of signal two times. The results of experiments, given in § 1.6, and also experiments in the measurement of the fluctuations of angles of arrival (see, for example [1.1; 1.13; 1.17, 1.18]) give values  $\Theta_{a0} \approx 1.7^\circ$  and  $\Theta_{r0} \approx 1^\circ$ .

Page 35.

In the case of applying the pencil-beam antennas the angular dimensions of the space of re-emission  $\Omega$  will be determined by the antenna radiation patterns. It is possible to approximate these diagrams with the aid of the functions:

$$f(\alpha_a) = e^{-1.39 \left( \frac{\alpha_a}{\alpha_{a0}} \right)^2}, \quad f(\alpha_r) = e^{-1.39 \left( \frac{\alpha_r}{\alpha_{r0}} \right)^2} \quad (1.30)$$

This approximation usually will agree well with real directional characteristic of antennas. Here  $\alpha_{a0}$  and  $\alpha_{r0}$  - angles of antenna directivity in the vertical and horizontal planes.

In the case of the directional antenna the dependence of signal level on angles  $\alpha_s$  and  $\alpha_r$  will be determined, on one hand, by angular characteristics (1.29), connected with the properties of the heterogeneities of the troposphere, and, on the other hand, by the angular characteristics of antennas (1.30). Dependences  $V(\alpha_r)$  and  $V(\alpha_s)$  will be equal to products (1.29) to (1.30). Thus,

$$\begin{aligned} V(\alpha_s) &= e^{-1.39 \left[ \left( \frac{\alpha_s}{\beta_{s0}} \right)^2 + \left( \frac{\alpha_s}{\alpha_{s0}} \right)^2 \right]} \\ V(\alpha_r) &= e^{-1.39 \left[ \left( \frac{\alpha_r}{\beta_{r0}} \right)^2 + \left( \frac{\alpha_r}{\alpha_{r0}} \right)^2 \right]} \end{aligned}$$

These dependences can be rewritten as follows:

$$\begin{aligned} V(\alpha_s) &= e^{-1.39 \left( \frac{\alpha_s}{\beta_s} \right)^2} \\ V(\alpha_r) &= e^{-1.39 \left( \frac{\alpha_r}{\beta_r} \right)^2} \end{aligned} \quad (1.31)$$

where

$$\beta_s = \frac{\theta_{s0} \alpha_{s0}}{\sqrt{\theta_{s0}^2 + \alpha_{s0}^2}}$$

and

$$\beta_r = \frac{\theta_{r0} \alpha_{r0}}{\sqrt{\alpha_{r0}^2 + \theta_{r0}^2}}$$

are effective angular width and height of space re-emissions in the case of the directional antennas. Now let us switch over to the determination of the losses of amplifications  $\delta_{yc}$ , which according to (1.28) are equal to the ratio of antenna volume  $\alpha_a$  to tropospheric space  $\alpha_r$ .

For the case of identical antennas on both points from the geometric relationships it is not difficult to obtain:

$$a_1 = c_1 \beta_r \beta_a^2$$

and

$$a_2 = c_2 \theta_{r0} \theta_{a0}^2$$

where  $c_1$  and  $c_2$  - constants. Taking into account that the fact that the angular dependences  $V(a)$  and  $V(\theta)$  are defined by the functions of one form (1.28) and (1.31), and also in view of the fact that distance from both corresponding points to the center of the space of re-emission  $a_1$  approximately the same, as to the center of space  $a_2$ , we will obtain  $c_1 = c_2$ .

In that case, substituting the value  $a_1$  and  $a_2$  in (1.28), we will have

$$\lambda_{yc} = \frac{\beta_r \beta_a^2}{\theta_{r0} \theta_{a0}^2}$$

Substituting the value  $\beta_r$  and  $\beta_a$  into the latter equality, we will obtain

$$\lambda_{yc} = \frac{1}{\left[1 - \left(\frac{\theta_{a0}}{x_{a0}}\right)^2\right] \sqrt{1 - \left(\frac{\theta_{r0}}{x_{r0}}\right)^2}} \quad (1.32)$$

When  $x_{a0} \gg \theta_{a0}$  and  $x_{r0} \gg \theta_{r0}$  the losses of amplification are absent.

When  $x_{a0} \ll \theta_{a0}$  and  $x_{r0} \ll \theta_{r0}$  when losses are great,

$$\lambda_{yc} = \left(\frac{x_{a0}}{\theta_{a0}}\right)^2 \left(\frac{x_{r0}}{\theta_{r0}}\right)^2 \quad (1.33)$$

Expressing  $\Delta_{\text{ant}}$  in (1.32) in the decibels, we will obtain

$$\Delta_{\text{ant}} = -10 \lg \left[ 1 - \left( \frac{\theta_{\text{a0}}}{\theta_{\text{a0}}} \right)^2 \right] - 5 \lg \left[ 1 - \left( \frac{\theta_{\text{a0}}}{\theta_{\text{a0}}} \right)^2 \right]. \quad (1.34)$$

With the pencil-beam antennas

$$\Delta_{\text{ant}} = 20 \lg \left( \frac{\theta_{\text{a0}}}{\theta_{\text{a0}}} \right) + 10 \lg \left( \frac{\theta_{\text{a0}}}{\theta_{\text{a0}}} \right). \quad (1.35)$$

If on the transmitting and receiving points are applied different antennas with the angles of directivity  $\theta_{\text{a0}}$ ,  $\theta_{\text{a0}}$  and  $\theta_{\text{a0}}$ ,  $\theta_{\text{a0}}$ , then formula (1.34) will take the form

$$\Delta_{\text{ant}} = -5 \lg \left[ 1 - \left( \frac{\theta_{\text{a0}}}{\theta_{\text{a0}}} \right)^2 \right] - 5 \lg \left[ 1 - \left( \frac{\theta_{\text{a0}}}{\theta_{\text{a0}}} \right)^2 \right] - 5 \lg \left[ 1 - \left( \frac{\theta_{\text{a0}}}{\theta_{\text{a0}}} \right)^2 \right] \quad (1.36)$$

or for the pencil-beam antennas

$$\Delta_{\text{ant}} = 10 \lg \left( \frac{\theta_{\text{a0}}}{\theta_{\text{a0}}} \right) + 10 \lg \left( \frac{\theta_{\text{a0}}}{\theta_{\text{a0}}} \right) + 10 \lg \left( \frac{\theta_{\text{a0}}}{\theta_{\text{a0}}} \right). \quad (1.37)$$

If one antenna not directed, then

$$\Delta = 10 \lg \left( \frac{\theta_{\text{a0}}}{\theta_{\text{a0}}} \right) + 10 \lg \left( \frac{\theta_{\text{a0}}}{\theta_{\text{a0}}} \right).$$

Page 37.

Transition from one directional antenna toward two directional antennas gives the addition in the losses of amplification only to value

$$\Delta = 10 \lg \left( \frac{\theta_{\text{a0}}}{\theta_{\text{a0}}} \right). \quad (1.38)$$

Therefore it cannot be considered that the losses of amplification in the case of applying two directional antennas are equal to the sum of the losses of amplification for each of the antennas. In reality the losses of the amplification of one antenna

differ only a little (to value  $\Delta$ ) from the losses of the amplification of system of two antennas.

Furthermore, in the measurement of the losses of antenna gain, which is usually conducted by the comparison of two signals, accepted from highly directional and weakly directed antennas. one should consider the directivity of the transmitting antenna which, as a rule, is not done.

The relationship between the losses of the amplification of one antenna and the losses of the amplification of two antennas was checked experimentally on the route 303 km at frequencies of 800-1000 MHz. Experiments showed that the equality given above for  $\Delta$  is justified experimentally. On the route 303 km of the loss of the amplification of the directional receiving antenna with  $\alpha_{r0} = \alpha_{d0} = 1^\circ$  and the omnidirectional transmitting antenna were 4 dB, and the losses of the amplification of the system of two such antennas - 6 dB. Taking into account that  $\theta_{90} = 1.7^\circ$  (see data § 1.6), formula (1.38) give  $\Delta = 2.3$  dB, which corresponds to experiment. From this conclusion follows practical the conclusion that on the tropospheric lines of communications to disadvantageously apply different antennas on the receiving and transmitters, since the losses of amplification in essence will be determined by the most directed antenna.

As showed the experiments (see § 1.6),  $\Theta_{a0} = 1.7^\circ$  and  $\Theta_{r0} = 1.7^\circ$ . Using formulas (1.34), (1.35) (1.36) and substituting in them these values  $\Theta_{a0}$  and  $\Theta_{r0}$ , it is easy to calculate the losses of amplification for any antennas. For example, for the system of identical symmetrical antennas ( $\alpha_{r0} = \alpha_{a0} = \alpha$ ) we calculated according to formula (1.34) the dependence of the losses of amplification  $\delta_{yc}$  first on  $\alpha$ , and then, since  $\alpha$  is determined the antenna gain, constructed the dependence of losses amplifications  $\delta_{yc}(\theta_0)$  on the value of the antenna gain (curve 1 on Fig. 1.16). The same figure gives the experimental dependence (curve 2), obtained in work [1.14]. Furthermore, are given the experimental points, obtained on the route 303 km with the antennas which have  $\alpha_{r0} = \alpha_{a0} = 1^\circ$  and  $6.7^\circ$ . As can be seen from Fig. 1.16, experimental data confirm obtained in this section dependence of the losses of amplification on their directivity. In the confirmation of this dependence it is possible, furthermore, to refer even to the series of experiments. As an example let us give the results of the experiences of Crawford which were conducted on the route 273 km at the frequency of 4110 MHz [1.3]. In these experiments on one of the ends of the route was applied the antenna by directivity of  $1.8^\circ$  and at other end - antenna with the angle of directivity of  $2.2^\circ$  and  $0.33^\circ$ .



According to the observations of Crawford the expansion of radiation pattern was approximately  $1^\circ$ , i.e., the angular dimensions of the space of re-emission comprised  $\Theta_{Bo} = \Theta_{To} = 1^\circ$ . According to (1.36) the losses of amplification had to be 6 dB. On the measurements of Crawford the losses of amplification proved to be equal to approximately 5.7 dB. As the confirmation of the derived relationships can serve also experiments which were conducted on the route 303 km at the frequency of approximately 1000 MHz in the central band of the European territory of the union where were applied antennas with the angle of directivity of  $1^\circ$  in both planes and antennas weakly directed with the angle of directivity of  $20^\circ$ . When from both sides were applied the omnidirectional antennas, the space of re-emission was determined by pillar by the properties of the heterogeneities of the atmosphere. Its angular dimensions according to the measurements, which were being carried out on this route, comprise approximately  $\Theta_{Bo} = 1.7^\circ$ ,  $\Theta_{To} = 1^\circ$ . Upon transfer to the directional antennas the space decreased also according to (1.34) the losses of amplification must be  $\delta = 9.4$  dB. Experimental measurements of the losses of the amplification of distance  $\delta = 8$  dB. The same result gives the comparison of calculation with the results of experiment on the route 300 km at the frequency of 2120 MHz of that carrying out in Japan [1.16].

As can be seen from equalities (1.34) - (1.36), the losses of

amplification depend only on the relative angular dimensions of the space of re-emission. If the angular dimensions of the space of re-emission in the case of omnidirectional antennas ( $\Theta_{so}$ ,  $\Theta_{ro}$ ) do not depend on distance, then the losses of amplification must not change with the distance.

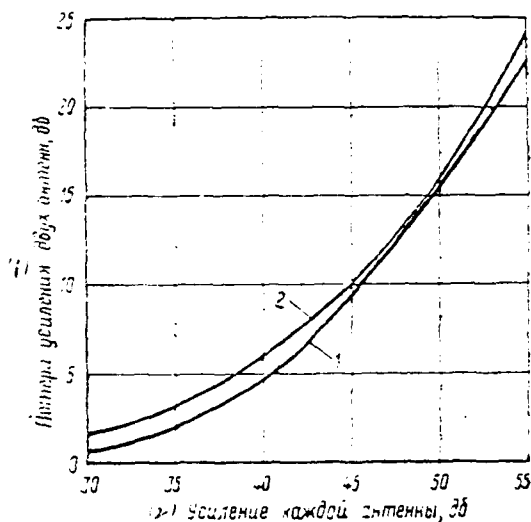


Fig 1.16. Dependence of the losses of the amplification of the system of antennas on the amplification of each antenna.

Key: (1). Losses of the amplification of two antennas, dB. (2). Amplification of each antenna, dB.

Page 39.

Angular dimensions ( $\Theta_{\text{до}}$ ,  $\Theta_{\text{го}}$ ). Judging according to the experimental data about the angles of arrival and other characteristics of the signal (see § 1.6), either they do not depend on distance or fall from the distance, what they indicate, for example, experiments [1.8]. Approximately it is possible to count value  $\delta$  of that not depending on the distance. Furthermore, as show experiments and as is evident

from expressions (1.34)-(1.36), the losses of amplification do not depend on wavelength. As can be seen from (1.34), (1.36), on the losses of amplification great effect exerts antenna directivity in the vertical plane; therefore from the point of view of the decrease of the losses of antenna gain to more favorably have the smaller angle of directivity in the horizontal plane and larger in the vertical plane.

Now let us pause at the question, to which usually is not turned the attention, although it has the vital importance during the determination of the losses of amplification. Discussion deals the fact that, strictly, to understand under this term. Above we defined it as the relation of the rms values of attenuation factor for the directional and omnidirectional antennas. But frequently under the term of the loss of amplification is understood a difference in the median values of the attenuation factor, expressed in the decibels,

$$\Delta' = 20 \lg \overline{V_o} - 20 \lg \overline{V_d}, \quad (1.39)$$

where  $V_o$  - an attenuation factor for the omnidirectional antenna,  $V_d$  - attenuation factor for the directional antenna.

In the majority of the works, dedicated to the determination of the losses of antenna gain, under this term (for example, [1.14; 1.15]) is understood value  $\Delta'_{(dB)}$ . But this value cannot characterize energy loss. The energy losses of random variable  $V$  can be

characterized only by a change in the rms value of this value. Meanwhile values  $\Delta'_{(\partial\delta)}$  and  $\delta_{yc(\partial\delta)}$  on the whole differ radically from each other:

$$\delta_{yc(\partial\delta)} = 10 \lg \overline{V_0^2} - 10 \lg \overline{V_1^2}. \quad (1.40)$$

It is not difficult to show analogously how was obtained expression (1.13), that in the case of the logarithmic normal law:

$$20 \lg \overline{V_0} = 10 \lg \overline{V_0^2} - 0,115 \sigma_0^2, \quad (1.41)$$

$$20 \lg \overline{V_1} = 10 \lg \overline{V_1^2} - 0,115 \sigma_1^2, \quad (1.42)$$

where  $\sigma_0$  and  $\sigma_1$  - the standard deviations of slow fadings for the omnidirectional and directional antennas respectively, expressed in the decibels. Substituting the value  $20 \lg \overline{V_0}$  and  $20 \lg \overline{V_1}$  from (1.41), (1.42) in (1.39), we obtain

$$\Delta'_{(\partial\delta)} = \delta_{yc(\partial\delta)} + 0,115 (\sigma_0^2 - \sigma_1^2). \quad (1.43)$$

Thus, value  $\Delta'_{(\partial\delta)}$  is connected not only with the value of the real losses of amplification  $\delta_{yc(\partial\delta)}$ , but also with a change in the depth of fadings upon transfer from the omnidirectional antenna toward that directed.

Page 40.

As it was shown earlier, this change is sufficiently considerable. Therefore value  $\Delta'_{(\partial\delta)}$  proves to be considerably more than the true losses of amplification. In summary value  $\Delta'_{(\partial\delta)}$  is not the value of the true losses of antenna gain and is inconvenient for the practical calculations, since it depends on the depth of slow fadings.

Thus, the account of the losses of amplification can be conducted only according to formulas (1.34), (1.35) or (1.36). Due to the phenomenon of the losses of antenna gain the value  $M_{\text{loss}}$  for the directional antennas proves to be less than for the omnidirectional antennas. Let us note that dependence  $M_{\text{loss}}$  on the distance (Fig. 1.5a, 1.5b) is constructed according to the experimental data which were obtained with the antennas of different directivity. Experimental values  $M_{\text{loss}}$  measured with the directional antennas for obtaining the dependence Fig. 1.5a, were recounted by us to the case of the omnidirectional antennas with the aid of the procedure given above. For obtaining the dependence 1.5b these data were recounted to the case of antennas with the angle of directivity of  $1^\circ$ . It should be noted that as a result of this translation, which considers directivities of antennas, scatter of the experimental values of attenuation factor it decreased. In many experiments regarding the losses of antenna gain was not considered the directivity of the transmitting antenna. In view of these deficiencies such data about the losses of amplification proved to be in many respects contradictory and inexplicable. The account of the effect of the directivity of the transmitting antenna made it possible to obtain the reliable experimental data about the losses of antenna gain.

§ 1.6. Determination of the angular dimensions of the tropospheric space of re-emission and optimum form of the antenna radiation patterns.

The losses of antenna gain, and also the depth of slow fadings they will be lower, greater the greater the part of the tropospheric space of re-emission is utilized for the re-emission, i.e., the nearer the form of antenna space is to the tropospheric space of re-emission. From an energy point of view to more favorably utilize antennas of the large amplification when  $\alpha \rightarrow 0$ . In this case we must be subdued with the fact that will be observed a phenomenon of the losses of amplification, and also an increase in the depth of slow fadings. However, that and another it is possible to reduce to a minimum with the aid of the rational selection of the antenna radiation pattern.

As we already spoke [this is evident from the formula (1.33)], the greatest losses of antenna gain cause the contraction of radiation pattern in the vertical plane, since  $S_{\theta} \sim \theta^2$  in horizontal plane  $S_{\phi} \sim \phi$ . Therefore to more favorably apply the antennas of different directivity in different planes.

It is most profitable an angle of directivity in the vertical plane to have to the equal angular dimensions of the tropospheric space of re-emission. Then the losses of amplification and increase  $\sigma$  due to the decrease of space in the vertical plane almost will not be. For obtaining the necessary amplification it is possible to increase antenna directivity in the horizontal plane. In that case of antenna they will have directivity in the horizontal plane more than in the vertical. Such asymmetric antennas will have considerably smaller losses of amplification, and value  $\sigma$  for the slow fadings will be substantially less. All this is directly evident from equalities (1.23), (1.24), (1.26), (1.38).

Thus, for the correct design of antennas are necessary the data about the angular dimensions of the tropospheric space of re-emission. For obtaining such data on routes in extent 270, 303 and 630 km were made special measurements. On one of the points was applied weakly directed antenna  $\alpha_{ro} = \alpha_{so} > 2^\circ$ , while on other point - pencil-beam antenna  $\alpha_{so} = \alpha_{ro} = 0.7^\circ$  (on routes 270 and 303 km) and  $\alpha_{so} = \alpha_{ro} = 1^\circ$  (on the route 630 km). The pencil-beam antennas rotated within limits of  $3^\circ$  on the vertical line and by  $2^\circ$  on the horizontal. Measurements consisted in the continuous recording of signal level during 3 min on each fixed antenna position. The distance between the fixed levels was  $0.4^\circ$ . First was removed radiation pattern on the vertical line, and then on the horizontal. The value of signal level



was averaged in every 3 min. Fig. 1.17 gives the diagrams in the vertical plane for three routes (1 - route 630 km, 2-270 km, 3-303 km), obtained as a result of averaging in a large quantity of performances of the measurements (several hundred), which were being carried out into different seasons of year.

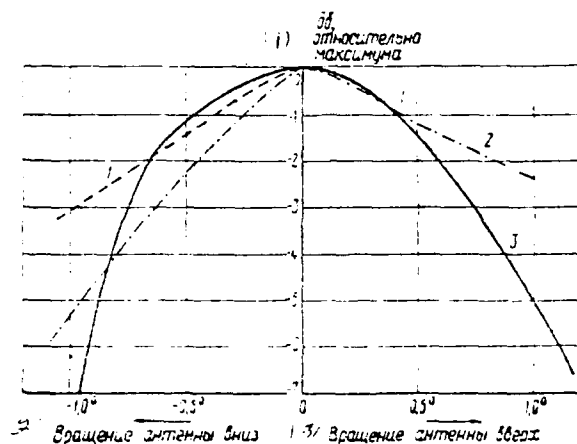


Fig. 1.17. Experimental diagram of re-emission in the vertical plane with the weakly directed transmitting antenna.

Key: (1) dB, relative to maximum. (2). Rotation of antenna down. (3). Rotation of antenna upward.

Page 42.

On the route 270 km the measurements were conducted only in spring and in summer. From Fig. 1.17 it is evident that the angular dimension of tropospheric space comprises approximately  $1.7^\circ$  for all routes. The angular diversion of tropospheric space in the horizontal plane on the same measurements was about  $1^\circ$ . Diversion we define, as it is accepted, on decay in the power of signal two times. The vertical dimension of the tropospheric space of re-emission is

greater horizontal, which indicates the large role of laminar heterogeneities in the formation of tropospheric field. Hence follows supplementary reason in favor of the contraction of the width of the antenna radiation patterns in the horizontal plane. The width of the antenna radiation pattern in the vertical plane, is most favorable from an energy point of view, it must be order of  $1.5-2^\circ$ . It is necessary to have in mind, of course, that with the wide antenna radiation patterns can arise the distortions of broadband signal due to the arrival of waves with the large time lag. Therefore during the transmission of broad band is necessary the special checking of possible distortions.

§ 1.7. Dependence of signal level on area relief and height of antennas.

During the remote tropospheric propagation area relief affects in the small sections, adjacent to transmitting and receiving ends of the route. The presence of the screening obstructions before the antennas causes the decrease of signal level the greater, the greater the angle of closing  $\theta$ , which is the angle between the line, drawn from the center of antenna to the apex of obstruction, and the horizontal plane (Fig. 1.18). The dependence of attenuation factor on the angle of obscuration is explained by a change in angle  $\gamma$  with a change in the angle of obscuration. With an increase  $\theta$  increases  $\gamma$ .

DOC = 80025103

PAGE

83

and since the scattering or wave reflection by atmospheric heterogeneities possesses the directed properties, then from increase of attenuation factor falls.

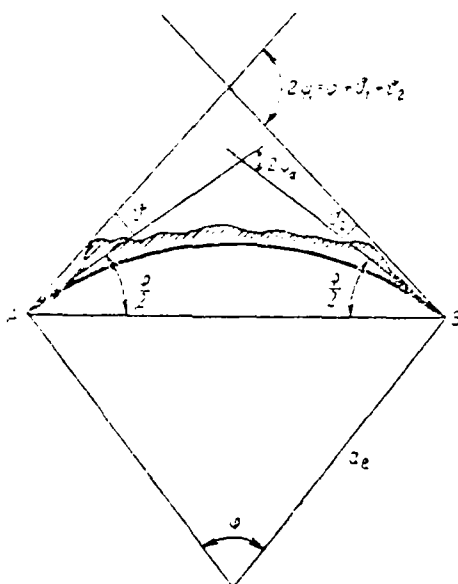


Fig. 1.18. Taking into consideration of the effect of area relief.

Page 43.

The experimental study of the effect of the shielding obstructions was conducted on routes with an extent 303 and 448 km [1.2], and also in the series of other routes [1.1] in extent 105 and 152 km. Experiments showed that the attenuation factor is changed inversely proportional to the square of angle  $\psi$ . On Fig. 1.19 is given the experimental dependence of attenuation factor on angle  $\psi$ , obtained on the route 450 km on the wave of approximately 30 cm. Designating through  $b$  the ratio of the rms value of attenuation factor  $V_{cp,KB}$  with  $\psi_1 = \psi_2 = 0$  to  $V_{cp,KB}$  with  $\psi_1 \neq 0$ ,  $\psi_2 \neq 0$ , in accordance with the experimental data

it is possible to record:

$$\dot{\delta} = \frac{V_{cp, \kappa \delta 0}}{V_{cp, \kappa \delta}} = \frac{\dot{\varphi}_0^2}{\dot{\varphi}_1^2}, \quad (1.44)$$

where  $\psi_0$  - slip angle for  $\vartheta_1 = \vartheta_2 = 0$ ,  $\psi_1$  - slip angle for  $\vartheta_1$  and  $\vartheta_2$ , not equal to zero. From the geometric relationships (see Fig. 1.18) we will obtain:

$$\psi \approx \frac{\varphi}{2}, \quad (1.45)$$

$$\psi_1 \approx \frac{1}{2}(\varphi + \vartheta_1 + \vartheta_2), \quad (1.46)$$

where  $\varphi \approx \frac{d}{a_e}$  - geocentric angle,  $a_e$  - equivalent radius of the Earth.

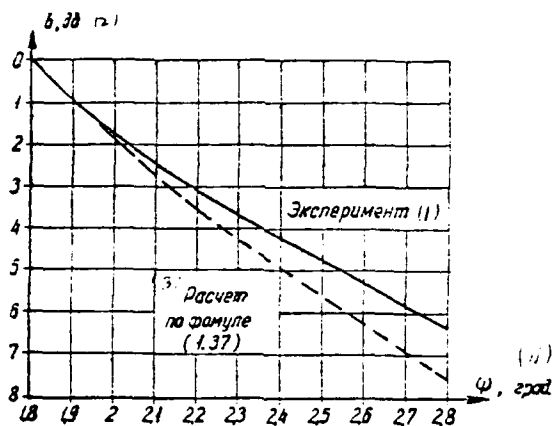


Fig. 1.19. Dependence of weakening on the angle of slip -  $\psi$ , for the route 448 km,  $\lambda=30$  cm.

Key: (1). Experiment. (2) dB. (3). Calculation according to formula. (4) deg.

Page 44.

Substituting these values of angles in (1.44), we will have

$$b = \frac{\varphi^2}{(\varphi - \alpha_1 - \alpha_2)^2} \quad (1.47)$$

or

$$b_{(dB)} = 40 \lg \varphi - 40 \lg (\varphi - \alpha_1 - \alpha_2). \quad (1.48)$$

As can be seen from (1.47), the dependence of weakening  $b$  on the angle of obscuration sufficiently weak. In this case, the greater the distance, the less the weakening, introduced by the shielding

obstructions.

§ 1.8. Statistical characteristics of signals with the space, frequency and angular diverse receptions.

General information.

On the tropospheric lines of communications for dealing with the rapid signal fading is used extensively the space diversity when the reception of signal is realized from several antennas, displaced relative to each other in the space, and also frequency diversity when signal simultaneously is transmitted and is accepted at two different frequencies.

Is less is propagated the method of the diverse reception over the angle, used only in the case of using the antennas with the very large directivity. All these methods of the diverse reception make it possible to considerably increase the stability of communication on the tropospheric lines; therefore it is of interest to come to light the fundamental laws, characteristic for the signals with the diversities of different form.

Correlation of signals with the space diverse reception.



If the reception of signals is conducted from two identical antennas, spread in the space, then in general rapid fadings occur on the different antennas nonsimultaneously. On the tropospheric lines of communications is applied the separation of antennas in the direction, perpendicular to route on the horizontal. The diversity of antennas along the route is ineffective, since for achievement of the necessary results is necessary the very large separation of antennas, considerably larger than with the transverse diversity. Therefore further the question will deal only with transverse horizontal separation.

Page 45.

The fluctuations of the instantaneous values of signal amplitude on different antennas prove to be to the certain degree uncorrelated. As usual, degrees of the correlation of signals can be determined with the aid of the coefficient of correlation R:

$$R = \frac{\overline{\Delta U_1 \Delta U_2}}{\overline{\Delta U^2}}, \quad (1.49)$$

where  $\Delta U_1$  - a change of the signal amplitude in the time relative to average value in the first antenna,  $\Delta U_2$  - the same change of the signal amplitude in the second antenna;  $\overline{\Delta U^2}$  - the mean square of the fluctuations of signal level.

Antennas are assumed to be identical ones; therefore  $\overline{\Delta U^2}$  it is

equal for both antennas. It proves to be that with an increase in the distance between the antennas  $l$  the coefficient of correlation  $R$  falls. Dependence of  $R$  on the distance is called space correlation function  $R(l)$ . The nature of this phenomenon can be explained based on this example. Let us examine two heterogeneities in the space of re-emission. Let one of them be located in the center of space  $a$  (Fig. 1.20) at point  $C_1$ , and the second - at a distance of  $L/2$  from the first heterogeneity at point  $C_2$  ( $L$  - a transverse dimension of space  $a$ ). At point  $A$  is located the transmitting antenna, while at points  $B_1$  and  $B_2$  - receiving antennas. If the wave amplitudes, reflected by heterogeneities  $C_1$  and  $C_2$ , are approximately identical, then with the small movements  $C_1$  relative to  $C_2$  in the place of reception will be observed deep fadings due to the interference of two waves reflected whose phase is changed in the time. A phase difference of two waves reflected in the first antenna will be

$$\Delta\varphi_1 = \kappa \left( 2 \sqrt{\frac{a^2}{4} + \frac{L^2}{4}} - d \right) \approx \frac{\kappa L^2}{2d}. \quad (1.50)$$

Phase difference in the second antenna

$$\Delta\varphi_2 = \kappa \left( 2 \sqrt{\frac{a^2}{4} + \frac{(L-l)^2}{4}} - d \right) \approx \frac{\kappa (L-l)^2}{2d}. \quad (1.51)$$

As can be seen from (1.50), (1.51), a phase difference of the waves reflected is different for antennas  $B_1$  and  $B_2$ , and, the greater  $l$ , the greater this difference.

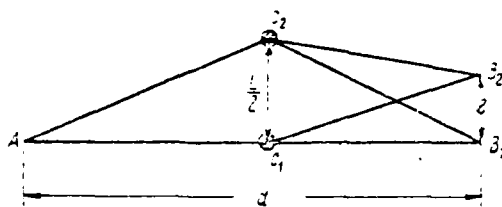


Fig. 1.20. Geometry of the diverse in the space reception.

Page 46.

Thus, the maximums and the minimums of signals will not coincide in these antennas. If  $\Delta\theta_1$ , it will differ from  $\Delta\theta_2$  to value  $\pi$ , then upon the appearance of an interference maximum in antenna  $B_1$  in antenna  $B_2$  there will be the minimum of signal, i.e., the coefficient of correlation of signals in  $B_1$  and  $B_2$  will be equal to zero. This will begin when

$$\frac{\pi(L-l)^2}{2L} - \frac{\pi L^2}{2L} = \pi,$$

or, taking into account that  $L \gg l$ , we will obtain

$$2\pi \frac{Ll}{L} = \pi, \quad (1.52)$$

whence we find value  $l=l_m$  which corresponds to the correlation coefficient, equal to 0:

$$l_m = \frac{L}{2}. \quad (1.53)$$

Thus, from an increase in  $l$  the degree of the correlation of signals falls. When  $l=l_m$  the correlation coefficient is approximately equal to zero. A radius of the correlation of signals on two

antennas, obviously, will be proportional to value  $l_0$ . Under a radius of correlation is understood the distance  $l_0$  at which the correlation function falls into e of times. Certainly, actually the space of re-emission contains many re-emitting heterogeneities; therefore interference fadings are caused by the arrival of many waves into the place of reception; however, the essence of phenomenon is not changed in comparison with the case examined. Approximately it is possible to consider that

$$l_0 \approx 2l = \frac{d \cdot \lambda}{L} = \frac{\lambda}{\sin \theta_0}, \quad (1.54)$$

where  $\theta_0$  - angular dimension of the space of re-emission in the horizontal plane.

As can be seen from (1.54), a radius of correlation is proportional to wavelength and it is inversely proportional to the angular dimensions of the space of re-emission. Since the angular dimensions of the space of re-emission according to § 1.5, and also to the measurements of angles of arrival [1.1] either do not depend on distance or they fall from the distance, then  $l_0$  apparently, must or not depend on distance or increase with the distance. In the case of the directional antennas a radius of correlation must increase inversely proportional to the angle of antenna directivity in the horizontal plane.

The experimental data about the dependence of a radius of

correlation on the distance have the large scatter of values [1.1], since in different experiments were applied different antennas.

Furthermore, pronounced climatic and geographical differences, and also differences in the time of observation. According to experimental data value  $\gamma_0/\lambda$ , apparently, does not depend on wavelength and varies for different experiments approximately from 10 to 70.

Page 47.

Therefore for guaranteeing the statistical independence of signals the diversity of antennas in the direction, perpendicular to route 1, must be selected not less (50-100)  $\lambda$ . Experimental space correlation function has a form, a close one to the exponential function:

$$R(l) = e^{-\left(\frac{l}{L}\right)} \quad (1.55)$$

Fig. 1.21 gives as an example the experimental space correlation function, obtained on the route in extent in 300 km on the wave 30 cm [1.2]. In this experiment were applied identical antennas, in which  $\gamma_{01} = \gamma_{02} = 10$ .

Correlation of signals with the diversity in the frequency. Frequency characteristics of signal.

AD-A883 445

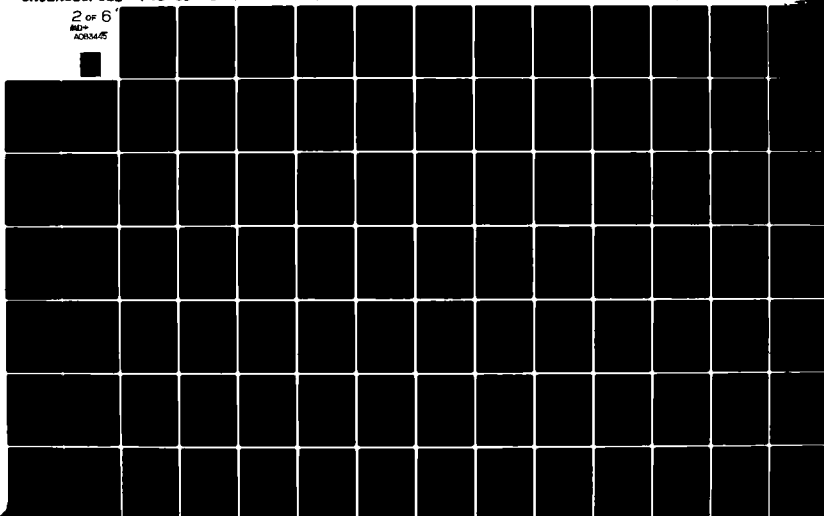
FOREIGN TECHNOLOGY DIV WRIGHT-PATTERSON AFB OH  
REMOTE TROPOSPHERIC RADIO COMMUNICATION, (U)  
MAR 80 I A GUSYATINSKIY, A S NEMIROVSKIY  
FTD-ID(RSI)-0251-80

F/0 17/001

UNCLASSIFIED

NL

2 of 6  
AD-  
A083445



During the remote tropospheric propagation into the place of reception come many waves with the randomly changing in the time phases. This leads to the fact that the amplitude-frequency characteristic of signal changes in the time randomly and it can be determined only statistically. For the quantitative estimate of random changes in the amplitude-frequency characteristic they use the coefficient of correlation

$$R(\Delta f) = \frac{\overline{\Delta U_1 \Delta U_2}}{\Delta U^2}.$$

where, as before  $\Delta U_1 = U_1 - \bar{U}_1$ ,  $\Delta U_2 = U_2 - \bar{U}_2$ ,  $U_1$  - signal level at frequency  $f$ ,  $U_2$  - signal level at frequency  $f_2 = f_1 + \Delta f$ .

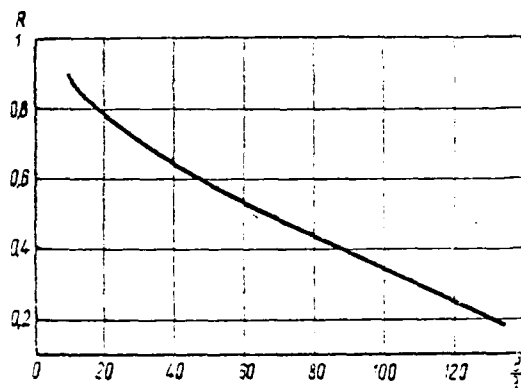


Fig. 1.21. space correlation function, obtained experimentally on the route 300 km on the wave 30 cm.

Page 48.

Dependence  $R(\Delta f)$  is nothing else but the frequency correlation function of signal. The nature of the variability of frequency characteristics it is easy to understand with the example of two heterogeneities which we give in the preceding section. In fact, according to (1.43) a phase difference of two signals, accepted at one point from two heterogeneities, located in the center and on the periphery of the space of re-emission, at frequency  $f_1$  will be

$$\Delta\phi_1 \approx \frac{\pi}{c} \frac{L^2}{d}, \quad (1.56)$$

and at frequency  $f_2$  -

$$\Delta\phi_2 \approx \frac{\pi}{c} \frac{L^2}{d}, \quad (1.57)$$

where  $c$  - the speed of light.

A phase difference is different at the different frequencies; therefore the maximums and the minimums of signal amplitude at the different frequencies do not coincide. With an increase  $\Delta f$  the correlation of signals decreases. With  $\Delta\phi_1 - \Delta\phi_2 = \pi$ , if on frequency  $f_1$  is observed the maximum of signal, then at frequency  $f_2$  there will be



the minimum. This will be according to (1.56), (1.57) when

$$\Delta f = c \frac{d}{L^2} \quad (1.58)$$

This value can serve as the measure for the correlation of signals at the different frequencies and is proportional to a radius of frequency correlation  $\Delta f_0$ :

$$\Delta f_0 \sim c \frac{d}{L^2} = \frac{c}{d_{r0} L} \quad (1.59)$$

In actuality picture will be, of course, more complicated, since in reality a quantity of heterogeneities is great, yes even are spread they they can be not only on the horizontal, but also on the vertical line. With the vertical separation

$$\Delta f_0 \sim c \frac{d}{L^2} \sim \frac{1}{d_{r0}} \quad (1.60)$$

so that dependence  $\Delta f_0$  on the distance differs somewhat from the first case. However, general laws are visible sufficiently well from this simple example. A radius of frequency correlation is inversely proportional to the square of the linear dimension of the space of re-emission and does not depend on wavelength. Therefore with an increase in the antenna directivity a radius of frequency correlation must sufficiently sharply rise. Dependence  $\Delta f_0$  on the distance is sufficiently complicated, since in (1.59) and (1.60) both the numerator and the denominator they change with change  $d$ . Since dependence of  $L$  on  $d$  is unclear, then is not defined dependence  $\Delta f_0$ .

on the distance.

Page 49.

As we already spoke, many experiments indicate that the angular dimensions of the space of re-emission do not depend on distance. In that case a radius of frequency correlation will be inversely proportional to distance.

Now let us pause at the experimental data about the frequency correlation of signals. According to these data [1.1] a radius of frequency correlation with the weakly directed antennas comprises at the distances of 200-400 km of approximately 0.8-1 MHz. With the antennas with the angle of directivity of  $1^\circ$  at the same distances it is equal to 1.5-2 MHz. At large distances there are only single measurements, which give the drop  $\Delta f_0$  with distance [1.1]. Judging according to the experimental data, a radius of frequency correlation, apparently, does not depend on wavelength. Utilizing experimental data about the value of a radius of correlation at the distances of approximately 300 km, it is possible to construct dependence  $\Delta f_0$  on the distance, taking into account that  $\Delta f_0$  it is inversely proportional to distance. Fig. 1.22 gives similar dependence for different angles of antenna directivity (for the case of identical antennas  $\alpha_{80} = \alpha_{r0}$ ). Water of frequency correlation function

it is possible to judge based on the example of the function, obtained on the route 303 km at the frequency of approximately 1000 MHz. This function is represented in Fig. 1.23. The form of correlation function is close to the Gaussian

$$R(\Delta f) = e^{-\frac{(\Delta f)^2}{\Delta f_0^2}} \quad (1.61)$$

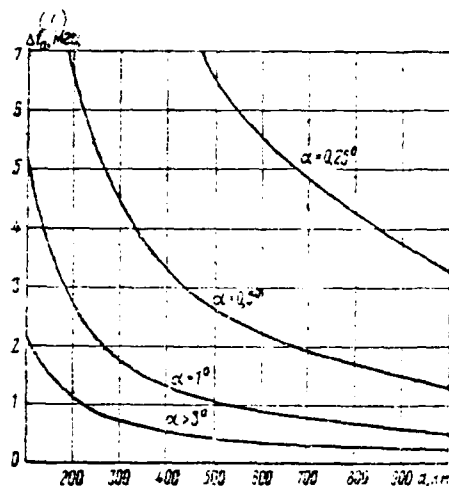


Fig. 1.22. Dependence of a radius of frequency correlation  $\Delta f_0$  for the system of identical antennas on the geographic distance  $d$ . Angle  $\alpha$  - the width of the antenna radiation pattern.

Key: (1). MHz.

Page 50.

Frequently in practice are applied another characteristic of the variability of the frequency characteristics of signal, so-called nonuniformity in band  $B$ . This value is the ratio of the highest value of signal amplitude to the lowest in the band  $\Delta f$ . In the case of the tropospheric propagation  $B$  it is random variable. Fig. 1.24 gives the integral distributions of value  $B_{0.99}$  for the different values  $\Delta f$ ,

received on the route with a length of 303 km at the frequency of approximately 1000 MHz.

Correlation of signals with the diversity on the angle.

With the pencil-beam antennas sometimes is applied the diverse in space reception, which is realized not with the aid of the diversity in the space of antennas themselves, but with the aid of the direction of each of the antennas into the different regions of the space of re-emission. This diversity in practice is realized in one antenna with parabolic reflector and several irradiators. Each irradiator gives its radiation pattern, shifted in the space relative to the radiation patterns of adjacent irradiators.

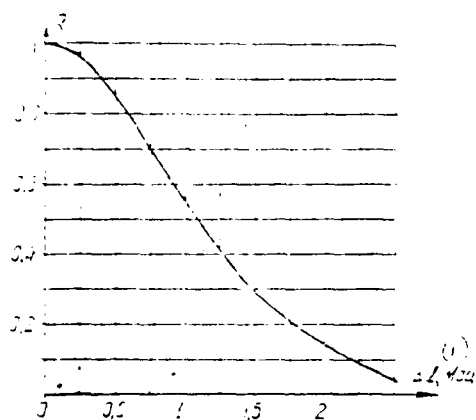


Fig. 1.23

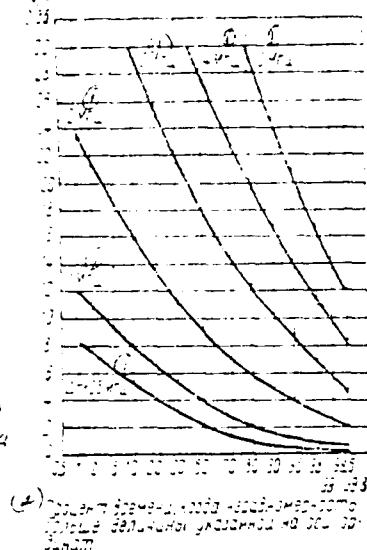


Fig. 1.24

Fig. 1.23. Frequency correlation function, obtained experimentally on the route 303 km,  $\lambda=30$  cm.

Key: (1). MHz.

Fig. 1.24. Nonuniformity of frequency characteristic for route  $d=330$  km and  $\lambda=30$  cm.

Key: (1). MHz. (2). Percentage of time when nonuniformity is more than value, indicated on axis of ordinates.

In the essence, angular separation in the nature of the phenomenon in no way differs from usual spatial separation. The shift of the radiation patterns, formed by adjacent irradiators, leads to the fact that the "centers of gravity" of the spaces of re-emission for each of the irradiators will be shifted relative to each other. This will lead to the fact that the difference of the phases of components, entering the received signal, will be different and, therefore, the correlation of signals for different irradiators will be disrupted. In this case, the greater the angular separation, the less the coefficient of correlation of signals. In [1.18] for the very pencil-beam antennas there was obtained following expression for the coefficient of angular correlation:

$$R(\Delta\beta) = \exp\left(-\frac{1.38\Delta\beta^2}{\alpha_{90}^2}\right), \quad (1.62)$$

where  $\Delta\beta$  - an angle of the separation between the diagrams of antenna directivity,  $\alpha_{90}$  - angle of antenna directivity in the vertical plane. Thus, a radius of angular correlation  $\Delta\beta_0$  according to (1.56) will be:

$$\Delta\beta_0 = 0.85\alpha_{90}. \quad (1.63)$$

When the dimensions of the space of re-emission are determined not only by antennas, but also by the properties of heterogeneities, a radius of correlation  $\Delta\beta_0$  will depend on the dimensions of the space of re-emission. The experimental data about the correlation with the angular diversity are given in [1.1]. Let us note that the

angular separation is effective only when divergence from the main direction does not cause the noticeable weakening of signal. With the angular separation to value  $\Delta\beta$  on the vertical line for second channel will be observed attenuation of signal. As in the presence of the shielding obstruction, this weakening is connected with an increase in angle  $\varphi$  (see Fig. 1.19). In this case, naturally, the weakening is expressed by the same formula, as in the case of the shielding obstruction

$$b = \frac{\varphi^2}{(\varphi + \Delta\beta)^2}. \quad (1.64)$$

Thus, diversity on the angle is effective with  $\varphi \gg \Delta\beta$ , i.e., either at large distances or with the very pencil-beam antennas.

Until now, the discussion dealt with the correlation of the instantaneous values of signal with the angular separation, i.e., about the correlation of rapid fadings. But with the considerable diversity on the angle when each irradiator cuts out in space its isolated space of re-emission, will be destroyed not only the correlation of the instantaneous values of signals (rapid fading), but also the correlation of five minute mean values (slow fading). In the examination of slow fadings we already said that the signals, which attached from different isolated parts of the space of re-emission, can be considered independent variables on the slow fadings.



Page 52.

Specifically, under this assumption the law of the distribution of slow fadings takes the logarithmic form and only under this assumption is observed that dependence of the depth of fadings from the antenna directivity which is justified experimentally. As a result of applying the diverse in angle reception, the dispersion of slow fadings decreases according to (1.23) or (1.24). Value  $n$  in this case will be equal to a number of isolated spaces of the re-emissions which are formed with the angular diversity. Angular diversity can be realized not only at receiving end, but also with the aid of the transmitting antenna with many irradiators. In this communicating system the losses of amplification decrease and become equal to the losses of antenna gain, which corresponds the space, equal to the sum of all spaces of re-emission, that are formed in the angular diversity. The losses of amplification decrease in  $n$  of times in comparison with the single reception, of course, when in all cases the space of re-emission is wholly determined by antennas.

On the route with a length of 303 km at the frequency of 1000 MHz were conducted the investigations of the effectiveness of diversity on the angle for dealing with the slow fadings. In the

experiments were utilized two receiving antennas, which had the angle of directivity of  $0.7^\circ$ . These antennas were shifted on the vertical line relative to each other on  $0.7^\circ$  so that the radiation patterns of these antennas intersected at the level of half power. From both receiving antennas was conducted simultaneously the prolonged recording of signal (approximately one month). The statistical analysis of recording showed that the correlation coefficient for the five minute mean values of signal on one and by another antennas comprised within entire period of observations 0.4-0.5. Thus, slow signal fading with the diversity to the angle, equal to the width of radiation pattern, are virtually not correlated. Consequently, conclusions about the effectiveness of angular diversity in the fight with the slow fadings and the losses of amplification are justified experimentally.

#### §1.9. Dependence of signal level on the form of polarization.

Experimental works [1.1; 1.2] showed that the mean signal level virtually does not depend on the form of polarization. Furthermore, the special investigations, which were being carried out at the frequency of approximately 1000 MHz at the distances 303 and 448 km, showed that rapid fadings with reception are simultaneously on the horizontal and vertical polarizations almost completely correlated (transmission was conducted during polarization of  $45^\circ$ ). The same

conclusion follows from the theoretical study of this problem. The measurements of the depolarization of signal on the route 303 km showed that the signal from the antenna, polarization which was perpendicular to the polarization of the transmitting antenna, on 18-25 dB is lower than from the normal antenna.

Page 53.

The value of depolarization continuously is changed in the time. The median value of polarizational weakening within the prolonged period of the measurements for the antennas by directivity of 1° was 20 dB. Depolarization depended on the directivity both transmitting and receiving of antennas. Polarizational weakening increased with an increase in their directivity.

§1.10. Dependence of the average signal level on the climatic conditions.

The mean signal level, as already mentioned, sufficiently strongly depends on the season or year. It is logical that the same reasons cause the dependence of mean level on the climatic conditions. The the climate warm and the more humid, the greater signal level during the remote tropospheric propagation, since with an increase in the temperature and humidity increases the intensity

of the heterogeneities of the dielectric permittivity of air, i.e., value  $\overline{\Delta\epsilon^2}$ . In many experiments [1.1] it was noted, that the daily mean value of signal level was correlated with the value of the dielectric permeability of air or the earth's surface, which is explained by the overall dependence both of value  $\overline{\Delta\epsilon^2}$  at the height of the space of re-emission and value  $\epsilon_0$  on the earth's surface from temperature and air humidity. This dependence is developed only with the very large periods of averaging, compared with the season of year, and is in many respects the reflection of that fact that both value  $\overline{\Delta\epsilon^2}$  and  $V$  have explicit seasonal behavior. Both values have a maximum in the summer months and the minimum in winter period. On the base of correlation of values  $V$  and  $\epsilon_0$  frequently are conducted the predictions of the mean signal levels for different geographical areas. Accordingly [1.1] the coefficient of conformity  $M$  between value  $V_{\text{exp-est}}(\text{dB})$  and value  $N = (V\overline{\epsilon_0} - 1) 10^6$  changes from the distance according to the law, represented in Fig. 1.25.

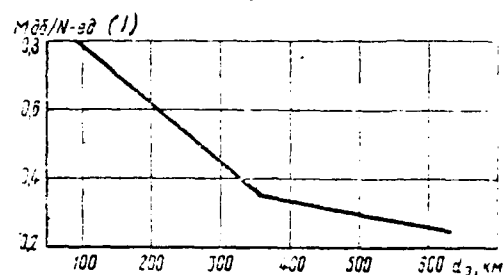


Fig. 1.25. Dependence of the coefficient of conformity  $M$  on the distance.

(1). dB/N-th.

Page 54.

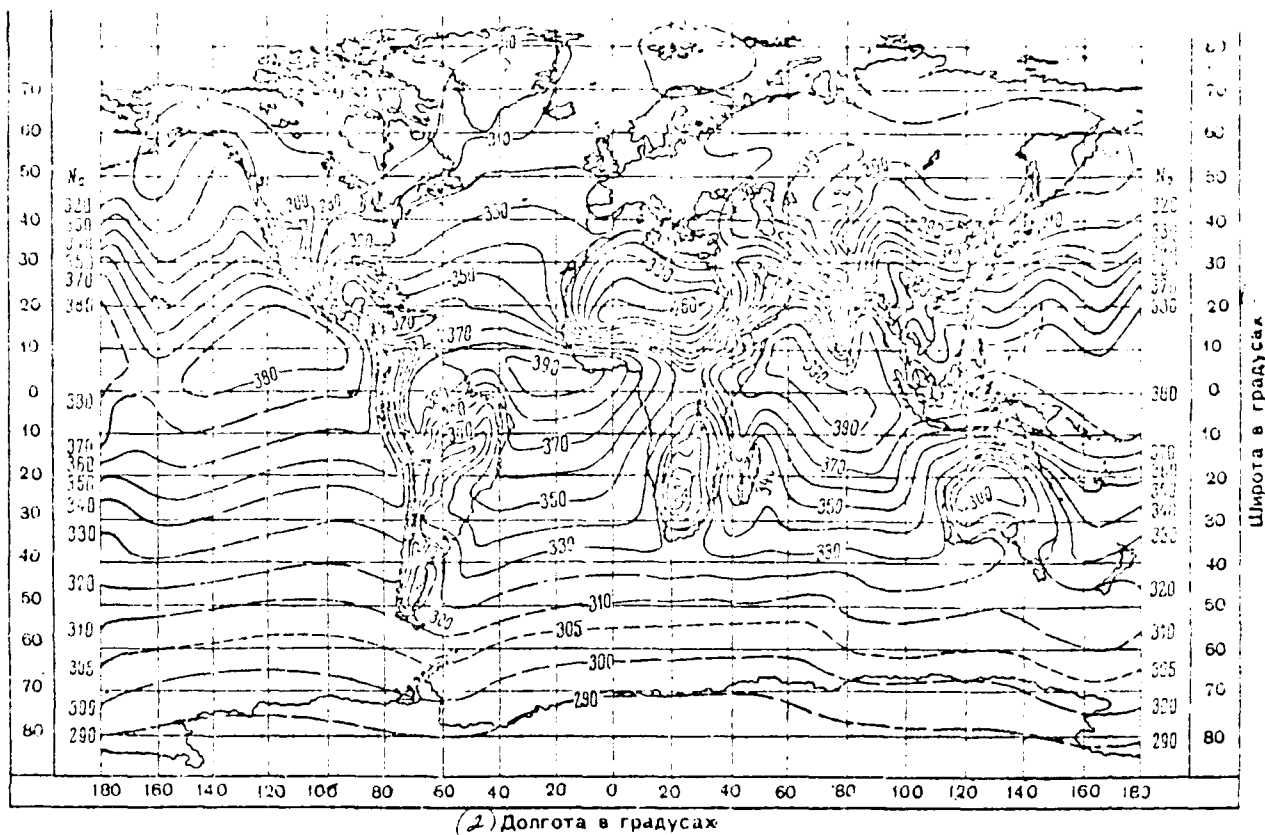


Fig. 1.26. Chart of value  $N_0 = (\sqrt{\epsilon_0} - 1) 10^6$  on earth's surface for worst month in year (when  $N_0$  is minimal).

Key: (1). Latitude in the degrees. (2). Longitude in degrees.

Page 55.

The coefficient of conformity  $M$  is the value of the change of the strength of field in the decibels, which arrives on  $1N$  - a unit change in the refractive index of air where  $N$  - a refractive index of air on the earth's surface. Thus, if are known the mean signal levels for one geographical area  $V_{cp, n_1}$ , then it is possible to find the same levels for other areas, if is known difference  $N_2 - N_1$ , where  $N_1$  - a surface value of refractive index in the first area, and  $N_2$  - surface value of refractive index in the area where it is necessary to determine the mean level of the signal

$$V_{cp, n_2}(\delta\delta) = V_{cp, n_1}(\delta\delta) + M(N_2 - N_1). \quad (1.65)$$

Values  $N$  for different geographical areas can be determined on the charts which are given in the documents of MKKR [International Radio Consultative Committee] [1.19]. Fig. 1.26 gives such charts of the average monthly value  $N_0$  in that month when this value is minimum. The coefficient of conformity in (1.65) is determined on the graph in Fig. 1.25.

In conclusion let us note that used this method should be with large care. The fact is that for many geographical areas it is not justified. In particular, under conditions of hot climate it proves to be unsuitable. Then it is possible to speak about winter period for many geographical areas. In winter the correlation between  $N_0$  and signal level proves to be very weak, and forecasting levels according to this method can give considerable errors. As it was already noted,

for the worst months of year, what are winter months, signal levels, obtained in different geographical areas with the moderate and subarctic climate, proved to be sufficiently close in the value with equidistances and the wavelengths (see Fig. 1.5). Therefore for the worst month of year<sup>1</sup> it is better to use directly values  $V_{cp-nz}$  from of the curves of Fig. 1.5a and b.

FOOTNOTE <sup>1</sup>. According to the norms of MKKR the stability analysis of the work of tropospheric line is conducted for the conditions of the worst month. ENDFOOTNOTE.

Page 56.

## REFERENCES

- 1.1. «Дальнее тропосферное распространение ультракоротких радиоволн». Под редакцией Б. А. Введенского, М. А. Колосова, А. И. Калинина, Я. С. Шергина. Изд. «Сов. радио», Москва, 1965.
- 1.2. Калинин А. И., Троицкий В. Н., Шур А. А. Статистические характеристики сигнала при дальнем тропосферном распространении унк. «Электросвязь» № 7, 1964, стр. 1—12.
- 1.3. A. B. Crawford, D. C. Hogg, W. H. Kummer. «Studies in tropospheric propagation beyond the Horizon». The Bell Syst. techn. Journ., v. 38, No. 7, sept. 1959, pp. 1067—1173.
- 1.4. Чихолом, Портман, Беттанкур, Хоп. «Исследование ультракоротких волн, рассеяния и микроволновых свойств при тропосферном распространении ультракоротких волн за пределами горизонта».
- Сб. «Вопросы дальней связи на ультракоротких волнах», под редакцией Сифорова В. И. М., Изд. «Сов. радио», 1957, стр. 215—266.
- 2.1. W. J. Inkster, W. J. Jinkster, A. L. Durkee. «Results of Propagation Measurements at 265 MC and 4090 MC on beyond-horizon paths». Proc. IRE, 42, 1955, pp. 1075—1076.
- 2.2. T. Fukami, S. Ueda, F. Ikegami, H. Fujimura. «Characteristics of tropospheric propagation over sea». Rev. Electr. commun. Japon., v. 5, No. 5—6, 1961, pp. 255—265.
- 2.3. A. Zuber, B. C. Foot, J. B. L. Lucas, W. J. Jinkster. «Propagation measurements at 265 MC over 173-mile path». Proc. IEE, 1958, pt. B, suppl. January, pp. 127—128.
- 2.4. G. S. Smith, J. H. Morrow, W. E. Nichols, B. E. Roche, J. E. Smith. «Properties of 400 MC S. long-distance tropospheric circuits». IRE, 1962, Dec. v. 50, No. 12, p. 2164.
- 2.5. H. G. G. «Ergebnisse und Bewertung von Messungen der troposphärischen Ausbreitung von Radiowellen auf mehreren verschiedenartigen Strecken in Europa und Südostasien». NTZ Heft 12 Dezember 1960, 368—370.
- 2.6. H. G. G. «Results of propagation measurements at 600 MC and 2120 MC over long-range beyond-horizon paths». Radiophys. Lab., No. 70, 311—329, 1963.
- 2.7. Д. Р. Рубин. «Электроника». Изд. 2, § 42а. М., ГИИТЛ, 1953, 56—63.
- 2.8. T. Hara, M. Inoue, R. Tschizawa, J. «Antenna-beam correlation and signal intensity correlation in angle-diversity reception in tropospheric communication». Journ. Radio Res. Lab., v. 9, No. 41, Feb.—Mar. 1962, 21—40.
- 3.1. J. B. B. «Etude expérimentale de la baisse de gain angulaire dans les ondes transhorizon». Annales des Telecomm. 1964, sept.—oct., 1964, pp. 121—129.
- 4.1. Шур А. А. «Расчет потерь сигнала при дальнем тропосферном распространении». «Электросвязь» № 1, 1963.
- 5.1. A. M. K. «Transmission of VHF and UHF over-land propagation beyond the horizon». J. Rad. Res. Lab., No. 53, 197—222.
- 6.1. И. И. «Экспериментальное исследование дальнего тропосферного распространения радиоволн». «Электросвязь» № 1, 1963.
- 7.1. Н. М. «Исследование особенностей сигнала, возникающего при дальнем тропосферном распространении унк». «Электросвязь» № 1, 1963.
- 8.1. «Справочник инженера МДР. Том II. Распространение радиоволн». стр. 227—231, «Связь» 1964.



Page 57.

## Chapter 2.

Diverse reception on the lines of remote tropospheric propagation of VHF (DTR).

### §2.1. Introduction.

In Chapter 1 it is shown that the signal in the place of reception with DTR is subjected to the rapid and slow fadings, which are determining multiplicative interference<sup>1</sup>.

FOOTNOTE <sup>1</sup>. Multiplicative interference is here assumed to be that operating immediately on entire spectrum of communication. The fluctuations of one spectral component of signal relative to others are considered insignificant. ENDFOOTNOTE.

The fundamental method of fight with the rapid fadings, caused by the multiple-pronged structure of the signal in the place of reception, is the diverse reception. The principle of the diverse reception lies in the fact that the signal at the output of receiver is formed by the combination of several input signals, which carry one and the

same information, but differently affected by multiplicative interference. This combined output signal will be considerably less affected by multiplicative interference. The informational evaluation carried out in [2.1], shows that the capacity of multibeam channel is less than the carrying capacity of single-ray channel (at the identical mean power); however, with the diverse reception with an increase in the multiplicity of diversity the capacity of multiple-pronged channel approaches the capacity of single-ray channel [2.2]. This confirms the possibility of the in practice complete elimination of rapid multiplicative interference by the use of the diverse reception.

Page 58.

§2.2. Statistical characteristics of the signal in the place of reception.

Let the transmitter emit the sinusoidal unmodulated oscillation with the frequency  $\omega_0$

$$u_{n\pi} = U_{n\pi} \cos \omega_0 t. \quad (2.1)$$

then the signal in the place of reception as a result of multiple-pronged propagation is equal to

$$V_{np} = \sum_{i=0}^n U_{np,i} \cos [\omega_0 (t - \tau_i)]. \quad (2.2)$$

Here  $U_{np,i}$  - amplitude of the  $i$ -th component of signal,  $\tau_i$  - the time lag of this component,  $n$  - total number of heterogeneities, which diffuse signal in the direction of reception.

Index  $i=0$  relates to amplitude and time lag of regular component, determined by the presence of diffraction field. Total signal can be recorded in the form

$$V_{np} = U_{np} \cos(\omega_0 t + \theta), \quad (2.3)$$

where the amplitude

$$U_{np} = \sqrt{X^2 + Y^2} \quad (2.4)$$

and the phase

$$\theta = \arctg \frac{Y}{X} \quad (2.5)$$

are determined through the projections of components on the orthogonal axes.

$$\left. \begin{aligned} X &= \sum_{i=0}^n U_{np,i} \cos \omega_0 \tau_i \\ Y &= \sum_{i=0}^n U_{np,i} \sin \omega_0 \tau_i \end{aligned} \right\} \quad (2.6)$$

Since scattering capacity (intensity) and position of the diffusers, located in the space of scattering, is changed randomly, amplitude  $U_{np}$  and phase  $\theta$  of the signal accepted are random functions which are slowly changed in the time. Slowness means that rate of change  $U_{np}$  and  $\theta$  is considerably lower than rate of change the slowest element of communication, i.e., that for the time, necessary for transmission of the longest element of the

communication (or for several periods of the quite low-frequency component of the spectrum of communication) of change  $\omega$  and  $\theta$  are negligible. According to the central limit theorem of Lyapunov the distribution of the sum of random components of the projections of amplitudes ( $i=1, 2, 3, \dots, n$ ) in formula (2.6) with sufficiently large  $n$  will strive how conveniently closely to the normal law of probability distribution.

Page 59.

In this case, since phase  $\theta$  evenly distributed in the limits  $0-2\pi$ , i.e.,

$$w(\theta) = \begin{cases} 1/2\pi & \text{при } 0 \leq \theta \leq 2\pi \\ 0 & \text{вне этого интервала.} \end{cases} \quad (2.7)$$

Key: (1). with. (2). out of this interval.

then signal amplitude will have the generalized Rayleigh distribution:

$$w(u) = \frac{u}{\sigma^2} e^{-\frac{u^2 + u_0^2}{2\sigma^2}} I_0\left(\frac{uu_0}{\sigma^2}\right). \quad (2.8)$$

In formula (2.8)

$$I_0(z) = \frac{1}{2\pi} \int_0^{2\pi} e^{z \sin \varphi} d\varphi \quad (2.9)$$

- the modified Bessel function,  $2\sigma^2$  is proportional to the power of

random (number of that scattered) signal,  $U_0^2$  is proportional to the power of regular (diffractive) the components of signal.

FOOTNOTE 1. Fluctuations in the signal, which are subordinated to other laws of distribution, here are not examined, since, as a rule, on the lines of DTR is correct the Rayleigh distribution. However, fundamental conclusions are valid also for them. Should be noted the very ordered theory of rapid fading with an  $\kappa$ -distribution by Nakagami, presented in [2.3]. ENDFOOTNOTE.

In the absence of regular components  $U_0=0$  law (2.8) is converted into the usual Rayleigh law

$$w(u) = \frac{u}{\sigma^2} e^{-\frac{u^2}{2\sigma^2}}. \quad (2.10)$$

In this case integral distribution, i.e., probability that the amplitude of received signal lies below certain threshold level  $U_{\text{пор}}$ , is equal

$$W(0 \leq u \leq U_{\text{пор}}) = \int_0^{U_{\text{пор}}} w(u) du = 1 - e^{-\frac{U_{\text{пор}}^2}{2\sigma^2}}. \quad (2.11)$$

Subsequently by us will be necessary the parameters of random variable, adhering to the Rayleigh law of the distribution:

$$\left. \begin{aligned} \text{— среднее значение } \bar{u} &= \sigma \sqrt{\pi/2}, \\ \text{— дисперсия } D\{u\} &= \frac{4-\pi}{2} \sigma^2, \\ \text{— медиана } U_{\text{мед}} &= \sqrt{\ln 2} \sigma \end{aligned} \right\}. \quad (2.12)$$

Key: (1). Mean value. (2). dispersion. (3). median.

FOOTNOTE 2. The median of the law of distribution is the value of signal, exceeded during 500/o of time of observation. It they use especially frequently, since it easily is found from experiment.

ENDFOOTNOTE.

Page 59.

Taking into account median value  $U_{med}$  distribution (2.11) we can write in the form

$$P\{0 \leq u \leq U_{med}\} = 1 - e^{-0.69 \left( \frac{U_{med}}{U_{med}} \right)^2} \quad (2.13)$$

In the process of experimental investigations the distribution of probability of signal amplitude is determined on the samples of the recording of signal, analogous those given in Fig. 1.7a and b. The results of treating such recordings usually are represented in the form of histograms (Fig. 2.1) and integral curves, represented in Fig. 1.8.

During the remote tropospheric propagation the VHF distance between the adjacent stations usually exceeds 150-200 km and the law of the probability distribution of rapid fadings is very close to the Rayleigh. With the decrease of distance in the received signal

appears diffraction component and distribution must be approximated by law (2.8). The duration of realization (recording, signal), which should be processed for obtaining the law of distribution, must be  $T_p = 4-7$  min, since during processing of the recording of the signal of larger duration will begin to be manifested the slow fluctuations of the median of signal, determined by damping change in the section of the propagation (see §1.4).

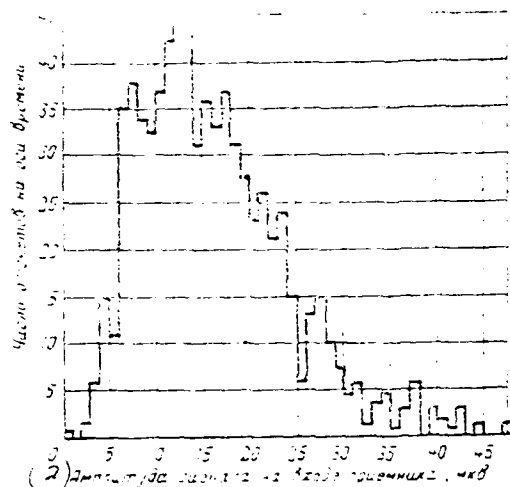


Fig. 2.1. Distribution of signal (histogram), received experimentally.

Key: (1). Number of readings on the time axis. (2). Signal amplitude at input of receiver,  $\mu V$ .

Page 61.

With the decrease of the time of observation can remain undetected the laws governing rapid fluctuations of the amplitude of received signal<sup>1</sup>.

FOOTNOTE 1. This will occur because in the interval of smaller length



will not be satisfied the condition of the ergodicity of the random process, which describes signal at the input of receiver.

ENDFOOTNOTE.

The methods of obtaining several spears of the fluctuating radio signals, i.e., the methods of diversity, are examined in §1.7.

Let us recall that on the lines of DTR is found a use, in the first place, the spatially distributed reception with which in the place of reception of the signal (with the  $N$ -fold reception), are accepted upon  $N$  of the antennas, spread usually perpendicular to the route; in the second place, the frequency-dispersed reception, in which is utilized one antenna and  $N$  of receivers and finally thirdly, diversity on the angle of arrival of the beam, with which is used one antenna the radiation pattern of which is done by multilobed, and  $N$  of receivers. The effectiveness of the diverse reception significantly affects the dependence of multiplicative interferences in the diverse channels. The effectiveness of the diverse reception is greater, the less are dependent these interferences. It should be noted that if for the first two methods of the diversity of signals obtaining the independent fluctuations of the envelopes of HF signal is relatively simple, then for the third method - angular diversity - it is considerably more complicated. The fact is that with an increase in the angle of diversity begins to fall the power of the

arriving signal (see Chapter 1). This means that during the design of systems with the angular diversity is necessary a reasonable compromise between a drop in power of signals with an increase in the angle of diversity and an increase in the correlation of signals with the decrease of this angle (see [2.4]). As the measure of the dependence of the Rayleigh fluctuations of the enveloping two diverse signals can serve the coefficient of correlation<sup>2</sup>.

FOOTNOTE 2. For non-Rayleigh distribution of fluctuations the correlation coefficient is not the adequate measure of their dependence. ENDFOOTNOTE.

Let the transmitter emit sinusoidal oscillation (2.1). Then with the diverse doubled reception in the place of reception are two signals:

$$\begin{aligned} V_1 &= U_{np1} \cos(\omega_0 t + \Theta_1), \\ V_2 &= U_{np2} \cos(\omega_0 t + \Theta_2). \end{aligned} \quad (2.14)$$

The two-dimensional probability density of the envelopes

$$p(U_{np1}, U_{np2}) = \frac{U_{np1} U_{np2}}{\sigma^4 (1-r^2)} e^{-\frac{U_{np1}^2 + U_{np2}^2}{2\sigma^2 (1-r^2)}} I_0 \left[ \frac{U_{np1} U_{np2}}{\sigma^2 (1-r^2)} \right], \quad (2.15)$$

where value  $r^2$  is almost accurately equal to the correlation coefficient between envelopes  $R_{U_{np1}, U_{np2}}$  [see formula (3.19)]:

$$r^2 \approx R_{U_{np1}, U_{np2}} = \frac{\overline{U_{np1} U_{np2}}}{\sqrt{\overline{U_{np1}^2} \overline{U_{np2}^2}}}, \quad (2.16)$$

$I_0$  - the modified Bessel function.

Page 62.

In works [2.5] and [2.6] it is shown that the Rayleigh fluctuations can be considered independent variable, if  $R_{u_{np1} u_{np2}} \leq 1/e = 0.37$ . Is the distance (in the space, in the frequency or on the angle of arrival of ray), to which it is necessary to spread signals for obtaining  $R_{u_{np1} u_{np2}} = 1/e = 0.37$ , is called a radius or an interval of correlation. Moreover, from these works it follows that the drop in the gain from the use of the diverse reception does not exceed 1.5 dB, if the coefficient of correlation of envelopes is equal to  $R_{u_{np1} u_{np2}} = 0.6$ . This means that in the calculations of the systems of the diverse reception it is possible to approximately consider fluctuations as those not correlated, if  $R_{u_{np1} u_{np2}} \leq 0.6$ . Further increase in the correlation coefficient leads to the sharp drop in the gain and in the limit with  $R=1$  the gain disappears (for the automatic selection). With the  $M$ -fold diverse reception the correlation is usually investigated in pairs, since the construction and investigation of the  $M$ -dimensional distribution function are combined with the great difficulties.

§2.3. Methods of the combination of the diverse signals.

After one of the methods presented above of diversity is obtained  $N$  of the spears of radio signal, affected by the independent multiplicative interferences, by primary task becomes the economical utilization of these signals, i.e., the use of such combination during which the losses of the transmitted information will be minimum.

In the communicating systems found use the methods of the linear combination of the diverse signals. During the use is calm methods the signal at the output of the device of  $N$ -fold addition  $S_z(t)$  it is determined by the equality

$$S_z(t) = \sum_{k=1}^N a_k S_k(t), \quad (2.17)$$

where  $S_k(t)$  - sum of useful signal in the  $k$ -th branch of diversity and additive noise, which operates at the input of the receiver of the same branch:

$$S_k(t) = V_k(t) + \xi_k(t), \quad (2.18)$$

For the case of the sinusoidal unmodulated signal in the transmission value  $V_k(t)$  is determined by formula (2.3). Natural is assumption about the fact that the median values of signals in the branches of diversity are equal to each other. Are also identical noisiness all  $N$  of receivers.

Value  $\alpha_k$  is the "weighing" coefficient which in general can depend on the value of signal or noise in the k-th or any other branch of diversity<sup>1</sup>.

FOOTNOTE <sup>1</sup>. In radar direction finding found use the methods of the nonlinear combination of the diverse signals (for example, signal at the output it was equal to the product of signals in the branches of diversity). ENDFOOTNOTE.

The methods of linear combination can be divided into the methods of switching and the methods of addition. During the switching at each given moment only one of coefficients  $\alpha_k$  is different from zero. In this case is possible, in the first place, the servo diversity when the signals in the place of reception test consecutively, until is located the signal, which exceeds the assigned threshold. This signal is supplied to the output of system until its level falls below threshold. As soon as this will occur, the system of the next diversity again will begin to search for the signal whose level is higher than the threshold value, etc. In the second place, is possible the system of optimum automatic selection, in which all N of signals are investigated simultaneously and it is selected for the connection to the output that from them whose level

is maximum. The statistical characteristics of the automatic selection of peak signal are better than with the servo diversity. Subsequently will be examined the automatic selection of peak signal.

The use of methods of addition provides for the simultaneous use of several spears of signals, obtained in the branches of diversity. In this case all coefficients  $a_k$  of formula (2.17) are different from zero. The greatest interest represent two methods additions. In the first all copies of signal received add up to the identical weight independent of their value. In this case  $a_1 = a_2 = \dots = a_N$ . This method is named linear addition. It will be shown below that it is most promising on the lines of LIS.

With the second method of addition the weighting factors are automatically regulated in such a way that at the output of add system would be provided the maximum value of signal-to-noise ratio. This method subsequently is named optimum addition. Find a use also the mixed methods. In one of them [2.7] the signals, accepted by two diverse receivers, add up linearly until their relation exceeds  $\sqrt{2}-1=0.41$ . When the ratio of signals in the branches of diversity falls below 0.41, weaker signal is disconnected also to the output of add system begins to enter one, more strong signal, system from the mode of linear addition passes into the mode of automatic selection. This method in its characteristics is most close to the optimum

addition (for more detail see §2.4).

The combination of signals by the diverse reception can be conducted either to the detector (in the linear part of receiver), or after detector.

Page 64.

In depending on this sharply they differ both methods and used for the combination equipment. With the combination to the detector is correct the assumption about the complete independence of the components of noise  $n(t)$  and signal  $s(t)$ . With the combination after the detector this assumption is correct, if the process of demodulation is linear as, for example, with AM. For FM this it is approximately correct only with the work of higher than its threshold. In the systems from FM, which found great use on the radio relay lines of tropospheric scattering, signal level at the output of the demodulator (with the work it is higher than the threshold) virtually does not depend on the power of signal at the input of receiver. A change in the power of signal at the input leads only to inversely scaling in the power of noises at the output of the FM discriminator. During the linear addition to the detector one should consider that the phases of the signals, which attached on different branches of dispersion  $\phi_1$  and  $\phi_2$  in formula (2.14)], are in general

different. Therefore for obtaining the maximum gain from the addition signals must be before the addition phased. For this are applied the special devices of the self-alignment of the phase (for details see Chapter 5). during the addition of post detection signals after the coherence of the added up signals is obtained automatically. For changing over type systems the place of combination role does not play. One should only have in mind that during the switching before the detector the automatic selection must be realized on the maximum signal level, and when selecting after detector (FM) on the minimum of noises.

#### §2.4. Statistics of signals with the diverse reception.

The use of the diverse reception improves the characteristics of communicating system. This improvement usually is evaluated one of the following criteria:

- 1) by an increase in the ratio of the power of signal to the power of noise at the output of the device of the addition of the diverse signals in comparison with this relation in the branches of the diversity;

- 2) by the decrease of the relative duration of the breaks of communication, caused by the fading;



3) by an increase in the authenticity of the transmission of binary information.

The first criterion determines an improvement in the most important parameter of communicating system at the transmission of analog signals - noise in the channel. In the subsequent calculations precisely this criterion is used as the basis of the comparison of different methods of combination. The second criterion determines the reliability of communication - percentage of time, during which the signal will be above the assigned threshold level. For the comparison of systems on this criterion it suffices to know the laws of the distribution of probabilities with the combination of the diverse signals. Finally, the third criterion is very important during the transmission of the discrete information (in more detail about this see in Chapter 6).

Page 65.

Let by the multiple-pronged tropospheric channel be transmitted by the FM signal

$$u_{\pi k} = U_{\pi k} \cos[\omega_0 t + \psi(t)],$$

where  $\psi(t)$  represents the modulating signal. Then in the k-th branch

of the diverse reception signal will be

$$S_k(t) = U_{npk}(t) \cos[\omega_0 t - \psi(t) + \theta_k(t)] + \xi_k(t) \quad (2.19)$$

also, with the  $N$ -fold linear combination.

$$S_z = \sum_{k=1}^N a_k S_k = \sum_{k=1}^N a_k U_{npk}(t) \cos[\omega_0 t - \psi(t) + \theta_k(t)] + \sum_{k=1}^N a_k \xi_k(t). \quad (2.20)$$

The first term in (2.19) and (2.20) determines useful signal, and by the second - additive interference before and after the device of addition. In accordance with the criterion of an improvement in the quality of communication accepted it is further necessary to make a comparison of the ratio of the averaged power of signal to the averaged power of noise in the branches of the diversity

$$r_k(t) = \frac{[U_{npk}(t) \cos[\omega_0 t - \psi(t) + \theta_k(t)]]^2}{\xi_k^2(t)} \quad (2.21)$$

and this ratio at the output of the device of addition

$$r_z(t) = \frac{\left[ \sum_{k=1}^N a_k U_{npk}(t) \cos[\omega_0 t - \psi(t) + \theta_k(t)] \right]^2}{\left[ \sum_{k=1}^N a_k \xi_k(t) \right]^2}. \quad (2.22)$$

Before passing to the calculation, let us note that the reaction rate, connected with HF modulated oscillation, at least, by an order higher than speed of the processes, connected with the fluctuations of signal, caused by multi-beam character. Actually, the highest frequency of fading does not exceed 5-10 Hz, whereas during the transmission of telephony lowest modulating frequency  $F_m = 300$  Hz,

but during the transmission of television  $F_u = 50$  Hz. Therefore during the investigation of fluctuations it is expedient to average the processes being investigated, moreover the interval of averaging  $T_u$  to select so that the envelope of fading  $U_{npk}(t)$  within time  $T_u$  would remain constant and at the same time the duration of the longest element of communication was much less  $T_u$ . For DTR value  $T_u = 0.1 \div 0.3$  s.

Page 66.

Root-mean-square (for time  $T_d$ ) the value of signal amplitude in the  $k$  branch of diversity will be equally

$$\frac{1}{T_d} \int_{-\frac{T_d}{2}}^{\frac{T_d}{2}} U_{spk}^2(t) \cos^2\{\omega_0 t - \varphi(t) - \Theta_k(t)\} dt = \frac{U_{spk}^2(t)}{2}, \quad (2.23)$$

since for time  $T_d$   $U_{spk}(t) = \text{const}$ .

The rms value of noise in the same branch

$$\frac{1}{T_d} \int_{-\frac{T_d}{2}}^{\frac{T_d}{2}} \xi_k^2(t) dt = \overline{\xi_k^2} \quad (2.24)$$

will be constant, since it depends only on the quality of receiver.

Then formula (2.21) can be recorded in the form

$$r_k(t) = \frac{U_{spk}^2(t)}{\overline{\xi_k^2}}. \quad (2.25)$$

Thus, the fluctuations of value  $r_k(t)$  are determined by random changes of the signal amplitude in transmitting. Again it is not superfluous to recall that during the study of the diverse reception

the probability distribution of envelopes  $U_{npk}(t)$  and respectively  $U_{npk}(t)$  are investigated in the time intervals

$$T_{yc} = 4 \div 7 T_{MH} \gg T_M.$$

For the convenience it is expedient to introduce the normalized ratio of the power of signal to the power of the noise

$$g_k(t) = \frac{r_k(t)}{(\sigma_k^2)^{1/2}}. \quad (2.26)$$

Here  $\frac{r_k(t)}{(\sigma_k^2)^{1/2}}$  - ratio of the root-mean-square deviation of signal at the input of receiver to the rms value of noise.

Since value  $U_{npk}(t)$  has the Rayleigh law of probability distribution, for  $g_k(t)$  integral distribution will be exponential:

$$W\{0 \leq g_k \leq Y_k\} = 1 - e^{-Y_k}. \quad (2.27)$$

From formula (2.27) it is possible to easily find the probability of the breaks of communication, i.e., the probability of the drop in the signal is lower than threshold level  $U_{npk}$ .

Page 67.

For this in formula (2.27) (and also in the subsequent formulas with  $Y$ ) it is necessary value  $Y_k$  to replace by  $\frac{U_{npk}^2}{2\sigma_k^2}$ . As an example, probability that the voltage of signal in the  $k$  channel there will be below threshold, will be determined by the expression

$$W\{0 \leq U_{npk} \leq U_{npk}\} = 1 - e^{-\frac{U_{npk}^2}{2\sigma_k^2}}. \quad (2.28)$$

Let us switch over to the determination of the rms values of the signal amplitude and noise at the output of add system (in interval  $T_u$ ). For the signal

$$\begin{aligned} & \overline{\left[ \sum_{k=1}^N a_k U_{npk}(t) \cos[\omega_0 t + \psi(t) + \Theta_k(t)] \right]^2} = \\ & = \sum_{i=1}^N a_i U_{npi}(t) \sum_{j=1}^N a_j U_{npj}(t) \overline{\{\cos[\omega_0(t) + \psi(t) + \Theta_i(t)] \cos[\omega_0(t) + \psi(t) + \Theta_j(t)]\}} = \\ & = \sum_{i=1}^N a_i U_{npi}(t) \sum_{j=1}^N a_j U_{npj}(t) \frac{\cos[\Theta_i(t) - \Theta_j(t)]}{2}, \quad (2.29) \end{aligned}$$

since value  $a$ ,  $U_{np}$  and  $\Theta$  they are permanent in the interval of averaging  $T_u$ .

For the noise

$$\overline{\left[ \sum_{k=1}^N a_k \xi_k(t) \right]^2} = \sum_{i=1}^N a_i \xi_i(t) \sum_{j=1}^N a_j \xi_j(t) = \sum_{k=1}^N a_k^2 \overline{\xi_k^2}, \quad (2.30)$$

since the noises in the branches of diversity are not depended, i.e.,

$$\overline{\xi_i(t) \xi_j(t)} = \begin{cases} \xi_i^2 & \text{при } i = j, \\ 0 & \text{при } i \neq j. \end{cases} \quad (2.31)$$

Key: (1). with.

Substituting (2.29) and (2.30) into formula (2.22), we obtain

$$r_z(t) = \frac{\frac{1}{2} \sum_{i=1}^N \sum_{j=1}^N a_i a_j U_{npi}(t) U_{npj}(t) \cos[\Theta_i(t) - \Theta_j(t)]}{\sum_{k=1}^N a_k^2 \overline{\xi_k^2}}. \quad (2.32)$$

From formula (2.32) it is evident that the signal-to-noise ratio depends substantially on the value of a phase difference

$\theta_i(t) - \theta_j(t)$ . Gain during the use of the diverse reception is maximum, when this difference is equal to zero.

Page 68.

Therefore with the combination is compulsory the phasing of signals. For this, as has already been spoken above, during the addition to the detector is utilized the self-alignment of the phase of the  $i$ -th signal under the phase of the  $j$ -th or vice versa. In this case  $\cos[\theta_i(t) - \theta_j(t)] = 1$  and

$$r_2(t) = \frac{1}{2} \frac{\left[ \sum_{k=1}^N a_k U_{npk}(t) \right]^2}{\sum_{k=1}^N a_k^2 \overline{U_k^2}} \quad (2.33)$$

Let us note that according to this formula it is possible to estimate maximum possible value  $r_2(t)$ . Utilizing Puniakowski-Schwarz's inequality, it is easy to show that

$$r_2(t) \leq \sum_{k=1}^N \frac{U_{npk}^2(t)}{2 \overline{U_k^2}} = \sum_{k=1}^N r_k(t). \quad (2.34)$$

Equal sign corresponds to a maximally possible gain from the diversity. Signal-to-noise ratio at the output of the device of addition in this case is equal to the sum of signal-to-noise ratios in all branches of diversity. So as for the separate branch of diversity, it is here expedient to introduce the normalized ratio of the power of signal to the power of the noise

$$\beta_k(t) = \frac{r_k(t)}{(\sigma_k^2)^{1/2}} \quad (2.35)$$

Here  $r_k$  since previously it was normalized relatively  $\sigma_k^2$ , assumed that the rms values of signal and noise in all branches of the diversity of identical  $\sigma_1 = \sigma_2 = \dots = \sigma_N = \sigma$  and  $\overline{\beta_1^2} = \overline{\beta_2^2} = \dots = \overline{\beta_N^2} = 1$ .

FOOTNOTE 1. This is not always correct. For example, with angular diverse reception  $\sigma_1 = \sigma_2 = \dots = \sigma_N$  it is necessary to use the calculation method, presented in [2.4] for the automatic selection. ENDFOOTNOTE.

Let us pass to the examination of the laws of distribution with different methods of combination.

Automatic selection. During the automatic selection coefficients  $\alpha_k$  are determined by the expression

$$\alpha_k = \begin{cases} 1 & \text{if } \beta_k = h \\ 0 & \text{if } \beta_k \neq h \end{cases} \quad (2.36)$$



Key: (1). for.

where  $h$  - number of channel with the maximum signal-to-noise ratio.  
The integral distribution of the normalized ratio of the power of signal to the power of noise will be equal [2.6]

$$W_{N_{\text{div}}} \{0 \leq y_1 \leq Y\} = (1 - e^{-Y})^N. \quad (2.37)$$

Page 69.

The means of distribution (2.37) is easily explained. Actually, since with the diverse reception with the automatic selection to the output is connected always the channel with the maximum value of  $Y$ , then in all remaining channels  $y_k < Y$ , and probability that in  $N$  channels  $y_k \leq Y$ , it is equal to

$$W_{N_{\text{div}}} \{0 \leq y_k \leq Y\} = \prod_{k=1}^N P \{0 \leq y_k \leq Y\} = (1 - e^{-Y})^N.$$

Probability density

$$w_{N_{\text{div}}} (y_1) = N e^{-y_1} (1 - e^{-y_1})^{N-1}. \quad (2.38)$$

Mean value  $\bar{y}_1$  can be accepted as the measure of gain from the use of the diverse reception  $Q$ . Computations give

$$Q_{\text{div}} = \int_0^{\infty} y_1 w_{N_{\text{div}}} (y_1) dy_1 = \sum_{k=1}^N 1/k. \quad (2.39)$$

From the latter formula it is evident that the gain from the use of the diverse reception rapidly falls from increase of  $N$ . The

addition of the  $k$  channel increases  $Q_{\text{div}}$  by value  $1/k$ . With large ones  $N$   $Q_{\text{div}} \rightarrow \ln N$ .

Optimum addition. Above [see formula (2.34)] it was shown that a maximally possible gain corresponds to the equality

$$r_z(t) = \sum_{k=1}^N r_k(t).$$

Brennan [2.8] demonstrated that in this case the form of weighting factors will be determined by the equality

$$a_k(t) = \frac{U_{npk}(t)}{\sqrt{2} \sigma_k^2}, \quad (2.40)$$

i.e., during the optimum addition amplification in the  $k$  channel must automatically be regulated so as at any moment of time to be proportional the  $k$  component of signal and inversely proportional to the rms value of noise in the  $k$  channel. Integral distribution  $y_z$  with the  $N$ -fold reception with the optimum addition will take the form (see, for example [2.8])

$$W_{N_{\text{opt}}} \{0 \leq y_z \leq Y\} = 1 - \sum_{\kappa=1}^N \frac{Y^{\kappa-1}}{(\kappa-1)!} e^{-Y}. \quad (2.41)$$

Gain from the use of the optimum addition

$$Q_{\text{div}} = N \quad (2.42)$$

increases linearly with a number of branches of diversity.

Linear addition. In this case all weighting factors are equal to each other:

$$a_1 = a_2 = \dots a_i = \dots a_N = a. \quad (2.43)$$

Virtually this means that the transfer functions of all diverse receivers must be identical and, therefore, the circuit of all ARU is in parallel. It is possible to place everything  $a_i = 1$ . The law of probability distribution during the linear addition for  $N > 2$  analytical expression does not have. The fact is that for the determination of the distribution of the sum, which stands in numerator (2.33), necessary to find the probability density of the sum of Rayleigh random variables, for which to take the integral of the form

$$W_z(u) = \overbrace{\int \int \int \dots \int}^N \frac{u_1 u_2 \dots u_N}{(2\pi)^N} e^{-\frac{u_1^2 + u_2^2 + \dots + u_N^2}{2\pi^2}} du_1 du_2 \dots du_N, \quad (2.44)$$

in which the integration is conducted from the  $N$ -dimensional space, limited by coordinate planes and hyperplane

$$\sum_{k=1}^N u_k = 1, \quad (2.45)$$

and then to find the integral law of sum.

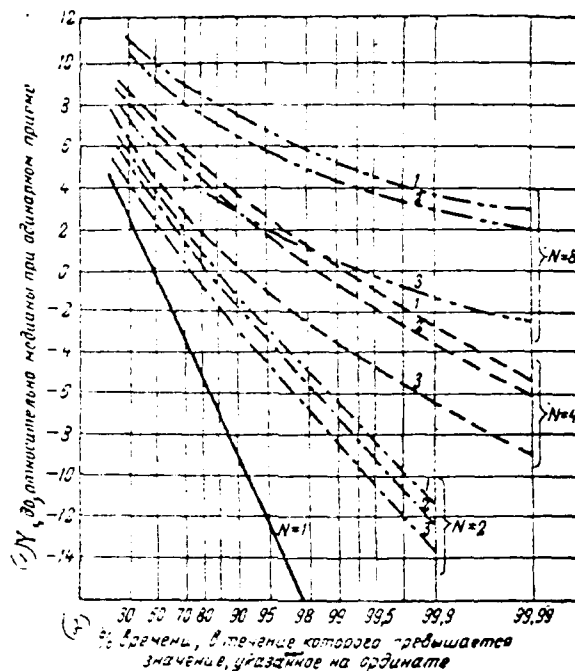


Fig. 2.2. Integral distribution  $Y$  for different methods of addition with  $N=2$ ,  $N=4$ ,  $N=8$ . 1 - optimum addition, 2 - linear additivity, 3 - automatic selection.

Key: (1).  $Y$ , dB, relative to median with the single receptor. (2). c/o time, during which is exceeded value, indicated on ordinate.

Page 71.

The results of numerical integration for  $N=4$  and 8 are represented in Fig. 2.2 (curves 2). Along the abscissa of this figure

are plotted the values, calculated by formula  $100(1-W) \cdot (0 \leq y \leq Y)!$  on the ordinate - the normalized ratio of the power of signal to the power of noise, expressed in the decibels relative to median value  $Y_{\text{med}}$  with the single reception. Gain from the use of linear addition can be calculated according to formula [2.8]:

$$Q_{\text{лин}} = 1 + \frac{\pi}{4}(N-1). \quad (2.46)$$

Fig. 2.2 gives the curved integral ones of the laws of distribution for all three methods of combination in question with the doubled, quadrupled and octuple reception, calculated according to formulas (2.37), (2.41) and (2.44). Values  $Q$  for all three methods of combination into the functions of a number of diverse receivers, calculated according to formulas (2.39), (2.42) and (2.46), are represented in Fig. 2.3. These curves characterize an equivalent increase in the median power of signal upon transfer from the single reception to that dispersion. From the figure one can see that with increase of  $N$  the difference in the gain between the linear and optimum additions does not exceed 1 dB, at the same time gain during the automatic selection increases considerably slower. Given in Fig. 2.2 and 2.3 curves characterize the double action of the diverse reception. On one hand, the diverse reception increases signal-to-noise ratio at the output, i.e., it makes it possible at the assigned quality of channels to decrease the energy parameters of system (power of transmitter, dimensions of antennas) or in the same energy parameters to improve the quality of channels.

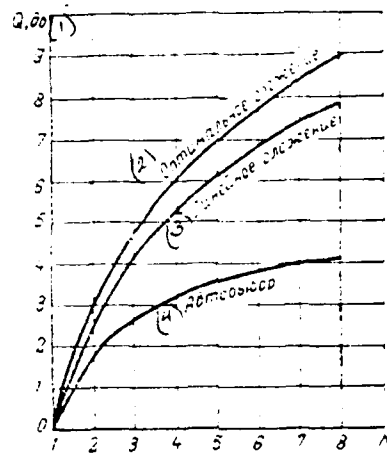


Fig. 2.3. Dependence of the coefficient of improvement  $Q$  on the order of diversity.

Key: (1). dB. (2). Optimum addition. (3). Linear addition. (4). Automatic selection.

Page 72.

On the other hand, the diverse reception sharply decreases the range of the rapid fluctuations (see Fig. 2.2), i.e., it decreases the percentage of time, during which the signal falls below the threshold of system and, therefore, raises the reliability of the transmission of information. One should note also that the diverse reception simultaneously provides an increase in the equipment reliability as a

result of the redundancy.

§2.5. Selection of the methods of the combination of the diverse signals on the lines DTR.

On multichannel radio relay lines, which use an effect of recte tropospheric propagation, almost always is applied frequency modulation. The conducted into §2.4 statistical analysis of the systems of the diverse reception makes it possible to make a comparison of the methods of combination for the line of DTR with the work of higher than the threshold of FM.

The power of noises at the output of the FM discriminator in general is determined by following formula [2.9]:

$$P_{\text{ш шх}} = P_{\text{с шх}} \left[ L_1 e^{-\left(\frac{P_c}{P_{\text{ш}}}\right)_{\text{шх}}} + L_2 \frac{1 - e^{-\left(\frac{P_c}{P_{\text{ш}}}\right)_{\text{шх}}}}{\left(\frac{P_c}{P_{\text{ш}}}\right)_{\text{шх}}} \right], \quad (2.47)$$

where  $L_1$  and  $L_2$  - the coefficients, which depend on the number of channel, the passbands of receiver and deviation of frequency. With the work it is higher than threshold  $\left(\frac{P_c}{P_{\text{ш}}}\right)_{\text{шх}} > 3 \div 10$ . In this case  $e^{-\left(\frac{P_c}{P_{\text{ш}}}\right)_{\text{шх}}} \rightarrow 0$  and formula (2.47) passes in the known relationship

$$P_{\text{ш шх}} = P_{\text{с шх}} \frac{L_2}{\left(\frac{P_c}{P_{\text{ш}}}\right)_{\text{шх}}}, \quad (2.48)$$

in which  $P_{\text{с шх}} \approx \text{const}$  and in depending on a change in the signal at the input is changed the power of noises at the output of the FM

discriminator (ChD). Value  $\left(\frac{P_c}{P_{\Sigma}}\right)_{\Sigma K}$  one should to replace by  $r(t)$ , also, taking into account formulas (2.25), (2.26) and (2.35) for the  $k$  branch of diversity record

$$P_{\Sigma \Sigma \Sigma K} = P_{c \Sigma \Sigma K} \frac{L_2 \frac{\sigma_K^2}{\sigma_K^2}}{y_K(t)} = \frac{v}{y_K(t)}, \quad (2.49)$$

and for the total signal

$$P_{\Sigma \Sigma \Sigma \Sigma} = P_{c \Sigma \Sigma \Sigma} \frac{L_2 \frac{\sigma^2}{\sigma^2}}{y_{\Sigma}(t)} = \frac{v}{y_{\Sigma}(t)}. \quad (2.50)$$

Page 73.

Here  $v = P_{c \Sigma \Sigma \Sigma} L_2 \frac{\sigma^2}{\sigma^2}$  and just as it is earlier, is assumed  $\sigma_1 = \sigma_2 = \dots = \sigma_N = \sigma$  and  $\overline{\varepsilon_1^2} = \overline{\varepsilon_2^2} = \dots = \overline{\varepsilon_N^2} = \overline{\varepsilon^2}$ . Knowing distributions  $y_K(t)$  and  $y_{\Sigma}(t)$  easy to find the distribution of power of noises at the output of ChD. In the integral laws of distribution, found in §2.4, one should simply  $v$  replace by  $v/P_{\Sigma \Sigma \Sigma \Sigma}$ .

The comparison of the methods of combination is most simple to produce for the doubled reception, i.e., with  $N=2$ , since in this case are obtained the relatively simple expressions for the distribution functions. The obtained output can be used also for  $N$ -fold reception, if we break it into  $N/2$  the doubled receptions, and then to each pair of twin circuits to use the same reasonings, etc.



During the automatic selection of the strongest of two signals the integral distribution of power of noise in the channel will be determined by the expression, which directly follows from formula (2.37) taking into account (2.50):

$$W_{2\text{opt}} \{0 \leq P_{\text{ш шмх}} \leq P_{\text{ш шмх}}\} = 1 - \left(1 - e^{-\frac{P}{P_{\text{ш шмх}}}}\right)^2. \quad (2.51)$$

The place, in which is realized the combination of signals, is unimportant; however, to FM detector - in the circuit DFCh - a combination must be conducted of signals  $U_{\text{мрх}}$  (Fig. 2.4a), and after detector - on noises  $P_{\text{ш шмх}}$  (Fig. 2.4b). For isolation of  $P_{\text{ш шмх}}$  in the branches of receiver with the diversity must be special monitoring noise channels. Hence the difference in the block diagrams during the automatic selection before and after FM detector. The control system on the signal, obtained from the device of comparison, disconnects the signal, which has smaller amplitude (or larger noise level). Matching device is necessary for maintaining the constancy of level at the output of receiver.

During the optimum addition the integral distribution of power of noise will be determined by the expression [see formula (2.41)]:

$$W_{2\text{opt}} \{0 \leq P_{\text{ш шмх}} \leq P_{\text{ш шмх}}\} = 1 - \left(1 - e^{-\frac{P}{P_{\text{ш шмх}}}}\right) e^{-\frac{P}{P_{\text{ш шмх}}}}. \quad (2.52)$$

System block diagram with the optimum addition is given in Fig. 2.5. The control systems regulate amplification in the branches of

DCC = 80025105

PAGE

144

diversity inversely proportional to the rms value of noise in accordance with formula (2.40).

For linear addition the significant role with FM begins to play the place of addition.

Page 74.

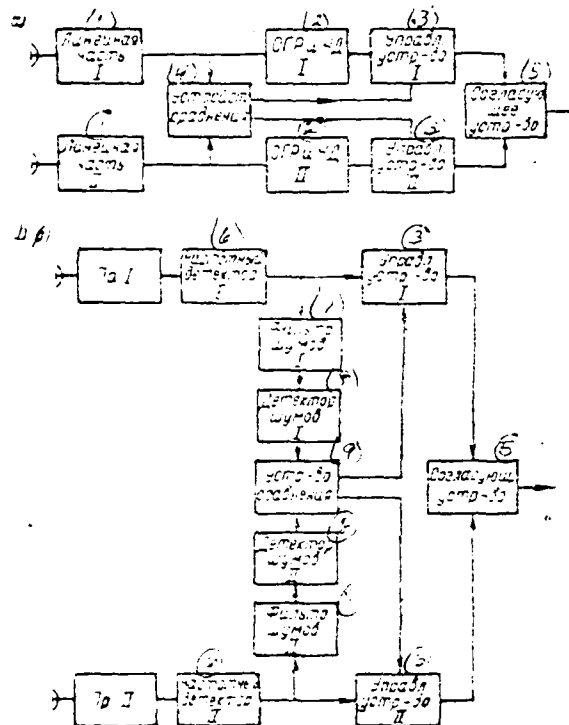
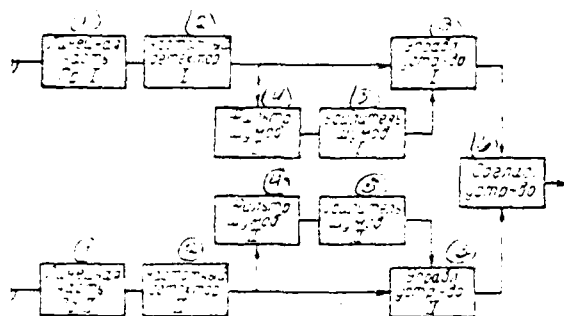


Fig. 2.4. Block diagram of automatic selection: a) on signal to FM detector; b) on noises after FM detector.

Key: (1). Linear part. (2). and. (3). Control device. (4). Comparison device. (5). Matching device. (6). FM discriminator. (7). Noise filter. (8). Detector of noises. (9). Device of comparison.



Key: (1). Linear part. (2). FM discriminator. (3). Control device.  
(4). Noise filter. (5). Amplifier of noises. (6). Matching device.

Page 75.

During the addition to FM detector in the high or intermediate frequency (Fig. 2.6a) the realization of gain from the diverse reception makes it necessary to produce the automatic tuning of the phases of the added up signals, since the phases of signals will differ from each other [see formula (2.14)]. For the determination of the distribution of power of noises in the channel it is necessary to take the integral of form (2.44) with  $N=2$ , and then to switch over from one voltage distribution to the next  $y_i$  and  $P_{\text{max}}$ . Found thus distribution takes the form

$$W_{2 \text{ ливн. до дет.}} (0 \leq P_{\text{ш. вхл.}} \leq \rho_{\text{ш. вхл.}}) = e^{-\frac{\rho_{\text{ш. вхл.}}}{2}} -$$

$$- \sqrt{\frac{\pi}{2 \rho_{\text{ш. вхл.}}}} e^{-\frac{\rho_{\text{ш. вхл.}}}{2}} \Phi \left( \sqrt{\frac{\rho_{\text{ш. вхл.}}}{2}} \right). \quad (2.53)$$

where  $\Phi(z) = \frac{2}{\sqrt{\pi}} \int_0^z e^{-z^2} dz$  - probability integral. A linear addition can be carried out, also, after FM detector (Fig. 2.6b). In this case integral noise distribution at the output will be determined by the convolution integral of noise distributions in the branches of diversity and take from [2.10]

$$W_{\text{2 лмш. после дет.}} \{0 \leq P_{\text{ш в мх}} \leq P_{\text{ш в мх}}\} = 1 - \frac{\nu}{P_{\text{ш в мх}}} e^{-\frac{\nu}{P_{\text{ш в мх}}}} \times K_1\left(\frac{\nu}{P_{\text{ш в мх}}}\right), \quad (2.54)$$

where  $K_1(z)$  - the modified function of Hankel.

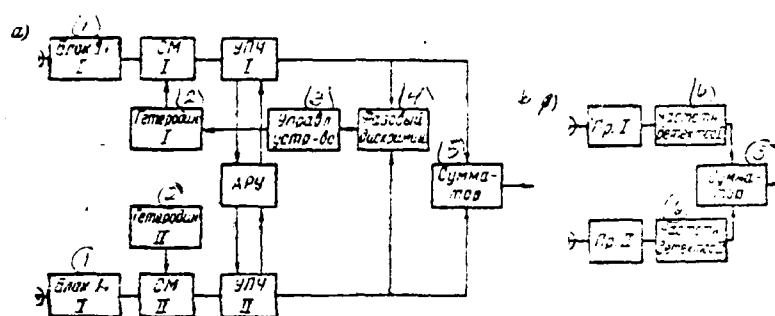


Fig. 2.6. Block diagram of the linear adder: a) to the detector FM, b) after detector FM.

Key: (1). Block. (2). Heterodyne. (3). Control device. (4). Phase discriminator. (5). Adder. (6). FM discriminator.

Page 76.

During the addition to the detector the identity of amplification the tractor [in accordance with the formula (2.43)] is reached by the device of the common for two receivers system of automatic gain control (ABU). In this case the factors of amplification of both branches of the diverse receiver will be equal and determined in essence by the strongest of two signals. The realization of gain from the diversity required the special system of the self-alignment of phase (APF), which consists of the phase discriminator and the control system, which affects phase of one of

the heterodynes. Since the ideal phasing of signals, naturally, is inaccessible, it is of interest to determine the drop in the gain from the diverse reception as a result of an inaccuracy in the phasing of the diverse signals. The corresponding curve is represented in Fig. 2.7. During the addition after detector the coherence of signals and the linearity of addition is obtained automatically; therefore the block diagram Fig. 2.6b is simpler. The integral distributions of power of noise on the output of the FM detector (with the work it is higher than the threshold) for the doubled reception and all methods of the combinations, constructed according to formulas (2.51)~(2.54), are given in Fig. 2.8 together with the distribution with the single reception. From Fig. 2.8 evidently:

- linear addition after FM detector gives considerably smaller gain in comparison with the addition to the detector. This is understandable from the physical considerations, since after the FM discriminators the signals in branches of diversity will be identical, and noises - determined by that signal whose level will be less to FM detector. If we consider threshold properties of FM, then the value of gain will become still less:

- of three remaining distributions quite worse in automatic selection. Moreover with an increase in the multiplicity of the

diverse reception N a difference in the automatic selection from add systems rises (see Fig. 2.3);

- linear addition to the detector insignificantly differs in the distribution from the optimum addition. It is necessary to keep in mind that during the addition to the detector, is improved the signal-to-noise ratio to the passage of mixture noise through the FM detector in which with the drop in the signal in lower than the threshold occur the irreversible deterioration in the output signal-to-noise ratio.

With the doubled reception is very graphic the method of the geometric interpretation of obtained results [2.11].



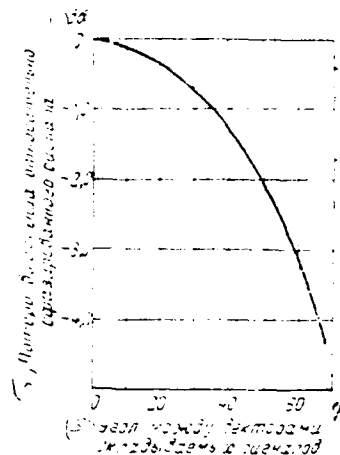


Fig. 2.7. Decrease of the coefficient of improvement due to an inaccuracy in the system APF.

Key: (1). dB. (2). Losses of gain relative to phased signal. (3). Angle between vectors of added up signals.

Page 77.

Let us examine the three-dimensional picture (Fig. 2.9a), in which along two axes are plotted the ratios of actual stress of signal to the rms value of noise in the first and second branches of the diversity:

$$\left( \chi_1 = \frac{U_{np1}}{\sqrt{2} \sigma}, \quad \chi_2 = \frac{U_{np2}}{\sqrt{2} \sigma} \right).$$

but along the third axis - the same relation at the output of the

system of combination

Let us examine automatic selection. Let in first channel  $x_1 = 0$  (since be equal to zero signal  $\bar{U}_{\text{ap1}}$ ). Then the line, which characterizes dependence  $x_2$  (at the output) on  $x_1$  (at the input of the system of the diverse receiver) will be straight line in plane  $x_2 O'x_1$  of that lying at angle of  $45^\circ$  to axes  $(C'F)$ . Value  $x_2$  will not be changed upon the appearance of a signal in the first branch of diversity ( $x_1 > 0$ ) until  $x_1$  becomes more than  $x_2$  since automatic selection system will work so that to the output nevertheless will be connected second channel. This means that all points, which characterize automatic selection, will lie in the plane, perpendicular to plane  $x_2 O'x_1$  of passing through  $O'F$ , i.e., in plane  $FO'H$ . In exactly the same manner, if signal in second channel  $x_2 < x_1$  then characteristic will pass in plane  $x_1 O'x_2$ . Thus, the locus of the characteristics of the system of automatic selection lies in two planes, perpendicular to coordinate planes  $x_2 O'x_1$  and  $x_1 O'x_2$  and which pass at angles of  $45^\circ$  to the axes.

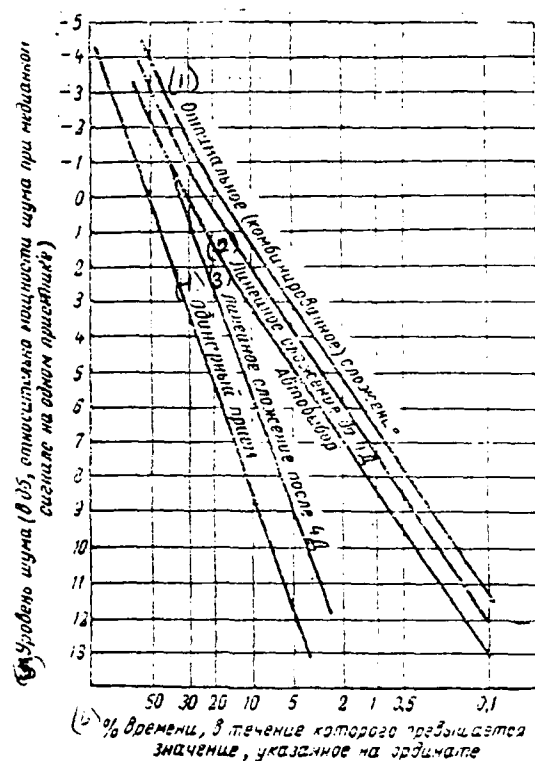


Fig. 2.8. Integral distributions of power of noise in telephone channel with the doubled reception  $N=2$ .

Key: (1). Optimum (combined) addition. (2). Linear addition to 4D. (3). Linear addition after 4D. (4). Single reception. (5). Noise level (8 dB, relative to power of noise with median signal on one receiver). (6). o/o time, during which is exceeded value, indicated on ordinate.

During the linear addition, if in first channel  $U_{np1}=0$ , then characteristic also will go in plane  $x_2 O'x_2$ . However, since during the linear addition

$$x_2 = \frac{U_{np1} + U_{np2}}{\sqrt{\frac{1}{2} + \frac{1}{2} - \frac{1}{2}}} = \frac{1}{\sqrt{2}} \left( \frac{U_{np1}}{\sqrt{\frac{1}{2}}} + \frac{U_{np2}}{\sqrt{\frac{1}{2}}} \right) \quad (2.55)$$

the slope of characteristic will be determined by factor  $\frac{1}{\sqrt{2}}$ , showing presence at the input of the system of the addition of receiver noise whose signal is equal to zero (line O'B). The same will be, if  $U_{np2}=0$ , but only in plane  $x_2 O'x_2$  (line O'G). If both signals are not equal to zero, then locus, which characterize the system of linear addition, will lie in the plane, passing through O'B and O'G.

Finally, for the optimum addition the locus of system will be the part of the surface of cone, which is located in I quadrant (FLEO'). This is explained by the fact that  $x_2$  at the output will be determined by the relationship:

$$x_2 = \sqrt{\frac{U_{np1}^2}{2\sigma^2} + \frac{U_{np2}^2}{2\sigma^2}} \quad (2.56)$$

directly following from (2.40).

The obtained geometric representation makes it possible to compare the methods of combination with any means of the probability distribution of signals. The two-dimensional differential probability distribution of signals in the chosen coordinates will be the surface above plane  $x_2 O'x_2$  (Fig. 2.9a).

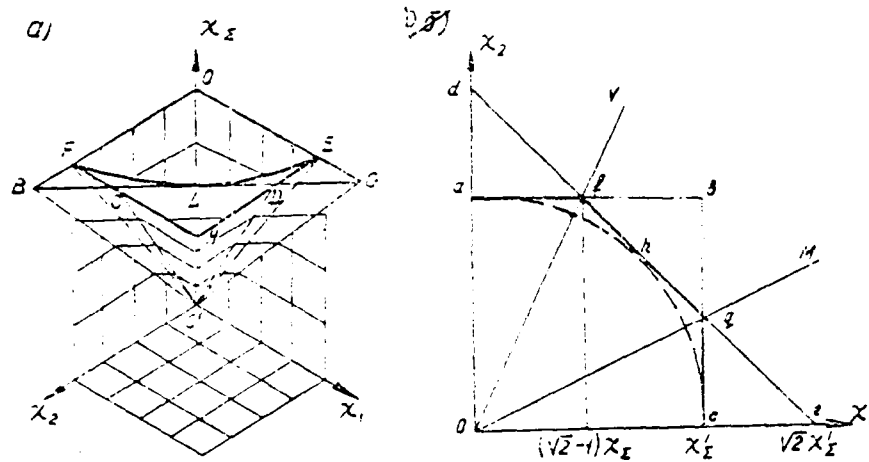


Fig. 2.9. Geometric interpretation of different types of addition (a), range of integration two-dimensional probability density (b).

Page 79.

The space, included between the part of the surface and its orthogonal projection on plane  $x_1O'x_2$ , is equal to the probability of simultaneous impingement  $U_{sp1}/\sqrt{2\sigma_1^2}$  and  $U_{sp2}/\sqrt{2\sigma_2^2}$  into the range of values, plotted along the coordinate axes. This means that the range of integration of two-dimensional distribution will take the form Fig. 2.9b, which there is a section of Fig. 2.9a by plane, perpendicular to  $x_3$ . The curve abc characterizes automatic selection, dfge - linear and ahc - optimum of addition. If is assigned certain value of the ratio of the voltage of signal to the rms value of noise

at the output of the system of addition  $X'_1$  or of the curves of Fig. 2.9b it is possible to determine, for what pairs  $X_1$  and  $X_2$  is reached  $X'_1$  at the different methods of combination. Value  $X'_1$  is plotted along the axis  $OX_1$ . It is evident that during the optimum addition for obtaining  $X'_1$  on the output add systems are required smaller value  $X_1$  and  $X_2$  than with other methods. Evident also that in the relation of signal amplitudes in the branches of diversity, which lie from  $\sqrt{2}-1$  to  $\frac{1}{\sqrt{2}-1}$ , the system of linear addition has characteristics best, than in automatic selection, and vice versa, out of this interval the automatic selection is better than the linear addition. If now during the study of the surface of two-dimensional probability density it seems that space, which is located within the sector, limited by the planes, perpendicular to Fig. 2.9b and passing through OV and OM, it is more than outside it, then system with the linear addition will give the best results, than automatic selection. This is correct, for example, for the Rayleigh law. Otherwise the automatic selection is better.

The made construction makes it possible to synthesize the system whose characteristics are very close to the characteristics of optimum addition. Let us examine curve afqc, which is determining the combination, in which in the relation of signal amplitudes from 0.414 to  $2.42(2-1 \text{ to } \frac{1}{\sqrt{2}-1})$  occurs the addition of the signals, obtained from both branches of diversity, and with drop in cre of the

signals of lower than 0.414 occurs the cutoff of weak signal. Since the results of integrating the two-dimensional probability density for afgc and for ahc will be close friend and to friend, both systems will virtually coincide in their characteristics. However, the technical embodiment of the proposed system, which can be called combined, is considerably simpler than the creation of system with the optimum addition. The block diagram of the construction of the combined system of pcst-detector addition is analogous Fig. 2.4b. However, the device of comparison in this case is not must simple to compare two signals, but to determine their relation and to disconnect the weakest signal, only if its level will be 2.5 times less than another signal. The combined addition to the detector is technically more complicated than after detector, and at the same time it has no advantages.

Page 80.

Comparing the systems of combination, one cannot fail to consider also that during the automatic selection at the moments of switching signal from one branch to another, is unavoidable the onset of the transient processes whose value can be inadmissibly great. In the system of the combined addition this transient process is considerably less, since the disconnected signal is 2.5 times less than remaining.

Thus, best methods of combination on the lines DTR they are, in the first place, linear addition to FM detector and, in the second place, the combined addition after FM detector. Both these of method are very used extensively on the lines of DTF.

Let us compare these methods between themselves. In favor of the combined addition after FM detector speak the following advantages.

1. With work in field of very weak signals, with linear addition and large difference signal level output power of noises will be determined by noises of both receivers, whereas with combination - by noises only of one.

2. Use of linear addition in FM detector with diversity in frequency requires sufficiently complicated device of automatic frequency control and phases of added up signals. However, as it will be shown below (see Chapter 5), there are satisfactory solutions of this technical problem. The combined addition after FM detector is technically more simply.

In favor of linear addition to FM detector operate the following factors.



1. In work [212] it is shown that during linear addition occurs considerable expansion of effective band width of circuit of propagation.

This can be explained by the fact that during the addition of two or several signals, which passed the four-poles with the random, but independent frequency characteristics, the spectrum of total signal it will prove to be that less distorted (by multiplicative interference) than the spectrum of each of the added up signals, while this means that the total signal seemingly passes four-pole with random, but more uniform response. Consequently, during the linear addition it is possible to pass through the line of DTR wider frequency spectrum or to obtain the smaller distortions of the spectrum. This means that during the transmission multichannel telephone signals during the linear addition the value of transient interferences will be substantially less.

2. During transmission of TV signals linear addition causes considerably less than distortions and disruptions of synchronization, than combined.

3. Operating misalignment of circuits of addition, unavoidable

in process of operation, it will cause during that combined, addition of inadmissibly large oscillation of signal level in circuit (oscillation of overall line attenuation in channels), whereas during linear addition this will cause only certain deterioration in signal-to-noise ratio as a result of incomplete realization of gain from diverse reception.

Page 81.

Generally, as show experimental investigations, the system of linear addition to FM detector is considerably less susceptible to any kind to operating changes in the circuits of the branches of diversity. The effect of operating misalignment on the effectiveness of the diverse reception is characterized by the curve of Fig. 2.10. Along the abscissa Fig. 2.10 is plotted the relation

$$\frac{\gamma_{\text{мсд}}}{\gamma_{\text{мсд}}} = \frac{U_{\text{пр1 мсд}}}{\sqrt{2 \sigma_1^2}} / \frac{U_{\text{пр2 мсд}}}{\sqrt{2 \sigma_2^2}}$$

in the branches of diversity. A change in relation  $\chi_{1 \text{ мсд}} / \chi_{2 \text{ мсд}}$  can occur both as a result of changing the amplification in the circuits of diversity and as a result of changing noisiness of the diverse receivers.

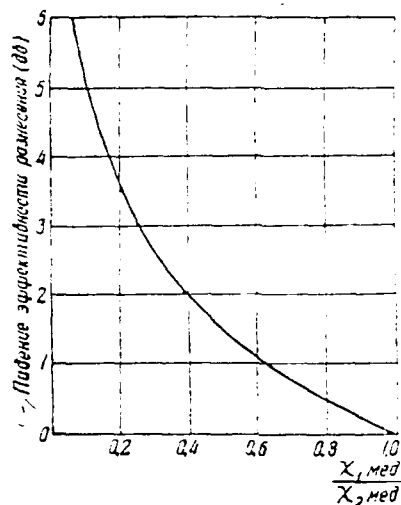


Fig. 2.10. Effect of operating misalignment on the effectiveness of the diverse reception.

Key: (1). Drop in the effectiveness of diversity (dB).

#### REFERENCES

21. Б. С. Шыбаков. О пропускной способности каналов с большим числом лучей. «Радиотехника и электроника», т. IV, вып. 9, 1959.
22. А. С. Немировский. О пропускной способности многолучевого канала при разнесенном приеме с автовыбором. «Радиотехника», № 3, 1961.
23. M. Nakagami. «The m-distribution a general formula of intensity distribution of rapid fading». Proc. of symposium held at the University of California, Los Angeles, June, 1958. Pergamon Press, 1960.
24. А. С. Немировский. О приеме со сложением сигналов, разнесенных по углу прихода луча при дальнем тропосферном распространении ука. «Электросвязь», № 8, 1960.
25. H. Staras Diversity reception with correlated signals. I. Apply Phys. 1956, January, v. 27.
26. Лекции по теории систем связи. Перевод с английского под ред. Б. Р. Левина (глава IV). Изд. «Мир».
27. D. G. Brennan. Linear diversity combining techniques. Proc. IRE, 1959, June, v. 47.
28. Э. Я. Рыский. О пороговом уровне ЧМ-приемника. «Электросвязь», № 6, 1954.
29. Е. Л. Геренрот. Помехозащищенность канала ЧТ тропосферной радиорелейной линии при линейном сложении. «Электросвязь», № 7, 1961.
30. F. I. Altman. A simplified diversity communication system for beyond-the-horizon links. IRE Trans. of Communication System, 1958, March, v. 4.
31. А. С. Немировский. О ширине полосы пропускания при одинарном и разнесенном приеме сигналов дальнего тропосферного распространения ука. «Электросвязь», № 5, 1961.

Page 82.

Chapter 3.

FREQUENCY CHARACTERISTICS OF THE SECTION OF RADIO WAVE PROPAGATION IN  
A TROPOSPHERE.

§ 3.1. Introduction.

On the tropospheric radio communication links the signal at input of receiver is the sum of a large number of components, re-emitted with the individual heterogeneities of the dielectric permeability of air. These components are propagated in the troposphere on different paths and, therefore, they have different time lag. If  $k$ -th component signal has time lag  $\tau_k$ , then at the frequency of transmitter, equal to  $\omega$ , the phase of this component is equal to  $\omega\tau_k + \varphi_k$ , where  $\varphi_k$  - time of reflection coefficient from a  $k$ -th of heterogeneity. Signal at the input of receiver is equal to the vector sum of the separate delaying components, which is illustrated by vector diagram Fig. 3.1a. With a change in the frequency of transmitter on  $\Delta\omega$  the phase of  $k$ -th components will

become equal to  $(\omega - \Delta\omega)t_0 + \varphi_0$ , i.e. with a change in the frequency of transmitter change the phases of all components of signal <sup>1</sup>.

FOOTNOTE <sup>1</sup>. With a change in the frequency of transmitter, generally speaking, change also the amplitudes of separate components, since the coefficient of reflection of radio waves from the heterogeneities of the troposphere depends on the frequency (see Chapter 1). However, with the small relative change the frequencies of the transmitter (order  $10^{-6}$ ) of the amplitude of the components of signal virtually do not change. ENDFOOTNOTE.

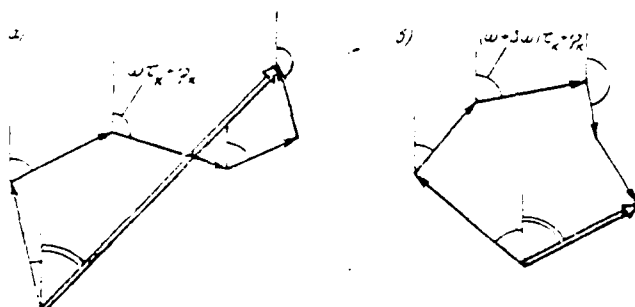


Fig. 3.1. Change in amplitude and phase of total signal at the input of the receiver of tropospheric line with a change in the frequency of transmitter.

Page 83.

Respectively will change amplitude and phase of total signal at the input of receiver as this shown in Fig. 3.1b. Thus, as a result of the multiple-pronged radiowave propagation in the troposphere signal at the input of receiver has different amplitude and phase at the different frequencies; furthermore, a change in the phase is in general disproportionate to a change in the frequency. Consequently, the section of radiowave propagation in the troposphere can be considered as certain linear four-pole with by nonuniform the amplitude-frequency and nonlinear phase-frequency by characteristics. Intensity and location of heterogeneities in the troposphere continuously change during randomly; respectively they change

amplitude and time lag of the separate components of multiple-pronged signal. Therefore the form of the amplitude-frequency and phase-frequency characteristics of the section of tropospheric line also continuously and randomly they change. In other words, these characteristics are the random functions of frequency.

During the transmission along the tropospheric lines of the modulated signals the nonuniformity of the amplitude-frequency and the nonlinearity phase response cause signal distortions. With multichannel telephony appear transient noises in the channels, with the television is lost the clearness and it appears "plastic" on the image, during the transmission of digital information are distorted "telegraph" impulses and is lost authenticity. Since the form of the frequency characteristics of section continuously changes, then value and character of these distortions also change randomly. In the incorrectly designed tropospheric communicating system signal distortions due to the multi-beam character of propagation can be considerable. Therefore the analysis of the amplitude-frequency and phase-frequency characteristics of the section of tropospheric line has great practical value.

Since the frequency characteristics of the section of tropospheric line are the random functions of frequency, then their analysis should be carried out the mathematical methods of the theory

of random functions. The theory of random functions is most completely developed in connection with by the random functions of time - to random processes. In particular, in radio engineering are sufficiently well studied the random processes, which are the fluctuation noises of radio engineering equipment [3.1-3.3]. The static characteristics of multiple-pronged signal at the output of the section of tropospheric line have much in common with statistical characteristics fluctuation noise. For this reason in the numerous works, dedicated to the analysis of the frequency characteristics of the section of tropospheric line, are used extensively the relationships of the theory of fluctuation noises <sup>1</sup>.

FOOTNOTE <sup>1</sup>. These relationships are applied also during the study of the characteristics of other multiple-pronged channels - with radiocommunications with the use of ionospheric scattering of ultrashort waves and during the use of the mcn as the passive communications relay. ENDFOOTNOTE.

Page 84.

However, one should have in mind that the analogy between the fluctuation noise and the signal with the multiple-pronged structure exists only in a sense and the arbitrary transfer of the positions of the theory of noises to the multiple-pronged signals can lead to



errors. Therefore in the beginning of this chapter briefly remind the reader of some relationships of the theory of fluctuation noises and further let us show how these relationships they can be used for the analysis of the frequency characteristics of multiple-pronged channel.

§ 3.2. Generalization of some relationships of the theory of fluctuation noises for the signals with the multiple-pronged structure.

Fluctuation noises. Fluctuation noise is stationary normal random process. If is specific  $k$ -th realization of this process  $\xi_k(t)$  (i.e. noise at the output of specific radio engineering equipment) and the values of this realization are known in entire time interval from  $-\infty$  to  $+\infty$ , then can be found the composite spectrum of this realization  $S_k(\Omega)$  moreover  $\xi_k(t)$  and  $S_k(\Omega)$  are connected with the pair of Fourier transforms, i.e.,

$$\begin{aligned} S_k(\Omega) &= \int_{-\infty}^{\infty} \xi_k(t) e^{-i\Omega t} dt, \\ \xi_k(t) &= \frac{1}{2\pi} \int_{-\infty}^{\infty} S_k(\Omega) e^{i\Omega t} d\Omega. \end{aligned} \quad (3.1)$$

The composite spectrum for another specific realization of noise will take already another form. The spectral composition of fluctuation noise as a whole for all possible realizations is determined by energy spectrum  $G(\Omega)$ . Energy spectrum is obtained as a

result of averaging on all possible realizations <sup>2</sup> of the square modulus of the composite spectrum of these realizations, i.e.,

$$G(\Omega) = \overline{|S(\Omega)|^2}. \quad (3.2)$$

FOOTNOTE 2. In the literature the energy spectrum is introduced usually as the result of averaging on the time of the square modulus of the current spectrum of one realization. We used here averaging on many realizations, which for the stationary process gives the same result. In this case to more easily establish analogy with the multiple-pronged signals; however, are here assumed to be known ones all values of noise in the time interval from  $- \infty$  to  $+\infty$ ; this assumption is, naturally, the mathematical fiction. ENDFOOTNOTE.

Energy spectrum gives only the averaged picture of the energy distribution of noise according to the frequencies of elementary harmonic components and it does not consider phase displacements of these components.

Page 85.

During calculations it is convenient to use the standardized energy spectrum which is determined from the formula

$$g(\Omega) = \frac{G(\Omega)}{G(0)}. \quad (3.3)$$

The static dependence between the values of fluctuation noise at

the moments of time  $t$  and  $t+\tau$  is characterized by correlation function by time. Frequently is utilized the normalized correlation function, which is called also the correlation coefficient. The correlation coefficient by time is determined from the formula

$$R(\tau) = \frac{\overline{u(t)u(t+\tau)}}{\overline{u^2(t)}}. \quad (3.4)$$

According to the theorem of A. Ya. Khirchin the correlation function of the time and the energy spectrum of fluctuation noise are connected with the pair of Fourier's transforms. The respectively normalized correlation function and the standardized energy spectrum are connected with relationships [13]:

$$g(\Omega) = \frac{\int_0^{\infty} R(\tau) \cos \Omega \tau d\tau}{\int_0^{\infty} R(\tau) d\tau}. \quad (3.5)$$

$$R(\tau) = \frac{\int_0^{\infty} g(\Omega) \cos \Omega \tau d\Omega}{\int_0^{\infty} g(\Omega) d\Omega}. \quad (3.6)$$

In radio engineering frequently is necessary to deal concerning the fluctuation noise, which passed through band-pass filter with the central frequency  $\omega_0$  and the passband, much less than central frequency. In this case fluctuation noise it is convenient to present as the quasi-harmonic oscillation which takes the form

$$u(t) = U(t) \cos[\omega_0 t + \phi(t)], \quad (3.7)$$

where  $U(t)$  - random amplitude, and  $\phi(t)$  - random phase of this

fluctuation.

FOOTNOTE 1. In the literature  $U(t)$  they frequently call also "envelope" of fluctuation noise [3.1-3.3]. ENDFCCTINCTE.

Central frequency it is expedient to select for the equal abscissa of the "center of gravity" of energy spectrum of noise as the plane figure, i.e.,  $\omega_0$  it is determined from the formula:

$$\omega_0 = \frac{\int_{-\infty}^{\infty} \omega g(\omega) d\omega}{\int_{-\infty}^{\infty} g(\omega) d\omega} \quad (3.8)$$

Page 86.

To the representation of fluctuation noise in the form (3.7) corresponds its vector image, shown in Fig. 3.2. With this image the instantaneous value of noise  $u(t)$  is equal to the projection of vector with an amplitude of  $U(t)$  and phase  $\phi(t)$  on the axis, which rotates with the circular velocity  $\omega_0$ . From Fig. 3.2 it directly follows that

$$U(t) = \sqrt{P^2(t) + Q^2(t)}, \quad (3.9)$$

$$\phi(t) = \arctg \frac{Q(t)}{P(t)}, \quad (3.10)$$

where  $P(t)$  and  $Q(t)$  - projections of vector to the motionless coordinate axes.

Processes  $P(t)$  and  $Q(t)$  have the normal law of probability distribution and the same energy spectrum, as the instantaneous value of noise  $u(t)$ , only the center of this spectrum is transferred from the frequency  $\omega_0$  to the zero frequency. From the theory of fluctuation noises it is also known that the correlation coefficients in time of processes  $P(t)$  and  $Q(t)$ , equal to each other, are connected with the standardized energy spectrum, displaced for the zero frequency, relationship [3.2; 3.3]:

$$R_P(\tau) = R_Q(\tau) = \frac{\int_{-\infty}^{\infty} g(\Omega) \cos \Omega \tau d\Omega}{\int_{-\infty}^{\infty} g(\Omega) d\Omega}$$

where  $\Omega = \omega - \omega_0$ .

(3.11)

The coefficient of cross correlation for processes of  $P(t)$  and  $Q(t)$  is determined by the relationship

$$R_{PQ}(\tau) = \frac{\int_{-\infty}^{\infty} g(\Omega) \sin \Omega \tau d\Omega}{\int_{-\infty}^{\infty} g(\Omega) d\Omega}, \quad (3.12)$$

from which evident that at the coinciding moments of time  $P(t)$  and  $Q(t)$  between themselves they are not correlated, i.e.,

$$R_{PQ}(0) = 0. \quad (3.13)$$

With the symmetrical relative to central frequency energy spectrum (i.e. with the symmetrical relative to zero frequency displaced spectrum) from (3.11) and (3.12) it follows that

$$R_P(\tau) = R_Q(\tau) = \frac{\int_0^{\infty} g(\Omega) \cos \Omega \tau d\Omega}{\int_0^{\infty} g(\Omega) d\Omega}, \quad (3.14)$$

$$R_{PQ}(\tau) = 0. \quad (3.15)$$

i. e.  $P(t)$  and  $Q(t)$  are not correlated at any moment of time.

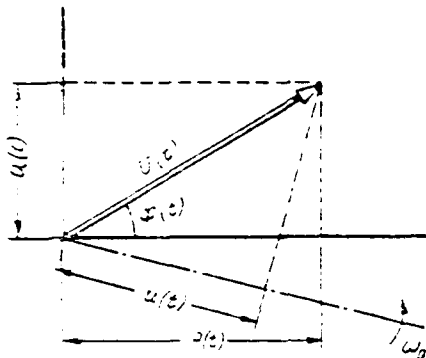


Fig. 3.2. Vector image of fluctuation noise as quasi-harmonic oscillation.

Page 87.

With the static properties of processes  $F(t)$  and  $Q(t)$  indicated the amplitude of the quasi-harmonic oscillation  $U(t)$ , connected with  $F(t)$  and  $Q(t)$  with relationship (3.9), is distributed according to the law of Rayleigh. The density of distribution of probabilities for the Rayleigh law takes the form [3.2; 3.3]:

$$W(U) = \frac{U}{\sigma^2} e^{-\frac{U^2}{2\sigma^2}}, \quad (3.16)$$

and the integral law of probability distribution - the form

$$F(u < U) = e^{-\frac{U^2}{2\sigma^2}}, \quad (3.17)$$

where  $2\sigma^2 = \overline{U^2}$  - the mean square of amplitude.

Is frequently examined also the combined passage through the filter of fluctuation noise and regular sine wave with an amplitude

of  $U_0$ . In this case the amplitude of total signal is distributed according to the generalized Rayleigh law, the density of distribution of probabilities for  $U$  which takes the form

$$W(U) = \frac{U}{\sigma^2} e^{-\frac{U^2 + U_0^2}{2\sigma^2}} I_0\left(\frac{UU_0}{\sigma^2}\right), \quad (3.18)$$

where  $I_0$  - a Bessel function of imaginary argument. The integral generalized Rayleigh law cannot be expressed in the analytical form and it is usually assigned graphically. During Rayleigh distribution for the amplitude its correlation coefficient is determined from formula [3.1]

$$R_U(\tau) = 0,921 p^2(\tau) + 0,0576 p^4(\tau) + 0,0144 p^6(\tau), \quad (3.19)$$

or according to the approximation formula

$$R_U(\tau) \approx p^2(\tau), \quad (3.20)$$

where

$$p^2(\tau) = R_p^2(\tau) + R_{pQ}^2(\tau). \quad (3.21)$$

With the combined passage through the filter of fluctuation noise and regular sine wave the correlation coefficient for the total amplitude is determined from very complicated formula [2.2; 3.3]. The approximate simple expression for this case obtained in [3.4] takes the form

$$R_U(\tau) \approx [p(\tau)]^2 e^{-S^2}, \quad (3.22)$$

where  $S^2 = \frac{U_0^2}{2\sigma^2}$  - ratio of the power of signal to the average power of noise. The phase of quasi-harmonic oscillation (3.7) is distributed evenly in the limits from 0 to  $2\pi$ , i.e., has probability density

$$W(\phi) = \frac{1}{2\pi}, \quad 0 \leq \phi < 2\pi. \quad (3.23)$$

The approximate simple expression for the coefficient of correlation of phase obtained in [3.4] takes the form

$$R_\phi(\tau) \approx \rho^{4/3}(\tau). \quad (3.24)$$

Page 88. P Quasi-harmonic oscillation (3.7) can be examined just as oscillation with the randomly instantaneous frequency  $\omega_0 + \Delta\omega(t)$ , moreover frequency  $\omega_0$  it is convenient to select for the equal abscissa of the "center of gravity" of energy spectrum, determined according to formula (3.8). The deviation of the instantaneous frequency from  $\omega_0$  the equally derived phase with respect to the time, i.e.,

$$\Delta\omega(t) = \frac{d\phi(t)}{dt}, \quad (3.25)$$

moreover phase  $\phi(t)$  is connected with  $P(t)$  and  $Q(t)$  with formula (3.10). During the symmetrical energy spectrum and the normal distribution of processes of  $P(t)$  and  $Q(t)$  the probability density for the deviations of the instantaneous frequency takes the form [3.2; 3.3]

$$W(\Delta\omega) = \frac{1}{\Delta\omega_1} \frac{1}{\left(1 - \frac{\Delta\omega^2}{\Delta\omega_1^2}\right)^{3/2}}, \quad (3.26)$$

and the integral law of probability distribution for the absolute value  $|\Delta\omega|$ :

$$P(|\Delta\omega| < \Delta\omega) = \frac{1}{\sqrt{1 - \frac{\Delta\omega^2}{\Delta\omega_1^2}}}. \quad (3.27)$$



Here  $\Delta\omega_1$  - average value for the absolute (on the sign) frequency deviation, i.e.,

$$\Delta\omega_1 = \overline{|\Delta\omega(t)|} \quad (3.28)$$

Value  $\Delta\omega_1$  is equal to the "radius of inertia" of energy noise spectrum as the plane figure and is determined from the formula

$$\Delta\omega_1^2 = \frac{\int_{-\infty}^{\infty} \Omega^2 g(\Omega) d\Omega}{\int_{-\infty}^{\infty} g(\Omega) d\Omega} \quad (3.29)$$

where  $\Omega = \omega - \omega_0$ ;  $\omega_0$  - central frequency, determined according to formula (3.8). the average significance of a deviation of frequency from  $\omega_0$  is equal to zero; the mean square of these divergences is calculated because it cannot, since the corresponding integral diverges.

Multiple-pronged signals. Let us now move on to the examination of signals with the multiple-pronged structure. Signal with the multiple-pronged structure is called signal at the output of the communication channel with the multiple-pronged (multipath) propagation of electromagnetic energy during the supplying to the input of the channel of sinusoidal oscillation with the frequency  $\omega_0$ ; it is assumed that this channel is linear four-pole has the random parameters. The dependence of amplitudes and phases of separate components of multiple-pronged signal on their time lag is determined, respectively, by the composite pulse reaction of channel

$S(\tau)$ , i.e., by response to the output of multiple-pronged channel, during the supplying to its input of "radio pulse" with the frequency  $\omega_0$  and the amplitude, which is changed according to the law of  $\delta$ -function <sup>1</sup>.

FOOTNOTE <sup>1</sup>. In the literature pulse reactor (or pulse transfer function) usually is called the response to the output of four-pole during the supplying to its input of the impulse of direct current [3.5]; response to the impulse with the high-frequency filling (radio pulse) in the literature occasionally referred to as pulse reaction on the envelope [3.6].

Page 89.

Actually for the multiple-pronged channel this response consists of the series/row of the delayed pulses which have amplitude and phase of filling correspond to amplitudes and to phases of the separate components of output multiple-pronged signal. For the estimate of distortions in the communication channel it is possible to utilize the composite transfer function of channel which characterizes a change in amplitude and phase of output signal with a change in the frequency of input signal. Composite transfer function can be recorded in the exponential form

$$\dot{K}(\Omega) = |K(\Omega)| e^{j\varphi(\Omega)}$$

(3.30)

or in the algebraic form

$$K(\Omega) = P(\Omega) + jQ(\Omega), \quad (3.31)$$

moreover

$$|K(\Omega)| = \sqrt{P^2(\Omega) + Q^2(\Omega)}, \quad (3.32)$$

$$\phi(\Omega) = \arctg \frac{Q(\Omega)}{P(\Omega)}. \quad (3.33)$$

Moreover  $|K(\Omega)|$  - amplitude-frequency, and  $\phi(\Omega)$  - phase-frequency of the characteristic of the channel;  $P(\Omega)$  and  $Q(\Omega)$  - with respect real and imaginary part of the transfer function. For the the specific  $k$ -th realization of the random parameters of multiple-pronged channel its composite transfer function and composite pulse reaction are connected with the pair of Fourier transforms [3.5]:

$$K_k(\Omega) = \int_{-\infty}^{\infty} S_k(\tau) e^{-j\Omega\tau} d\tau, \quad (3.34)$$

$$S_k(\tau) = \frac{1}{2\pi} \int_{-\infty}^{\infty} K_k(\Omega) e^{j\Omega\tau} d\Omega$$

Let us recall that in this examination  $S_k(\tau)$  - response to the effect of radio pulse with the frequency  $\omega_0$ . Therefore in (3.32)  $\Omega$  is detuning relative to frequency  $\omega_0$ , i.e.,  $\Omega = \omega - \omega_0$ .

Let us determine now, what analogy occurs between the fluctuation noise and the multiple-pronged signal. For the specific realization of fluctuation noise the dependence of amplitudes and phases of elementary harmonic components on the frequency is

determined by the composite spectrum  $S(\Omega)$ ; for the specific realization of multiple-pronged channel the dependence of amplitudes and phases of the separate components of signal at the output of their time lag is determined by the composite pulse reaction  $S(\tau)$ . The specific realization of fluctuation noise and its composite spectrum are connected with the pair of Fourier transforms (3.1). For the specific realization of multiple-pronged channel composite transfer function and composite pulse reaction are connected with the pair of Fourier transforms (3.34). Consequently, for the transfer function of multiple-pronged channel pulse reaction plays the same role, as the spectrum for the fluctuation noise. However, in the examination of one realization still there is no complete analogy between the spectrum of fluctuation noise and the pulse reaction of multiple-pronged channel. Actually the "spectrum" <sup>1</sup> of composite transfer function is obtained from it with the aid of the direct Fourier transform, while the pulse reaction  $S(\tau)$  is obtained from  $K(\Omega)$  with the aid of inverse transformation of Fourier.

FOOTNOTE <sup>1</sup>. Here and throughout word the spectrum is placed into the quotation marks, since discussion deals with the spectrum for functioning the frequency, but not the function of time, as this usually has the place in radio engineering.

Thus, the composite "spectra" of functions  $K(\Omega)$  and  $S(r)$  are characterized by sign with the imaginary part, i.e., have identical moduli, but different phases. The analogy indicated will be, however, complete, if we examine not one realization, but fluctuation noise and multiple-pronged channel as a whole. The spectral structure of fluctuation noise as a whole for all possible realizations is characterized by energy spectrum  $G(\Omega)$ ; for the characteristic of multiple-pronged channel as a whole it is possible to introduce the energy pulse reaction which is obtained as a result on all possible realizations of the square modulus of pulse reaction, i.e.,

$$G(\tau) = \overline{|S(\tau)|^2}. \quad (3.35)$$

During calculations it is convenient to use the standardized energy pulse reaction which is determined from the formula

$$g(\tau) = \frac{G(\tau)}{G(0)}. \quad (3.36)$$

A similar to energy spectrum energy pulse reaction characterizes only the averaged energy distribution according to the delaying components and does not consider the phase shifts between them.

Above it was shown that for one realization the "spectrum" of transfer function to the pulse reaction of multiple-pronged channel they coincide in the modulus. It is obvious, the same modulus have

the "spectra"  $P(\Omega)$  and  $Q(\Omega)$ , i.e., the real and imaginary parts of the transfer function. Therefore according to (3.2) the energy pulse reaction of multiple-pronged channel with the random parameters is the "energy spectrum" for real and imaginary parts and transfer function <sup>1</sup>.

FOOTNOTE <sup>1</sup>. For the composite function it is possible to speak only about the energy spectrum of real and imaginary parts, since for the complex quantity concept "energy" is deprived of sense. ENDFCCTNCTE.

Of this consists the analogy between the fluctuation noise and the multiple-pronged signal, from which follows this rule:

during the analysis of the transfer function of multiple-pronged channel with the random parameters it is possible to use the relationships of the theory of fluctuation noises, after replacing in these with relationships time by the frequency and the energy noise spectrum  $G(\Omega)$  for the energy pulse reaction of the multiple-pronged channel  $G(\tau)$ .

The rule indicated will be used for determining the static properties of the transfer function of multiple-pronged channel and, in particular, section of radiowave propagation in the troposphere. First of all, let us determine the static dependence between the

values of the real part of the transfer function of multiple-pronged channel at frequencies  $\omega$  and  $\omega + \Omega$ . This statistical dependence is described by the correlation coefficient in the frequency, which is determined by the relationship

$$R_p(\Omega) = \frac{\overline{P(\omega) P(\omega + \Omega)}}{\overline{P^2(\omega)}} \quad (3.37)$$

For the energy pulse reaction it is expedient to introduce the concept of the "central" time lag, equal to the abscissa of its center of gravity as the plane figure. Analogous with the central frequency of spectrum (3.8) this central time lag can be determined according to the formula:

$$\tau_0 = \frac{\int_{-\infty}^{\infty} \tau g(\tau) d\tau}{\int_{-\infty}^{\infty} g(\tau) d\tau} \quad (3.38)$$

Page 91.

Then, by analogy with (3.11) the correlation coefficients in the frequency for the real and imaginary parts of the transfer function  $P(\Omega)$  and  $Q(\Omega)$  they are connected with the energy pulse reaction whose center is displaced to the zero time lag, by the relationship/ratio

$$R_p(\Omega) = R_Q(\Omega) = \frac{\int_{-\infty}^{\infty} g(\tau_1) \cos \Omega \tau_1 d\tau_1}{\int_{-\infty}^{\infty} g(\tau_1) d\tau_1} \quad (3.39)$$

where  $\tau_1 = \tau - \tau_0$ ;  $\tau_0$  it is determined according to formula (3.38). The

coefficient of cross correlation for random functions  $P(\Omega)$  and  $Q(\Omega)$  by analogy with (3.12) is determined by the relationship

$$R_{PQ}(\Omega) = \frac{\int_{-\infty}^{\infty} g(\tau_1) \sin \Omega \tau_1 d\tau_1}{\int_{-\infty}^{\infty} g(\tau_1) d\tau_1}, \quad (3.40)$$

from which it follows that

$$R_{PQ}(0) = 0, \quad (3.41)$$

i.e. values  $P(\Omega)$  and  $Q(\Omega)$  are not correlated at the coinciding frequencies. If energy pulse reaction is symmetrical relative to its central time lag, determined according to formula (3.38), then from (3.39) and (3.40) it follows that

$$R_P(\Omega) = R_Q(\Omega) = \frac{\int_0^{\infty} g(\tau_1) \cos \Omega \tau_1 d\tau_1}{\int_0^{\infty} g(\tau_1) d\tau_1} \quad (3.42)$$

and

$$R_{PQ}(\Omega) \equiv 0, \quad (3.43)$$

i.e. values of the real and imaginary parts of the transfer function they are not correlated for any frequencies. The projections of the amplitude of total signal on the coordinate axes, considered as the functions of frequency, depict, obviously, the real and imaginary parts of the transfer function of multiple-pronged channel (on the specific scale). From Fig. 1 it follows that

$$\left. \begin{aligned} P(\Omega) &= \sum_{k=1}^n U_k \cos(\Omega \tau_k + \varphi_k) \\ Q(\Omega) &= \sum_{k=1}^n U_k \sin(\Omega \tau_k + \varphi_k) \end{aligned} \right\} \quad (3.44)$$



Let us assume now that the signal at the output of multiple-pronged channel is created by a large quantity of uniform reemitters, moreover signal amplitudes, reflected from these reemitters, are statistically not depended, and the phases of signals evenly distributed in the limits from 0 to  $2\pi$ .

Page 92.

Under the assumptions of value  $F(\Omega)$  and  $Q(\Omega)$  indicated are the sums of a large quantity of independent and equally distributed components with amplitudes of  $U_k$  and time lags  $\tau_k$ . Consequently, according to central limit theorem the probability theory (to Lyapunov theorem) values  $P(\Omega)$  and  $Q(\Omega)$  are distributed according to the normal law [3.2; 3.3]. Since the phases of components  $\varphi_k$  are distributed evenly from zero to  $2\pi$ , then all composed and, consequently, also values  $P(\Omega)$  and  $Q(\Omega)$  have zero average value. Furthermore, as it was shown above,  $P(\Omega)$  and  $Q(\Omega)$  between themselves were not correlated. From the theory of fluctuation noises it is known [for 3.2; 3.3], that with the statistical properties of values  $F(\Omega)$  and  $Q(\Omega)$  indicated the values of amplitude-frequency characteristic of multiple-pronged channel, connected with  $F(\Omega)$  and  $Q(\Omega)$  with relationship (3.32), are distributed according to the law of Rayleigh, i.e., have density probabilities (3.16) and integral law of probability distribution (3.17). The values of the phase-frequency characteristic, connected

with  $P(\Omega)$  and  $Q(\Omega)$  with relationship (3.33), are distributed evenly from 0 to  $2\pi$ , i.e., they have a probability density (3.23).

During the Rayleigh distribution for the values of the amplitude-frequency characteristic the correlation coefficient between these values at frequencies  $\omega$  and  $\omega + \Omega$  it is analogous (with 3.19), (3.20) and (3.21) it can be determined according to the formula

$$R_{\rho}(\Omega) = 0.921 \rho^2(\Omega) + 0.0576 \rho^4(\Omega) + \dots \quad (3.45)$$

or according to the approximation formula

$$R_{\rho}(\Omega) \approx \rho^2(\Omega), \quad (3.46)$$

where

$$\rho^2(\Omega) = R_p^2(\Omega) + R_Q^2(\Omega). \quad (3.47)$$

Besides the random components, at the output of multiple-pronged channel can be present also regular component with the permanent time lag and with a permanent amplitude of  $U_0$ . In particular, this situation can occur during the remote tropospheric propagation of VHF, when at the input of receiver is regular component, caused by refraction or reflection from inversion layer. This case is analogous to the combined passage through the filter of fluctuation noise and regular sine wave. Therefore when, at the output, the multiple-pronged channel of regular component is present, the amplitude of total signal is distributed according to the generalized Rayleigh law, i.e., has probability density (3.18); the integral law

of probability distribution is assigned graphically [3.2, 3.3].

The correlation coefficient in the frequency for the values of the amplitude-frequency characteristic in the presence of regular component analogous (with 3.22) can be calculated according to the approximation formula

$$R_{\omega}(\Omega) \approx [\rho(\Omega)]^{2e^{-S^2}}, \quad (3.48)$$

where  $\rho(\Omega)$  is determined by relationship (3.47);  $S^2$  - relation of the power of regular component and mean total power of the scattered components.

The correlation coefficient between the phases of signal at frequencies  $\omega$  and  $\omega + \Omega$  can be calculated according to formula (3.24), where  $\rho(\Omega)$  is determined by relationship (3.47).

For the evaluation of signal distortions in the multiple-pronged communication channels important value has the derivative of the phase-frequency characteristic of this channel, which is usually called "group time lag" <sup>1</sup>.

FOOTNOTE <sup>1</sup>. Sometimes also is utilized term "the group propagation time. ENDFOOTNOTE.

In the theory of fluctuation noises to group time lag corresponds,

obviously, instantaneous frequency, as the derivative of the phase of noise on the time. For the evaluation of distortions and multiple-pronged channel importantly not value itself  $\tau_p$  and divergence  $\tau_p$  from the central time lag which are called the fluctuations of the group time of propagation  $\Delta\tau_p$ .

Page 93.

If central time lag is defined as the abscissa of the center of gravity of an energy-pulse reaction according to formula (3.38), then in the presence of the symmetrical pulse reaction probability density for the fluctuations of group time lag by analogy with (3.26) takes the form

$$W(\Delta\tau_p) = \frac{1}{\Delta\tau_1} \cdot \frac{1}{\left(1 + \frac{\Delta\tau_p^2}{\Delta\tau_1^2}\right)^{\frac{3}{2}}} \quad (3.49)$$

The integral law of probability distribution for  $|\Delta\tau_p|$  by analogy with (3.27) takes the form

$$F(|\Delta\tau_p| < \Delta\tau_p) = \frac{1}{\sqrt{1 + \left(\frac{\Delta\tau_1}{\Delta\tau_p}\right)^2}} \quad (3.50)$$

Here  $\Delta\tau_1$  - mean value for the absolute (on the sign) value of fluctuations, i.e.,

$$\Delta\tau_1 = \overline{|\Delta\tau|} \quad (3.51)$$

By analogy with (3.29)  $\Delta\tau_1$  equal to the "radius of inertia" of

energy pulse reaction as the plane figure it can be calculated according to the formula

$$\Delta \tau_1^2 = \frac{\int_{-\infty}^{\infty} \tau_1^2 g(\tau_1) d\tau_1}{\int_{-\infty}^{\infty} g(\tau_1) d\tau_1} \quad (3.52)$$

where  $\tau_1 = r - r_0$ ;  $r_0$  it is determined according to formula (3.38).

Mean value of the fluctuations of the group propagation time is equal to zero. The mean square of these fluctuations is calculated but it cannot, since corresponding integral diverges.

Concluding the examination of the analogy between the fluctuation noises and the multiple-pronged signals let us touch one additional question. All relationships for the transfer functions of multiple-pronged channel, given in this section, are correct only during the normal probability distribution for the real and imaginary parts of the transfer function  $F(\omega)$  and  $Q(\omega)$ .

Normal distribution for  $F(\omega)$  and  $Q(\omega)$  in this examination was obtained from formulas (3.44). It follows, however, it remembers that expressions (3.44) for  $F(\omega)$  and  $Q(\omega)$  correspond to the so-called "incoherent" scattering of radio waves on the discrete reemitters. But, as shown in Chapter 1, incoherent scattering is only the simplified model of the exact tropospheric propagation of VHF. In

actuality the mechanism of this propagation is more complicated and in general at the output of the section of propagation is not a discrete, but continuum of signals, how conveniently which differ little in the time lag. Therefore in general expressions (3.44) for  $P(Q)$  and  $Q(Q)$  must be recorded in the form of integral sums, elementary terms in these sums can be dependent and distributed not identical. Thus, Lyapunov theorem here is not applied, and therefore there are no foundations for asserting that  $P(Q)$  and  $Q(Q)$  will be compulsorily distributed according to the normal law. However, with satisfaction of the specified conditions the sum of a large number of terms is distributed normally [3.2; 3.3] and with dependent and different of distributed terms. However, to establish that during the tropospheric propagation of VHF these conditions are satisfied, very complex. For this it is necessary to know the statistical properties of the separate components of multiple-pronged signal, meanwhile the study of the signals, re-emitted with elementary ones they are distributed normally.

Page 94.

Nevertheless, for determining signal distortions on the tropospheric lines of communications nevertheless it is possible to use the relationships given in this section. The fact is that the Rayleigh distribution for the signal amplitude at the output of

FD-302 (Rev. 4-15-64)

FOREIGN TECHNOLOGY DIV WRIGHT-PATTERSON AFB OH  
REMOTE TROPOSPHERIC RADIO COMMUNICATION, (U)  
MAR 80 I A GUSYATINSKIY, A S NEMIROVSKIY  
FTD-ID(RS)T-0251-80

F/O 27/21

**UNCLASSIFIED**

**E**

3 of 6'  
ADA  
A063455

[illegible]

section of tropospheric propagation experimentally is confirmed for the majority of the used in practice routes, is experimentally confirmed also that the phase of signal is distributed evenly in the limits from 0 to  $2\pi$ . But Rayleigh distribution for the signal amplitude and uniform for the phase can occur only during the normal distribution for  $P(\Omega)$  and  $Q(\Omega)$ . But this, in turn, it means that for the transfer function of multiple-pronged tropospheric channel will be valid the given above relationships. Let us recall that these relationships are obtained under the most general assumptions about the pulse reaction of channel, which for all or some realizations can be continuous function  $\tau$ . Let us note also that on comparatively short and marine routes for the signal amplitude experimentally is confirmed the generalized Rayleigh law.

### § 3.3. Frequency and phase responses of the section of tropospheric line.

In this section will be examined the statistical properties of the amplitude-frequency and phase-frequency characteristics of the section of tropospheric line. The analysis of the statistical properties of these characteristics will be carried out for the tropospheric lines, intended for multichannel telephony and television. As has already been indicated, on such lines the length of section does not exceed 250-300 km, and the width of radiation



pattern of antenna comprises not more than  $1-15^\circ$ .

Energy pulse reaction of the section of line. In § 3.2 it was shown that the statistical properties of the frequency and phase responses of the section of tropospheric line can be determined, if it is known the energy pulse reaction of this section. Thus, it is first of all necessary to find expression for the energy pulse reaction of the section of line, i.e., the dependence of the mean power of the components of multiple-pronged signal on their time lag. Total multiple-pronged signal at the output of the section of line is created as a result of the re-emission of electromagnetic energy by a large quantity of heterogeneities of the troposphere. In this case the signals with the identical time lag are re-emitted by a whole series of the heterogeneities, located on the surface whose all points have the identical sum of distances of the transmitting and receiving antennas. For determining the shape of surface of "equal time lag" let us examine Fig. 3.3a and b. Fig. 3.3a shows the section of the section of tropospheric line by the plane, passing through the center of the earth and the line, which connects the points of reception and transmission ("section along the route"). The points, which have identical total distance of the transmitting and receiving antennas, in this plane are located on the ellipses with the foci in points of reception and transmission; several such ellipses are shown in Fig. 3.3a.

Page 95.

Fig. 3.3b shows section perpendicular to route. In this plane the points with the identical total distance of the transmitting and receiving antennas lie on the circumferences whose centers are located on the middle of the cut between the points of transmission and reception (point 0 in Fig. 3.3a and b). Several such circumferences are shown in Fig. 3.3b. Thus, "surfaces with the equal time lag" are ellipsoids of rotation with the axis, passing through the points of reception and transmission, and with the foci at these points.

Further during the determination of the pulse reaction it is necessary to keep in mind that the signal at the reception is created only by those heterogeneities which they lie within the limits of the "space of the scattering", formed by the intersection of the radiation patterns of the transmitting and receiving antennas. The section of the space of scattering by section plane along the route has a form of quadrangle and is shown in Fig. 3.3a by twin circuits.

Usually on the tropospheric center lines of the antenna radiation patterns they are raised relative to horizontal line to the

small angle of order of  $1-2^\circ$ . Therefore, as can be seen from Fig. 3.3a, section plane of the perpendicular to route cuts the cone of the antenna radiation pattern at angle relative to axis, close one to  $90^\circ$ . Consequently, the section of the space of scattering by this plane virtually has a form of circle with the center at the point of intersection of the axes of radiation patterns (strictly speaking, this section it has a form of ellipse with the ratio of axes, by close one to the unit). This circumference is shown in Fig. 3.3b by twin circuits. During the determination of energy pulse reaction us interest only those sections of the planes with the equal time lag which lie within the space of scattering. Fig. 3.3a and b the sections of these sections shows by thick lines.

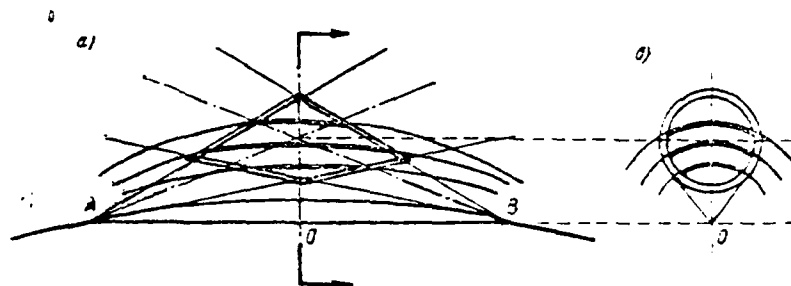


Fig. 3.3. Surfaces with equal signal lag: a) section along the route,  
b) section is perpendicular to route.

Page 96.

During the determination of energy pulse reaction it is necessary to know the mean power of signals with the data by time lag. The power of signals at the reception depends on that, in what part of the space of scattering is located the re-emitting heterogeneity. The heterogeneities, located in the area of the intersection of the axes of the radiation patterns of the transmitting and receiving antennas, create the signals of larger intensity than the heterogeneities, located on the periphery of the space of scattering. This is determined by the directivity of the transmitting and receiving antennas. Furthermore, the heterogeneities, located in the lower part of the space of scattering, better re-emit energy than heterogeneity in the upper part of the space. This they expect energy, than heterogeneity in the upper part of the space. This is explained, mainly, by an increase in the angle of "scattering" with the height. The angle of "scattering" increases also, if heterogeneities are located "to the right and to the left" of the direction of main antenna radiation. Thus, the energy pulse reaction of the section of tropospheric line is

determined by the geometry of surfaces with the equal time lag, by the geometry of the space of scattering, by the antenna radiation pattern and by a change in the angle of the "dissipation" of electromagnetic energy. In general the computation of energy pulse reaction is fairly complicated problem. For this it is necessary to conduct integration for the surface of equal time lag in the limits of the space of scattering taking into account the directivity of antennas and change in the scattering angle. However, for the real tropospheric lines, intended for multichannel telephone and television, this problem it is possible substantially to simplify, on the basis of the following considerations:

1. On the real tropospheric lines the altitude of the space of scattering by the Earth comprises several kilometers, and the distance between the points of reception and transmission - several hundred kilometers. Therefore in the ellipses with the equal time lag, depicted in Fig. 3.3a minor axis much less than the distance between the foci <sup>1</sup>.

FOOTNOTE 1. Figure 3.3a for the clarity is made without the observance of scale. ENDFOOTNOTE.

In other words, these ellipses are strongly elongated along the route, and therefore their cuts in the limits of the space of

scattering can be replaced with the cuts of straight lines. On the basis of the geometric ratios of Fig. 3.3b, it is possible to show also that at the length of section 250-300 km and directivity of antennas of 1-1.5° circular arcs with the equal time lag, which are located within the limits of the space of scattering, have central angle on the order of 30-40°. Consequently, without the large error these arcs also can be replaced with the line segments. Thus, for the real tropospheric lines of the "surface of equal time lag" in the limits of the space of scattering it is possible to replace with parallel planes. Respectively time lag for each such plane is determined by its altitude above the ground.

Page 97.

2. With pencil-beam antennas scattering angle of electromagnetic energy within limits of space of scattering changes insignificantly. Therefore, as shown in [3.4], the mean power of the delaying components of signal at the point of receptor is determined in essence by the antenna radiation pattern, but not by a change in the scattering angle.

3. Area of sections of surfaces with equal time lag, situated within space of scattering, depends on their altitude. As can be seen from Fig. 3.3a and b, this area is maximum for the center of the

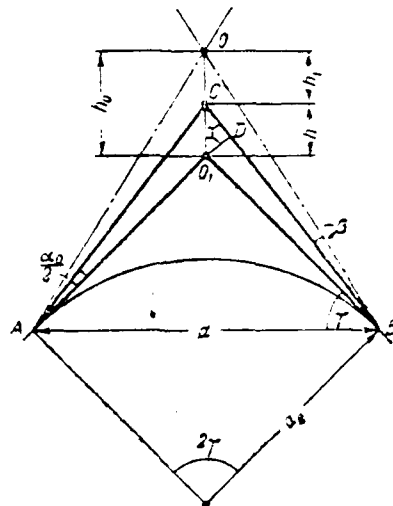
space of scattering and decreases for its upper and lower parts. With respect to different ones there will be a quantity of heterogeneities, which participate in the creation of component with the specific time lag. Strictly speaking, this one must take into account during the computation of the pulse reaction of the section of propagation. However, during the use of the pencil-beam antennas by this fact also it is possible to disregard.

Thus, from entire aforesaid it follows that with the sufficiently pencil-beam antennas the time lag of the components of signal at the receptor depends, in essence only from the altitude of the heterogeneities above the ground and the mean power of these components virtually is determined only by the antenna radiation pattern. During the use of this simplified model of multiple-pronged propagation the computation of the energy pulse reaction of the section of propagation substantially is facilitated. Let us note, however, that the given above considerations carry purely qualitative character. Therefore it is necessary to explain, what must be directivity of antennas and length of section, so that during the use of the simplified model error during the computation of pulse reaction would not exceed the specific value. To this question we still will return after will be obtained expression for the coefficient of frequency correlation. And let us thus far calculate energy pulse reaction for the simplified model of multiple-pronged



propagation, assuming that the conditions for using this model are satisfied.

Let us examine Fig. 3.4, in which are shown the paths of propagation for two components: one component is re-emitted by the heterogeneity, located at the lower point of the space of scattering  $O_1$ , time lag for this component we will consider zero; the second component is re-emitted by the heterogeneity, located on altitude  $h$  above point  $O_1$  (point  $G$ ).



Page 98.

$$\Delta S \approx 2CD = 2h \sin \gamma \approx 2h \gamma. \quad (3.53)$$

From the geometric ratios of Fig. 3.4 it is evident that

$$\gamma \approx \frac{d}{a_e}, \quad (3.54)$$

where  $d$  - length of the section of the tropospheric line;  $a_e$  - equivalent radius of the Earth. From (3.53) and (3.54) it follows that the relative time lag for the component of signal, re-emitted with heterogeneity at altitude  $h$ , is determined by the ratio

$$\tau = \frac{\Delta S}{c} = \frac{hd}{ca_e}, \quad (3.55)$$

where  $c$  - velocity of propagation of electromagnetic energy. As has already been spoken, the mean power of the delaying components is determined in essence by the total radiation pattern of the transmitting and receiving antennas, which can be approximated by Gaussian curve <sup>1</sup> and recorded in the form

$$g(\theta) = e^{-\frac{\theta^2}{2\alpha_0^2}}, \quad (3.56)$$

where  $\theta$  - angle between the axis of antenna and the direction in the heterogeneity, located on altitude  $h$  (see Fig. 3.4);  $\alpha_0$  - width of the antenna radiation pattern on the angle of half power.

FOOTNOTE <sup>1</sup>. The correctness of this approximation is confirmed by the experimental measurements of the diagram of the antennas of the tropospheric lines (see §3.4). ENDFOOTNOTE.

Permanent factor in the index of exponential curve is selected so, in order to with  $\beta = \alpha_0/2$   $g(\beta) = 1/4$  (due to two antennas). We will consider that the positive angles  $\beta$  are calculated "upward" from the center of the volume of scattering 0. Then from the geometric ratios in Fig. 3.4 we have

$$-\beta \approx \frac{h_1}{d/2} = \frac{h_0 - h}{d/2}. \quad (3.57)$$

Let us introduce also the relative time lag, which corresponds to the center of the space of scattering, which in accordance with (3.55) is equal

$$\tau_0 = \frac{h_0 d}{c a_0}. \quad (3.58)$$

Further let us determine from (3.55) and (3.58)  $h$  and  $h_0$  and let us substitute them in (3.57), after which let us substitute (3.57) in (3.56).

Page 99.

As a result we will obtain final formula for the energy pulse reaction of the section of tropospheric line in the form:

$$\left. \begin{aligned} g(\tau) &= e^{-\Delta \sigma_1^2 (\tau - \tau_0)^2} & \text{при } \tau > 0 \\ g(\tau) &= 0 & \text{при } \tau < 0 \end{aligned} \right\}. \quad (3.59)$$

Key: (1). with.

where  $\Delta\Omega_1$  - parameter, which has the dimensionality of angular frequency and determined by the ratio

$$\Delta\Omega_1 = 2\pi \left( 0,75 \frac{ca_e}{d^2 a_0} \right). \quad (3.60)$$

The energy pulse reaction of the section of tropospheric line is shown in Fig. 3.5 on relative scale  $\Delta\Omega_1\tau$ ; its maximum it corresponds to time lag  $\tau_0$ , i.e., to time lag for the center of the space of scattering. Let us recall that the energy pulse reaction takes this form, only if the axes of antennas are raised to the angle  $\alpha_0/2$  relatively tangential to the ground at points of reception and transmission. On the real tropospheric lines for obtaining the maximum power of signal at the reception the antennas orient approximately thus.

Coefficient of frequency correlation. Now, after using ratios §3.2 it is possible to obtain formula for computing the correlation coefficient between the values of the amplitude-frequency characteristic. For this at first should be determined the "central time lag" of energy pulse reaction according to formula (3.38). However, before it is necessary to make one observation: function  $g(\tau)$ , determined by Gaussian curve (3.59), rapidly decreases in the region of negative time lags. Therefore without the essential error it is possible to consider that in the region of negative time lags the energy pulse reaction is not equal to zero, but it is determined by Gaussian curve (3.59) (dotted line in Fig. 3.5).

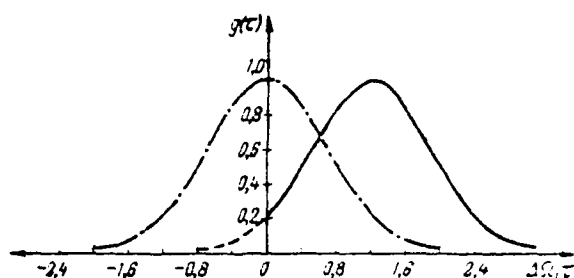


Fig. 3.5. The energy pulse reaction of the section of radiowave propagation in the troposphere (axes of antenna are directed at angle  $\alpha_0/2$  to the horizon).

Page 100.

Then the central time lag of pulse reaction, defined according to formula (3.37) as the abscissa of its "center of gravity", is equal, obviously,  $\tau_0$ . Consequently, for the energy pulse reaction whose center is displaced to the zero time lag, instead of (3.59) we have

$$g(\tau_1) = e^{-\frac{1}{2} \frac{\tau_1^2}{T^2}}, \quad (3.61)$$

where  $\tau_1 = \tau - \tau_0$ . This displaced pulse reaction is constructed dot-dash line in Fig. 3.5. Since the energy pulse reaction can be considered symmetrical relative to its center, then for determining the coefficients of correlation and cross correlation of the real and imaginary parts of the transfer function should be used relationships

(3.42) and (3.43). Substituting (3.61) in (3.42) and after producing the computation of integrals [3.7], we will obtain the following expression for the correlation coefficient between the values of the real (or imaginary) of the parts of the transfer function on frequencies  $\omega$  and  $\omega + \Omega$

$$R_p(\Omega) = R_q(\Omega) = e^{-\frac{1}{2} \left( \frac{\Omega}{\Delta\Omega_0} \right)^2}, \quad (3.62)$$

where

$$\Delta\Omega_0 = \sqrt{2} \Delta\Omega_1. \quad (3.63)$$

According to (3.43) the coefficient of the cross correlation between the values of the real and imaginary parts of the transfer function is equal to zero with any frequency separation; i.e.

$$R_{pq}(\Omega) \equiv 0. \quad (3.64)$$

Further, after using formula (3.46), it is possible to determine the correlation coefficient for the values of the modulus of transfer function, i.e., values of frequency characteristic. After substituting (3.62) and (3.64) in (3.47) and the result of this substitution in (3.46), after switching over from the angular frequencies to frequencies in the hertz, we will obtain the following expression for the correlation coefficient between the values of frequency characteristic at frequencies  $f$  and  $f + F$ :

$$R_c(F) = e^{-\left( \frac{F}{\Delta f_0} \right)^2}, \quad (3.65)$$

moreover according to (3.60) and (3.63)

$$\Delta f_0 = \frac{\Delta \Omega_0}{2\pi} = 1.06 \frac{ca_e}{j^2 x_0} \approx \frac{ca_e}{j^2 x_0}. \quad (3.66)$$

Value  $\Delta f_0$  is usually called a "band or a radius of correlation". From (3.65) it is evident that  $\Delta f_0$  there is the band on edges of which the values of frequency characteristic have a correlation coefficient, equal to  $1/e$ .

Page 101.

If at the output of the section of tropospheric line, besides the random components, is present regular component, then the correlation coefficient between the values of the amplitude-frequency characteristic can be obtained according to formula (3.48) taking into account (3.47), (3.62) and (3.64). Let us recall that expression (3.65) is obtained for the simplified model of tropospheric propagation, moreover this model is valid at the pencil-beam antennas and too great a length of section<sup>1</sup>.

FOOTNOTE <sup>1</sup>. Analogous expression is obtained in (3.8) somewhat by other means. ENDFOOTNOTE.

The computation of the coefficient of frequency correlation taking into account all factors, which are determining the pulse reaction of



section (geometry of the space of scattering, change in the scattering angle, etc.) is carried out [3.9]. Obtained in [3.9] the fairly complicated expression correctly also for the weakly directed antennas. With  $\alpha_0 \leq 1.5^\circ$  and  $d \leq 300$  km dependence  $R_c(F)$ , obtained in [3.9], very closely coincides with (3.65). This defines the boundaries of the applicability of the simplified model of tropospheric propagation, i.e., it is possible to consider that all relationships of this section are valid, if the width of the antenna radiation pattern does not exceed  $1.5^\circ$ , and the length of the section of tropospheric line comprises not more than 300 km. On the real tropospheric lines, intended for the transmission multichannel telephony and the televisions, these conditions usually are fulfilled. Calculations according to formula (3.65) coincide well with the results of experimental measurements in the sections of different length [3.10].

Frequency characteristic of the section of line. The correlation coefficient between the values of the frequency characteristic of section gives the evaluation of the band of the signal which can be transmitted along the tropospheric line without the essential distortions. If into limits the bands of the signal of the value of frequency characteristic have a correlation coefficient, close one to the unit, distortions will be small. However, this evaluation is tentative, purely qualitative, since the correlation coefficient

gives only the averaged picture of distortions and it does not make it possible to judge possible short-term distortions of frequency characteristic. Meanwhile such short-term distortions can be considerable, even if in the apparatus of the frequency band in question is large correlation of values of frequency characteristic. Distortions of the frequency characteristic of the section of tropospheric line considerably more complete it is possible to estimate with the aid of the relation of signal amplitudes on the edges of the assigned band. This estimate is used extensively in radio engineering; however, it is necessary to keep in mind that in our case the form of the frequency characteristic of the section of tropospheric line continuously changes in the time randomly. Consequently, it is necessary to find the law of probability distribution for the relation of signal amplitudes on the edges of the assigned band.

As has already been indicated into §3.2, signal amplitude at any frequency was distributed according to the law of Rayleigh, i.e., has probability density (3.16).

Page 102.

Furthermore, it is known that with the assigned frequency separation the correlation coefficient between the signal amplitudes can be

calculated according to formula (3.65). Thus, it is necessary to find the law of probability distribution for relation two sublimity with the Rayleigh distribution; the correlation coefficient between these values is known and, therefore, known their two-dimensional law of distribution [3.2, 3.3]. The methods of the probability theory make it possible to find the law of distribution for the quotient, if is known the two-dimensional law of the distribution of dividend and divider. With the aid of these methods in [3.8] is found the probability density for relationship of the values of the frequency characteristic of the section of line on the edges of band  $\Delta f$ . This probability density takes the form

$$W(k) = \frac{2k}{(1+k^2)^2} \cdot \frac{1 - R_U(F)}{\left[1 - R_U(F) \left(\frac{2k}{1+k^2}\right)^2\right]^{\frac{3}{2}}}, \quad (3.67)$$

where  $k$  - a relation of the values of frequency characteristic on the edges of band  $\Delta f$ ;  $R_U(F)$  - correlation coefficient between these values, determined according to formula (3.65). From (3.67) can be obtained the integral law of probability distribution for the relation  $k$  indicated which is determined by the expression

$$W(k < K) = \int_0^K W(k) dk = \frac{1}{2} \left[ 1 - \frac{1 - K^2}{\sqrt{(1+K^2)^2 - 4R_U(F)K^2}} \right]. \quad (3.68)$$

Integral law (3.68) determines probability that relation  $k$  does not exceed value  $K$ . However, frequency characteristic has identical

nonuniformity, if the amplitude ratio on the edges of band is equal to  $K$  or  $1/k$ . Probability that the frequency characteristic has relationship of amplitudes on the edges of band gain  $K$  or not less than  $1/k$  is equal to the association of the probabilities of these incompatible events. Consequently, according to the theorem of addition [3.1-3.3] this probability is equal to

$$W\left(k < K, k > \frac{1}{K}\right) = W(k < K) + W\left(k > \frac{1}{K}\right). \quad (3.69)$$

For the integral law of probability distribution (3.68) it is possible to show that

$$W(k < K) = W\left(k > \frac{1}{K}\right). \quad (3.70)$$

Consequently, taking into account (3.68-3.70) the integral law of probability distribution for the nonuniformity of the frequency characteristic section of tropospheric line takes the form

$$W\left(k < K, k > \frac{1}{K}\right) = \left[1 - \frac{1 - K^2}{\sqrt{(1 - K^2)^2 - 4R_c(F)K^2}}\right]. \quad (3.71)$$

Page 103.

The curves of the integral law of probability distribution for the nonuniformity of frequency characteristics are shown by solid lines in Fig. 3.6. These curves are constructed according to formula (3.71) for different values  $R_c(F)$ .

In a number of cases in the section of tropospheric line at the point of reception besides the random scattered components, is present also regular component of signal. In these cases for determining the distortions of the frequency characteristic of section it is necessary to find the law of probability distribution for the relation of two values, distributed according to the generalized Rayleigh law (3.18). This problem is solved in [3.11], where is found integral law of probability distribution for the nonuniformity of frequency characteristic in the presence of regular component. Expression for this law takes the fairly complicated form and here is not given <sup>1</sup>.

FOOTNOTE <sup>1</sup>. This expression, besides [3.11], is given also in [3.10].  
ENDFOOTNOTE.

Considerably more simply is obtained approximation in the presence of the regular component whose power not less than 1.5-2 times exceeds the power of the scattered components. This case is of greatest interest for the practice, since only essential regular component noticeably improves the nonuniformity of the frequency characteristic of the section of line. In the presence of considerable regular component for the integral law of the nonuniformity of frequency characteristic in the band  $\Delta f$  in [3.12] is obtained the approximation

$$W\left(k < K, k > \frac{1}{K}\right) = \Phi(S^2 \sqrt{2}) - \Phi(S^2 \sqrt{2}) \times \\ \times \frac{1-K}{\sqrt{K^2 - 2R_G(F)K + 1}}. \quad (3.72)$$

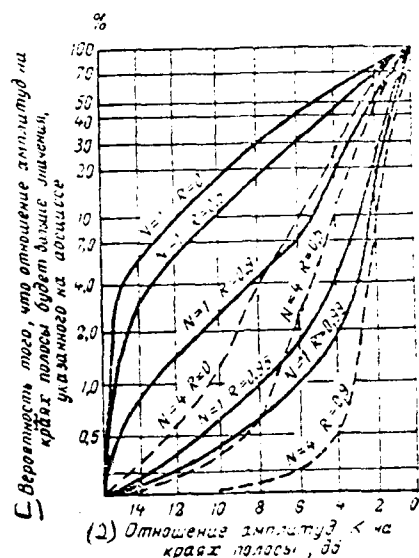


Fig. 3.6. Integral law of probability distribution for the nonuniformity of the frequency characteristic of the section of tropospheric line with the single ( $N=1$ ) and combined in fours ( $N=4$ ) receptions.

Key: (1). Probability that the amplitude ratio on the edges of band will be more than the value, indicated on the abscissa. (2). Ratio of amplitudes  $K$  on edges of band, dB.

Page 104.

Here  $S^2$  - ratio of the power of regular component to the mean

total power of the scattered components;  $\Phi(z)$  - probability integral. Expression (3.72) is correct with  $S^2 \leq 1.5-2$ ,  $R_c(F) \leq 0.9$ .

On the tropospheric lines of communications frequently is utilized the diverse reception during the addition of signals in the circuit of intermediate frequency to the detector. In this system of the diverse reception is conducted the automatic tuning of the phases of the stored signals, as a result of signal amplitude they are summarized arithmetically. Therefore the amplitude of total signal is the sum of the Rayleigh distributed values, i.e., has a law of probability distribution (2.44). Respectively for the evaluation of the nonuniformity of frequency terminal characteristic of this system of the diverse reception it is necessary to find law of probability distribution for the quotient two values, distributed according to the law [2.44]. This is made in [3.12], where is found the law of probability distribution for the nonuniformity of frequency characteristic during the diverse reception and the addition of signals in the circuit of intermediate frequency. This law takes the form:

$$W\left(k < K, k > \frac{1}{K}\right) = \Phi\left(\sqrt{\frac{\pi N}{4-N}}\right) - \Phi\left(\sqrt{\frac{\pi N}{4-N}} \times \left(\frac{1-K}{\sqrt{K^2 - 2R_c(F)K + 1}}\right)\right), \quad (3.73)$$

where  $N$  - a multiplicity of the reception;  $\Phi(z)$  - probability integral.

FOOTNOTE 1. Expression (3.73) approximately describes the law of probability distribution for nonuniformities of frequency characteristic, moreover its accuracy increases with increase of  $N$ . With  $N=4$  the error is insignificant. ENDECCINCTE.

In Fig. 3.6 dotted line showed the curves of the law of probability distribution for nonuniformities of frequency characteristic with quadrupled reception ( $N=4$ ). These curves are constructed according to formula (3.73) for different values  $R_0(F)$ . In Fig. 3.6 it is evident that in the system of the diverse reception during the addition of signals to the detector occurs the considerable decrease of the nonuniformity of the frequency characteristic of the section of line. Respectively in this system decrease distortions of the signals, transmitted by the line; however, in regard to this it is necessary to make one observation: expression (3.73) is correct when the phasing of signals occurs at all frequencies in the limits of band  $\Delta f$ . Virtually this not thus: the signals, transmitted by the line, can have sufficiently wide spectrum, meanwhile the phasing occurs only at one frequency<sup>2</sup>.

FOOTNOTE 2. With CHM, which usually is utilized on the tropospheric lines, this frequency corresponds to the constant component of the



modulating signal (see Chapter 2). ENDOCTNCTE.

At other frequencies the spectral components of the stored signals have different and random phases, and therefore system of addition does not give here the gain, which corresponds to formula (3.73). However, virtually this incomplete phasing within the limits of band does not strongly impair total frequency characteristic.

Page 105.

The fact is that on the tropospheric lines to avoid strong distortions for the transmission of signals is utilized the band of the strongly correlated values of frequency characteristic. In this case the correlation between the phases of the spectral components of signal is also great [3.2; 3.3]. Therefore it is possible to consider that in the limits of band is a complete phasing of the stored signals. Thus, expression (3.73) and graphs of Fig. 3.6 it is possible to use, if the correlation coefficient between the amplitudes on the edges of band  $\Delta f$  is virtually not less than 0.9.

The experimental measurements of the frequency characteristic of the section of tropospheric line repeatedly were made on many routes; the results of these measurements are given in Chapter I and in [3.10, 3.13]. Since the form of frequency characteristic continuously

changes in the time, then these measurements cannot be conducted with a slow change in the frequency of transmitter ("on the points"). Therefore on the tropospheric lines for measuring the frequency characteristic of the section of radiowave propagation is utilized a rapid change in the frequency of transmitter in the saw-tooth law ("sweeping"). For this to the input of the frequency shift key of transmitter is supplied the saw-tooth voltage with the frequency of 50-100 Hz. On receiving dead ending the voltage from the output of amplitude detector is supplied to the vertical plates of the oscillograph; sweep of oscillograph is synchronized by signal from the output of the FM discriminator. The quasi period of the fluctuations of signal amplitude comprises fractions of a second, and the period of a saw-tooth change in the frequency of transmitter - the hundredth fractions of a second. Therefore during the period of "sweeping" parameters of multiple-pronged channel in the troposphere virtually do not manage to change and on the oscilloscope face are obtained the images of the "instantaneous" frequency characteristics of the section of line (Fig. 3.7)<sup>1</sup>.

FOOTNOTE <sup>1</sup>. These photographs are undertaken from [3.13], where are given results of the measurements of the frequency characteristic of the section of tropospheric line with a length of 300 km with the width of the antenna radiation pattern of 1°. ENDFOOTNOTE.

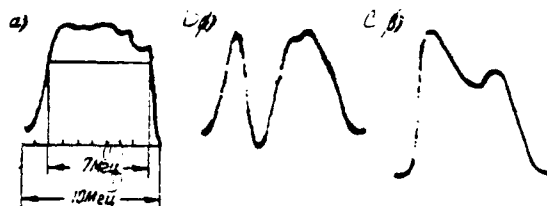


Fig. 3.7. Samples of the frequency characteristics of the section of line with the doubled (a) and single (b, c) receptions:  $d=300$  km,  $\alpha_0=1^\circ$ .

Key: (1). MHz.

Page 106.

Characteristic of group time lag. In §3.2 it was shown that with the known correlation coefficient for the real and imaginary parts of the transfer function can be determined the fundamental statistical properties of the phase-frequency characteristic of the section of line. This can be made by analogy with the phase of fluctuation noise [3.1-3.3]. However, for calculating the distortions on the tropospheric lines it is important to know not the phase-frequency characteristic of section, but its derivative, i.e., the characteristic of group time lag, since signal distortions are determined by the nonuniformity of this characteristic. On the tropospheric lines the nonuniformity of the characteristic of group

time lag continuously changes in the time and it is important to know the law of probability distribution for its fluctuation. As it was shown into §3.2, the integral law of probability distribution for divergence  $r_p$  from the central time lag takes form (3.50). This law is completely determined, if is known its parameter  $\Delta r_1$ , computed from formula (3.52). After substituting in (3.52) expression (3.61) for the energy pulse reaction, displaced to the zero time lag, we will obtain

$$\Delta r_1^2 = \frac{\int_0^\infty r_1^2 e^{-\Delta \Omega_0^2 r_1^2} dr_1}{\int_0^\infty e^{-\Delta \Omega_0^2 r_1^2} dr_1}. \quad (3.74)$$

After calculating integrals in (3.74) [3.7] taking into account (3.63), we have

$$\Delta r_1 = \frac{1}{\Delta \Omega_0} = \frac{1}{2\pi \Delta f_0}, \quad (3.75)$$

where  $\Delta f_0$  - the band of correlation, determined according to formula (3.66). After substituting (3.66) in (3.75), we will obtain

$$\Delta r_1 = 0,15 \frac{d^2 r_0}{ca_e}. \quad (3.76)$$

Let us recall that value  $\Delta r_1$  is an average value of absolute (on the sign) divergence  $r_p$  from the central time lag  $r_0$ . Knowing this value, it is possible according to formula (3.50) to determine the integral law of probability distribution for the values of the

characteristic of group time lag. Curve this law for relative values  $\frac{\Delta \tau_p}{\Delta \tau_1}$  is shown in Fig. 3.8. Direct measurement  $\tau_p$ , i.e. derived phase response, is connected with the great difficulties. Therefore in practice they use the usually following method: is supplied to the input of the measured circuit the high-frequency signal, frequency-modulated or in the amplitude by sine voltage with the frequency  $\Omega$ . At the output of circuit this signal is detected, and is measured the phase of sinusoidal output potential of detector.

Page 107.

It is known that if within the limits of the spectrum of modulated signal  $\tau_p$  practically it does not change, then the phase of sinusoidal output potential of detector is approximately equal to

$$\varphi \approx \Omega \tau_p. \quad (3.77)$$

Consequently, after measuring this phase, it is possible at the known frequency  $\Omega$  to determine  $\tau_p$  <sup>1</sup>.

FOOTNOTE <sup>1</sup>. This method the measurements of group time lag in the literature frequently call Nyquist's method. In Chapter 4 it is shown, under what conditions approximate equality (3.77) is fulfilled on the tropospheric lines for the frequency modulation by the simple tone. ENDFOOTNOTE.

The described method is utilized in the special instruments IVZ, intended for characteristic measurement of the group time lag of the circuit of radio relay line. Block diagram for these measurements is shown in Fig. 3.9. The transmitting part of the instrument IVZ realizes frequency modulation of transmitter by sine wave with the relatively small frequency (of the order of 100 kHz) and by small deviation (also order 100 kHz). Furthermore, is conducted a change in the carrier frequency of transmitter in the saw-tooth law with the frequency of 50-100 Hz - "sweeping." With this sweeping in accordance with the characteristic of group time lag changes the phase of the modulating output potentials circuit. The measurement of this phase is realized in the receiving part of the instrument IVZ. For this signal from the output of the FM discriminator it is supplied to two inputs of the phase discriminator (PD), moreover to one input it is direct, and on another - through the quartz filter (KF) with the passband a total of several hertz. A change in the phase of the modulating voltage occurs with the frequency of sweeping, i.e., with the frequency of 50-100 Hz. Therefore these changes are not passed by quartz filter and at its output the phase of signal is retained constant. This signal can be used as reference in the phase discriminator.

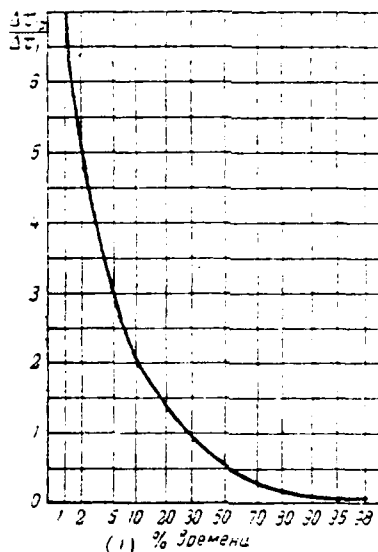


Fig. 3.8. Integral law of probability distribution for the fluctuation of group time lag.

Key: (1). Time.

Page 108.

Output potential of the phase discriminator is proportional to the changing in the process of sweeping phase of the modulating signal, i.e., it is proportional to the characteristic of group time lag. This voltage is supplied to the vertical plates of oscillograph. Sweep of oscillograph is synchronized by voltage by the frequency of

50-100 Hz from the output of frequency detector. This signal of synchronization preliminarily passes through the low-pass filter (PNCh), which does not pass modulating frequency on the order of 100 kHz. On the oscilloscope face is obtained the image of the characteristic of the group time lag of the measured circuit in the band of sweep.



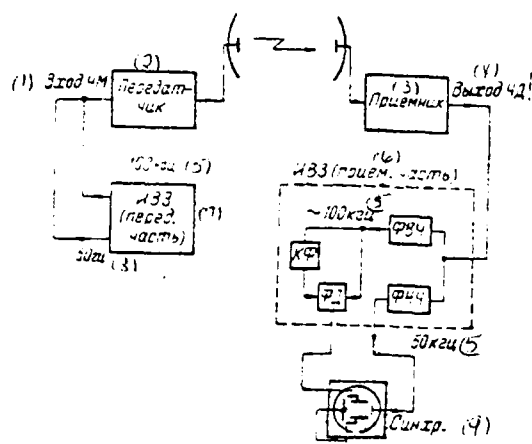


Fig. 3.9. Block diagram of instrument for measuring the group time lag (IVZ) .

Key: (1) . Input ChM. (2) . Transmitter. (3) . Receiver. (4) . Output ChD. (5) . kHz. (6) . Reception part. (7) . transmission part. (8) . Hz. (9) . Synchronizer.



Fig. 3.10. Samples of characteristics of group time lag of section of line (characteristics are obtained on oscilloscope face with the aid

of instrument IVZ).

Page 109.

In the measurements with the aid of the instrument IVZ on the tropospheric lines of communications on the oscilloscope face is obtained the image of "instantaneous" characteristics of the group time lag of the section of line<sup>1</sup> (Fig. 3.10) <sup>2</sup>.

FOOTNOTE <sup>1</sup>. In this case the instrument IVZ measures also characteristics  $\tau_{\text{gr}}$  of equipment circuit. However, with the correctly designed equipment the nonuniformity of characteristic  $\tau_{\text{gr}}$  in the service band by an order is less than divergence  $\tau_{\text{gr}}$  due to the multiple-pronged radiowave propagation in the section of line.  
ENDFOOTNOTE.

FOOTNOTE <sup>2</sup>. Photographs are made from the oscilloscope face in the measurements on section of tropospheric line with a length of 300 km with the width of the antenna radiation pattern of 1°. ENDFOOTNOTE.

The form of this characteristic continuously changes in the time randomly in accordance with a change in the structure of the multiple-pronged tropospheric channel; the speed of these changes is from the portions of the hertz to several hertz. Characteristic

measurements of the group propagation time with the aid of the instrument IVZ repeatedly were made in the section of the tropospheric line; the results of these measurements coincide well with theoretical relationships [3.10, 3.14].

Measurement  $\tau_p$  with the aid of the described instrument IVZ is in principle possible only during sweeping of the frequency of transmitter. For the more precise measurements of fluctuations  $\tau_p$  at one frequency can be used the method, presented in [3.15]. The results of measurements  $\tau_p$ , carried out by the method indicated in the section of tropospheric line, are given in [3.16]. These results also coincide well with the conclusion of theory.

In conclusion let us note that the methods, used in this section for determining the statistical properties of transmission function, benefit not only for the section of tropospheric line, but also generally for the multiple-pronged channel with the random parameters at output of which is Rayleigh amplitude distribution of signal [3.17]. In particular, by these methods in [3.18] are obtained relationships for the frequency of the characteristics of the section of the line of ionospheric scattering.

§3.4. Synthesis of the model of the section of tropospheric line.

Utilizing statistical laws for the transfer function of the section of the tropospheric line, given in §3.3, it is possible to construct the specific model of radiowave propagation in this section. The synthesis of this model represents interest, since in a number of cases it can prove to be useful for calculating the distortions on the tropospheric line of communications. To synthesize this model is possible, on the basis of the following considerations: the signals, transmitted by the tropospheric line, virtually have a spectrum with limited bandwidth. Therefore signal distortions due to the multiple-pronged propagation of radio waves are determined by the transmission function of the section of line in this limited band.

Page 110.

In the limited frequency band indicated the composite transfer function of section can be represented Fourier series whose composite coefficients are determined according to formula [3.5]:

$$C_{q,t} = \frac{1}{\Delta\Omega} \int_{-\frac{\Delta\Omega}{2}}^{\frac{\Delta\Omega}{2}} K_t(\Omega) e^{i\Omega t} d\Omega, \quad (3.78)$$

where  $K_t(\Omega)$  - transfer function for the concrete realization of multiple-pronged channel at the moment of time  $t$ ;  $\Delta\Omega$  - period of resolution in terms of the frequency axis and, therefore,

$$\tau_0 = \frac{2\pi}{\Delta\Omega} = \frac{1}{\Delta F}. \quad (3.79)$$

Fourier series for the composite transfer function in the limited band may be recorded in the form

$$K_f(\omega) = \sum_{k=-\infty}^{\infty} |C_{k_f}| e^{j(2\pi k_f \tau - \varphi_{k_f})}, \quad (3.80)$$

where  $|C_{k_f}|$  - modulus and  $\varphi_{k_f}$  - the phase of the  $k$ -th composite coefficient. Here we have somewhat unaccustomed resolution in the Fourier series the function of the frequency; in radio engineering more frequently is encountered the resolution in the Fourier series the function of time. Therefore one should remember that in (3.80) in comparison with the customary recording of Fourier series the time and frequency interchanged the position themselves. Let us note also that in radio engineering we usually deal concerning the expansion in the Fourier series of the real function of time and then the moduli of the coefficients of series for the positive and negative frequencies are equal, i.e.,  $C_{k_f} = C_{-k_f}$ . In our case Fourier series is represented the composite function of frequency, and therefore the moduli of the coefficients of series (3.80) for the positive and negative time lags, generally speaking, are not equal, i.e.,  $C_{k_f} \neq C_{-k_f}$ . Utilizing the known Euler formula for composite numbers, from (3.80) we will obtain for the real and imaginary parts of the transfer function in the limited frequency band:

$$\begin{aligned} P(\Omega) &= \sum_{k=-\infty}^{\infty} [C_{k1}] \cos(\Omega k \tau_1 - \varphi_{k1}) \\ Q(\Omega) &= \sum_{k=-\infty}^{\infty} [C_{k2}] \sin(\Omega k \tau_1 + \varphi_{k2}) \end{aligned} \quad (3.81)$$

Let us compare now expressions (3.81) with expressions (3.44). Let us recall that expressions (3.44) are recorded for actually and imaginary of the parts of the transfer function of multiple-pronged channel with the time lag of separate components on  $\tau_1$  by the amplitudes of these components  $C_k$  and by phases  $\varphi_k$ . Consequently, expressions (3.81) correspond to multiple-pronged radiowave propagation, moreover separate components differ from each other in terms of identical time lag  $\tau_1$ , have amplitudes  $C_{k1}$  and phases  $\varphi_{k1}$ .

Thus, for the limited band of frequencies  $\Delta\Omega$  can be proposed the following equivalent model of the section of the tropospheric line: in the section of line electromagnetic energy is propagated in the form of digital components, moreover the time lag of each component differs from adjacent by identical value  $\tau_1$ ; amplitude and phase of signal in the  $k$  beam is determined by the  $k$  composite coefficient during the expansion in the Fourier series in the band of the transfer function of section indicated.

Let us emphasize that these discrete components are not in any way the delaying signals, re-emitted with real heterogeneities in the troposphere: the signals, re-emitted with the heterogeneities of the troposphere differ from each other identical, only by the arbitrary time lag; furthermore, in general at the output of the section of tropospheric line is not a discrete but continuum of the beams (see Chapter 1). However, as far as the model indicated is concerned, then it is only the equivalent of the section of propagation, valid for the limited frequency band. Out of this band the transfer function of equivalent model no longer coincides with the transfer function of the section of tropospheric line.

Fourier series (3.80) is recorded for the actual realization of the transfer function of the section of line, taking place at the moment of time  $t$ . However, transmission of the function of section continuously changes in the time randomly. Consequently, randomly change there will be amplitudes and phases of the delaying signals in the equivalent model of the section of line. During the use of this model in calculations it is important to know, what law of probability distribution will occur for amplitudes and phases of the delaying signals. For determining this law let us rewrite expression (3.78) into somewhat other form, namely: express the transfer

function through its real and imaginary parts we will use the Euler formula. As a result we will obtain

$$\begin{aligned} \dot{C}_{k_t} &= \frac{1}{\Delta\Omega} \int_{-\frac{\Delta\Omega}{2}}^{\frac{\Delta\Omega}{2}} [P_t(\Omega) + jQ_t(\Omega)] e^{jk\tau_3\Omega} \Delta\Omega = \\ &= \frac{1}{\Delta\Omega} \int_{-\frac{\Delta\Omega}{2}}^{\frac{\Delta\Omega}{2}} (P_t(\Omega) \cos k\tau_3\Omega + jP_t(\Omega) \sin k\tau_3\Omega + jQ_t(\Omega) \cos k\tau_3\Omega - \\ &\quad - Q_t(\Omega) \sin k\tau_3\Omega) \Delta\Omega = (C_{P_{k_t}} - S_{Q_{k_t}}) + j(S_{P_{k_t}} + C_{Q_{k_t}}). \end{aligned} \quad (3.82)$$

Here  $C_{P_{k_t}}$ ,  $S_{P_{k_t}}$ ,  $C_{Q_{k_t}}$  and  $S_{Q_{k_t}}$  - coefficients with cosines and sines of expansion in the Fourier series of functions  $P_t(\Omega)$  and  $Q_t(\Omega)$  for the actual realization of multiple-frequency channel. In §3.3 it was shown that the random changes in the time of the real and imaginary parts of the transfer function are subordinated to the normal law of probability distribution for any frequency  $\Omega$ . From the theory of random functions [3.19] it is known that during the expansion in the Fourier series of normal function the coefficients with sines and cosines of this expansion are also normal values. Consequently, in our case of value  $C_{P_{k_t}}$ ,  $S_{P_{k_t}}$ ,  $C_{Q_{k_t}}$  and  $S_{Q_{k_t}}$  they are distributed normally. In accordance with (3.82) the modulus of the coefficient of series (3.80), obviously, is equal to

$$|\dot{C}_{k_t}| = \sqrt{(C_{P_{k_t}} - S_{Q_{k_t}})^2 + (S_{P_{k_t}} + C_{Q_{k_t}})^2}. \quad (3.83)$$

In §3.2 it was shown that on the real tropospheric lines the



energy pulse reaction is virtually symmetrical relative to a certain central time lag. In the presence of the symmetrical energy pulse reaction the values of functions  $P(\Omega)$  and  $Q(\Omega)$  are not depended for any frequency  $\Omega$ . Furthermore, from the theory of random functions it is known ~~that~~ [3.19] that during the expansion in the Fourier series of random function the coefficients with sines and cosines of this expansion between themselves are not correlated. Taking into account this, we see that the values in the brackets in expression (3.83) between themselves are not correlated.

Page 112.

Furthermore, these sums have normal probability distribution as the sums of normal values. Consequently, probability distribution for  $|C_k|$  obeys the law of rayleigh [3.2; 3.3]. The phase of the coefficient of the expansion of transfer function in the Fourier series is determined by the expression:

$$\varphi_k = \arctg \frac{S_{p_k} + C_{q_k}}{C_{p_k} - S_{q_k}}. \quad (3.84)$$

Consequently, with those normally distributed and not correlated  $(S_{p_k} + C_{q_k})$  and  $(C_{p_k} - S_{q_k})$  phase  $\varphi_k$  has uniform probability distribution, in the limits from 0 to  $2\pi$ . Again let us recall that the probability distributions indicated, occur for the delaying signals in the equivalent model, but not for the signals, re-emitted with the real

heterogeneities of the troposphere; probability distribution for amplitudes and phases of the real components of multiple-pronged signal, generally speaking, can be any.

During the use of an equivalent model in the calculations it is necessary to know also the rms values of the amplitudes of the delaying signals. From relationship (3.83) and lack of correlation of values  $C_{P_k}$ ,  $C_{Q_k}$ ,  $S_{P_k}$  and  $S_{Q_k}$  it follows that

$$\overline{|C_k|^2} = \overline{C_{P_k}^2} + \overline{C_{Q_k}^2} + \overline{S_{P_k}^2} + \overline{S_{Q_k}^2} \quad (3.85)$$

From the theory of random functions [3.19] it is known that during the expansion in the Fourier series of random function the rms values of coefficients with sines and cosines of this series are equal to the appropriate coefficients of expansion into Fourier's poisson correlation function. Furthermore, as it was shown into §3.2, correlation function for  $P(\Omega)$  and  $Q(\Omega)$  were equal to each other. Consequently, in accordance with (3.85)

$$\overline{|C_k|^2} = 4b_k^2, \quad (3.86)$$

where  $b_k$  - k coefficient of expansion in the Fourier series correlation function for the real part of the transfer function. Let us recall that according to (3.37) the correlation function for  $P(\Omega)$  is an even function  $\Omega$ , and therefore formulas for determination must be recorded in the form of cosine-conversion. Furthermore, let us note that during the use of an equivalent model in the

calculations it is necessary to know only relative values of the amplitudes of the delaying signals. Therefore during computation  $b_1^2$  it is expedient to introduce standardization, after accepting  $b_0^2=1$ . Taking into account all this, formula for determining the rms value of the amplitudes of the delaying signals in the equivalent model can be recorded in the form

$$b_k^2 = \frac{\int_0^{\frac{\Delta\Omega}{2}} R_p(\Omega) \cos k \tau_0 \Omega d\Omega}{\int_0^{\frac{\Delta\Omega}{2}} R_p(\Omega) d\Omega} \quad (3.87)$$

where  $R_p(\Omega)$  - correlation coefficient for the real part of the transfer function.

Page 113.

In §3.3 it is shown that at the length of the section of tropospheric line not more than 300 km and to the width of the diagram of antennas not more than 1.5° correlation coefficient for  $P(\Omega)$  is determined by expression (3.62). After substituting (3.62) in (3.87), we will obtain

$$b_k^2 = \frac{\int_0^{\frac{\Delta\Omega}{2}} e^{-\frac{1}{2}\left(\frac{\Omega}{\Delta\Omega_0}\right)^2} \cos k \tau_0 \Omega \, d\Omega}{\int_0^{\frac{\Delta\Omega}{2}} e^{-\frac{1}{2}\left(\frac{\Omega}{\Delta\Omega_0}\right)^2} \, d\Omega} \quad (3.88)$$

Integrals in (3.88) cannot be calculated in the elementary functions. However, formulas for determination  $b_k^2$  nevertheless can be obtained, moreover it is here expedient to examine two interesting ones for the practice of the case:

1. Tropospheric communicating systems usually are designed so that width of band of the transmitted signals not more than twice exceeds the band of correlation, i.e.,  $\frac{\Delta\Omega}{\Delta\Omega_0} < 2$ . In this case quadratic exponential curve under the integral sign in numerator and denominator of expression (3.88) can be with a high degree of accuracy represented three first members of Maclaurin series. After this computation of integrals in (3.88) to produce simply. From (3.88) it directly follows that

$$b_0^2 \equiv 1. \quad (3.89)$$

For the 1st and 2nd component after the computation of integrals in (3.88) we will obtain:

$$\left. \begin{aligned}
 b_1^2 &\approx \frac{2,5 \left( \frac{\Delta\Omega}{\Delta\Omega_0} \right) + 0,2 \left( \frac{\Delta\Omega}{\Delta\Omega_0} \right)^4}{1 - 0,04 \left( \frac{\Delta\Omega}{\Delta\Omega_0} \right)^2 + 0,0016 \left( \frac{\Delta\Omega}{\Delta\Omega_0} \right)^4} \cdot 10^{-2} \\
 b_2^2 &\approx \frac{0,6 \left( \frac{\Delta\Omega}{\Delta\Omega_0} \right) + 0,135 \left( \frac{\Delta\Omega}{\Delta\Omega_0} \right)^4}{1 - 0,04 \left( \frac{\Delta\Omega}{\Delta\Omega_0} \right)^2 + 0,0016 \left( \frac{\Delta\Omega}{\Delta\Omega_0} \right)^4} \cdot 10^{-2}
 \end{aligned} \right\} \text{ when } \frac{\Delta\Omega}{\Delta\Omega_0} < 2. \quad (3.90)$$

Values  $b_1^2$  for the components with the more by fine numbers when  $\frac{\Delta\Omega}{\Delta\Omega_0} < 2$  are negligible.

Fig. 3.11 shows the graph of the dependence of the mean squares of amplitudes the 1st and 2nd component on relationship of bands  $\frac{\Delta\Omega}{\Delta\Omega_0}$ . From the figure one can see that when  $\frac{\Delta\Omega}{\Delta\Omega_0} < 2$  values  $b_2^2$  are low in comparison with  $b_1^2$ . Therefore for the investigation of distortions on such lines it is possible to examine the equivalent model, consisting of all or three "beams": one with the zero time lag and the amplitude, equal to 1, and two more with the rms values of amplitudes  $b_2^2$ , and the time lag on  $+\tau_2$  and  $-\tau_2$ .

Page 114.

It should be noted that in many instances the analysis distortion can be even more simplified, on the basis of the following considerations: as can be seen from Fig. 3.11, even when  $\frac{\Delta\Omega}{\Delta\Omega_0} = 2$   $b_1^2$  is

composes only 15c/o of  $b^2_0$ . During the introduced by us normalization we assume that the signal amplitude with the zero time lag is always equal to the unit; the amplitudes of remaining beams experience the random changes, distributed according to the law of rayleigh. Therefore at the separate moments of time the amplitudes of beams with the zero time lag and with the time lag on  $\pm\tau_3$  can become commensurable, which will cause essential signal distortions. However, the simultaneous increase of the amplitudes of beams, which delay on  $\pm\tau_3$  and  $-\tau_3$ , has very small probability. Therefore for the analysis of distortions it is possible to use the equivalent model, which consists in all of two beams: zero and delaying either on  $\pm\tau_3$  or for  $-\tau_3$ . This representation of the channel of tropospheric communication it can greatly facilitate analysis, since the distortions ChM of signals during the double-beam propagation are well studied<sup>1</sup>.

FOOTNOTE 1. The distortions of the simple tone during the double-beam propagation are examined in [3.20]; transient noises with multichannel telephony - in [3.21]. ENDFOOTNOTE.

2. Second case takes place when frequency band being investigated is much more than band of correlation, i.e.,  $\frac{\Delta\Omega}{\Omega} \gg 1$ . In this case it is not the possible to obtain through the elementary functions even approximations for  $b^2_x$ . However, formula for the

computation nevertheless can be obtained with the aid of the special function whose values are tabulated. For this should be cosinusoidal function in the numerator of relationship (3.88) expressed by the exponential functions from the imaginary argument (according to the Euler formula). Expression in the numerator can be further reduced to special function from complex variable, which takes the form

$$\phi(z) = u(z) + jv(z) = \int_0^z e^{x^2} dx. \quad (3.91)$$

Here  $z = \rho e^{j\theta}$ , moreover  $\rho$  - modulus and  $\theta$  - argument complex variable  $z$ . Integral in the denominator of expression (3.88) can be easily expressed by the special function - probability integral. Then after simple conversions it is possible to obtain the following formula for determining the mean square of signal amplitudes in the equivalent model:

$$b_k^2 = e^{-\frac{\Delta\Omega_0^2}{2}} (2\pi)^{-1} \frac{\frac{2}{\sqrt{\pi}} U(\rho, \theta)}{F\left(\frac{\Delta\Omega}{2\sqrt{2}\Delta\Omega_0}\right)}. \quad (3.92)$$

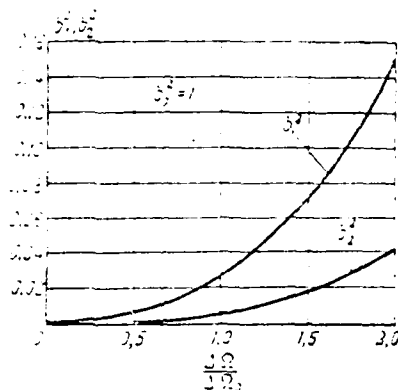


Fig. 3.11. The mean squares of signal amplitudes in the equivalent model of the section of tropospheric line.

Page 115.

Here  $U(\rho, \theta)$  - coefficient with the imaginary part of function  $\phi(z)$ , of that determined by relationship (3.91),

$$\rho = \sqrt{20k^2 \left( \frac{\Delta\Omega}{\Delta\Omega_0} \right)^2 + 0.124 \left( \frac{\Delta\Omega}{\Delta\Omega_0} \right)^2} \quad (3.93)$$

$$\theta = \arctg \frac{0.08}{k} \left( \frac{\Delta\Omega}{\Delta\Omega_0} \right)^2$$

Functions  $U(\rho, \theta)$  are tabulated for the different values  $\rho$  and  $\theta$  [3.22],  $P(z) = \frac{2}{\sqrt{\pi}} \int_0^z e^{-x^2} dx$  - a function of probability integral.

Let us note that formula (3.92) is valid for any, including for low values  $\frac{\Delta\Omega}{\Delta\Omega_0}$ . However, function  $U(\rho, \theta)$  is tabulated only for values



is not less than  $45^\circ$  and the values  $\rho$  not more than 1.5. As it follows from (3.93), this corresponds  $\frac{\Delta\Omega}{\Delta\Omega_0} \approx 3.5$ , therefore for low values  $\frac{\Delta\Omega}{\Delta\Omega_0}$  should be used formulas (3.90).

From comparison (3.92) and (3.61) it is evident that the 1st exponential factor in formula (3.92) is the value of the energy pulse reaction of the section of line, undertaken at point  $k\tau_3$ .

Consequently, the mean squares of amplitude of signals in the equivalent model can be obtained as the readings of energy pulse reaction at points  $k\tau_3$ , multiplied by correction factor

$\frac{2}{V\pi} U(2,9)/F\left(\frac{\Delta\Omega}{2\sqrt{2}\Delta\Omega_0}\right)$ . It is possible to easily show that with an increase in the relation of bands  $\frac{\Delta\Omega}{\Delta\Omega_0}$  this correction factor approaches unity [3.22, 3.23]. In the interesting us case when  $\frac{\Delta\Omega}{\Delta\Omega_0} \gg 1$ , it is possible to accept this factor equal to unit, i.e., to consider that values  $\sigma_k^2$  are equal to the readings of energy pulse reaction at points  $k\tau_3$ , i.e.,

$$\sigma_k^2 \approx g(k\tau_3) \frac{1}{\text{dph}} \frac{\Delta\Omega}{\Delta\Omega_0} \gg 1. \quad (3.94)$$

Key: (1). with.

This is illustrated by Fig. 3.12, where the readings of the pulse reaction, determined by relationship (3.61), they are shown for case  $\frac{\Delta\Omega}{\Delta\Omega_0} = 7$ . When  $\frac{\Delta\Omega}{\Delta\Omega_0} > 4$  formula (3.94) gives error not more than 2-30/c. From relationship (3.94) follows the interesting method of

the experimental measurement of the form of the energy pulse reaction of the section of line. For this it is necessary to measure the frequency and phase responses of section during different realizations of multiple-pronged channel. These measurements must be carried out in the band  $\Delta\omega$ , several times of the exceeding band correlation  $\Delta\omega_0$ . Then for each realization it is necessary to expand the composite transfer function of section in the interval  $\Delta\omega$  in the Fourier series. After determining the moduli of the coefficients of this series and after conducting averaging in a large number of random realizations, we will obtain values  $b_j^2$ , i.e. the readings of energy pulse reaction at points  $\pm k\tau_j$ .

As it was shown in Fig. 3.3, the frequency characteristic of the section of line can be experimental obtained by the method of sweep and the phase response (is more precise, its derivative) - with the aid of the instrument IV2.

Page 116.

Thus the described above method of measuring the energy pulse reaction can be realized in practice. However, does arise the question: and it is worth measuring the energy pulse reaction of section with this sufficiently complex method? Making these measurements, in the principle, can be carried out and by the simpler

method with which the transmitter emits narrow pulses, and with receiving end are recorded the pulses, reflected from the individual heterogeneities of the troposphere.

In regard to this it must be noted that on the real ones are tropospheric lines a single "pulse" method the measurements cannot be utilized virtually. The fact is that on the real tropospheric lines the width of the antenna radiation pattern does not usually exceed  $1^\circ$ , and the length of section comprises not more than 300 km, the respectively relative time lag of the components of multiple-pronged signal does not exceed 0.2-0.3  $\mu$ s. Therefore with the pulse method of measurement transmitter must emit pulses on the order of 0.1 and even 0.05 ns. Only then at receiving end it will be possible to in sufficient detail obtain the form of the pulse reaction of the section of line. But for observing such pulses it is necessary to have a passband of receiver on the order of 10 MHz. In this broad band in the existing energy parameters of tropospheric systems the signal-to-noise ratio will be close to unity; this strongly impedes recording pulse reaction at receiving end. Not randomly in the literature completely there is no information about measurements of the pulse reaction of the section of tropospheric line with the pencil-beam antennas.

Another matter is the measurement of energy pulse reaction by

the described above method with the aid of the spectral analysis of the composite transfer function of section. True, and in this case for the investigation is necessary the broad band (on the order of 10 MHz), in which is realized the measurement of the frequency and phase responses of section. However, signals from the outputs of the amplitude detector of receiver and instrument IVZ, which are determining the form of these characteristics, have a band only several hundred hertz. This allows also in a small signal-to-noise ratio in the broad band at the input of receiver to successfully conduct the measurement of the energy pulse reaction of section.

As it was already shown, for obtaining the readings of energy pulse reaction it is necessary to expand in Fourier series the composite transfer function of section. This can be made, for example, graphically, after using the photographs of frequency characteristics and characteristics of group time lag, photographed from the oscilloscope face (see, for example Fig. 3.7 and 3.10).

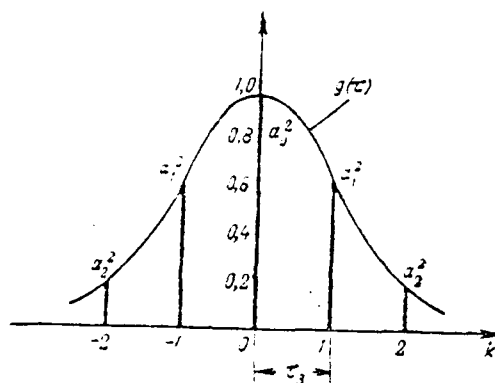


Fig. 3.12. Energy pulse reaction and mean squares of signal amplitudes in the equivalent model when  $\frac{\Delta\omega}{\Delta\omega_0} > 1$

Page 117.

However, it is considerably more effective to obtain these readings automatically, with the aid of the special measuring installation whose block diagram is shown in Fig. 3.13. This installation contains auxiliary generator with frequency  $f_2$  (on the order of 100 kHz) and spectrum analyzer. Auxiliary generator is modulated in the signal frequency from the output of instrument IVZ and in the amplitude - signals from the output of the amplitude detector of receiver with a change in the frequency characteristic by sweep. Signal from the output of amplitude detector periodically, with the frequency of sweep  $F$ , repeats the form of the frequency characteristic of the

section of line. Consequently, the amplitude of auxiliary generator proves to be the modulated "form" of the frequency characteristic of section. Signal from the output of instrument IV2 periodically, with the frequency of sweep  $F$ , repeats the form of the characteristic of the group time lag of section. Consequently, the frequency of auxiliary generator proves to be modulated characteristic  $\tau_{gp}$  of section. As is known, with the frequency modulation the laws of a change in the phase and frequency are connected with the relationship

$$\varphi(t) = \int \omega(t) dt. \quad (3.95)$$

Therefore the phase of auxiliary generator proves to be that modulated according to the law of integral of characteristic  $\tau_{gp}$ . But integral of  $\tau_{gp}$  it defines, as is known, the single characteristic of section. Therefore the phase of auxiliary generator periodically, with the frequency of sweep  $F$ , repeats the form of the phase response of section. Thus, in the described installation is obtained the signal, amplitude and phase of which periodically repeat the frequency and phase responses of section. This signal, naturally, has line spectrum with the spectral lines, distant for the frequency of sweep  $F$ . It is easy to understand that this linear spectrum corresponds to the expansion of the composite transfer function of the section of line in the Fourier series in the interval of sweep. Thus, it suffices to analyze the spectrum of the signal of auxiliary generator in order to determine the discrete readings of the pulse reaction of the section of line.

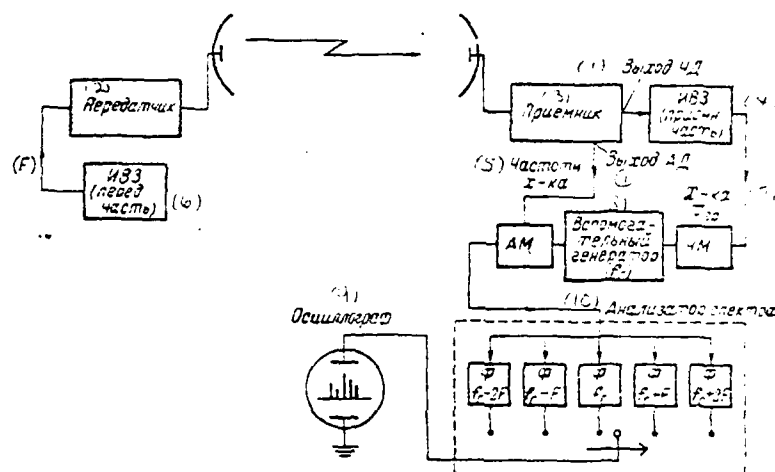


Fig. 3.13. Block diagram of installation for measuring the readings of energy of the pulsed reaction of the section of line.

Key: (1). Output ChD. (2). Transmitter. (3). Receiver. (4). IVZ (receiving part). (5). It is frequency. characteristic. (6). IVZ transmitting part). (7). Characteristic. (8). Auxiliary generator. (9). Oscillograph. (10). Spectrum analyzer.

Page 118.

In the described installation this is realized with the aid of the special spectrum analyzer, which consists of several quartz filters: "central" filter is tuned to a frequency of auxiliary generator  $F_1$  and remaining filters - for frequencies  $F_1 \pm F$ . The output signals of

all filters are detected and with the aid of the electron commutator automatically, alternately are connected to the vertical plates of oscillograph. As a result on the oscilloscope face is obtained the panorama of the amplitudes of the delaying signals of the equivalent model of propagation. It is logical that the values of these amplitudes continuously change in the time as a result of a change in the structure of multiple-pronged tropospheric channel<sup>1</sup>.

FOOTNOTE <sup>1</sup>. The given here method of measurement of pulse reaction should be carried to the methods of frequency radar, just as the mentioned it is above method of measurement with the pulse modulation of transmitter - to the methods of pulse radar. The respectively described here installation for measuring the pulse reaction of the section of tropospheric line is, actually, multipurpose two-position frequency radar.

To utilize for measuring the pulse reaction of the section of line other known methods of frequency radar are cannot, since all known frequency radars are single-position, i.e., work only during the location of transmitter and receiver in one point (for example, see [3.24]). ENDECCCTNCTE.

With the aid of the described installation were carried out the measurements of the pulse reaction of the section of tropospheric



line with a length of 300 km with the antennas with the width of the radiation pattern of  $1^\circ$ . Sweep was realized in the band  $\Delta f = 8$  MHz, which five times exceeds the band of correlation. Fig. 3.14a and b shows signal amplitudes in the equivalent model, photographed from the oscilloscope face at different moments of time. With the selected band of sweep  $\Delta f = 8$  MHz these signals are located on the time lag on  $\tau_s = 1/\Delta f = 0.125$   $\mu$ s. In the upper right-hand corner of Fig. ~~3.13a~~<sup>3.13u</sup> is shown the signal of auxiliary generator, modulated the amplitude of the corresponding frequency characteristic of the section; in the upper right-hand corner of Fig. 3.14b - the corresponding characteristic of group time lag, obtained at the output of instrument IVZ.

According to a large number of photograph it was established that the probability distribution for the signal amplitudes in the equivalent model obeys the law of Rayleigh, this confirms the conclusions of theory, given above. Were also calculated the rms values of amplitudes, i.e., the readings of the energy pulse reaction of the section of line. These readings are shown in Fig. 3.15. According to the discrete readings is constructed energy pulse reaction of section of line, shown in Fig. 3.15 by solid line. For the comparison of theory and experiment, in the same figure dotted line showed the theoretical curve of energy pulse reaction, constructed in accordance with formula (3.61).

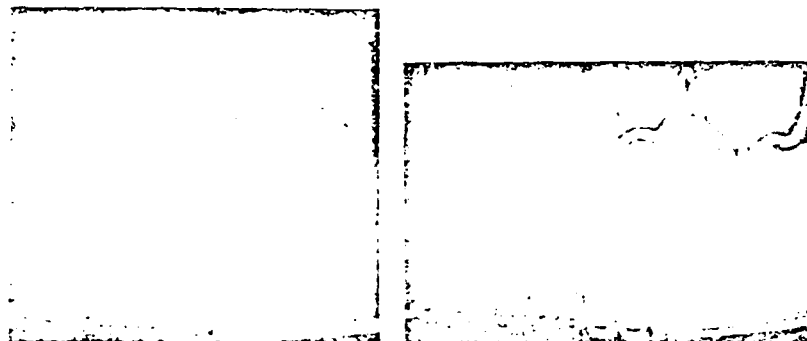


Fig. 3.14. Signal amplitudes in the equivalent model, obtained by the method of Fig. 3.13; AM the signal of auxiliary generator (a) and characteristic  $V_{sp}$  (b).

Page 119.

As it was shown into §3.3, the energy pulse reaction of the section of tropospheric line with the pencil-beam antennas is completely determined by the total radiation pattern of receiving and transmitting antennas in the vertical plane; this radiation pattern is approximated by quadratic exponential curve (3.56). For the confirmation of this position in Fig. 3.15 dash line showed the experimental total antenna radiation pattern. This diagram is obtained as a result of measurements with the aid of the receiver, established on the helicopter. For convenience in the comparison of radiation pattern is energy of pulsed reactors along the horizontal

axis, besides time lag  $\tau$ , are plotted also the angles  $\beta$ , calculated in the vertical plane relative to the axis of the antennas; the connection between  $\tau$  and  $\beta$  is determined by relations (3.55), (3.57) and (3.58). A good coincidence of all three curves in Fig. 3.15 shows the correctness of the premises, made in this chapter during the analysis of the frequency and time characteristics of the section of tropospheric line.

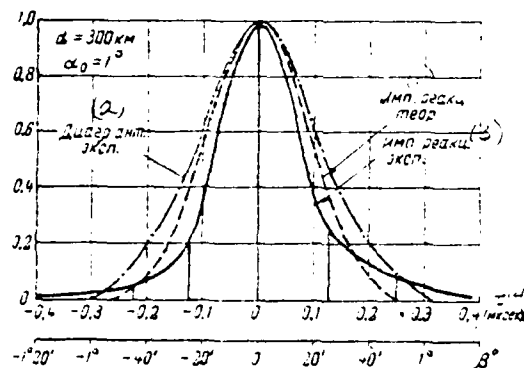


Fig. 3.15. Experimental energy pulse reaction of the section of line and antenna radiation pattern.

Key: (1). Pulse reaction theory. (2). Diag. arta. of exp. (3). Pulse reactionary exp. (4). ps.

Page 120.

## REFERENCES

- 3.1. В. И. Бунимович. Флуктуационные процессы в радиоприемных устройствах. «Советское радио», 1951.
- 3.2. Б. Р. Левин. Теория случайных процессов и ее применение в радиотехнике. «Советское радио», 1960.
- 3.3. Б. Р. Левин. Теоретические основы статистической радиотехники. «Советское радио», 1966.
- 3.4. И. А. Гусятинский. Искажения сигнала при распространении ука за пределами прямой видимости. Сборник трудов Государственного НИИ Министерства связи СССР, 1959, вып. 1(15).
- 3.5. А. А. Харкевич. Спектры и анализ. Физматгиз, 1962.
- 3.6. А. А. Ризкин. Основы теории усилительных схем. «Советское радио», 1958.
- 3.7. И. С. Градштейн, И. М. Рыжик. Таблицы интегралов, сумм, рядов и произведений. Физматгиз, 1962.
- 3.8. И. А. Гусятинский. Ширина полосы и мощность переходных помех при радиосвязи рассеянием в тропосфере. «Электросвязь», 1959, № 4.
- 3.9. А. В. Прессин, В. Ф. Губский. К теории разносигнального приема при дальнем тропосферном распространении ука. «Радиотехника», 1959, № 5.
- 3.10. Дальнее тропосферное распространение ука. Под ред. Б. А. Васильевского. «Советское радио», 1963.
- 3.11. А. В. Прессин. К расчету полосы пропускания тропосферы при дальнем тропосферном распространении ука. «Радиотехника и электроника», 1961, № 5.
- 3.12. А. С. Немировский. Ширина полосы пропускания при одинарном и разносигнальном приеме сигналов дальнего тропосферного распространения ука. «Электросвязь», 1961, № 5.
- 3.13. И. А. Гусятинский, А. С. Немировский. Экспериментальное исследование полосы пропускания при одинарном и разносигнальном приеме сигналов дальнего тропосферного распространения ука. «Электросвязь», 1964, № 7.
- 3.14. И. А. Гусятинский, Э. Я. Рыжик. Теоретическое и экспериментальное исследование флуктуаций амплитуды и фазы модулирующего сигнала в многолучевом канале с ЧМ. «Электросвязь», 1965, № 2.
- 3.15. А. А. Шур, Г. С. Максимов. Об одном методе измерения флуктуаций фазы радиосигнала при излучении дальнего тропосферного распространения. «Радиотехника и электроника», 1961, № 5.
- 3.16. В. Н. Троицкий. Исследование флуктуаций группового времени задерживания при дальнем тропосферном распространении. «Электросвязь», 1964, № 5.
- 3.17. Ю. А. Бунимович. Частотная корреляция при радиосвязи с использованием рассеянных волн. «Радиотехника», 1963, № 9.
- 3.18. Я. А. Фикс. Об искажениях сигнала, обусловленных многолучевым характером механизма рассеяния в ионосфере. «Электросвязь», 1964, № 10.
- 3.19. В. С. Пуганова. Теория случайных функций. Физматгиз, 1960.
- 3.20. С. В. Барондас. Статистический расчет нелинейных переходов, вызванных отражением в антенных фидерах многоканальных радиорелейных систем. «Электросвязь», 1963, № 9.
- 3.21. В. А. Немиров. Основы радиосвязи на ука. Связьиздат, 1957.
- 3.22. К. А. Карлов. Таблицы функций в комплексной плоскости. Изд. АН СССР, 1958.
- 3.23. Е. Янке, Ф. Эмде. Таблицы функций с формулами и кривыми. Гостехиздат, 1948.
- 3.24. А. С. Винницкий. Обзор основ радиолокации при непрерывном излучении радиоволн. «Советское радио», 1961.

Page 121.

#### Chapter 4.

POWER OF NOISES IN TELEPHONE CHANNEL AT THE OUTPUT OF ONE SECTION OF LINE DTR.

##### §4.1. Introduction.

One of fundamental qualitative indices of any communication is signal-to-noise ratio at the output of channel. Noise sources in the channels of communication of radio relay line can be divided into two fundamental forms: the first includes the inherent noise, determined by the thermal agitations of input circuits of receiver (noises of the independent origin); the second noise source are the transient interferences, which appear during the transmission multichannel telephony (noises of the dependent origin).

With the frequency modulation, which found widest use on the radio relay lines, including on the lines DTF, the power of own

thermal noises in the channel with the work of higher than the threshold is inversely proportional to the power of signal at the input of receiver. In this case, since the signal at the input of receiver has rapid and slow fluctuations, the power of inherent noise in the channel is also subjected to fluctuations.

The reason for transient interferences with ChM is the inadequacy of the circuit of line. In the lines DTR, besides the sources of the transient interferences, characteristic to the usual radio relay lines (for greater detail, see chapter 6) there is also a specific source - multi-beam character of the signal in the place of reception.

In this chapter will be examined the methods of calculation of thermal noises and transient interferences, caused by the multi-beam character of signal, and is also found the optimum value of the deviation of frequency, which corresponds to the minimum of their sum. Here (§4.3) will be examined one additional means of distortions, characteristic to channel DTR: the linear distortions, which are determining the fluctuations of overall line attenuation in the channel and changes of the phase of the fundamental harmonic.

## §4.2. Thermal noises at the output of the section of line DTR.

The psophometric power of thermal noises in  $i$  telephone channel of radio relay line with ChM is determined by the following formula (at point with the level of useful signal  $P_{\text{н}}$   $N_{\text{p}}$ ):

$$P_{\text{r}} = \frac{n k T \Delta F_{\text{н}} K_{\text{ac}}^2}{P_{\text{с вх}}} \left( \frac{F_i}{\Delta f_{\text{н}}} \right)^2 e^{2p_{\text{н}}}, \text{ мВт}, \quad (4.1)$$

Key: (1). 7.

where  $n$  - a coefficient of receiver noise;

$kT$  - product of Boltzmann's constant ( $k=1.38 \cdot 10^{-23}$ ) to the absolute temperature;

$\Delta F_{\text{н}}$  - width of band of telephone channel;

$K_{\text{ac}}$  - psophometric coefficient;

$P_{\text{с вх}}$  - power of signal at the input of the receiver;

$F_i$  - the medium frequency of the  $i$  channel in the group spectrum;

$\Delta f_{\text{н}}$  - effective deviation of frequency to one channel.

Formula (4.1) is valid only with the signals, which exceed threshold values  $ChM^1$ ).

FOOTNOTE 1. If signal falls below the threshold of improvement  $ChM$ , then noises in the channel sharply grow. The time, during which occurs this drop in the signal, determines the reliability of the work of line. ENDFOOTNOTE.

$$P_{c\text{ox}} \geq P_{c\text{nop}} = (3 \div 10) P_{\text{шш}}, \quad (4.2)$$

where  $P_{\text{шш}}$  — the inherent noise of receiver. In this case the power of noises at the output of the FM discriminator of receiver has the triangular spectrum. This means that upper telephone channel is located in the worst conditions. For the equalization of the noise characteristics of channels are applied the special four-poles: the pre-distorting filter in the transmission increases the deviation of frequency in the upper channels due to the decrease of the deviation of the frequency of lower channels and the restoring filter, leveling level of useful signal at the reception. The characteristic of the pre-distorting filter according to the recommendations of МККР [ - International Radio Consultative Committee] is approximated by curve  $B^2(F) = 0.4 + 1.35 \left(\frac{F}{F_s}\right)^2 + 0.75 \left(\frac{F}{F_s}\right)^4$ , in which  $F_s$  — upper cut-off frequency of the group spectrum. For the upper, the worse, channel the coefficient of predistortions is equal to

$$B^2(F_s) = b_{\text{np}} = 2.5. \quad (4.3)$$



The power of signal at the input of receiver is determined by the parameters of equipment and by total attenuation between the output of transmitter and input of the receiver:

$$P_{\text{свх}} = \frac{P_{\text{пт}} G_{\text{т}}}{A_{\text{с}}}, \quad (4.4)$$

where  $P_{\text{пт}}$ — power of the transmitter;

$G_{\text{т}}$ — total amplification of the transmitting and receiving antennas taking into account the losses of antenna gain with DTR.

For the pair of antennas with the factors of amplification  $G_{\text{пт}}$  and  $G_{\text{пр}}$  the losses of amplification  $\delta_{\text{yc}}$  are determined on the curve Fig. 1.16 (in the times). Then

$$G_{\text{т}} = \frac{G_{\text{пт}} G_{\text{пр}}}{\delta_{\text{yc}}}. \quad (4.5)$$

Page 123.

Total attenuation  $A_{\text{с}}$  with DTR is determined by fading  $A_{\text{св}}$  signal in the feeder lines, which connect transmitter and receiver with the antennas, free-space attenuation

$$A_{\text{св пр}} = \left( \frac{4\pi d}{\lambda} \right)^2, \quad (4.6)$$

where  $d$  - a distance between the transmitting and receiving antennas,  $\lambda$  - wavelength, and finally by attenuation factor  $A_{occ}$ , by that considering weakening signal during the remote tropospheric propagation relative to the field of free space and fluctuation of this weakening in the time.  $A_{occ}$  - random function of time. It is determined, in the first place, by average annual value  $A_{cr}$ , in the second place, seasonal changes  $A_{ces}$  and, thirdly, random rapid  $A_c$  and slow  $A_u$  fluctuations:

$$A_{occ} = A_{cr} A_{ces} A_u A_c. \quad (4.7)$$

Since the line of communications must operate satisfactorily in the worse (from the point of view of radiowave propagation) conditions, value  $A_{ces}$  should be to take by the equal to attenuation in the worse winter month and entire calculation made for the product

$$A_{cr} A_{ces} = \bar{A}, \quad (4.8)$$

where  $\bar{A}$  - a rms value of signal in the worse according to propagation conditions month. After substituting into formula (4.1) value  $P_{occ}$  from formula (4.4) taking into account (4.5) - (4.8), we will have for the upper worse channel at the point of zero relative level ( $\alpha = 0$ )

$$P_r = \frac{\pi k T \Delta F \kappa_{nc}^2}{P_{nA} \left( \frac{G_{nA} G_{np}}{b_{np}} \right) b_{np}} \left( \frac{F_r}{\Delta f_{\kappa}} \right)^2 A_{\phi} A_{canp} \bar{A} A_u A_c. \quad (4.9)$$

In the qualitative examination of telephone channel vital importance has the average-minute power of noises in the channel; and

MKKT [MKKT - International Telegraph and Telephone Consultative Committee] and MKKR in their recommendations (see Chapter 6) normalize precisely it. Therefore in formula (4.9) it is necessary to pass from instantaneous power of noise in the channel to the average-minute ones. For this value  $P_T$  must be averaged from the rapid fadings, i.e., to find  $\bar{A}_6$ ).

FOOTNOTE 1. It should be noted that with the averaging on the rapid fadings is obtained not the average-minute value, but average in 3-5 min. This time is determined the need for the development of the statistics of signal during the rapid fluctuations. Averaging in 1 min would accurately give for the complete ("Rayleigh") performance 3-5 different average-minute values. ENDFOOTNOTE.

From formula (4.4) taking into account (4.7) it is evident that  $A_5$  is inversely proportional to the power of signal at the input of receiver  $P_{cax}$ .

Page 124.

Knowing the distribution of power of signal with the rapid fadings, presents no difficulties to find  $\bar{A}_6$  from the formula:

$$\bar{A}_5 = \int_0^{\infty} \frac{1}{P_{cax}} W(P_{cax}) dP_{cax} \quad (4.10)$$

where  $W(P_{\text{ср}})$  — probability density of the power of signal with the single or diverse reception.

Thus, for the optimum addition with the  $N$ -fold reception into formula (4.10) it is necessary to substitute distribution (2.41) taking into account (2.26) and (2.25). As a result of computing the integral we will obtain value  $\bar{A}_0$  in the function of a number of diverse receivers  $N$  in the form 1)

$$\bar{A}_0 = \frac{U_{\text{ср}}^2}{2(N-1)} \quad (N > 1), \quad (4.11)$$

where  $\frac{U_{\text{ср}}^2}{2}$  — value of signal amplitude (see formula 2.23).

FOOTNOTE 1. With single reception  $\bar{A}_0$  there does not exist, since integral (4.10) diverges. ENDFOOTNOTE.

Formula (4.11) makes it possible to determine the coefficient of improvement, obtained from the use of the diverse reception with optimum addition  $Y_{\text{ср}}$  in the form:

$$Y_{\text{ср}} = \frac{\bar{A}_0}{U_{\text{ср}}^2/2} = \frac{1}{2(N-1)}. \quad (4.12)$$

Coefficient  $\gamma_w$  determines the ratio of the median value of the average-minute power of noise with the diverse reception to the power of noise, which corresponds to the rms value of signal with the single reception. For other methods of the combination of the diverse signals the computation of integral (4.10) presents considerable difficulties. For the linear addition, which is of greatest interest, was carried out numerical integration. The values of the coefficients of improvement are given in Table 4.1.

Table 4.1.

Состояние (1)	Прием (2)	
	двоенный (3)	четверный (4)
Оптимальное (5)	0,5	0,17
Линейное (6)	0,3	0,28

Key: (1). Addition. (2). Reception. (3). doubled. (4). quadrupled.  
(5). Optimum. (6). Linear.

Page 125.

As a result of the slow fluctuations of signal the average-minute value of thermal noises at the output of one section of tropospheric line  $P_r$  changes according to a normal-logarithmic law together with  $A_m$ . Coefficient when  $A_m$  in formula (4.9) determines the rms value of signal (on the slow fadings)  $\bar{P}_r$ . Taking into account (4.6) and (4.12) value  $\bar{P}_r$  for the upper channel at zero-level point can be determined according to the formula:

$$\bar{P}_r = \frac{(4\pi)^2 n k T \Delta f_k \kappa_{nc}^2 d^2 A_p \gamma_v}{P_{na} \left( \frac{G_{na} G_{np}}{z_{yc}} \right) \lambda^2 b_{np}} \left( \frac{F_a}{\Delta f_k} \right)^2 \bar{A}. \quad (4.13)$$

For standard telephone channel (0.3-3.4 kHz) with uniform noise distribution ( $\kappa_{nc}=0,75$ )

$$\bar{P}_r = 0,45 \cdot 10^{-15} \frac{n d^2 A_p \gamma_v F_a^2}{\gamma^2 P_{na} \left( \frac{G_{na} G_{np}}{z_{yc}} \right) \Delta f_k^2} \bar{A}. \quad (4.13a)$$

The average-minute value of noise changes around its median value according to the normal-logarithmic law whose distribution is represented in Fig. 4.1.

§4.3. Transient noises, caused by multiple-pronged radiowave propagation.

As it was shown in chapter 3, multiple-pronged radiowave propagation in the section of tropospheric line causes the nonuniformity of the amplitude-frequency characteristic and characteristic of the group propagation time. It is known that with the frequency modulation, which as a rule, it is utilized on the tropospheric lines, the nonuniformity of these characteristics leads to the distortions of modulating signal [4.1]. In particular, with multichannel telephony in this case appear transient noises in telephone channels.

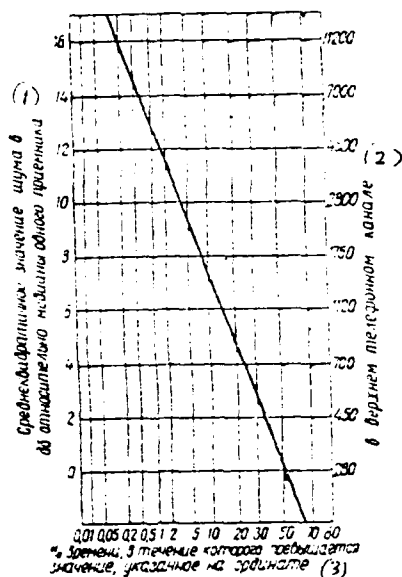


Fig. 4.1. Law of the distribution of the average-minute value of noise.

Key: (1). Rms value of noise in dv relative to the median of one receiver. (2). In upper telephone channel. (3). Time, during which is exceeded value, indicated on ordinate.

Page 126.

For the section of tropospheric line the form of the amplitude-frequency characteristic and characteristic of the group propagation time continuously changes in the time randomly. Respectively changes the crosstalk volume in telephone channels.



Therefore during the design of tropospheric lines it is important to know the law of probability distribution for the power of transient noises. It is necessary to also have a formula for calculating the average-minute power of transient noises, since in the norms of MKKR for the tropospheric lines is indicated precisely the average-minute power of noise [4.1]. Furthermore, it is important to estimate the decrease of transient noises during the use of the diverse reception.

Formulas for the calculation of power of the transient noises, caused by the multi-beam character of radiowave propagation, will be obtained in this section, they are valid for the existing in practice tropospheric multichannel systems. In such systems the length of section, the width of the antenna radiation pattern, and also the deviation of frequency depend on a number of telephone channels, moreover with an increase in the number of channels usually the foreshortened length of section and decreases the width of the antenna radiation pattern (i.e. increases their amplification). This is explained by the fact that with an increase in the number of channels increases the passband of receiver, and therefore for guaranteeing the threshold C/N necessary the higher signal level at the input of receiver. On the other hand, with an increase in the number of channels for guaranteeing the necessary relation of signal/thermal noise usually is necessary to increase the effective deviation, which corresponds to the measuring level of one telephone

channel (deviation "to the channel"). The aforesaid is illustrated by Tables 4.2, where are given the values of the parameters, typical for multichannel tropospheric systems.

Power of transient interferences. With the frequency modulation multichannel communication  $u(t)$  the signal at the output of transmitter takes the form

$$u_{\text{out}} = U_0 \cos[\omega_0 t - \Delta\omega_m s(t)], \quad (4.14)$$

where

$$s(t) = \int_0^t u(t) dt, \quad (4.15)$$

moreover

$$-1 \leq u(t) \leq 1 \quad (4.16)$$

with the probability, the close one to the unit;  $\Delta\omega_m$  - maximum deviation of the frequency;  $U_0$  - signal amplitude.

Table 4.2.

Число каналов (1)	Длина участка, км (2)	Ширина диаграммы направленности антенн град (3)	Девияция «на канал» кГц (4)
50	500	1	100
120	200	0,5	200

Key: (1). Number of channels. (2). Length of section, km. (3). Width of antenna radiation pattern deg. (4). Deviation "to channel" of kHz.

Page 127.

As a result of the multiple-pronged propagation of radio waves in the section of tropospheric line the signal on the input of receiver consists of a large quantity of delaying components. We will thus far consider that at the input of receiver there are by  $n$  of discrete components, the  $k$ -th component having amplitude  $U_k$ , delay  $\tau_k$  and phase  $\varphi_k$ .

As has already been indicated in chapter 3, in actuality multiple-pronged signal at the input of receiver has more complicated structure and is in general continuous of the components, how conveniently which differ little in the time lag. However, assumption about the discrete set of the delaying components makes analysis more

demonstrative.

Under the made assumption about the discrete structure of multiple-pronged signal channel (4.14) at the input of receiver takes the form

$$u_{np} = \sum_{k=1}^n U_k \cos[\omega_0(t - \tau_k) + \Delta\omega_m s(t - \tau_k) + \varphi_k]. \quad (4.17)$$

After simple trigonometric conversions the signal at the input of receiver can be presented in the form of the quasi-harmonic oscillation

$$u_{np} = U(t) \cos[\omega_0 t + \Delta\omega_m s(t) + \Theta(t) + \varphi_k], \quad (4.18)$$

where  $U(t)$  - the amplitude of this oscillation, and  $\Theta(t)$  - its phase, moreover

$$U(t) = \sqrt{X^2(t) + Y^2(t)}, \quad (4.19)$$

$$\Theta(t) = \text{arctg} \frac{Y(t)}{X(t)}, \quad (4.20)$$

where

$$X(t) = \sum_{k=1}^n U_k \cos\{\omega_0 \tau_k + \Delta\omega_m [s(t) - s(t - \tau_k)] + \varphi_k\}, \quad (4.21)$$

$$Y(t) = \sum_{k=1}^n U_k \sin\{\omega_0 \tau_k + \Delta\omega_m [s(t) - s(t - \tau_k)] + \varphi_k\}. \quad (4.22)$$

From expression (4.18) it is evident that as a result of the multiple-pronged radiowave propagation the signal at the input of receiver acquires "parasitic" amplitude modulation. This amplitude modulation must be substantially suppressed by limiter, otherwise it

will cause the considerable crosstalk volume in telephone channels [4.1]. Furthermore, from (4.18) and (4.15) it follows that the instantaneous frequency at the input of receiver as the derivative of its phase is determined by the expression

$$\omega^*(t) = \omega_0 + \Delta\omega_m u(t) + \frac{d\theta}{dt}. \quad (4.23)$$

Page 128.

Consequently, signal at the output of the FM discriminator of receiver takes the form 1)

$$e^*(t) = u(t) + \frac{1}{\Delta\omega_m} \frac{d\theta}{dt}. \quad (4.24)$$

FOOTNOTE 1. During this recording it is assumed that the product of the transmission factors of the frequency shift key and the FM discriminator to equal 1, i.e., during the undistorted transmission the signal at the output of detector is equal to signal at the input of modulator [4.2]. ENDFOOTNOTE.

In the latter expression first term is the undistorted communication and the second - distortion product which taking into account (4.20) is equal to

$$e(t) = \frac{1}{\Delta\omega_m} \frac{d\theta}{dt} = \frac{1}{\Delta\omega_m} \cdot \frac{X(t)Y'(t) - X'(t)Y(t)}{X^2(t) - Y^2(t)}. \quad (4.25)$$

Here and throughout prime designates the operation of differentiation.

Further analysis will be carried out taking into account the indicated in Table 4.2 limitations which occur for the existing multichannel tropospheric systems. In chapter 3 was obtained expression (3.61) for the energy pulse reaction of the section of tropospheric line. From this expression taking into account (3.60) and with  $d_r = 8500$  km (average conditions of refraction) is easy to find that for the parameters of a 60-channel system  $g(\tau_1) = 0.1$ , if  $\tau_1 = 0.2$   $\mu$ s, and for the parameters of a 120-channel system  $g(\tau_1) = 0.1$ , if  $\tau_1 = 0.05$   $\mu$ s. This means that the appearance of components with delay relative to the center of pulse reaction is respectively more than 0.2  $\mu$ s and 0.05  $\mu$ s have small probability. Consequently, it is possible to consider that in expressions (4.21) and (4.22):

$$\left. \begin{array}{l} \tau_k \leq 0,2 \text{ мксек при } N = 60 \\ \tau_k \leq 0,05 \text{ мксек при } N = 120 \end{array} \right\} \quad (4.26)$$

Key: (1). with.

Further from (4.15) it follows that

$$s(t) - s(t - \tau_k) = \int_{t - \tau_k}^t u(t) dt. \quad (4.27)$$

During the use of standard equipment for multiplexing the upper cut-off frequency multichannel communication with 60 channels is

equal to 252 kHz and with 120 channels - 552 kHz. Consequently, the period of upper cut-off frequency is approximately 4  $\mu$ s and 2  $\mu$ s. Taking into account (4.26) this means that in expressions (4.27) the period of the most rapid changes in integrand  $u(t)$  is much more than the interval of integration  $\tau_k$ .

Page 129.

Therefore in the interval of integration function  $u(t)$  can be considered in effect permanent and, therefore, instead of (4.27) it is possible to record the approximate equality

$$s(t) - s(t - \tau_k) \approx u(t) \tau_k. \quad (4.28)$$

Let us further note that with 60 telephone channels the effective deviation of multichannel communication exceeds deviation to the channel 2 times, and with 120 channels - 2.3 times [4.1]. Therefore according to data from Table 4.2 for the existing tropospheric systems the effective deviation of multichannel communication composes with 60 channels 200 kHz and with 120 channels - 460 kHz. It is also known that the maximum deviation multichannel communication  $\Delta f_m$  with probability 95% not more than 1.5 times exceeds its effective deviation [4.2]. Consequently,

$$\left. \begin{aligned} \Delta f_m &\leq 300 \text{ kHz при } N = 60 \\ \Delta f_m &\leq 690 \text{ kHz при } N = 120 \end{aligned} \right\} \quad (4.29)$$

Key: (1). with.

with the probability, the close one to the unit.

It is easy to show that during limitations (4.16), (4.26) and (4.29) occur the approximate equalities:

$$\sin[\Delta\omega_n u(t) \tau_k] \approx \Delta\omega_n u(t) \tau_k, \quad (4.30)$$

$$\cos[\Delta\omega_n u(t) \tau_k] \approx 1 \quad (4.31)$$

(error does not exceed 70/0). Taking into account (4.28), (4.30) and (4.31), expressions (4.21) and (4.22) can be approximately presented in the form:

$$X(t) = \sum_{k=1}^n U_k \cos(\omega_0 \tau_k - \varphi_k) - \Delta\omega_n u(t) \sum_{k=1}^n U_k \tau_k \sin(\omega_0 \tau_k - \varphi_k), \quad (4.32)$$

$$Y(t) \approx \sum_{k=1}^n U_k \sin(\omega_0 \tau_k - \varphi_k) - \Delta\omega_n u(t) \sum_{k=1}^n U_k \tau_k \cos(\omega_0 \tau_k - \varphi_k). \quad (4.33)$$

Let us examine now first terms in expressions (4.32) and (4.33). From the comparison with expressions (3.44) is evident that these terms are real and imaginary parts of the transfer function of the section of tropospheric line, i.e.,  $P(\Omega)$  and  $Q(\Omega)$ . Evident also that the sums of second terms of expressions (4.32) and (4.33) are the result of differentiation  $P(\Omega)$  and  $Q(\Omega)$  with respect to the frequency; let us designate these sums through  $P'(\Omega)$  and  $Q'(\Omega)$ . Let us recall further that the real and imaginary parts of the transfer function of the section of tropospheric line are the projection of



the amplitude of total signal, at the point of reception with the vector image of the signal (see Chapter 3). Page 130.

Consequently,  $P(\Omega)$  and  $Q(\Omega)$  can be recorded in the form

$$\begin{cases} P(\Omega) = V_0 \cos \phi_0 \\ Q(\Omega) = V_0 \sin \phi_0 \end{cases} \quad (4.34)$$

where  $V_0$  - amplitude of total signal at the point of reception and  $\phi_0$  - its phase. By analogy  $P'(\Omega)$  and  $Q'(\Omega)$  it is possible to consider the projections of certain "modified" signal, and, as can be seen from (4.32) and (4.33), the components of this signal have amplitude  $U_1$ , time lag  $\tau_1$  and phase  $\phi_1$ . Respectively can be recorded

$$\begin{cases} P'(\Omega) = V_1 \sin \phi_1 \\ Q'(\Omega) = V_1 \cos \phi_1 \end{cases} \quad (4.35)$$

where  $V_1$  - amplitude of the modified signal, and  $\phi_1$  - its phase. Taking into account (4.34) and (4.35) expression (4.32) and (4.33) it is possible to rewrite in the form:

$$X(t) = V_0 \cos \phi_0 - \Delta \omega_m u(t) V_1 \sin \phi_1 \quad (4.36)$$

$$Y(t) = V_0 \sin \phi_0 - \Delta \omega_m u(t) V_1 \cos \phi_1 \quad (4.37)$$

Let us determine first the power of transient interferences for the "frozen troposphere", i.e., in the constant parameters of multiple-pronged channel. Therefore we will thus far consider values  $U_1$ ,  $\tau_1$  and  $\phi_1$  as constants, then in (4.36) and (4.37) on time depends only  $u(t)$ . Taking into account this, let us differentiate (4.36) and (4.37) on the time and we will use relationship (4.25). As a result

after simple conversions we will obtain for the product of the distortions

$$z(t) = \frac{u'(t) V_0 V_1 \cos \Phi}{V_0^2 + 2\Delta\omega_{\pi} u(t) V_0 V_1 \sin \Phi + \Delta\omega_{\pi}^2 u^2(t) V_1^2} \quad (4.38)$$

Let us further expand the right side of expression (4.38) in series according to degrees of  $u(t)$ , moreover we will be restricted to terms of expansion not higher than the second degree. As a result after obvious conversions we will obtain

$$z(t) = \frac{V_1}{V_0} \cos \Phi u'(t) - \frac{1}{2} \Delta\omega_{\pi} \left( \frac{V_1}{V_0} \right)^2 \sin 2\Phi [u^2(t)]' + \frac{1}{3} \left( \frac{V_1}{V_0} \right)^3 \Delta\omega_{\pi}^2 \cos \Phi (1 - 2\cos 2\Phi) [u^3(t)]', \quad (4.39)$$

where

$$\Phi = \Phi_0 - \Phi_1$$

(prime designates the process of differentiation). The first member of expression (4.39) contains the derivative of the modulating function  $u(t)$ . Since spectrum  $u'(t)$  does not contain new spectral components in comparison with  $u(t)$ , then the first term determines the so-called "coherent" product of distortions. This term does not bring about transient interferences, but gives only change in the level of useful communication in channels [4.1]. The second term determines distortion products, incoherent with  $u(t)$ , and therefore characterizes the level of transient interferences.

The third term also in essence contains noncoherent products; however, it has also coherent with  $u(t)$  part. Thus, transient noises are determined by the second and third members of expression (4.39).

For convenience in further computations it is expedient to introduce standardized values, after designating

$$v_0^2 = \frac{V_0^2}{\bar{V}_0^2}, \quad (4.40)$$

$$v_1^2 = \frac{V_1^2}{\bar{V}_1^2}, \quad (4.41)$$

where  $\bar{V}_0^2$  and  $\bar{V}_1^2$  — mean squares of values  $V_0$  and  $V_1$ , and  $v_0$  and  $v_1$  — the standardized values of these values; it is obvious that

$\bar{v}_0^2 = 1$ ,  $\bar{v}_1^2 = 1$ . Let us note now that according to (4.34) and (4.35)

$$\left. \begin{aligned} \bar{V}_0^2 &= \bar{P}^2(\Omega) + \bar{Q}^2(\Omega) = 2\sigma_0^2 \\ \bar{V}_1^2 &= \bar{P}'^2(\Omega) + \bar{Q}'^2(\Omega) = 2\sigma_1^2 \end{aligned} \right\} \quad (4.42)$$

where  $\sigma_0^2$  and  $\sigma_1^2$  — the mean squares of the projections of the amplitude of basis and modified signals. As shown in chapter 3 energy pulse reaction of the section of tropospheric line plays for random functions  $P(\Omega)$  and  $Q(\Omega)$  the same role, as energy spectrum for the random process. It is known that the mean square of process is equal

to integral of the energy spectrum all over frequency region. Consequently, by analogy between the fluctuation noise and the signal with the multiple-pronged structure value  $\sigma_0^2$  is equal to integral of the energy pulse reaction all over region of time lags. For the existing in practice tropospheric systems energy pulse reaction is even function  $\tau$ . Therefore  $\sigma_0^2$  is determined by the relationship

$$\sigma_0^2 = 2 \int_0^{\infty} g(\tau_1) d\tau_1. \quad (4.43)$$

Values  $P'(\Omega)$  and  $Q'(\Omega)$  are derivatives of  $P(\Omega)$  and  $Q(\Omega)$  in the frequency. It is known that the energy spectrum of derived process can be obtained from the spectrum of fundamental process by multiplication on  $\Omega^2$ . Therefore by analogy between the fluctuation noise and the signal with the multiple-pronged structure "energy spectrum" for  $P'(\Omega)$  and  $Q'(\Omega)$  can be obtained from the energy pulse reaction  $g(\tau_1)$  by multiplication on  $\tau_1^2$ .

Consequently, value  $\sigma_1^2$  is determined by the relationship

$$\sigma_1^2 = 2 \int_0^{\infty} \tau_1^2 g(\tau_1) d\tau_1. \quad (4.44)$$

Page 132.

Now according to (4.42), (4.43) and (4.44) it is possible to record the following equality:

$$\frac{\overline{V_1^2}}{\overline{V_0^2}} = \frac{\int_{-\infty}^{\infty} \tau_1^2 g(\tau_1) d\tau_1}{\int_{-\infty}^{\infty} g(\tau_1) d\tau_1} \quad (4.45)$$

After comparing the right sides of expressions (3.52) and (4.45), we will obtain

$$\frac{\overline{V_1^2}}{\overline{V_0^2}} = \Delta\tau_1. \quad (4.46)$$

Let us recall that  $\Delta\tau_1$  — the mean value of the absolute divergence of group time lag from mean value  $\tau_{rp}$  — is calculated from formula (3.76). Express in (4.39) values  $V_0$  and  $V_1$  through their standardized values. Furthermore, let us consider (4.46) and will drop in (4.39) the first term, which is determining the coherent product of distortions. Let us designate also:

$$\varphi_2 = \Delta\tau_1 \left[ \frac{1}{2} - \frac{\overline{\tau_1^2}}{\overline{\tau_1}} \sin 2\phi \right] = \Delta\tau_1 \rho_2. \quad (4.47)$$

$$\varphi_3 = \Delta\tau_1 \left[ \frac{1}{3} - \frac{\overline{\tau_1^3}}{\overline{\tau_1}} \cos \phi + 1 - \cos 2\phi \right] = \Delta\tau_1 \rho_3. \quad (4.48)$$

As a result we will obtain expression for the incoherent products of the distortions

$$z_{ik}(t) = \varphi_2 \Delta\omega_{\pi} [\omega^2(t)]' + \varphi_3 \Delta\omega_{\pi}^2 [\omega^3(t)]'. \quad (4.49)$$

Let us note now that in work [4.4] during the computation of the

power of transient noises is obtained the expression, which has the same form, as expression (4.49) <sup>1</sup>).

FOOTNOTE 1. The presentation of work [4.4] can be found also in [4.1]. ENDFOOTNOTE.

True, this expression in work [4.4] is obtained for the product of the distortions, which appear in the apparatus circuit with the constant parameters, and therefore coefficients  $\varphi_2$  and  $\varphi_3$  are here constant values. In our case multiple-pronged tropospheric channel has the variable parameters, and therefore coefficients  $\varphi_2$  and  $\varphi_3$  randomly change in the time. However, these changes occur much slower than change in the signal multichannel communication. Therefore it is possible to consider these coefficients as constants and, after using the relationships of work [4.4], to determine the power of transient noises at the output of telephone channel.

Page 133.

Obtained thus power will depend on the slowly changing parameter which determines the law of probability distribution for the crosstalk volume.

Let us note also that for the real tropospheric lines, taking

into account (4.48), and also the statistical properties of random variables  $v_0$ ,  $v_1$  and  $\phi$ , it is possible to show that during the high percentage of time the power of transient noises is determined in essence by the first member of expression (4.49). Therefore let us leave in expression (4.49) only first term and will make the same conversions, as in work [4.4]. As a result taking into account (3.76) we will obtain final formula for the power of transient noises at the output of telephone channel at point with the zero relative level.

$$P_n = 10^{-3} \frac{\Delta F_k \kappa_{nc}^2}{\Delta F} (2\pi F_i)^2 (2\pi \Delta F_k)^2 e^{4\rho_{cp}} y_2(\sigma) \frac{\int_0^1 d^2}{c^4 a_i^4} p_{2, \text{norm}}^{(1)} \quad (4.50)$$

Key: (1) . mW.

where  $\Delta F_k$  — band of telephone channel;  $F_i$  — the medium frequency of the  $i$  channel,  $\kappa_{nc}$  — the psychometric coefficient;  $\Delta F = F_2 - F_1$  — width of the spectrum multichannel communication;  $F_1$ ,  $F_2$  — respectively lower and upper cut-off frequencies multichannel communication  $\Delta f_k$  — deviation "to the channel";  $\sigma = \frac{F_i - F_1}{F_2 - F_1}$  — dimensionless coordinate of the medium frequency of the channel;  $y_2(\sigma)$  — function, which calculates the distribution of transient noises on the basis of the spectrum multichannel communication (in Fig. 4.2, undertaken from [4.4], is shown the graph of this function);  $\rho_{cp}$  — difference in the nepers between the average level  $N$  of telephone channels and the measuring level of one telephone channel; with  $N < 240$   $\rho_{cp}$  it is determined from formula [4.1]:

$$\rho_{cp} = (-1 + 4 \lg N), \text{ dB.} \quad (4.51)$$

In expression (4.50)  $p_2$  it is the random variable, determined by relationship (4.47). Probability distribution for value  $p_2$  depicts on the relative scale distribution for the power of transient interferences. Value  $p_2$ , in turn, depends on random variables  $v_0$ ,  $v_1$  and  $\phi$ . The statistical properties of these values to us are known.



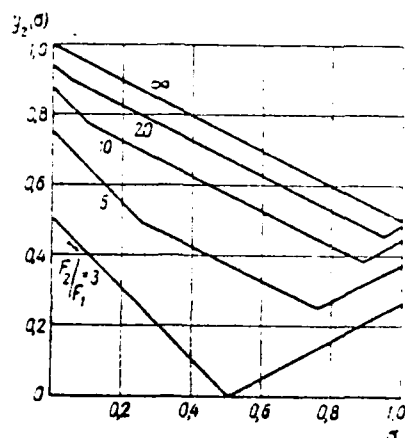


Fig. 4.2. Distribution of power of transient noises in the group spectrum (in the relative units).

Page 134.

As has already been indicated in chapter 1 and 3, the amplitude of the total signal  $v_0$  is distributed according to the law of rayleigh, and its phase  $\phi_0$  was distributed evenly in the limits from 0 to  $2\pi$ . Projections of the amplitude of modified signal  $P'(\Omega)$  and  $Q'(\Omega)$ , being derivatives of the normal distribution of values  $P(\Omega)$  and  $Q(\Omega)$ , are also distributed normally [4.3]. Consequently, the amplitude of the modified signal  $v_1$  is distributed according to the law of rayleigh, and its phase  $\phi_1$  is distributed evenly in the limits from 0 to  $2\pi$ . Further, since  $P'(\Omega)$  and  $Q'(\Omega)$  is

statistically not depended from  $P(\Omega)$  and  $Q(\Omega)$  [4.3], then values  $v_0$  and  $v_1$  are not depended, and a difference in their phases  $\phi$  is distributed evenly from 0 to  $2\pi$ . The methods of the probability theory make it possible to find the law of probability distribution for the function from several random variables, if are known the static properties of these values [4.2], [4.3]. With these methods in [4.5] is found the integral law of distribution for value  $p_2$ , which takes the form:

$$W(p_2 < P_1) = \begin{cases} \frac{4P_2}{\pi \sqrt{1-4P_2^2}} \ln \left| \frac{\sqrt{1-4P_2^2} + 1 + 2P_2}{1 - \sqrt{1-4P_2^2} - 1 - 2P_2} \right|, & 0 \leq P_2 < \frac{1}{2} \\ \frac{4P_2}{\pi \sqrt{4P_2^2-1}} \operatorname{arctg} \frac{\sqrt{4P_2^2-1}}{2P_2-1}, & P_2 > \frac{1}{2} \end{cases} \quad (4.52)$$

The curve of the integral law of probability distribution for value  $p_2$  is shown in Fig. 4.3.

Let us examine now expression (4.50), which is determining the power of transient noises in telephone channel. From this expression taking into account (4.47) it is evident that the power of transient noises grows with decrease of  $v_0$ , i.e., with the decrease of signal at the input of receiver. This is an important fact, since from the signal at the input of receiver depend thermal noises in telephone channel (see §4.1). Consequently, the increase of thermal noises with the rapid signal fading is connected with the increase of transient noises. This connection however, is not single-valued, but has

DCC = 90025108

PAGE

~~27~~  
280

statistical (correlative) character, since crosstalk volume depends not only on  $v_0$ , but also on random variables  $v_1$  and  $\phi$ .

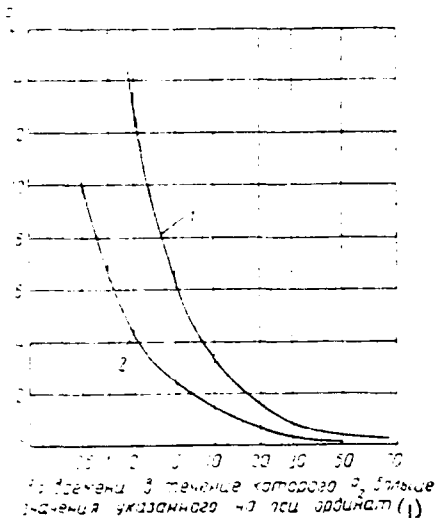


Fig. 4.3. Integral law of probability distribution for the transient noises, caused by multiple-pronged radiowave propagation: 1 - single reception 2 - the doubled reception.

Key: (1). The time during which  $P_2$  is longer than the value, indicated on axis of ordinates.

Page 135.

Further from expression (4.50) it is evident that the power of the transient noises, caused by the multi-beam character of propagation, is proportional to the width of the antenna radiation pattern to the fourth degree and to the length of the section of line to the eighth degree. Thus, the power of transient noises sharply grows with an increase in the length of section and expansion of the antenna

radiation pattern. Furthermore, from (4.50) evident also that the power of transient noises depends substantially on the value of an equivalent radius of Earth  $R_e$ , i.e. from the conditions of refraction. Physically this is explained by the fact that with deterioration in the refraction grows the scattering angle and, therefore, increases the relative time lag of the components, re-emitted with the heterogeneities of the troposphere. The conditions of refraction slowly change in the time. Consequently, crosstalk volume, besides the rapid fluctuations, caused by a change in the multiple-pronged structure of signal, has also relatively slow changes. It is important to note that the level of thermal noises also has the slow changes, connected with the slow signal fading at the input of the receiver (see Chapter 1). Moreover, slow changes in the thermal and transient noises have statistical connection and this must be had in mind during the design of the tropospheric lines of communications.

Gain with the diverse reception. On the tropospheric lines for dealing with the rapid signal fading is utilized the diverse reception moreover in practice for guaranteeing the necessary for stability of communication usually is utilized the quadrupled reception. For adding four signals accepted in essence are utilized two systems of the addition:

1) the addition of signals in pairs in the circuit of intermediate frequency to the detectors, after which the signals from the output of two detectors store in the circuit of the low frequency:

2) the addition of all four signals in the circuit of intermediate frequency to the detector.

In both systems during the addition of signals in the circuit of intermediate frequency with the aid of the special devices is provided the coincidence of frequency and phase of the stored signals.

Let us examine first how influences the power of transient noises the diverse reception during the use by the 1st of the systems indicated. During the addition of two signals in the circuit of intermediate frequency value  $v_0$  in expression (4.47) is an arithmetical sum of two values, distributed according to the law of rayleigh, the law of probability distribution for this sum is determined by expression (2.44). Let us note that the addition "in the phase" is realized only for the fundamental signals, but not for those modified. As has already been indicated, the modified signals are statistically not depended from the bases, and therefore they are added vectorially.

Page 136.

Meanwhile it is known that vector sum of two values, distributed according to the law of Rayleigh, is also distributed according to the law of Rayleigh [4.2], [4.3] and, therefore, in expression (4.47) value  $v_1$  has Rayleigh probability distribution. The phases of the total vector  $v_0$ , and also the total vector  $v_1$  in add in question system, as before, are distributed evenly from 0 to  $2\pi$ . Consequently, in expression (4.47) a difference in these phases  $\Phi$  is also distributed evenly from 0 to  $2\pi$ .

Taking into account the statistical properties of values  $v_0$ ,  $v_1$  and  $\Phi$  indicated in [4.5] is found the integral law of the probability distribution of value  $P_2$  during the doubled reception and the addition of signals to the detector. This law takes the form:

$$W(P_{\text{rec}} < P_2) = \frac{4P_2 \ln \left( \frac{1}{2P_2} + \sqrt{\frac{1}{4P_2^2} - 1} \right)}{\pi \sqrt{1 - 4P_2^2}} + \frac{4P_2 \arccos \frac{1}{2P_2}}{\pi \sqrt{4P_2^2 - 1}}$$

where  $R$  - function  $P_2$ , expression for which see in [4.5].

The curve of the integral law of the probability distribution for value  $P_2$  is

AD-A883 445

FOREIGN TECHNOLOGY DIV WRIGHT-PATTERSON AFB OH  
REMOTE TROPOSPHERIC RADIO COMMUNICATION.(U)  
MAR 80 I A BUSYATINSKIY, A S NEMIROVSKIY  
FTD-ID(R&T)-0251-80

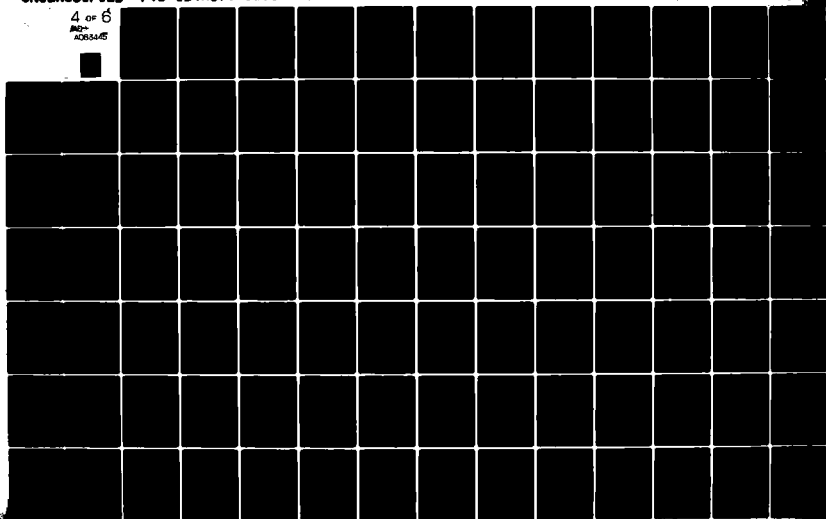
F/8 17/80

UNCLASSIFIED

NL

4 OF 6

AD-A883 445





constructed in Fig. 4.3 next to the curve for the single reception. From Fig. 4.3 it is evident that the use of the doubled reception during the addition of signals to the detector significantly decreases the power of transient noises. This is understandable, since in this system of addition occurs an improvement in the uniformity of the amplitude-frequency characteristic and characteristic of the group time of propagation of the section of the line (see Chapter 3). During the addition of two signals in the circuit of intermediate frequency to the detector at the output of detector are summarized thermal and transient noises. Then are summarized low-frequency signals from the outputs of two detectors, moreover in the system in question is realized the linear addition (see Chapter 2). However, with sufficient for the practice accuracy it is possible to consider that here is conducted the automatic selection of that of the low-frequency signals, for which the power of noises is minimum.

Thus it is first necessary to find the integral law of probability distribution for the sum of thermal and transient noises on the output of detector. Further it is possible to calculate probability that the total noise at output of both detectors does not exceed the specific value. This probability gives the integral law of distribution for the sum of noises in the low-frequency circuit, i.e., for the system of the quadrupled reception as a whole. Since

the total noises at the output of detectors are not depended and detectors are identical, then according to product rule [4.2], [4.3] this integral law is determined by the relationship

$$\begin{aligned} W(n_{\text{счета}} < N_{\text{счета}}) &= 1 - W(n_{\text{счета}} > N_{\text{счета}}) = \\ &= 1 - W^2(n_{\text{сдв}} > N_{\text{сдв}}). \end{aligned} \quad (4.54)$$

Page 137.

Main difficulty with the solution of this problem consists of the determination of the law of probability distribution for the sum of thermal and transient noises with doubled reception i.e., in the determination of function  $W(n_{\text{сдв}} > N_{\text{сдв}})$ . The fact is that, as it was already shown, fluctuations of the level of thermal and transient noises at the output of detector are statistically dependent, which considerably complicates the determination of the law of distribution for their sum. Nevertheless, by the methods of the probability theory this problem can be solved; however, mathematical calculations are very complicated. Therefore these calculations here are not given, but is given only final result, i.e., the law of probability distribution for the sum of noises during the quadrupled reception and the addition of signals in the circuit of low frequency. This law is obtained by the method of numerical integration in electronic computer and it is analytically expressed to it cannot. Graphically this law of distribution is depicted as the curve, shown in Fig. 4.4.

the vertical axis is here given relation  $N_{\text{trans}}/N_{\text{th}}^2$  where  $N_{\text{th}}$  is the power of transient interferences, designed according to (4.50) with  $p_2=1$ . The curve in Fig. 4.4 corresponds to the average power of thermal and transient noises; as it is shown in Fig. 4.4, this equality corresponds to the optimum value of frequency in which the average total power of thermal and transient noises is minimum. However calculations show that in other cases of the average power of thermal and transient noises the curve of the integral law of probability distribution for their sum deviates little from the curve in Fig. 4.4.

When a curve of the law of distribution for the sum of noises at the output of detector, after using relationship (4.54), it is not difficult to find a curve for the total power of noise during the operation of the circuit of low frequency, i.e., with that quadrupled value of  $N_{\text{th}}$ . This curve is also shown in Fig. 4.4. From the comparison of curves in this figure it is evident that the quadrupled receiver sensitivity decreases the overshoots of noises in comparison with the case of  $N_{\text{th}}$ .

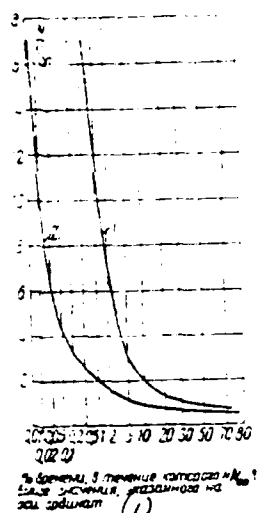


Fig. 4.4. Integral law of probability distribution for the sum of the thermal and transient rises: 1 - the doubled reception; 2 - the quadrupled reception.

Key: (1). the time during which is higher than the value, indicated on the axis of ordinates.

Here  $P(\alpha, \beta, \gamma, z)$  - the designation of the hypergeometric function whose values are tabulated.

Average-minute power of transient noises. Formula (4.50) determines the power of transient noises, measured during the short period of time (of second), until the multiple-pronged structure of signal can be considered constant. Meanwhile in the recommendations of MKKR for the tropospheric lines is normalized the average-minute power of noises [4.1]. It is obvious, for computing the average-minute power it is necessary to find the rms value of value  $p_2$  in accordance with its law of distribution. Certain difficulty here lies in the fact that the theoretically root-mean-square value of value  $p_2$  does not exist. This is obtained because the theoretical laws of probability distribution for  $p_2$ , determined by expressions (4.52), (4.53) and (4.55), assume possible the how conveniently large "overshoots" of transient noises. It is in actuality certainly, such "overshoots" on the real lines do not occur. Therefore during the computation of the rms value of  $p_2$  upper integration limit should be restricted. Is expedient to accept this limit equal to  $p_{max} = 15$ . This value  $p_2$  corresponds on the real tropospheric lines to the overshoots of transient noises to 10% pW. As it is

Page 138.

Let us examine now add system, in which is realized the addition of all four signals before the detector (linear addition, see chapter 2). In this system of addition value  $v_0$  in expression (4.47) is obtained as a result of the addition of four values, distributed according to the law of rayleigh. However, the law of probability distribution for the sum of four such values to obtain complicatedly. Therefore to it is more convenient consider that value  $v_0$  is distributed according to the law for the so-called optimum addition (see Chapter 2). This law is very close to the law for the linear addition. As far as value is concerned  $v_1$ , entering expression (4.47), then, as has already been indicated, the modified signals store without the tuning of the phase; therefore  $v_1$  is as before distributed according to the law of rayleigh. The phases of total fundamental and total of that modified of signals and, consequently, also their difference  $\phi$  are as before distributed evenly in the limits from 0 to  $2\pi$ . Taking into account the statistical properties of values  $v_0$ ,  $v_1$  and  $\phi$  indicated by the methods of the probability theory [4.3] can be found the density of distribution of probabilities for value  $p_2$  during the addition of four signals to the detector. This density of distribution takes the form

$$W(p_{2\text{overs}} < p_{2\text{overs}}) = 0,08 F(2,5; 3; 5,5; 1 - p_{2\text{overs}}^2). \quad (4.55)$$

established/installed experimentally, the overshoots, which exceed this value, do not occur.

Page 139.

Thus, according to the rule of the determination of average value [4.2], [4.3] the rms value of value  $p_2$  can be determined by the method of computing the integral

$$\overline{p_2^2} = \int_0^{p_2^{\text{maxc}}} p_2^2 W(p_2) dp_2, \quad (4.56)$$

where  $W(p_2)$  - the density of distribution of probability for  $p_2$  with the single and diverse receptors determined by expressions (4.52), (4.53) and (4.55). Analytically integral in (4.56) is calculated very complicatedly, and therefore more simply to resort to the numerical integration. Graphic calculation of integral in (4.56), carried out in accordance with the curves in Fig. 4.3, and also expression (4.55), gives following values  $\overline{p_2^2}$ :

$$\overline{p_2^2} = 1.3, \quad (4.57)$$

with the single receptor

$$\overline{p_2^2} = 0.3, \quad (4.58)$$

during the doubled reception and the addition of signals to the detector

$$\overline{p_2^2} = 0.17. \quad (4.59)$$

In the system of the quadrupled receiver during the addition of the pair of signals to the detector, and then by the addition of signals from the output of two detectors to determine the average-minute power of transient interferences is impossible. As has already been indicated, in this system is conducted the automatic selection on the sum of transient and thermal noises, and therefore here has sense he speaks only about the total average-minute power. Furthermore, this total average-minute power will depend on the relationship between the thermal and transient noises. There is greatest interest for the practice in case, when with the single reception the average-minute power of thermal and transient noises are equal. This corresponds to the minimum total power of the noises (see §4.4).

Calculated average value in accordance with curved 2 in Fig. 4.4 it shows that in this case in the system of the quadrupled reception in question the total average-minute power of thermal and transient noises 3 times (to 5 dB) is less than total average-minute power with the single reception.

In conclusion let us note that the calculated here average power of transient noises, strictly speaking, is not average-minute. The



fact is that the speed of signal fading and, consequently, also the frequency of the "overshoots" of transient noises on the real lines comprises the portions of hertz. Therefore during the minute usually are observed a total of several considerable overshoots of transient noises, which is clearly insufficient for determining the average value for the minute. Therefore it is necessary to keep in mind that the calculated here values of average power are average for a few minutes.

Page 140.

Transient noises due to the parasitic amplitude modulation. From expressions (4.15), (4.18), (4.19), (4.21) and (4.22) it is evident that as a result of the multiple-pronged radiowave propagation the signal amplitude at the point of reception is modulated multichannel communication  $u(t)$ . It is known that if this parasitic AM completely is not eliminated in the limiter, then it causes transient noises in telephone channels [4.1]. We will not be it here gives the derivation of formula for computing the power of transient noises due to parasitic AM, but let us give only the method of obtaining this formula.

For obtaining this formula one should substitute (4.36) and (4.37) in (4.19). Further expression for the signal amplitude it is

possible to lead to the form, the analogous expression from [4.6] <sup>1)</sup>, where are examined transient interferences due to parasitic AM, appearing in the circuit equipment.

FOOTNOTE <sup>1</sup>. The presentation of this work is given also in [4.1].  
ENDFOOTNOTE.

Then, after making the same conversions, that also in [4.6], is easy to obtain final formula for the calculation of power of transient noises due to parasitic AM. This formula for the point with the zero relative level of useful signal takes the form

$$P_{nAM} = (0.15)^2 \frac{2 \Delta F_k}{\Delta F} K_{nc}^2 K_{orp}^2 (2\pi \Delta f)^2 e^{4P_{cp}} \frac{x_1^2 x_2^4}{c^2 x_1^2} p_1^2, \text{ msm}, \quad (4.60)$$

Key: (1). W.

here  $K_{orp}$  — coefficient, which considers suppression AM by limiter,  
 $p_1$  — random variable, equal to

$$p_1 = \frac{v_1}{v_0} \sin \phi, \quad (4.61)$$

remaining designations in (4.60) the same as in (4.50). Parameter  $p_1$ , depending on random variables  $v_0$ ,  $v_1$  and  $\phi$ , determines the fluctuations of crosstalk volume. Taking into account statistical properties indicated above of values  $v_0$ ,  $v_1$  and  $\phi$  it is possible to find the laws of probability distribution for value  $p_1$  with the

single and diverse receptions. These laws are obtained into §4.3; Let us here point out only that in the receivers of tropospheric lines is required the very strong suppression by parasitic AM in the limiter for guaranteeing a small crosstalk volume. Calculations according to formula (4.60) and experimental measurements show that with the coefficient of suppression AM in the limiter  $K_{AM} = 0.003-0.004$  power of transient noises due to parasitic AM compares with the diverse reception only several ten picowatts.

Gain from the introduction of predistortions. On the radio relay lines with ChM with multichannel telephony usually are utilized the predistortions of the group spectrum, with which increases the deviation in "upper" telephone channels and it decreases in the "lower ones" [4.1]. The introduction of predistortions changes the level not only of thermal ones, but also transient noises. This question is examined in [4.7], where is determined the corresponding gain from the introduction of predistortions. As it was shown above, on the real tropospheric lines transient noises due to the multi-beam character of propagation are determined in essence by the 1st member of expression (4.49), i.e., by the product of the distortions of the 2nd order.

In [4.7] it is shown that the predistortions, introduced in accordance with the curve of MKPB [4.1], decrease the power of the transient noises of the 2nd order (on the 2nd harmonic) to 5 db, or 3 times. Consequently, and for the transient noises due to the multi-beam character of propagation in upper telephone channel we have a gain from the introduction of predistortions.

$$b_{\text{пред}} = 5 \text{ дб (3 раза)}. \quad (4.62)$$

Key: (1). time.

Experimental measurements. The experimental measurements of the power of transient noises repeatedly were conducted on the routes of different extent and with different antenna directivity. The results of these measurements, given in [4.5] and [4.6], coincide well with the calculations according to the formulas of this section<sup>1</sup>.

FOOTNOTE <sup>1</sup>. Exception are the routes above sea where the presence of the strong regular component of signal significantly decreases the crosstalk volume. ENDFOOTNOTE.

In Fig. 4.5, undertaken from [4.5], is shown the sample of the recording of crosstalk volume on recorder tape. This recording is made in the section of tropospheric line with a length of 300 km with the single and doubled receptions (during the addition of signals to the detector). Crosstalk volume was recorded at the output of

telephone channel with the frequency that "presenting" to 275 kHz. The effective deviation of frequency, which corresponds to measuring level of one telephone channel, was 100 kHz; the width of the antenna radiation pattern of  $-10^\circ$ . From Fig. 4.5 it is evident that the crosstalk volume continuously is changed due to a change of the multiple-pronged structure of signal and at the separate moments of time they take place the sharp "overshoots" of this level; the doubled reception substantially decreases a quantity and a value of such overshoots.

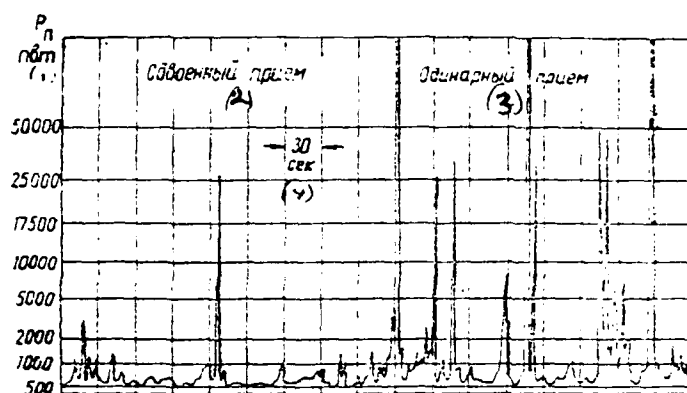


Fig. 4.5. Sample of the recording of the fluctuations of crosstalk volume on recorder tape.

Key: (1). pW. (2). Doubled reception. (3). Single reception. (4). ALC

Page 142.

The simultaneous recording of signal level conducted at the input of receiver showed that a sharp increase in the crosstalk volume is connected, although it is ambiguous, with deep signal fading.

§4.4. Fluctuations of overall line attenuation and phase of signal in telephone channel.

In §4.2 it was shown that 1st term of expression (4.39)

determines the coherent product of distortions which has the same spectral components, as useful communication. Coherent product is summarized with the useful communication geometrically (it is vector) and are produced change in level and phase of signal at the output of telephone channel. It is known that signal level at the output of telephone channel is determined by so-called "overall line attenuation" in channel [4.1]. Thus, the appearance of a coherent product, caused by the multi-beam character of propagation, is equivalent to the fluctuations of overall line attenuation in the channel, which produce change in the volume in subscriber, and also they can lead to self-excitation in the channel. Therefore these fluctuations must not exceed the specific value<sup>1</sup>.

FOOTNOTE 1. Norms to changes in overall line attenuation on the lines "direct visibility" are given in 4.1. For the tropospheric lines of such norms thus far there does not exist. ENDFOOTNOTE.

Changes in the phase of signal during the transmission of voice communications do not have a value. However, these changes can lower the stability of communication during the secondary multiplexing of telephone signal channel of telegraph or binary information (see Chapter 7). In accordance with (4.39) the coherent product of the distortions, caused by the multi-beam character of propagation, is equal to

$$\varepsilon_K(t) = \frac{V_1}{V_0} \cos \varphi u'(t). \quad (4.63)$$

For determining the fluctuations of overall line attenuation and phase of useful signal let us assume that to the input of telephone channel is given the single tone. Let after the transfer into the spectrum of group frequencies this modulating signal have frequency

The amplitude of the modulating signal, as into §4.3, let us take as equal to 1. Then the modulating signal takes the form

$$u(t) = \sin \Omega t. \quad (4.64)$$

Differentiating (4.64) on  $t$  and after substituting result in (4.63), we will obtain for the coherent product

$$z_k(t) = \Omega \frac{V_1}{V_0} \cos \Phi \cos \Omega t. \quad (4.65)$$

Page 143.

Let us explain the now physical sense of value  $\frac{V_1}{V_0} \cos \Phi$ . For this express the derivative of the phase response of section, i.e., group time lag, through the real and imaginary parts of the transfer function (see Chapter 3). In accordance with (3.33) we have

$$\Delta \tau_{rp} = \frac{d\theta(\Omega)}{d\Omega} = \frac{P'(\Omega)Q(\Omega) - P(\Omega)Q'(\Omega)}{P^2(\Omega) + Q^2(\Omega)}. \quad (4.66)$$

After substituting (4.34) and (4.35) in (4.66), after simple conversions taking into account (4.40), (4.41) and (4.42) we will



obtain

$$\Delta \tau_{rp} = \frac{V_1}{V_0} \cos \phi. \quad (4.67)$$

From comparison (4.65) and (4.67) it is evident that the coherent product of distortions is determined by expression

$$\epsilon_x(t) = \Omega \Delta \tau_{rp} \cos \Omega t. \quad (4.68)$$

The fundamental harmonic of signal at the output of the FM discriminator is composed of the undistorted communication  $u(t)$  and coherent product  $\epsilon_x(t)$ . Consequently, the fundamental harmonic of signal is determined by the expression

$$u_1(t) = \sin \Omega t + \Omega \Delta \tau_{rp} \cos \Omega t. \quad (4.69)$$

Expression (4.69) is easy to reduce to the form

$$u_1(t) = U_{m1} \sin(\Omega t + \beta_1). \quad (4.70)$$

where

$$U_{m1} = \sqrt{1 + (\Omega \Delta \tau_{rp})^2}, \quad (4.71)$$

$$\beta_1 = \Omega \Delta \tau_{rp}. \quad (4.72)$$

Group time lag changes randomly as a result of a change in the multiple-pronged structure of the signal (see Chapter 3). Respectively randomly change amplitude  $U_{m1}$  and phase  $\beta_1$  for the fundamental harmonic of signal at the output of the FM discriminator. The frequency of these fluctuations has the same order, as the frequency of rapid signal fading.

From the examination of expressions (4.70), (4.71) and (4.72) it

is possible to draw two important conclusions:

1) with any changes  $\Delta\tau_p$  occurs only a increase in the amplitude of the fundamental harmonic, i.e., the decrease of overall line attenuation;

2) the fluctuation of the phase of signal can be considered as its delay to period  $\Delta\tau_p$ . Furthermore, from (4.72) it follows that, measuring the phase of signal at the output of the FM discriminator, it is possible with the known  $Q$  to obtain value  $\Delta\tau_p$ ; this method of measurements is used extensively on the tropospheric lines (see Chapter 3).

Page 144.

Thus, amplitude and phase of the modulating signal at the output of the FM discriminator are completely determined by value [words not found in document]  $\omega_0$  <sup>1</sup>.

FOOTNOTE <sup>1</sup>. This is correct for any four-pole, if in the limits of the spectrum of the modulated signal the value practically is not changed; hence occurs term "group time lag", i.e., the delay time of the modulating signal. ENDFOOTNOTE.

It is necessary, however, to keep in mind that relationship (4.39) and, consequently, also relationships (4.71) and (4.72) are approximate and give sufficient accuracy only with the fulfillment of limitations (4.26) and (4.29). As it was shown in §4.2, on the tropospheric lines, intended for multichannel telephony, these limitations in the high percentage of time are fulfilled. But at the separate, rare moments of time the limitations indicated can and not occur. Therefore with small probability are nevertheless possible the cases when signal amplitude does not increase, but it decreases, and the phase of signal no longer is determined by value  $\Delta\tau_{rp}$  at the frequency  $\omega_0$ .

The integral law of probability distribution for  $\Delta\tau_{rp}$  is obtained in chapter 3 and takes form (3.50). This law determines probability distribution for the fluctuations of amplitude and phase of useful signal with the single receptor if  $\Delta\tau_{rp}$  with probability  $W$  does not exceed  $\Delta\tau_{rp}$ , then with the same probability  $W$  signal amplitude does not exceed  $\sqrt{1 - 2\Delta\tau_{rp}}^2$ , and the phase of signal does not exceed  $\Delta\Omega\tau_{rp}$ . During the doubled receptor and the addition of signals to the detector we do not thus far have a law of probability distribution for  $\Delta\tau_{rp}$ . This law can be determined, on the basis of relationship (4.67). As it was shown in §4.2, in this system of the diverse reception value  $V_0$  has density of distribution (2.44), value  $V_1$  is distributed according to the law of Rayleigh, and value  $\phi$  is

distributed evenly in the limits from 0 to  $2\pi$ . Taking into account the statistical properties of values  $V_0$ ,  $V_1$ , and  $\phi$  indicated in accordance with expression (4.67) in [4.9] is found the integral law of probability distribution for value  $\Delta r_p$  during the doubled reception and the addition of signals to the detector. This law takes the form

$$W\left(\frac{\Delta r_p}{V_1} > S\right) = 1 - \frac{S}{1+S^2} \left(1 - \frac{1}{1+S^2}\right), \quad (4.73)$$

where  $\Delta r_1$  it is calculated from formula (3.76).

During the quadrupled reception and the addition of signals to the detector values  $V_1$  and  $\phi$  as before have Rayleigh and uniform probability distributions, and value  $V_0$  has a law of distribution for the sum of four values, distributed according to the law of Rayleigh. However, analysis considerably is simplified, if we consider that the amplitude of the input signal  $V_0$  has probability distribution the same as in the system of the automatic selection of the best of the signals. As shown in chapter 2, probability distribution during the quadrupled reception and the automatic selection is close to the distribution during the addition of signals to the detector.

Page 145.

Taking into account the statistical properties of values  $V_0$ ,  $V_1$ , and

$\phi$  indicated in [4.9] is obtained the integral law of probability distribution for  $\Delta\tau_p$  during quadrupled reception and addition of signals to the detector. This law takes the form

$$W_{\text{сверт}}\left(\left|\frac{\Delta\tau_p}{\Delta\tau_1}\right| > S\right) = 1 - \frac{4S}{\sqrt{S^2-1}} + \frac{6S}{\sqrt{S^2-2}} - \frac{4S}{\sqrt{S^2-3}} + \frac{S}{\sqrt{S^2-4}}. \quad (4.74)$$

Let us note that with  $S \gg 1$  occur the asymptotic formulas:

$$W_{\text{сверт}}\left(\left|\frac{\Delta\tau_p}{\Delta\tau_1}\right| > S\right) \approx \frac{1}{S^4}. \quad (4.73a)$$

$$W_{\text{сверт}}\left(\left|\frac{\Delta\tau_p}{\Delta\tau_1}\right| > S\right) \approx \frac{6}{S^3}. \quad (4.73b)$$

The curves of the laws of probability distribution for value  $\Delta\tau_p$  with the doubled and quadrupled receptions are constructed to Fig. 4.6. Is here for the comparison constructed the corresponding curve for the single reception undertaken from Fig. 3.8. Comparing (4.61) and (4.67), we see that these curves correspond also to probability distribution for value  $p_1$ .

As it follows from (4.72), measurement of the phase of the fundamental harmonic of signal to the output of the FM discriminator gives value  $\Delta\tau_p$ . Experimental measurements  $\Delta\tau_p$  were conducted in the section of tropospheric line with a length of 300 km with the antennas with the width of the radiation pattern of  $1^\circ$ . The results of these measurements both with doubled and with the single receptions coincide well with the theoretical laws of distribution

DOC = 30025108

PAGE

~~57~~  
306

for  $\Delta\tau_p$ . Measurements were conducted with the aid of the instrument IVZ and it is in detail described into §3.3. On the route indicated were conducted also the measurements of the fluctuations of the amplitude of the fundamental harmonic of signal at the output of the FM discriminator.

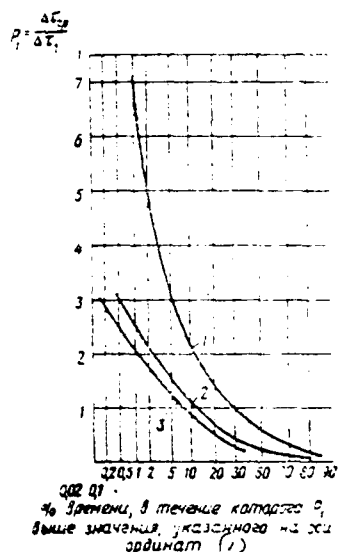


Fig. 4.6. The integral law of probability distribution for fluctuations  $P_1$  with the single and diverse receptions; 1 - single, 2 - doubled, 3 - quadrupled receptions.

Key: (1). Time during which  $P_1$  is higher than the value, indicated on the axis of ordinates.

Page 146.

In these measurements to the input of the frequency shift key of transmitter was supplied sinusoidal signals with the frequency of 275 kHz and the level, which corresponds to deviation 140 kHz. with receiving dead ending the level of the fundamental harmonic of the

detected signal was recorded with recorder tape (Fig. 4.7). In this figure it is evident that for the fundamental harmonic a characteristically sharp increase in the level at the separate moments of time ("overshoots"). Evident also that the voltage of the fundamental harmonic does not fall below the specific level. Was carried out the recording of the fluctuations of the fundamental harmonic at different modulating frequencies from 14 to 275 kHz. This recording showed that the fluctuations of the fundamental harmonic increase with an increase in modulating frequencies. All this is in complete agreement with conclusions of theory. According to the data of tape recording of chart-recording instrument were constructed the experimental curves of probability distribution for the fluctuations of the fundamental harmonic with the single and doubled receptions. These curves coincide well with theoretical, designed according to formulas (4.71), (4.76) and (4.73).

§4.5. Determination of the optimum deviation of frequency on the lines DTR.

In §§2 and 3 this chapter were determined the thermal and transient noises of multiple-pronged origin at the output of one section of line DTR [see formulas (4.13) (4.50)].

The total power of noises at the output of one section

$$P_{\Sigma} = P_T + P_n \quad (4.75)$$



will depend substantially on deviation of frequency, since from an increase in the deviation the value of thermal noises falls:

$$P_T = \frac{1}{\Delta f_k^2} \quad (4.76)$$

but the value of transient noises increases

$$P_n = \beta \Delta f_k^2. \quad (4.77)$$

FOOTNOTE 1. Without taking into account the noises of the equipment origin (for details see chapter 6). ENDPCCOTINCIE.

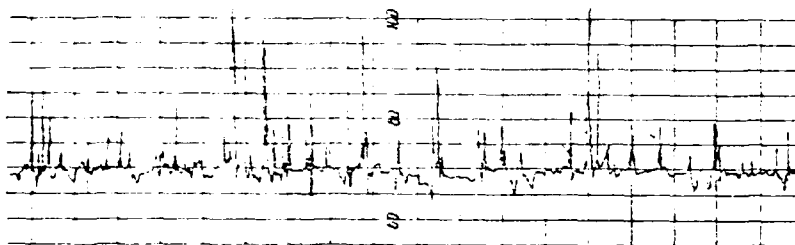


Fig. 4.7. Sample recording of fluctuations of residual attenuation in a telephone channel on an automatic recorded tape ( $\Delta f = 100$  kHz,  $\Delta f_k = 100$  kHz,  $F_k = 275$  kHz).

Page 147.

Values  $\alpha$  and  $\beta$  determine from formulas (4.13) and (4.50). for the upper, the worse, channel they are equal to:

$$\alpha = \frac{(4\pi)^2 \pi \kappa T \Delta F_k \kappa_{nc}^2 d^2 A_{\Phi} \bar{A} \sqrt{F_n^2 \lambda_{yc}}}{P_{nA} G_{np} G_{nA} \lambda^2 b_{np}}. \quad (4.78)$$

$$\beta = 10^{-3} \frac{\Delta F_k \kappa_{nc}^2}{\Delta F b_{np}} (2\pi F_n)^2 (2\pi)^2 e^{4\theta_{cp}} y_2(\sigma) \frac{z_0^4 d^8}{c^4 d_c^4} \bar{P}_N. \quad (4.79)$$

After substituting (4.76) and (4.77) in (4.75), it is possible to determine the optimum deviation of frequency to channel  $\Delta f_{opt}$  corresponding to the minimum of the total power of noises at the output of section<sup>1</sup>.

FOOTNOTE 1. The account of the transient noises of the apparatus origin whose value usually is substantially less than  $P_{\Sigma}$  somewhat decrease the obtained lower value of the optimum deviation of frequency. ENDFOOTNOTE.

The minimum of function  $P_{\Sigma}(\Delta f_N)$  corresponds

$$\Delta f_{\text{конт}} = \sqrt[4]{\frac{\alpha}{\beta}}. \quad (4.80)$$

In this case  $P_T = P_{\Sigma} = \sqrt{\alpha\beta}$ . After substituting in (4.80) the values  $\alpha$  and  $\beta$ , we will obtain the optimum deviation of frequency in depending on the parameters of equipment and line DTR

$$\Delta f_{\text{конт}} = \sqrt[4]{\frac{10^3 n \kappa T \Delta F A_{\Phi} \bar{A} \gamma_N \gamma_{\Sigma} \alpha^4 \alpha_e^4}{\pi^2 P_{\Sigma A} G_{\Sigma A} G_{\Sigma P} \lambda^2 y_2(\sigma) \tau_0^4 \alpha^2 \rho_N^2}} e^{-\rho_{\Sigma P}}. \quad (4.81)$$

Formula 4.81 can be converted taking into account the following: amplification factors flatten and transmitting of antennas is usually equal to  $G_{\Sigma A} = G_{\Sigma P}$  and connected with the width of radiation pattern according to half power with relationship (for the parabolic antennas)

$$G \approx \frac{8}{\alpha_0^2(\rho_{ad})};$$

relation  $\frac{\gamma_N}{\rho_N^2}$  depends on a number of diverse receivers and for the doubled and quadrupled recaptions is close to value of 1.15

$$\left( \frac{\gamma_2}{\rho_2^2} = 1.2; \quad \frac{\gamma_4}{\rho_4^2} = 1.1 \right);$$

for the upper channel  $y_2(\sigma) = 0.47$ ; the numerical values  $\kappa T = 4 \cdot 10^{-21}$ ;

$$c = 3 \cdot 10^8 \text{ km/s}; \quad a_e = 8.5 \cdot 10^3 \text{ km}.$$

Page 148.

Then

$$\Delta f_{\text{конт}} = 0,87 \cdot 10^4 \sqrt{\frac{\Delta F n \lambda_{yc} A_p \bar{A}}{P_{\text{нд}} \lambda_{(M)}^2 d_{(KM)}^6}} e^{-P_{\text{ср}}} \quad (4.81a)$$

For example, for a 60-channel line in the section with a length of  $d = 300 \text{ km}$  in the parameters of the equipment:  $\lambda = 0.35 \text{ m}$ ,  $P_{\text{нд}} = 3 \text{ kW}$ ,  $n = 2$ ,  $A_p = 2 \text{ dB}$  and to loss of the amplification of the pair of antennas  $\Delta_{yc} = 10 \text{ dB}$  optimum deviation  $\Delta f_{\text{конт}} = 65 \text{ kHz}$ .

#### REFERENCES

41. И. А. Гусятинский, Е. В. Рыжков, А. С. Немировский. Радиорелейная линия связи. «Связь», 1965.
42. Б. Р. Левин. Теория случайных процессов и ее применение в радиотехнике. «Советское радио», 1960.
43. Б. Р. Левин. Теоретические основы статистической радиотехники. «Советское радио», 1966.
44. С. В. Бродич. Расчет шумов в каналах радиорелейной линии с частотным уплотнением и частотной модуляцией. «Электросвязь», 1956, № 1.
45. И. А. Гусятинский, Э. Я. Рыжкий. Теоретическое и экспериментальное исследование мощности переходных помех при многолучевом приеме. «Электросвязь», 1962, № 12.
46. С. В. Бродич, В. П. Миннашин, А. В. Соколов. Радиорелейная связь. «Связьиздат», 1960.
47. Е. И. Гершенрот. Расчет шумов в каналах радиорелейной линии при введении предвысокочастотных. «Электросвязь», 1960, № 6.
48. Дальнее тропосферное распространение дкв. Под ред. Б. А. Введенского и др. «Советское радио», 1965.
49. И. А. Гусятинский, Э. Я. Рыжкий. Теоретическое и экспериментальное исследование флуктуаций амплитуды и фазы модулирующего сигнала в многолучевом канале с ЧМ. «Электросвязь», 1965, № 2.

Page 149.

Chapter 5.

#### EQUIPMENT FOR TROPOSPHERIC RADIO RELAY LINES.

§5.1. Characteristic features and content of the equipment of stations tropospheric radio relay lines (TRI).

Stations of tropospheric radio relay lines - complex of the most diverse equipment and installations. Stations of TRI, as a rule, are located far from the populated areas and, consequently, also far from the centralized electric power sources; therefore they have their self-contained power supplies. At present all stations of TRI are serviced and greatly frequently are combined with the stations of radio relay lines of sight or by the points of cable main lines for the association of these all means into the common communicating system.

In the tropospheric radio relay lines it is possible to isolate three types of stations.

The terminal station, located in the beginning or at the end of the entire line, exists independently or is a transitional link from the radio relay line of sight or cable main line to the tropospheric line. Terminal stations can be utilized with the complete assembly of equipment in the beginning of communication network or in the reduced space, for example, only for the reception of television program at the ends of the branchings.

Transit exchange, in contrast to the transit exchange RFL of direct visibility, always provides the demodulation of the high-frequency signal accepted to the group or video-spectrum. Transit exchanges it is possible to divide into two categories: stations with isolation and introduction of telephone channels and television program and station without the isolation of telephone channels and introduction of television program.

Stations with the branching provide tee-off of high-frequency shafts - telephone or television. Stations of complete branching, actually, consist of two stations - terminal both intermediate and during the organization of communication branching is considered as independent line.

Page 150.

Equipment TRL has much in common with equipment RRL of direct visibility [5.1-5.4], but at the same time individual equipment strongly differs from analogous equipment. In the transmitters are applied special powerful output amplifiers for obtaining on the output of large high-frequency power. This draws the appearance of special water-air cooling systems of the output units of transmitter.

In the receivers are applied the highly sensitive low-noise amplifiers - parametric or on the tunnel diodes and special equipment for a decrease in the threshold level of received signal. Appear need the protection of this equipment from the different interferences and, on the contrary, the need for the protection of other systems from the interferences from the side of stations of TRL. Arise the questions of the protection of the service personnel from the harmful biological radiation effect of transmitters.

Into the content the equipment of stations of TRL is included the following equipment and the equipment: the transceiver equipment with the systems of repeated reception, monitoring and measuring, antenna-waveguide, heating, ventilation, input-commutational equipment, the equipment of illumination and diesel-generator installations.

Depending on the purpose of station into it can enter television equipment and apparatus for multiplexing or isolation of telephone channels.

The electronic equipment of stations is located in the technical building, constructed between the antenna systems. At the stations with the antenna systems in the form of parabolic rectangular mirrors with the horn feed, referred from the mirrors to the large distance, the equipment is connected with the irradiators by the waveguides with a length of 50-70 m. During the use of parabolic antennas with the reemitters equipment it is expedient to install in the three-storied buildings, which substantially decreases the length of waveguides and it makes it possible to place equipment in three independent instrument rooms: receiving instrument room - third landing, by the transmitting instrument room - the second landing and by low-frequency instrument room - the first landing.

#### §5.2. Block diagrams of the stations of tropospheric radio relay lines.

Let us examine the block diagrams of the stations of tropospheric radio relay lines with a different number of

high-frequency shafts and with the different methods of the diversity of received signals. Since in the majority of the cases terminal station composes the half intermediate, then let us examine the block diagram of transit exchange of TRL with the system of quadrupled reception (Fig. 5.1) and by the diversity of received signals in the space and in the frequency, intended for the transmission of the signals multichannel telephony. At this station for the work in each direction are utilized two transmitters and or four receivers.

Page 151.

The use of two transmitters, through which is transmitted one and the same communication, and four receivers not only raises the quality of transmission in accordance with an increase in the multiplicity of reception, but it also increases equipment reliability of station.

The adopted on two antennas the signals of the preceding station enter four receivers -  $Pr_1$ ,  $Pr_2$ ,  $Pr_1'$  and  $Pr_2'$  through separation filters  $RF_1$  and  $RF_2$ . Since each antenna picks up signal from two transmitters, which work at the different frequencies, then in order to direct the signals of these frequencies toward the appropriate receivers they are applied separation filters indicated. On this block diagram are also depicted the antennas, which consist of parabolic reflector Z and horn emitter RC, which ensures emission and



reception of the electromagnetic vibrations of different polarization. Signals from the horn feed to separation filters fall on the waveguides V. Two receivers, connected to different antennas, are inclined for one frequency, and two of others - to another. The addition of signals is realized in pairs. First store/add up the signals of the receivers, inclined for one frequency. Addition is realized in the intermediate frequency before the demodulation in the equipment of addition  $Sl_1$ , and then the addition of signals from two pairs of receivers tuned to the different frequencies; this addition is realized after demodulation in the group frequency in other equipment of addition  $Sl_2$ .

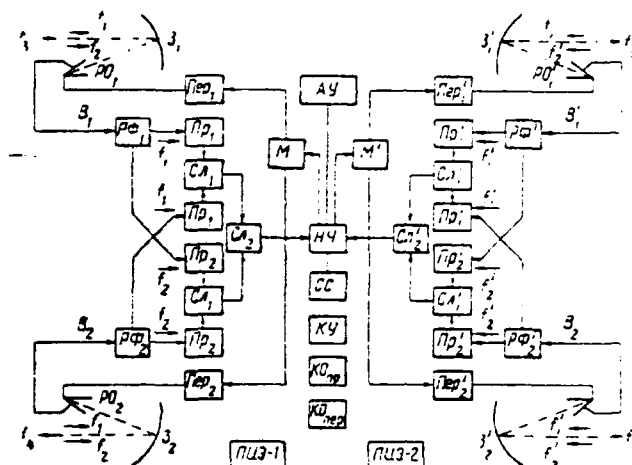


Fig. 5.1. Block diagram of the transit exchange of the tropospheric radio relay line with the system of the quadrupled reception.

Page 152.

The added-up and modulated signal of group frequency enters the stand of low frequency NCh, and then multichannel equipment for multiplexing or isolation of channels AU and the equipment of service communication SS.

On the side of transmission the signals from the equipment for multiplexing and equipment of official communication through the stand NCh are supplied to the common for two transmitters modulator M, in which is realized frequency modulation. Further transformation

of the frequency-modulated signals into the signals of higher frequency and bringing power up to the necessary value in several kilowatts occurs in two separate transmitters  $Per_1$  and  $Per_2$ , which work at the different frequencies. High-frequency energy from these transmitters on the waveguides is supplied respectively to the irradiators of two antennas. At this station for the work in each direction are utilized two transmitters. Each transmitter works on its antenna, and each antenna is utilized for the reception and for the transmission.

At the station is provided the monitoring and measuring equipment for checking qualitative indices of receivers  $KO_{\text{qual}}$ , equipment for checking the parameters of transmitters  $KO_{\text{par}}$ , special monitors for the measurements and the group circuit KU. The electric power supply of entire station is realized from two primary sources of electric power supply PLE-1, PLE-2. In this case all the equipment of station is distributed so that the half the receiving equipment, which works at one frequency, and the half the transmitting equipment, which corresponds to these receivers, are supplied from one of the sources of primary electric power supply, and other half - from other. During the malfunction of one of the sources the efficiency of station is retained.

Fig. 5.2 give the block diagram of the transit exchange of the

tropospheric radio relay system, designed for two high-frequency shafts, each of which can be used both for the transmission of telephone signals and for the transmission of television program, moreover sonic tracking is transmitted in the same shaft, as picture signals. Station is constructed so that are provided for the possibility of the simultaneous use of two shafts for the transmission of the signals multichannel telephony, the possibility of isolation and introduction of telephone channels and television program at each station. For this introduction and isolation of channels as, however, and in the preceding block diagram, at each station are realized demodulation and repeated modulation of signals. For an improvement in the quality and reliability of communication is utilized the quadrupled reception with the angular and frequency diversity of signals. On the transit exchange are installed two transceiver parabolic antennas with re-emitters and two horn emitters for the angular diversity of signals.

Page 153.

One antenna, which consists of the large mirror EZ, the re-emitting mirror PZ and two horn emitters EC<sub>1</sub>, EC<sub>2</sub>, is utilized for communication with the preceding station, and other - for the work with the subsequent station.

On the block diagram all elements of the first shaft have numeral 1, all elements of the second shaft numeral 2. All elements which work in the direction of the preceding station, they are noted by prime, the elements which work in the direction of the preceding station, prime they do not have.

On the block diagram are depicted the in principle important assemblies of high-frequency circuit, circuit of addition, video- and group circuits, and also the most important elements of commutation and checking. The first shaft works in the mode of television, by the second - in the mode multichannel telephony.

Signals from the preceding station, accepted by antenna and two horn feed, through separation filters  $BF_1$  and  $BF_2$  reach the inputs of four receivers of the first shaft  $PR_1-1$ ,  $PR_2-1$ ,  $PR_3-1$  and  $PR_4-1$ , and then to the equipment  $SI-1$ . The folded signals are demodulated in the demodulator  $D-1$  and after distributor  $RU-1$  enter the equipment of the separation of picture signals and sonic tracking  $PIZ$ , into the equipment of the correction and of regeneration  $UKR$ , and then through input-commutation equipment  $VKO$  they are supplied to the telecast station or the repeater.

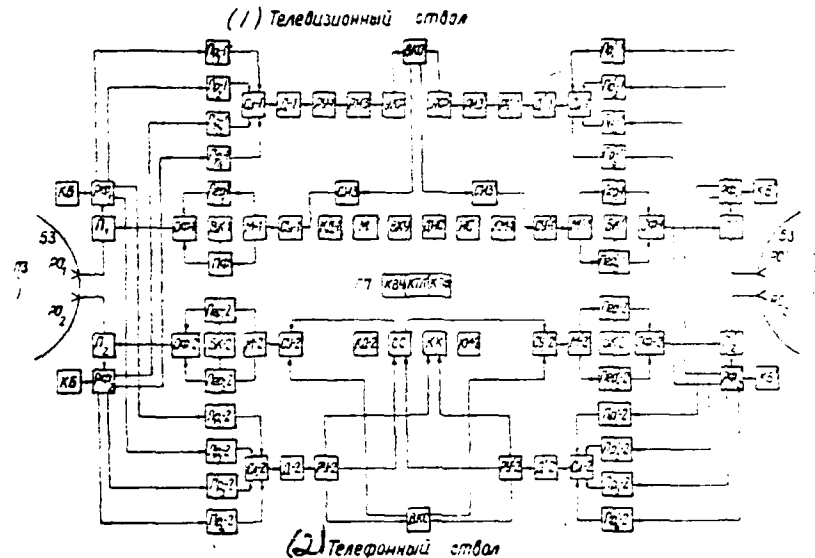


Fig. 5.2. Block diagram of transit exchange of TBL to two shafts for the transmission of the signals of telephony and television.

Key: (1). Television shaft. (2). Telephone shaft.

Page 154.

If at this station is realized only the branching of television program, then picture signals and sound after distributor are supplied through the matching device SU-1 to the modulator M-1 of transmitter. On the transit exchanges are installed four doubled transmitters. Each of the doubled transmitters has one common modulator. High-frequency oscillations from the transmitters Per,-1,

Per<sub>2</sub>-1, and Per<sub>1</sub>-2, Per<sub>2</sub>-2, through the uniting filters OF<sub>1</sub> and OF<sub>2</sub> are supplied to the horn feed. The connection of transmitters and receivers to the common horn is realized through the polarizational selector P.

If at this transit exchange occurs the introduction of television program, then picture signals and sound from telecast station come input-comutation equipment VKC, and then the equipment for the coincidence of signals of image and sound SIZ, the combined signals are supplied to the modulators M-1 and M'-1 the corresponding doubled transmitters, which work at two different frequencies.

For checking of the transmitting circuit at the output of each doubled transmitter are control r-f units BK, which convert output high-frequency signal into the signal of intermediate frequency for its supply to the control demodulator KD. After control demodulator picture signals are supplied to the equipment of measurement and checking VKU, where is provided television monitoring system, oscillograph with the attachment for the isolation of the experimental row, which makes it possible to produce the continuous checking of the characteristics of television channel without the break of communication.

For the tuning works and the preventive measurements on the

points are installed the monoscope M, the sensor of test signals DIS and the stand of experimental row IS. Signals from this equipment can be supplied into different points of the circuit of image [5.5].

On the side of reception the videosegment can be monitored with the aid of the television monitoring system and the oscillograph with the attachment for the isolation of the signals of experimental row. These measurements can be conducted at different points of circuit.

For tuning of receivers and conducting of preventive measurements are provided control modulators MM and monitor units of high frequency KB, which ensure the supply of high-frequency pilot signals to the inputs of receivers.

In the telephone shaft the signals from the multiplexing equipment come to the input-commutation stand VKS, and then the matching device SU, which matches the levels of signals and resistances of equipment for multiplexing, official channels, levels of pilot frequencies. Total signal enters the modulator M of the doubled transmitter.

Page 155.

On the side of reception after addition and demodulation the signals



enter the separating equipment, where they are branched in accordance with their purpose and enter through input-commutation stand the equipment of the isolation of channels or terminal multichannel equipment, and also the equipment of link between operators SS and monitoring channels KK.

Since transit exchange contains a large quantity of the most diverse equipment, distant from each other up to the considerable distance, the general control of entire station is realized from main panel GP. The equipment installed on it makes it possible to produce the inclusion and different commutation in the high-frequency equipment for any shaft KVCh, and also different measurements, checking and commutation in the circuits of television KTL and telephony KTF.

The block diagrams of the corresponding terminal stations include the half high-frequency equipment and all elements of control and accessory equipment.

The first of the given block diagrams was acceptance for the work in the range 500-1000 MHz, where is most effective the use of spatial separation of signals, and the third - at the more high frequencies where it is more expedient to combine frequency separation with the angular diversity of received signals.

It should be noted that the transmission of television program is possible along the lines, equipped by the stations, constructed according to the first block diagram, of course, with the appropriate supplement with their necessary television equipment.

### §5.3. Antennas of tropospheric radio relay lines.

On the tropospheric radio relay lines are commonly used the optical-type antennas with the reflector in the form of the part of the surface of paraboloid of revolution. As the irradiator of parabolic surface can be utilized the weakly directed horn antenna or mirror system from the horn antenna and the supplementary mirror Fig. 5.3 and 5.4. Single-reflector antennas with the horn feed are created with the use of a symmetrical reflector (Fig. 5.3a), possibly also the creation of single-reflector antenna with the asymmetric relative to focal line reflector (Fig. 5.3b).

The principle of the work of dish antennas is widely known [5.6] and consists in the fact that the emission in the direction of the focal axis of paraboloid in view of the geometric properties of parabolic surface proves to be phased; therefore electromagnetic energy is concentrated near the focal axis of parabolic surface. The

degree of concentration of electromagnetic energy, i.e., the width of the antenna radiation pattern, is determined by linear superficial dimensions of the aperture of antenna relative to wavelength.

Page 156.

In the two-mirror parabolic antennas, besides fundamental parabolic reflector, is installed also supplementary hyperbolic or elliptical mirror. In this case is utilized the known geometric property of the hyperboloid (ellipsoid) of rotation. With the coincidence of one point of the focus of hyperboloid with the focus of parabolic reflector and another focal point with the source of spherical wave - by irradiator, occurs the transformation of spherical wave with the center at point C' (Fig. 5.4) into the spherical wave with the center at point C and this two-mirror antenna system, just as single-reflector, provides the concentration of electromagnetic energy near the focal axis of system. Two-mirror antennas [5.7] have a number of advantages before the single-reflector ones. Calculations show that with identical superficial dimensions of aperture the factor of amplification of the two-mirror antenna somewhat higher than single-reflector one. Furthermore, the directivity pattern of two-mirror antenna is characterized by the substantially smaller side-lobe level in the space after the surface of parabolic reflector, which increases the interference shielding of antenna.

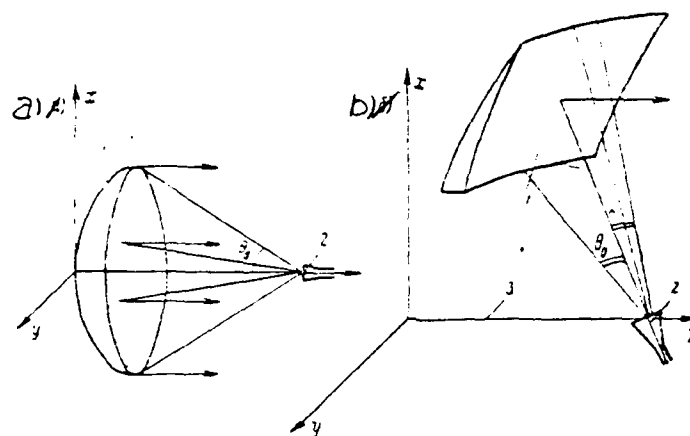


Fig. 5.3. The single-reflector parabolic antenna: a) with symmetrical reflector, b) with the asymmetric reflector: 1 - parabolic reflector, 2 - horn feed, 3 - focal axis of antenna.

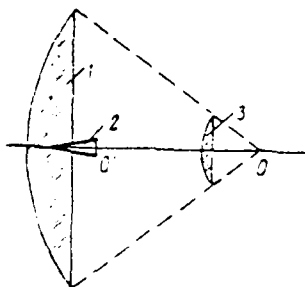


Fig. 5.4. Two-mirror parabolic antenna: 1 - parabolic reflector, 2 - horn feed, 3 - supplementary mirror (hyperboloid).

Page 157.

The required factor of amplification and antenna matching in

range of the frequencies of the order 1000 MHz can be provided with the use of any of the diagrams; therefore selection is conducted from the considerations of simplicity of design. Are most suitable single-reflector antennas. Widest use received single-reflector antennas with the symmetrical reflector, the design of the reflecting mirror of which is characterized by greatest simplicity. However, these antennas according to electrical and performance data are somewhat inferior to single-reflector antennas with the asymmetric reflector. Thus, in the antennas with the symmetrical reflector certain part of the electromagnetic energy, reflected from the surface of parabolic reflector, falls to the surface of the aperture of irradiator and in the form of the electromagnetic wave reflected is propagated in the feed line of irradiator. As a result of reacting the mirror to the irradiator deteriorates the agreement, which causes the appearance of noises. This deficiency to a considerable degree can be compensated by the use of ferrite gates or by the introduction of equivalent components of tuning to the feed line of irradiator, which create an additional wave reflected, equal in the amplitude and opposite on the phase to the wave reflected, caused by the reaction of mirror.

Another deficiency in the antenna, which uses a symmetrical reflector, is the fact that the antenna feeder and design of the attachment of irradiator is located in the field of the

electromagnetic wave, reflected from the parabolic reflector, and therefore certain part of the energy is scattered during these designs, which leads to the decrease of the antenna gain. A supplementary deficiency in this diagram is the need for the installation of irradiator at the considerable height above the ground, which hampers operation and tuning of antennas. It is not difficult to see that the use of an asymmetric part of the parabolic reflector makes it possible considerably to decrease and in a number of cases to completely remove the reaction of mirror. Thus, for instance, in the antenna, depicted in Fig. 5.3b, the reflected from parabolic reflector electromagnetic wave passes by irradiator, and the reaction of mirror virtually is absent. During the use of this diagram has the capability to arrange irradiator in immediate proximity on the earth's surface, which facilitates the operation of antenna. Besides the noted above special features of antenna with the asymmetric reflector, essential for the practice, especially during the installation of antenna in the snow and glare ice areas, is the fact that the asymmetric reflector is installed inclined relative to the earth's surface; which blocks deposition on the surface of the reflector of snow and ice-covered surface. On the schematic of single-reflector antenna with the symmetrical parabolic reflector is carried out the antenna of tropospheric radio relay communicating system "White Alisa", realized in the USA. Operating frequencies of this system - order 1000 MHz. Surface of antenna aperture is a square

(18x18 m) with the blunt angles. Irradiator is located on the tower and is raised above the ground approximately by 15 m.

Page 153.

In the areas of the extreme north for some of the antennas is applied the heating of the reflecting surface by hot oil, since formation on the surface of the reflector of the layer of ice or snow substantially makes the electrical parameters worse of antenna.

Fig. 5.5 shows the general view of the antenna with the asymmetric parabolic reflector (surface area of aperture - 20x20 m), utilized on the Soviet tropospheric radio relay lines in the range of the frequencies of the order 1000 MHz. It consists of parabolic reflector and horn pyramidal irradiator which provides the emission of the wave of two mutually perpendicular polarizations. The geometric parameters of horn feed are selected from the condition of obtaining the greatest antenna gain. For this, as is known, the dimensions of horn emitter must be such that the width of the radiation pattern of irradiator on the level - 10 dB would be equal approximately to angular superficial dimension of antenna aperture. In practice it is not the possible to satisfy this condition accurately, since the radiation patterns of pyramidal horn are different in different planes. Therefore is provided the approximate

DOC = 80025109

PAGE

~~4~~332

fulfillment of conditions, in this case the width of the radiation pattern of irradiator in plane E is obtained somewhat smaller, and the width of radiation pattern in plane H - larger angular dimension

29.



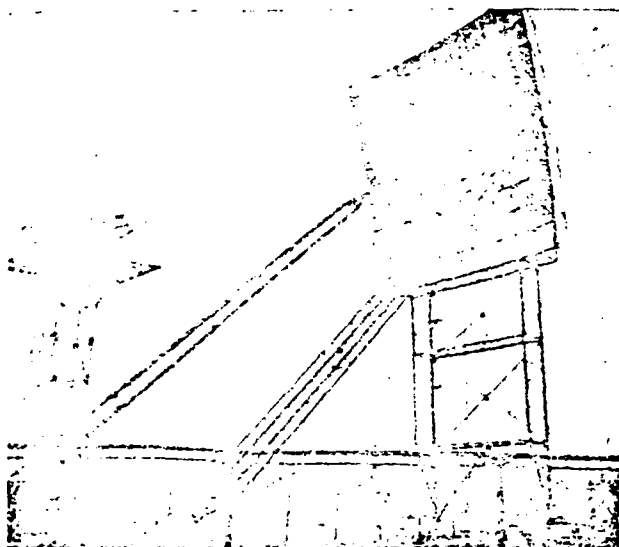


Fig. 5.5. Antenna of six-ten-channel tropospheric communicating system.

Page 159.

It is also known that the assigned width of the directivity pattern can be ensured, utilizing pyramidal horns of different length. The relationship between the size of the aperture of horn, its length and length of transmitting wave determines phase distortions in the aperture of horn [5.6]. With an increase in the phase distortions is required larger superficial dimension of aperture for obtaining the required width radiation pattern. simultaneously with an increase in the phase distortions increases the side-lobe level of radiation

pattern and, therefore, grow electromagnetic energy losses in the minor lobes. Therefore it is expedient to apply horn feed with small phase distortions. In practice good results are obtained with the value of phase distortions  $\leq \pi/4$ . In this case the directivity patterns of horn antennae virtually coincide with the radiation patterns of cophasal surface antennas with the appropriate geometric dimensions and the amplitude distributions and energy losses in the minor lobes of radiation pattern are minimum.

A general view of horn antenna feeder is shown in Fig. 5.6. Horn feed is fulfilled by airtight. For this horn from the side of aperture it is capped from the foam plastic. The elimination of the effect of cover on matching of horn emission is achieved by its inclination relative to the axis of horn. The angle of inclination is selected by such, that the cover is installed perpendicularly to the earth's surface and the formation of the layer of snow and ice is eliminated.

The adjustment of antenna system is realized by movement of horn feed.

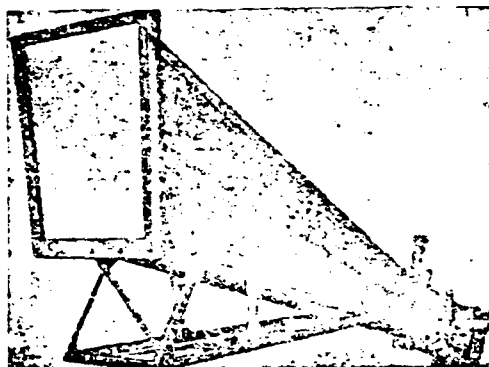


Fig. 5.6. The general view of horn feed.

Page 160.

For guaranteeing the tropospheric radio communication in the range of several thousand megahertz are necessary antennas with the very high amplification factor. In practice on these lines are utilized antennas with the surface of aperture 100-200 m<sup>2</sup>, as a result of which the antenna radiation pattern considerably becomes narrow. With an increase in the operating frequency increases the required accuracy of the fulfillment of the surface of the reflecting mirror and, consequently, also the required rigidity of the metallic frameworks of the reflecting mirror, their weight and cost. Therefore at the more high frequencies it is preferable to utilize structurally a simpler symmetrical parabolic reflector. In this case the antenna feeder must be rigidly connected with the surface of mirror, since in

this case during the strain of the surface of reflector due to the wind and glare ice loads the position of irradiator relative to the surface of mirror will change insignificantly and the distortion of radiation pattern will be less than in the case of the location of irradiator on the separate support, as shown in Fig. 5.5. At these frequencies becomes possible angular separation; therefore antennas must be designed so that they would work simultaneously according to several radiation patterns, turned relative to each other to certain angle. The problem of developing several radiation patterns in one mirror parabolic antenna can be solved by the method of arrangement near the point of the focus of several irradiators Fig. 5.7.

In this case during the supply to the irradiators of electromagnetic energy from the separate transmitters or the connections to them of receivers, antenna radiation pattern for each of the transmitters (receivers) will prove to be turned relative to each other in the space to the angle, determined by geometric parameters the antennas and value the angle of rotation of irradiator relative to focal line. This diagram can be realized both in the single-reflector ones and in the multireflector parabolic antennas.

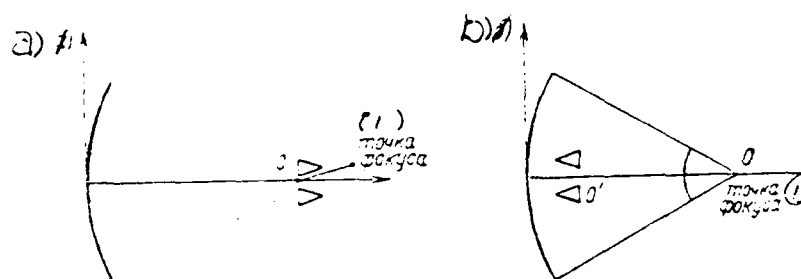


Fig. 5.7. Single-reflector (a) and two-mirror (b) antennas of the angular diverse receiver.

Key: (1). the point of focus.

Page 161.

The second possible method of the realization of angular separation in one antenna is the use of an antenna system of several emitters of smaller size and corresponding system of the distribution of electromagnetic energy between these emitters [5.8]. For obtaining assigned gain factor of this system it is necessary that the total surface area of the aperture of all emitters would be approximately equal to the surface area of antenna aperture of larger size. The use of this system can give certain economic effect, since the cost of several mirrors of the smaller size lower than cost of one large mirror in the different areas of aperture.

Let us examine based on the example of the antenna, which consists of two emitters, the diagram of feed (Fig. 5.8) of which ensures angular separation. As can be seen from figure, antenna feeders are connected up the lateral arms of dual waveguide tee, in this case the lengths of connecting lines 1 and 2 are distinguished to the value, equal to quarter wavelength in the waveguide. The connection of equipment is realized to arms E and H. Electromagnetic energy from arm E is divided into the equal parts between the lateral arms of dual waveguide tee, moreover electromagnetic energy in the lateral arms proves to be in the antiphase. Electromagnetic energy from arm H is divided equally between the lateral arms, phase shift in this case is equal to zero.

taking into account that the lengths of connecting lines are distinguished to quarter wavelength in the waveguide, which gives the supplementary phase shift, the equal to ninety degrees  $\Delta\psi=90^\circ$ , we obtain, that with the feed of emitter system from the side of arm E electromagnetic field in irradiator 1 advances in phase the electromagnetic field in emitter 2 by  $90^\circ$ . With the feed from the side of arm H the field in irradiator 1 lags on the phase on  $90^\circ$  behind the field in irradiator 2. In this case it proves to be that with the feed from the side of arm E the radiation pattern is deflected to the side of emitter 1.

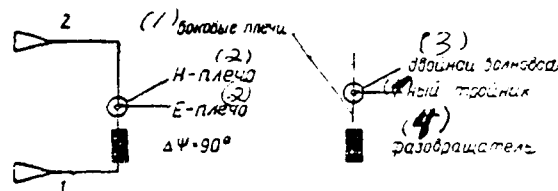


Fig. 5.9. Schematic of the feed of antenna system of two emitters for the angular diverse reception.

Key: (1). lateral arms. (2). arm. (3). dual waveguide tee. (4). phase inverter.

Page 162.

The value of the angle of rotation of radiation pattern depends on the distance between the emitters and, as show the results of calculation, with the utilized in practice sizes of antennas the described diagram makes it possible to carry out rotation to the necessary angle. The deficiency in this system is the increased side-lobe level of radiation pattern. In view of the known property of dual waveguide tee the interconnection between arms E and H is absent, if tee is matched from the side of lateral arms. A similar system can be created, also, for a larger quantity of antennas. Fig. 5.9 shows the power-supply system of the antenna, which consists of four emitters and realizing four partial radiation patterns.

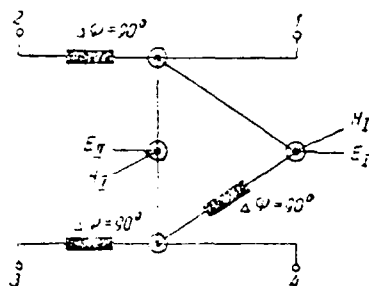


Fig 5.9. Schematic of antenna feed of four emitters for the angular diverse reception.

#### §5.4. Feed lines of antennas.

For the connection of antenna feeder with the high-frequency equipment for message center are applied coaxial and waveguide feed lines. The use of lines of ground wave is impossible, since they are subjected to the action of atmospheric conditions.

Wide acceptance on the radio relay lines received the waveguides which provide the transfer of electromagnetic energy with the smallest losses, possess high dielectric strength, they are reliable. they are applied, in particular, rectangular waveguides excited on fundamental type wave  $H_{10}$ , they possess the smallest geometric dimensions and the smallest cost.



For the propagation in rectangular waveguide of wave  $H_{10}$  the size of the wide wall of waveguide  $a$  must be equal to:

$$a > \frac{\lambda}{2},$$

where  $\lambda$  - maximum wavelength.

The size of the narrow wall  $b$  is usually selected equal to:

$$b = \frac{\lambda}{2}.$$

Page 163.

Fig. 5.10 gives curves, which make it possible to determine the attenuation in a rectangular waveguide by tubes. Waveguide lines are comprised from the separate segments with a length of 4-5 m at ends of which flanged, which ensure the reliable contact between the combinable cuts; within waveguide flanged connection for airtightness is installed rubber packing. The produced by industry waveguide tubes are allowed radio relay lines. In the range of the frequencies on the order of 1000 MHz, besides waveguide feed lines, possibly also the use of coaxial lines. At the more high frequencies due to an increase in the attenuation the use of coaxial line is inexpedient. The maximum sizes of coaxial line are determined by the condition of the absence in the line of the waves of highest types [5.6]

DOC = 80025109

PAGE

~~34~~ 342

$$\lambda_{\text{pas}} > \pi(a_1 + a_2),$$

(5.1)

where  $a_1$  and  $a_2$  - radii of the internal and external conductors of line.

In practice find use flexible and rigid coaxial lines. Structurally rigid coaxial line is fulfilled of two copper or brass tubes one of which performs the role of external conductor, the second - internal conductor of line.

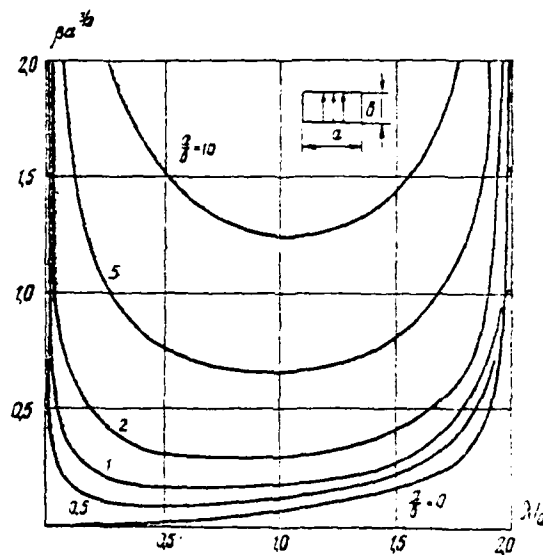


Fig. 5.10. Attenuation in the copper waveguide of the rectangular section:  $\beta$  - attenuation in the decibels,  $a$  and  $b$  - in the centimeters.

Page 164.

Available experimental and calculated data show that the rigid coaxial lines can be used in the receiving and transmitting feed lines, since during the appropriate selection of the sizes of cross section the energy losses in the line by length 50-100 m do not exceed 1-2 dB, but throughput can reach the value of 10 kW. Rigid coaxial lines require for the production considerably less copper than waveguide; however, differ from waveguide lines in terms of the

large complexity of design and in terms of larger magnitude of losses power.

Is possible also the use of cable lines. Throughput in them at frequency  $f \sim 1000$  MHz reaches 7.5 kW.

For exciting horn feed simultaneously by the electromagnetic waves of two independent communication channels, one of which is utilized for transmission of signals of communication, and other - for the reception of information, serve polarizational selectors.

The polarization selector consists of the cut of the waveguide, in which are created the waves of two polarizations, and the equipment, which ensures the excitation of these waves in the waveguide. Polarizational spectra differ in form of the cross section of waveguide and in the method of exciting the waves in the waveguide. The electromagnetic waves of two mutually perpendicular polarizations can be excited in the cut of the waveguide of rectangular, square, round or elliptical cross section. The excitation of electromagnetic waves can be realized with the aid of the coaxial or waveguide feed line.

In Fig 5.11 is shown the diagram of the polarizational sector with a square cross section excited by coaxial lines.

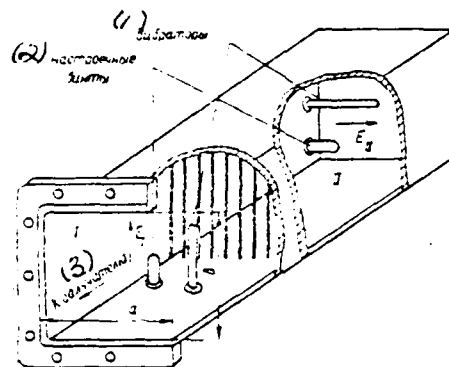


Fig 5.11. Diagram of the polarizational selector, excited by coaxial lines.

Key: (1). Vibrators. (2). Adjustment screws. (3) To emitter.

Page 165.

These a diagram it is expedient to utilize with the work in the range of the decimeter waves when electromagnetic energy is supplied to the antenna by coaxial lines. The external conductor of coaxial line is connected with the waveguide, and internal conductor passes in the waveguide into the vibrator. In order to ensure the transfer of electromagnetic energy in the waveguide in the direction to the horn feed, in the polarizational selector near the vibrator is installed the shorting device, made in the form of grating from the wires. The site of installation of shorting device and length of vibrator

determine the agreement of polarizational selector with the coaxial line. The second part of the polarizational selector is made analogously. Difference consists of that, the coaxial line and vibrator of the second part of the polarizational selector are installed perpendicular to coaxial line and vibrator of the first part of the selector. Furthermore, in this case the short-circuiter is carried out in the form of metallic plate. In view of the fact that the vibrators of polarizational selector are mutually perpendicular, and the wires of polarizational grating are perpendicular to the vector of the strength of the field of the wave, excited by the second part of the selector, the elements of the construction of the first part of the selector virtually do not influence its agreement for wave  $E_{11}$ . Agreement for wave  $E_1$  also is not connected with the sizes of the second part of the selector, since for this wave the polarization grid is shorting device and blocks the propagation of wave  $E_1$  in the second part of the selector. Due to the perpendicularity of the vibrators of selector the connection between the coaxial lines I and II in the selector is very small. The dimensions of transverse cross section of the waveguide of selector are selected by such that there are no conditions of exciting the waves of the highest types. For the waveguide whose cross section is close to the square, by second type wave is an electromagnetic wave of the type  $H_{11}$ ; therefore this condition takes following form [5.6]:

$$\left. \begin{aligned} \lambda_{kpH_{10}} &> \lambda_{pod} \geq \lambda_{kpH_{11}} \\ \lambda_{kpH_{11}} &= \frac{2ab}{\sqrt{a^2 + b^2}} \end{aligned} \right\} \quad (5.2)$$

where  $\lambda_{pod}$  - working wavelength,

$\lambda_{kpH_{10}}$  - critical wavelength of fundamental type,

$\lambda_{kpH_{11}}$  - critical wavelength for wave  $H_{11}$ .

The agreement of the cut of rectangular waveguide with the coaxial lines I and II is realized by selection of the length of vibrators in the waveguide and by selection of distance from the vibrator to the short-circuiting grating or the plate. In view of the fact that the design of the moving in the cross section of waveguide polarizational grating or plate is very complicated and does not provide reliable contact with the waveguide, it is expedient to realize tuning polarizational selector with the motionless plate or the grating.

Page 166.

The action, equivalent to the movement of shorting device in the small limits, exerts the capacitive screw, located in the same plane,

as vibrator. Therefore in practice tuning polarizational selector can be realized by selection of the length of vibrator and submersion depth of tuning screw.

In practice can be encountered the cases, when the polarization selector, which works in the decimeter range, it is necessary to connect directly with the waveguide line. This can be necessary, for example, during the use of transmitters of this power, which cannot be transmitted along the coaxial line. In this case the receiving part of the polarizational selector is made by the connection of waveguide with the coaxial line, as it was described above; the equipment of the transmitting part of the selector of such type is clear from Fig. 5.12. The dimensions of the cross section of a waveguide of such type are determined by the given above condition is realized in the waveguide of the waves of the highest types. Tuning of the polarization selector from the side of coaxial line is realized in the manner that it is described above.

Tuning from the side of waveguide line is conducted by tuning screws, knobs and other tuning elements placed in rectangular waveguide, and also by the selection of the position of shorting device.

A deficiency in the systems described above of the polarized



DOC = 80025109

PAGE

349

selectors is the narrow band of the passed frequencies, which is caused by small dimensions of the cross section of waveguide. For an increase in the passband should be increased the dimensions of cross section and simultaneously used such diagrams, which would exclude the possibility of existence in the common waveguide of the oscillations of types  $H_{11}$  and  $E_{11}$ .

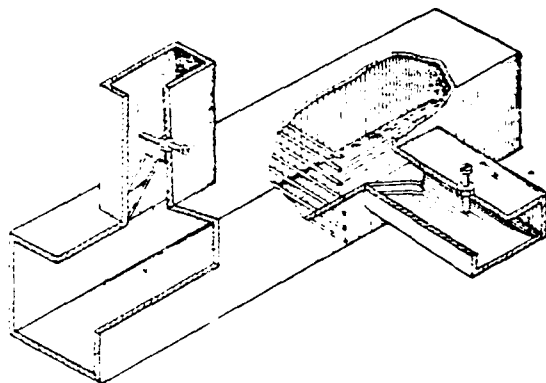


Fig. 5.12. Diagram of the polarizational selector, excited by two waveguide lines.

Page 167.

Fig. 5.13 shows the lines of force of electrical and magnetic (dotted line) fields in the waveguide for the wave of the type  $H_{11}$  and  $E_{11}$ , and the strength of field  $E_0$ , which excites this waveguide with the connection of rectangular waveguide [5.6].

Of the exciting field  $E_0$  at the symmetrical points identical with respect to the value and direction, and during the excitation of polarizational selector waveguide and with the sufficient precise fulfillment of the waveguide of polarizational selector waves  $E_{11}$  and  $H_{11}$ , be excited will not be and the dimensions of the cross section of

the waveguide of selector can be selected large. The condition of the absence of the waves of the highest types in this case will take following form [5.6]:

$$\left. \begin{aligned} \lambda_{\text{кр}H_{10}} &\geq \lambda_{\text{раб}} \geq \lambda_{\text{кр}H_{21}} \\ \lambda_{\text{кр}H_{21}} &= \frac{2ab}{\sqrt{(2b)^2 + a^2}} \end{aligned} \right\} \quad (5.3)$$

where  $\lambda_{\text{раб}}$  - working wavelength,

$\lambda_{\text{кр}H_{10}}, \lambda_{\text{кр}H_{21}}$  - critical wavelengths for fundamental type waves  $H_{10}$  and  $H_{21}$ .

The special feature of the polarizational selector, excited by rectangular waveguides, are the considerable dimensions of opening in the common waveguide, which influences the agreement of selector. Fig. 5.14 shows the structure of the currents on the wall of the waveguide of selector, excited by rectangular waveguide 2. Opening in the common waveguide to which is connected rectangular waveguide 1, it breaks currents and therefore is exerted a substantial influence on the agreement of selector from the side of waveguide 2.

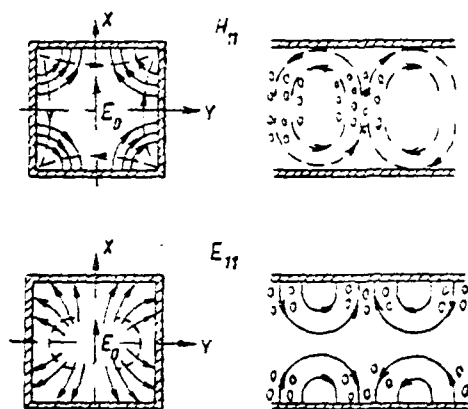


Fig. 5.13. Structure of electromagnetic field in the cross section of square waveguide.

Page 168.

The effect of opening can be reduced, if we in it place certain quantity of stubs in the manner that this is shown in Fig. 5.14, which remove gap for the longitudinal currents. The effect of these stubs on the agreement in waveguide 1 will be small, since stubs are perpendicular to the vector of electric intensity in this waveguide. The best results can be obtained, if we instead of the stubs place into waveguide 1 of plate, as shown in Fig. 5.12, whose length is equal to the half wavelength in the waveguide. Such plates, virtually without influencing agreement in waveguide 1, form four-wave extended waveguides whose input resistance is close to zero. This system of

DOC = 80025109

PAGE

4/ 353

plates apparently, closes also transverse currents.

The systems described above of polarizational selectors with the excitation of common waveguide by coaxial lines are applied in the range of the frequencies of the order 1000 MHz. At these frequencies can be used also the selectors, excited by rectangular waveguides. At the more high frequencies should be applied the diagrams, which are based on the excitation of selector by rectangular waveguides.

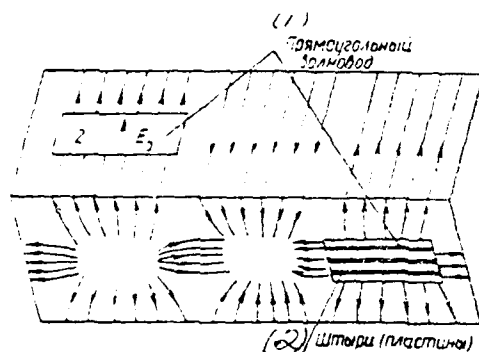


Fig 5.14. Currents on the walls of the waveguide of polarizational selector, excited by rectangular waveguide.

Key: (1). Rectangular waveguide.

#### §5.5. Filters and ferrite valve devices.

During the quadrupled reception and the use of a frequency separation is necessary the use of separation filters, which make it possible to conduct the reception of signals of two different frequencies on one antenna. The filter, intended for the separation of the signals of two frequencies, taken by one antenna, can be carried out on the parallel diagram, given in Fig. 5.15.

Separation filter consists of splitter and band-pass filter, tuned to frequencies  $f_1$  and  $f_2$ .

FOOTNOTE 1. Is possible the construction of separation filter with the use of band rejection filters, which reflect the signals of frequency, on which the band rejection filter is inclined.  
ENDFOOTNOTE.

The separation of signals in the filter is realized as follows. The signal of frequency  $f_1$  by bandpass filter 1 without the reflection, and without the essential losses it arrives at the input of receiver  $P_1$ . For frequency  $f_2$  this filter is short circuit and signal of this frequency it does not fall to the input of receiver. Analogously occurs the isolation of the signal of frequency  $f_2$ . In view of the fact that band-pass filter 2 at frequency  $f_1$  is short circuit, with the distance from the branch point to the connection point of band-pass filter, equal to quarter wavelength  $\lambda_2/4$ , we obtain, that the arm of 1 filters is infinitely large resistance for frequency  $f_2$  and does not influence the agreement of separation filter at frequency  $f_2$ . Certain deterioration in the agreement due to the reflection of electromagnetic energy by branching off is compensated by the use of equivalent components of tuning. Analogously is provided the agreement of separation filter at frequency  $f_1$ .

The described diagram can be realized for the separation at the reception of two frequencies of communication. In practice, however, can be encountered the cases when for an increase in the capacity of radio relay line is applied transmission along the line of several shafts at different frequencies. In this case appears the need for the use of separation filter for separation of four, six or more number of frequencies of communication. The use of the system described above of the parallel separation of frequencies meets with considerable difficulties due to the complexity of agreeing the filter. Actually, with the connection to the filter Fig. 5.15 in third band-pass filter for the frequency discrimination  $f_3$  we obtain, that at this frequency the distances  $\lambda_1/4$  and  $\lambda_2/4$  differ from the wave  $\lambda_3/4$  and therefore the arms of the first and second filters at this frequency are some reactance, which influence agreement. Furthermore, branching for the frequency discrimination  $f_3$  at frequencies  $f_1$  and  $f_2$  will be certain reactance and have an effect on the agreement of equipment also at frequencies  $f_1$  and  $f_2$ . Tuning a filter of this type for a large number of frequencies is very complex problem.

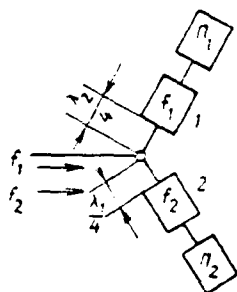


Fig. 5.15. Schematic of parallel separation filter, intended for the separation of the signals of two frequencies of communication.



Page 170.

In this case should be applied series circuit of the frequency separation of the signals Fig. 5.16. A difference in this diagram lies in the fact that by filter section is isolated the signal of one frequency  $f_1$ , the signals of remaining frequencies pass without the distortions; then is isolated signal  $f_2$ , etc. This diagram is based on the use of dual waveguide ones it is branch or three-decibel directional couplers [5.9]. The principle of the work of separation filter is identical during the use of a dual waveguide tee and three-decibel directional coupler. Below give the description of the work of consecutive separation filter with the use of dual waveguide ones it is branch.

From Fig. 5.16a it is evident that the cell contains two dual waveguide tees (VT) and two band or band rejection filters, tuned to frequency  $f_1$ . To the input of filter (Fig. 5.16b) into arm E of the dual waveguide tee VT<sub>1</sub> enter the signals of several frequencies  $f_1$ ,  $f_2$ , .... In the tee the electromagnetic wave is divided into the equal by amplitude, but opposite on the phase waves between the

lateral arms of tee. Waves, passing through the band or band rejection filters, tuned to frequency  $f_1$ , are divided in the frequency. Band rejection filters reflect the signals of frequency  $f_1$  and pass entire remaining frequency spectrum, band-pass filter pass the signal of frequency  $f_1$  and reflect the signals of other frequencies of the communication. Due to a difference in the distances from branch point to the connection points of filters, equal to quarter wavelengths, reflected by filters the signals of the lateral arms come the waveguide tee in the phase and pass therefore into arm H of tee 1. The signals, which passed band or band rejection filters, enter arm E of tee 2. The described diagram provides the separation of a large number of shafts of communication.

The important element of separation filters, which work on the parallel and on the consecutive circuits, are band and band rejection filters. The simplest type of band-pass filter is branching from the waveguide or coaxial line with the short-circuiting piston (Fig. 5.17a).

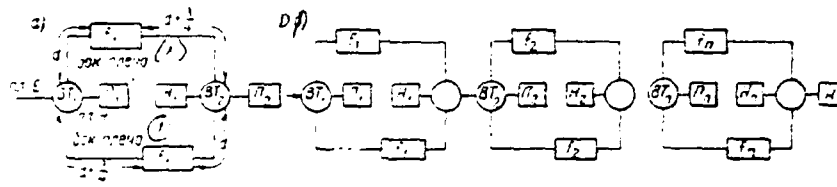


Fig. 5.16. Schematic of separation filter, made on series circuit.

Key: (1). side is arm.

Page 171.

With the equivalent distance from the branch point to the short-circuiting piston, equal to quarter wavelength, the input resistance of cell is very great and electromagnetic waves pass along the fundamental line without the reflection. At other frequencies this branching off is the reactance, which reflects electromagnetic wave. For obtaining the required frequency selectivity are applied several such elements connected in series. As the element of band-pass filter can be used the cut of waveguide or coaxial line with the inductive heterogeneities on the leads (Fig. 5.17b). During the appropriate selection of the length of the cut of line and construction of heterogeneities the equivalent length of cut can be made to be equal half wavelength  $\lambda/2$  in the waveguide. This cut of

waveguide (coaxial) is equivalent to parallel resonant circuit, tuned to frequency  $f_1$ . Possibly also series connection of such several elements; in this case the best results can be obtained in the filter with the quarter-wave communications. Fig. 5.17c shows one of the versions of the construction of the cell of band rejection filter [5.9]. This filter is equivalent to consecutive resonant circuit whose input resistance at the frequency of resonance is close to zero. Filter reflects electromagnetic waves in the frequency of resonance and passes the waves of other frequencies.

Besides separation filters, on the tropospheric radio relay lines are applied also the filters of harmonics [5.9]. Is possible the use of two types of the filters of harmonics.

First type filters are fulfilled thus. Electromagnetic energy of fundamental frequency by acceptor circuit, and energy of harmonics is reflected to the transmitter. Filters of this type can consist of the series of resonance elements (LCRs) by length  $\lambda_0/4$ , where  $\lambda_0$  - a wavelength of transmitter.

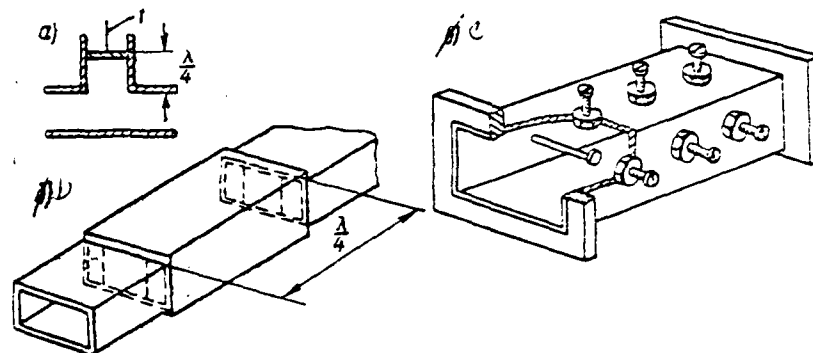


Fig. 5.17. Band and band rejection filters: 1 - short-circuiting piston.

Page 172.

At frequencies of even harmonics the length of such loops will compose the whole number of half-waves, and loop resistance will be very little; therefore for these frequencies the feed line will prove to be short-circuited. At the fundamental frequency input loop resistance is very great and the agreement of feed line virtually does not change. This filter is simple device; however, it possesses that deficiency which suppresses the emission of transmitter only on the even harmonics, the odd harmonics and other spurious radiations they pass through the filter without difficulty.

From the deficiency indicated are free the aperiodic filters, which are high-pass filters, all reflecting spurious radiations, which are found in the range of frequencies, situated it is higher than the operating frequencies of the equipment for tropospheric radio relay lines. In Fig. 5.18a and b they are shown general view to the construction of internal rod of one of the versions of the high-pass filters of the transmitter 1000 MHz [5.9].

Overall deficiency for first type filters is the fact that electromagnetic energy of the spurious radiations of transmitter it is reflected by filter to the transmitter it has an effect on the mode of its operation. This deficiency is absent in second type filters, which are fulfilled in such a way that energy of harmonics does not fall to the input of transmitter, but it is absorbed by filter itself.

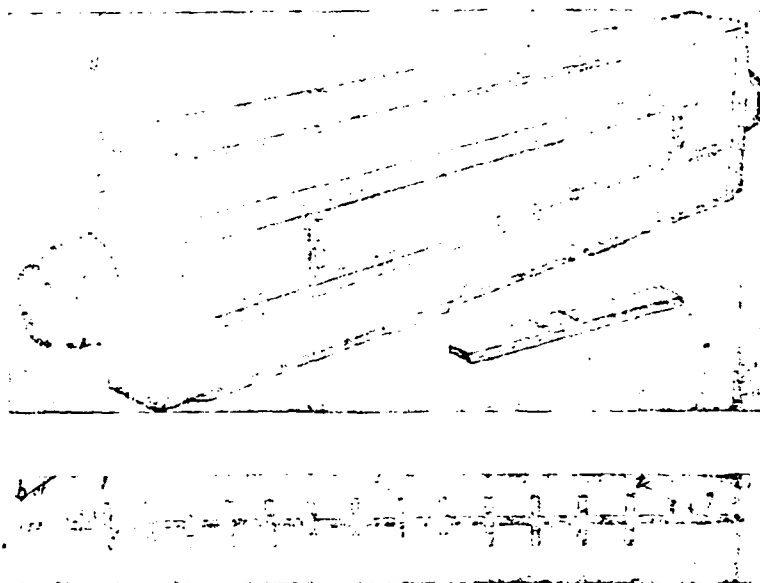


Fig. 5.18. The general view of the aperiodic filter of harmonics (a) and internal rod (b): 1 - the inclined sections, 2 - rods.

Page 173.

Filters of this type can utilize an effect of resonance energy absorption in the ferrite, placed within the cut of feed line. Can be designed the filters in which the energy of parasites is reflected by resonance elements and is absorbed in the special loads. Fig. 5.19 gives the general view of waveguide filter with the absorption of the power of harmonics. Filter is the cut of the waveguide of the

rectangular cross section, in wide wall of which is gashed the series of slots. Each slot is the open end of the waveguide of the reduced section, partially filled by attenuating material. The dimensions of slot and cross section of supplementary waveguides are selected in such a way that they would be less than the critical dimensions in the limits of the service band of frequencies and it is more than critical for the harmonic frequencies. Therefore, the energy of fundamental frequencies passes on the waveguide without difficulty, without being shunted into the supplementary waveguides and without experiencing noticeable absorption. Energy of harmonics, being propagated along the waveguide, is shunted into the supplementary waveguides where it is absorbed in the load.

At present ferrite devices are applied very widely in the technology SVCh.



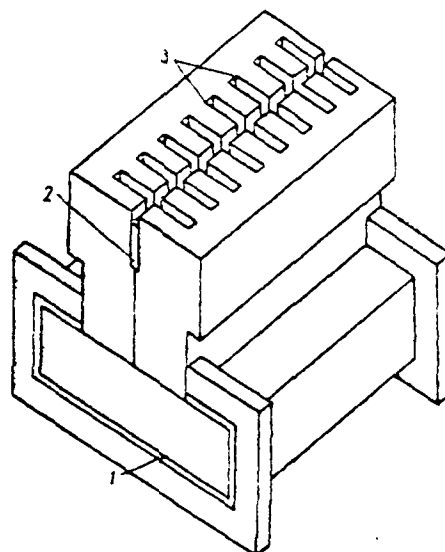


Fig. 5.19. Waveguide filter with the absorption of the power of the harmonics: 1 - fundamental waveguide, 2 - the absorbing load, 3 - supplementary waveguides.

Page 174.

In the antenna-waveguide circuits TRL are utilized ferrite gates [5.10], which possess low losses for the electromagnetic wave, which is propagated in the forward direction, and by large losses for the wave reflected. The use of such gates makes it possible to obtain the high agreement of transmitter with the antenna-waveguide circuit, to exclude interferences between telephone channels with multichannel telephony. The solution of this problem is possible in the devices

which use ferromagnetic resonance, and also in the devices with the nonreciprocal phase shifts in the magnetized ferrites. Fig. 5.20 shows the schematic of the ferrite gate, which uses ferromagnetic resonance. Ferrite gate is the cut of waveguide <sup>1</sup>, placed into the transverse magnetostatic field, created by permanent electromagnet.

FOOTNOTE <sup>1</sup>. Analogous devices can be created with the use of coaxial feed lines. ENDFOOTNOTE.

Within the waveguide are placed the ferrite and dielectric plates, fastened together. By the method of the appropriate selection of the dimensions of the ferrite plate, electrical parameters of ferrite and dielectric and constant value of magnetic field it is possible to obtain a considerable increase in the attenuation for the wave, passing through the gate in certain direction, with small attenuation for the electromagnetic wave of opposite direction. The agreement of gate for the transmitted electromagnetic wave with its connection to the matched load is determined in essence by dimensions and form of dielectric plate, since the dielectric permeability of contemporary ferrite materials is small. Strict calculation of ferrite gates can be made only for some idealized cases, and therefore in practice the dimensions of gate and the parameters of dielectric plate and ferrite are selected experimentally. It is known from the practice that the system described above of ferrite gate is realized in the centimeter

frequency band where succeeds in obtaining attenuation for direct wave of the order of tenths decibel. This means that with the work with the transmitter in power 3-4 kW in the ferrite plate is scattered power on the order of 300 W, which is provided because of the use of air or water cooling of that wall of waveguide to which is attached the plate. Besides direct losses in the ferrite plate is also scattered virtually all power of the electromagnetic wave reflected. However, in view of the fact that the agreement in the feed lines high, power of the wave reflected, as a rule, is approximately by an order less than the power of direct losses and therefore virtually it does not affect the thermal condition of ferrite plate.

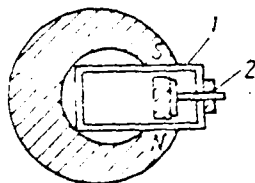


Fig. 5.20. Schematic of the ferrite gate: dielectric (1) and ferrite (2) plates.

Page 175.

The use of the described schematic of ferrite gate at frequencies of order 1000 MHz meets with great difficulties due to a considerable increase in the direct losses during these frequencies, and also complicated and bulky construction. In this frequency band of the loss of ferrite gate are 0.6-1 dB, which corresponds to 10-20% of power of transmitter, scattered by ferrite plate. At the power of transmitter 3-4 kW the scattered by ferrite plate power is equal to approximately 500-800 W, which requires the use of a complicated cooling system. In the decimeter range the best results can be obtained during the use of the ferrite circulator where the ferrite creates nonreciprocal phase shifts. The diagram of one version of the ferrite circulator, intended for the work with the transmitter of tropospheric radio relay line in the range 1000 MHz,

is given in Fig. 5.21a. Circulator [5.10] is the coaxial branching cff <sup>1</sup>, in which is placed the magnetized ferrite.

FOOTNOTE <sup>1</sup>. Circulators of this type can be made also on the waveguide branching cff. ENDFOOTNOTE.

Circulator is formed with the aid of three connected at angle of  $120^\circ$  cuts of coaxial lines. In the center of this connection is located the ferrite cylinder, magnetized along its axis by magnetostatic field  $H_0$ . In the absence of ferrite cylinder the power of electromagnetic wave, applied to arm I, is divided into equal parts between arms II and III. Ferrite excites in arms the II and III electromagnetic waves  $E_2$  and  $E_3$ . In this case it proves to be possible to fit the parameters of ferrite cylinder so that the intensity of field  $E_2$  would be equal in magnitude and on the phase of the intensity of field  $E_2$  of the wave, which existed in arm of the II in the absence ferrite cylinder; electromagnetic fields  $E'_2$  and  $E_3$  in arm III prove to be equal in magnitude and opposite on the phase.

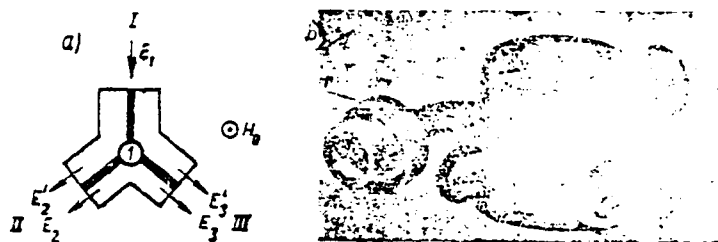


Fig. 5.21. Diagram (a) and general view (b) of the ferrite circulator: 1 - ferrite.

Page 176.

In this case electromagnetic energy from arm I completely passes into arm the II, and electromagnetic energy of the wave reflected from arm II passes into arm III and is absorbed by the matched load. Fig. 5.21b gives the general view of the ferrite circulator, intended for the work in the range of frequencies  $f=1000$  MHz. Cooling circulator water, direct losses are 0.2 dB, inverse losses - 20 dB. The greatest throughput is 3-4 kW.

#### §5.6. Systems of repeated reception.

The simplest system of the doubled reception is the system with the optimum addition, examined theoretically into §2.4. The detailed block diagram of the receiver, designed for the doubled reception

with the space diversity of received signals, is given in Fig. 5.22. The accepted by two antennas  $A_1$  and  $A_2$  signals through band-pass filter  $PF_1$  and  $PF_2$  which provide the necessary selectivity along second channel and selectivity for the protection from their own transmitter, they enter the high-frequency amplifiers  $UVCh_1$  and  $UVCh_2$  and the mixers  $SM_1$  and  $SM_2$ , to which are supplied the oscillations from the common heterodyne  $G$ . The voltage of intermediate frequency is amplified by  $UPCh_1$  and  $UPCh_2$  and is demodulated in frequency demodulators  $DM_1$  and  $DM_2$ . The obtained signals of low frequency are supplied to the stage of addition. The latter is two cathode followers with the total cathode load, which are controlled by the special amplifiers of noises in depending on the noise level of receiver so that in that receiver, in which the noise level is more, the amplification of cathode follower is less. Noise voltages from the output of each demodulator are isolated by noise filters  $FSh_1$  and  $FSh_2$  in the frequency region, situated are above the group spectrum multichannel communication. This voltage is amplified by the amplifiers of noise  $USb_1$  and  $USb_2$  and after detection  $D_1$  and  $D_2$  is utilized for the appropriate adjustment of the stage of addition. To the total load of cathode followers is connected group amplifier  $GU$ .

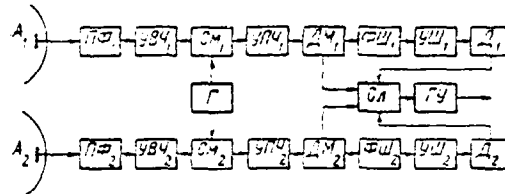


Fig. 5.22. Block diagram of receiver for the doubled reception with the space diversity of signals and the addition in the low frequency.

Page 177.

This diagram of control works well in such a case, when the total power of noises at outputs of both receivers remains constant, and occurs only its redistribution. Since cathode followers are included by a deep direct-current feedback, then in this case is provided the constancy of overall line attenuation of circuit without depending on noise distribution in the receivers. Since on the tropospheric lines, besides rapid incoherent signal fading, which enter from two antennas, there are slow fadings, virtually identical for these two signals, then the stages of addition can simultaneously to the identical degree be triggered or be cut off, and consequently, considerably change overall line attenuation of diagram. For eliminating this deficiency the amplifiers of noise are encompassed by the parallel system ARU (Fig. 5.23), because of which the total



power output of the amplifiers of noises remains constant, and the levels of control voltages, the applicable to the stages additions, they are distributed in accordance with the levels over the inputs of the amplifiers of noise. Fig. 5.24 gives another version of the diagram of control, in which is utilized one common amplifier of noise, included by ARU [5.11]. To the receivers are secured the shifted in the frequency regions of noise which are isolated with the aid of four band-pass filter, installed at input and output of amplifier.

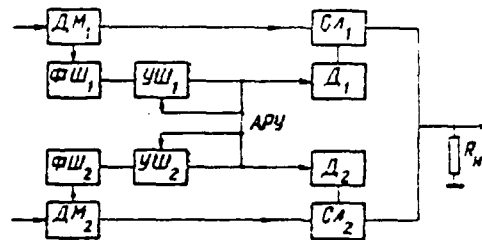


Fig. 5.23. Block diagram of addition in the low frequency with the use of parallel ARU.

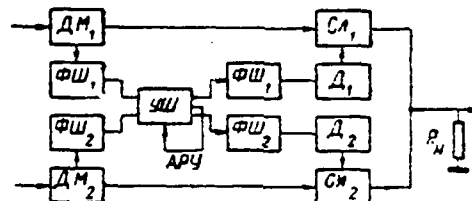


Fig. 5.24. Block diagram of addition in low frequency with use of common amplifier of noise.

Page 178.

A deficiency in this diagram is the presence of four filters requirements for which very rigid, since inlet filters must completely separate the working spectrum multichannel communication, the considerably exceeding noise level in the filter pass band, and output filters - reliably divide noise channels. However, in the first diagram of control is inherent another deficiency. In it two

amplifiers of noise, which require balance and constancy of the parameters in the time.

Fig. 5.25 gives the curves, which characterize the work of add system in the low frequency with the doubled reception. Curves show the dependence of the power of noise in telephone channel with single and doubled trimmers. Line 1 shows the theoretical dependence of the power of noise with the single reception on the value of signal at the input of receiver. Change in the power of noises and value of signal is given in the relative units. Dotted curve 2 shows the experimental dependence of noises on the value of signal for one receiver, while dotted curve 3 - for another receiver. A sharp increase of noises corresponds to the decrease of signal of lower than the threshold value for the sensing transducer of the frequency-modulated. Unbroken curve 4 shows the theoretical dependence of the power of noises with a decrease of signal on one of the receivers and a constant value of signal on other. Gain on the thermal noises with the doubled reception and the identical signals is 3 dB (points a and A). The maximum value of noise with decrease of one of the signals to zero theoretically increases on 6 dB (point E), due to the absence of one signal on 3 dB and presence of noise from the second receiver also by 3 dB. The experimental curves for this case, depicted as dotted lines 5 and 6, coincide sufficiently well with the theoretical curves for the values of signal of more than threshold level and go below on signal levels of less than the threshold level.

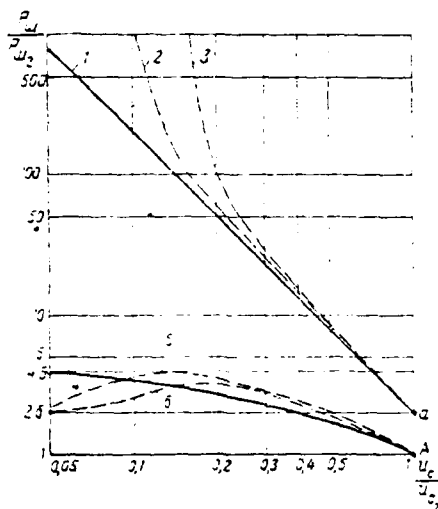


Fig. 5.25. Dependence of the power of noises in the channel in add system in the low frequency on the value of signal at the input.

Page 179.

This is explained by a sharp increase of noises during the breakdown of threshold relationships and by a complete closing of the corresponding stage of addition.

As noted into §2.4, it is most expedient to produce the linear addition of signals with the repeated reception at the intermediate frequency. But to produce this addition of signals is possible only in such a case, when these signals have identical phase. Since

signals at the output of IF amplifiers with the doubled reception with the space diversity of signals differ from each other in the phase due to a difference in the circuits of high and intermediate frequencies and as a result of a continuous change in phase of both signals with their passage through the troposphere, receiver must have a system of the automatic tuning of the phase of arriving at the stage of addition signals. Fig. 5.26 gives the system block diagram of addition in intermediate frequency [5.12]. The accepted by two antennas signals of one and the same frequency, but of different phase through band-pass filter  $PF$  and ferrite gates  $PV$  enter the mixers  $S_m$ , where they are converted into the oscillations of intermediate frequency and are amplified by IF amplifiers  $PUFCh$

[intermediate-frequency preamplifier] and  $UPCh$ . The addition of signals is conducted in the stage of addition  $S_1$ . The necessary for the transformation of high-frequency signals into the signals of intermediate voltage frequency of heterodyne is created by the method of frequency multiplication of common crystal oscillator  $KG$  to the necessary value in the multipliers  $UM$ .

Since crystal oscillator for both receivers common then the oscillations of intermediate frequency are always equal in the frequency, but they can differ in the phase. The signals accepted after  $UPCh$  through the limiters of  $Ogras$  [Osp = Oyr] [Soviet thermonuclear mirror machine] are supplied to the phase discriminator

DOC = 80025110

PAGE

378

FD, in which is developed the error signal, which affects the phase modulators FM, connected between the crystal oscillator and the multipliers.

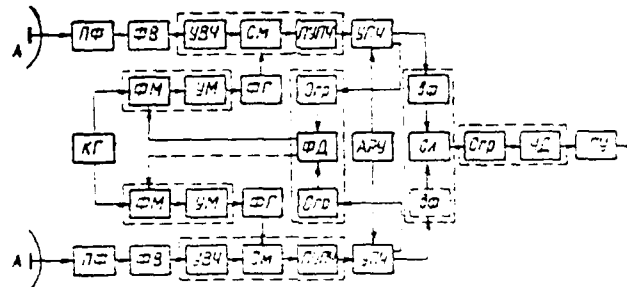


Fig. 5.26. Block diagram of receiver for the decoupled reception with the addition in the intermediate frequency.

Page 180.

The changes in the phase, obtained in the phase modulators, are multiplied into the appropriate number of times and are transferred to the intermediate frequency. This device provides the high accuracy of the phasing of received signals without the use of dc amplifiers due to the effect of the multiplication of phase divergences and virtually it does not depend on frequency stability of common heterodyne. The effectiveness of the work of phase tuning is characterized by the coefficient of control or by the coefficient of tuning, equal to the ratio of an initial phase difference  $\phi_0$  (with the switched-off automatic tuning) to a residual phase difference  $\delta\phi_0$  (with the connected tuning) [5.13]. The coefficient of control is equal to

$$K = \frac{\phi_0}{\delta\phi_0} = 1 - S_{\text{ODI}} \cdot S_{\text{OM}} \cdot n.$$

where  $S_{p.d.}$  - mutual conductance of the phase discriminator,  $S_{p.m.}$  - mutual conductance of phase modulator,  $n$  - the multiplication factor of frequency.

For the compensation for an initial phase difference in two receivers is utilized the equalizer of phase VP, included in one or the other arm of the stage of addition.

Heterodyne filter FG serves for the suppression of the combination oscillations, which appear in the stages of multiplication. After the stage of addition the signals enter the demodulator, which consists of the limiter of Cgras and FM discriminator ChD. From the output of demodulator the signals of low or group frequency are supplied to the group amplifier GU.

Linear conditions of the addition of the output signals of each of the receivers is provided by the use of parallel automatic gain control ARU of both IF amplifiers. With parallel ARU both amplifiers at any moment have the identical amplification, determined by the receiver on input of which larger signal, i.e., summarized signals, it is located in the same ratio as input signals. Phase modulator of this system consists of two tubes, interconnected (Fig. 5.27a)



85-0083 445

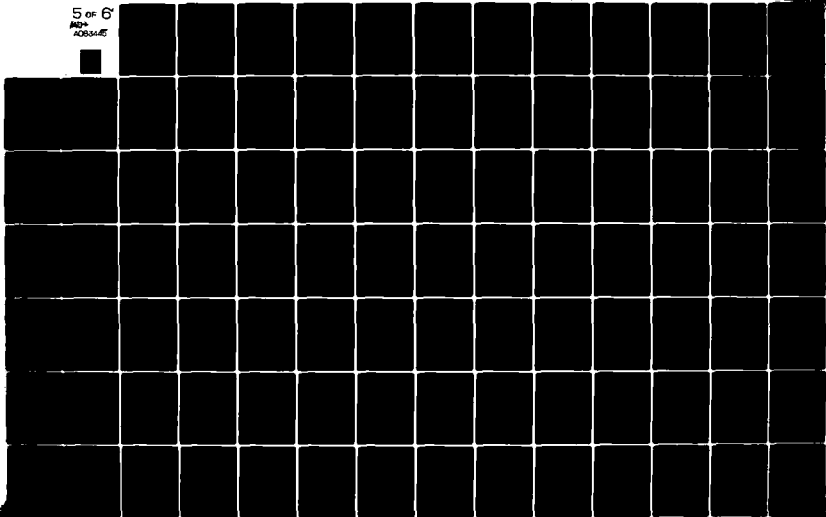
FOREIGN TECHNOLOGY DIV WRIGHT-PATTERSON AFB OH  
REMOTE TROPOSPHERIC RADIO COMMUNICATION (U)  
MAR 80 I A BUSTATINSKIY, A S NEMIROVSKIY  
FTD-ID(RS)T-0251-80

F70 17/80

UNCLASSIFIED

NL

5 of 6  
AND  
ACQUISIT



[5.14]. The oscillations, which come to the grids of these tubes from crystal oscillator, are out of phase relative to the supplied signal on  $\pm\alpha$ . This is reached by the fact that between the input stage of modulator and the grids of modulator tubes are connected the phase-shifting circuits, which ensure the necessary change in the phase. Error voltage from the phase discriminator is fed to the grids of modulator tubes. If error voltage is equal to zero, then the amplification of tubes identical and, as can be seen from vector diagram Fig. 5.27b, vectors of the total voltage  $\bar{u}$  is located in same conditional zero position, and the vectors of stress components  $\bar{u}_1$  and  $\bar{u}_2$  are shifted relatively to  $\pm\alpha$ .

Page 181.

If the polarity of error voltage is such, that the amplification of the first tube increases, and by the second it decreases, then occurs an increase in the phase of total oscillation by the angle  $+\phi$ , as it is clearly evident from the diagram where  $\bar{u}'_1$  and  $\bar{u}'_2$  - stress components, and  $\bar{u}'$  - a total voltage. With a change in the polarity of error voltage the phase of total voltage changes in the other direction. The output voltage of modulator  $u$  is the sum of two sine voltages  $u_1$  and  $u_2$ , equal in the frequency, but which differ in the phase on  $\pm\alpha$  from the phase of total voltage. Fig. 5.28 depicts the dependence  $\phi$  on the parameter  $k=u_1/u_2$  at different angles  $\alpha$ . From the

graph it is evident that mutual conductance of phase modulator increases with an increase in the initial angles  $\alpha$ , but in this case decreases the amplitude of total vector and increases its relative change in the process of tuning. On the basis of these considerations, the initial phases of vectors it is expedient to select order of  $\pm 70^\circ$ . In this case the relatively linear section of modulation characteristic is obtained with  $k$ , that is changed within the limits from 1 to 2, which corresponds to the rotation of total vector at an angle of  $\phi = \pm 43^\circ$ .

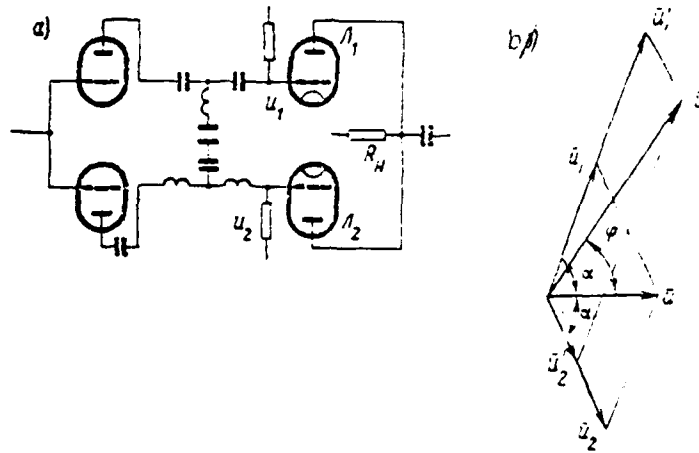


Fig. 5.27. Diagram and vector diagram of phase modulator.

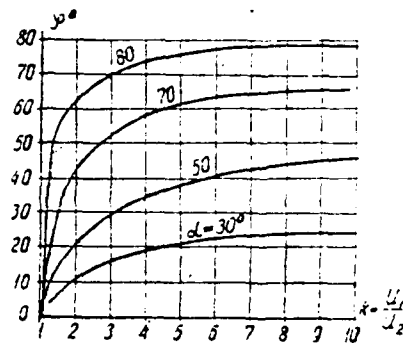


Fig. 5.28. Dependence of angle  $\varphi$  on parameter  $k$  at different angles  $\alpha$ .

Page 182.

In the selected diagram of the tuning of phase the control of the

amplitude of stress components is realized simultaneously so that  $u_1 = ku$ ,  $u_2 = (1/k)u$  and  $u_1/u_2 = k^2$ .

In this modulator circuit the voltage is developed on the total load of tubes in anode circuits  $R_H$ , therefore  $u_1 \equiv S_1 R_H$ ,  $u_2 \equiv S_2 R_H$ ,  $u_1/u_2 = k^2 = S_1/S_2$ .

For obtaining the phase shift on  $\pm 43^\circ$  is necessary a change of the slope of each tube 1.4 times. Since even at the values of the circuit parameters indicated in it occurs essential parasitic amplitude modulation, then after phase modulator it is expedient to introduce amplitude limiter. The characteristic of phase modulator is given in Fig. 5.29. As the phase discriminator is utilized balance phase discriminator. With a change in the phase of the stored up vibrations relative to each other to one or other side on the loads of detector will be developed error voltage for different polarity and different value.

The characteristic of the phase discriminator has many zero, distant behind each other to  $\pi$ , and period of change, equal  $2\pi$ . As a result of the peculiarity of the phase discriminator indicated, the dynamic system characteristics with the phase tuning has complicated form and behavior of entire system it can be different in depending on initial conditions and further change in the phase shifts. Dynamic

DOC = 80025110

PAGE

305

characteristic represents the dependence of the residual detuning of phase  $\delta\phi_0$  on initial  $\delta\phi_0$ . Fig. 5.30 depicts the possible dynamic system characteristics.

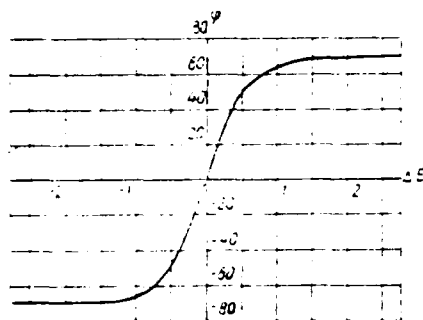


Fig. 5.29

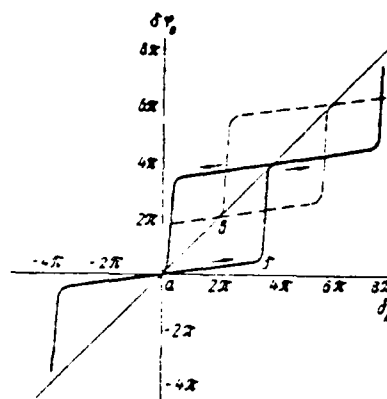


Fig. 5.30

Fig. 5.29. Characteristic of phase modulator.

Fig. 5.30. Dynamic characteristics of system of automatic tuning of phase.

Page 183.

Thus far a change in the phase shift is located in the band of the retention of system (segment of the curve a-b), i.e., thus far residual detuning does not exceed value  $\pi/2$ , system is held about conditional zero. As soon as residual detuning it will exceed value  $\pi/2$ , system "jumps" to another conditional zero, with further increase in the phase shift again will occur the jump. With an inverse change in the phase shift first will occur the retention of system about the conditional zero, equal to  $4\pi$ , and then follows

inverse jump. Upon the initial connection the system can be retained about the nearest of zero relative detunings of the phases of the arriving signals - point c. So that the jumps would not cause disturbance in the work of entire receiver, it must be designed so that the possible relative changes in the phase of two signals with their passage through the troposphere would not exceed the region of the retention of system. Fig. 5.31 gives the experimental curve, which shows a change in the phase difference between the arriving signals, which enter from two antennas. In the curve are plotted changes in output potential of the phase discriminator from the time. In the time interval of 0-1 min the system of the automatic tuning of phase is switched off, in this case in the curve recorded change in the phase from  $-\pi/2$  to  $+\pi/2$ , which is determined by the property of the phase discriminator to react to a phase difference, multiple  $2\pi$ , in an identical way. In the connected system are noted insignificant changes in the phase difference. On dotted curve is plotted the actual value of a phase difference between two signals, defined as product of droop and the coefficient of control.



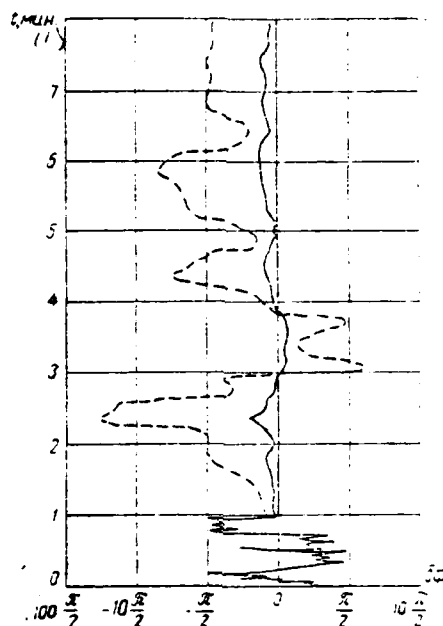


Fig. 5.31. Change of the phase difference in the system with the automatic tuning of phase.

Key: (1). min.

Page 184.

Fig. 5.32 gives the experimental curves, which characterize the dependence of thermal noise in telephone channel of receiver with the addition in the intermediate frequency on the identical high-frequency signal levels at inputs of both receivers on a phase difference between these signals with connected and switched-off APF.

As the zero noise level is accepted the level, which corresponds to equality phases. From the examination of these curves it is evident that the disagreement of phases on  $30-40^\circ$  causes an increase in the noise on 1 dB. With connected Aft virtually of an increase in the noise it is not observed.

For the addition in the intermediate frequency sometimes in the systems of the doubled reception is utilized the device of addition with the frequency control of the stored vibrations with an accuracy to phase [5.15]. In such devices is applied the second frequency conversion and addition is realized at the second intermediate frequency. The block diagram of the part of the receiver with this addition is given in Fig. 5.33. The oscillations of the stored signals from two amplifiers of the second intermediate frequency enter the phase discriminator. In one of the circuits of transformation is utilized the mixer with the quartz heterodyne, in the second circuit - mixer and generator with the reactance tube. Error voltage, developed at the output of the phase discriminator, is supplied to the reactance tube and oscillator frequency is adjusted slightly so, in order to frequency at outputs of both amplifiers coincide with an accuracy to phase. This system is suitable for the composition of vibrations, modulated by the signals multichannel telephony or by the signals of the television image, but it has two essential deficiencies. This system during the repeated addition

first requires the pairwise addition of signals, and then addition the vapor between themselves. The system of the automatic frequency control with an accuracy to phase has very narrow band of trapping and, besides in addition to this, the heterodynes of receivers and the generators of transmitters must have very high stability.

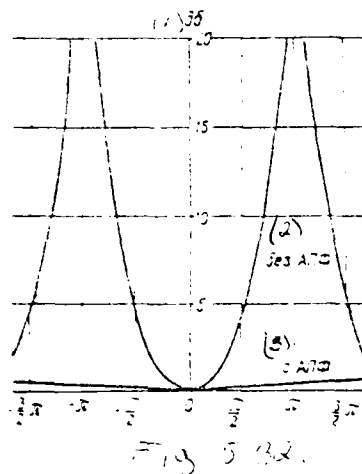


Fig. 5.32. Dependence of thermal noises on a phase difference between the received signals.

Key: (1). dB. (2). without. (3). with.

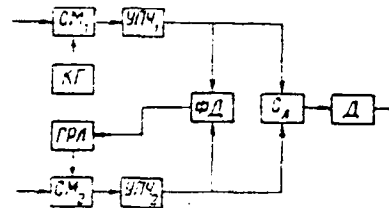


Fig. 5.33. System block diagram of addition with frequency control with an accuracy to phase.

Page 185.

Quartzes of the combined receiving-transmitting devices must be adapted to each other.

For the creation of the devices of the quadrupled reception are utilized the combined systems of addition. For adding the signals,

spread in the space, is applied the addition of signals in the intermediate frequency in pairs for each frequency and the subsequent addition - combining in fours the pairs between themselves in the low frequency. For the repeated addition of signals at the intermediate frequency is proposed the new system of the addition of Fig. 5.34, which has a whole series of the essential advantages in comparison with those earlier existed, basis of which lies in the fact that the system does not require special devices for the frequency control and phase of stored vibrations [5.16]. The frequency-modulated signals of intermediate frequency from the output of four IF amplifiers enter the synchronizing units  $SU_1-SU_4$ . Each of these devices consists of fundamental OS and auxiliary VS of mixers. Auxiliary mixer serves for forming the heterodyne frequency for the fundamental mixer. To both mixers are supplied the oscillations of intermediate frequency, while to the auxiliary are supplied even oscillations from the reference oscillator OG. During interaction of the oscillations of intermediate frequency and oscillations of reference oscillator at the outputs of auxiliary mixers are formed the oscillations with the frequencies:

$$f_{BC_1} = f_{or} + f_{np_1},$$

$$\dots\dots\dots$$

$$f_{BC_4} = f_{or} + f_{np_4}.$$

In the fundamental mixer interaction of the oscillations of the obtained frequencies and signals intermediate of frequency leads to the formation of the second intermediate frequency:

$$f_{2np_1} = f_{BC_1} - f_{np_1} = f_{or} + f_{np_1} - f_{np_1} = f_{or};$$

$$\dots\dots\dots$$

$$f_{2np_4} = f_{BC_4} - f_{np_4} = f_{or} + f_{np_4} - f_{np_4} = f_{or}.$$

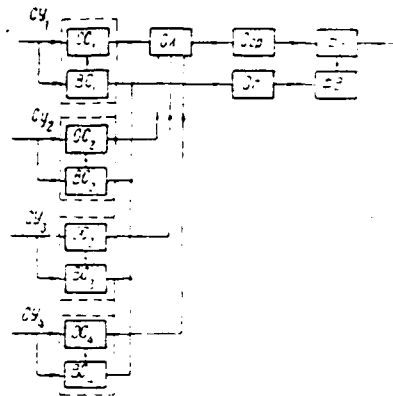


Fig. 5.34. System block diagram of addition with the synchronizing units.

Page 186.

From these expressions it is evident that the signal frequencies at the outputs of the fundamental mixers of each synchronizing unit are equal to the frequency of reference oscillator. This equality frequencies is maintained with an accuracy to phase and all signals can be simply stored on the total load. Passing through this synchronizing unit, the frequency-modulated signal is converted into the signal, modulated on the phase. This occurs as a result of the fact that in the fundamental mixer of synchronizing unit interact two frequency-modulated oscillations, which have the identical deviation of frequency -  $\Delta\omega$ , but dephased of the modulating signal by  $\Delta\phi = 2\pi F\tau$ ,

where  $F$  - the modulating frequency.

This displacement is caused by the fact that the signal due to all delays in the synchronizing unit delays to the period  $\tau$  relative to fundamental signal. At the output of the fundamental mixer of each synchronizing unit

$$\begin{aligned} f(t) &= \Delta f_c \sin 2\pi F t - \Delta f_c \sin 2\pi F(t-\tau) = \\ &= 2\Delta f_c \sin \frac{2\pi F \tau}{2} \sin 2\pi F(t-\tau) = \Delta f \sin 2\pi F(t-\tau), \end{aligned}$$

i.e. the deviation of frequency at the output

$$\Delta f = 2\Delta f_c \sin \frac{2\pi F \tau}{2}.$$

With satisfaction of condition  $2\pi F_{\max} \tau \ll 1$  - where  $F_{\max}$  - maximum modulating frequency, deviation at the output

$$\Delta f \approx 2\pi \Delta f_c F \tau$$

is proportional to the modulating frequency, and the index of modulation at the output

$$m = \frac{\Delta f}{F} = 2\pi \Delta f_c \tau,$$

is constant for any modulating frequency, i.e., signal has at the output frequency, but phase modulation. Since  $\Delta f \ll 1$ , the index of modulation in this phase modulated signal of small and signal can be modulated in the phase discriminator during the small distortions. Since the disagreement of signals in view small  $\tau$  is considerably less than  $2\pi$ , then all signals can be folded on one load in the stage of addition  $S_1$  and after limitations are demodulated in the phase discriminator PD. As the reference voltage for the phase

discriminator is utilized the same voltage from the reference oscillator, shifted on  $90^\circ$  in the phase inverter PV. Linear conditions of addition in this system is provided by the common parallel gain control of all IF amplifiers.

The described synchronizing unit somewhat improves the threshold properties of receiver due to the transformation of the frequency modulated signal into the signal, modulated on the phase, and its detection in the single detector, and also due to pumping of the oscillation, synchronous with the carrier of signal [5.17].

Page 187.

#### §5.7. Transmitters with the powerful amplifier klystron.

Widest use in the tropospheric systems received transmitters with the frequency modulation of generators at the intermediate frequency, the subsequent transformation of the oscillations of intermediate frequency into the high-frequency oscillations and the amplification of these oscillations to the necessary power. Fundamental vacuum-tube instruments for amplifying the high-frequency oscillations are multicavity span klystrons, travelling-wave tubes and powerful triodes. Fig. 5.35 gives the block diagram of the transmitter, used in the tropospheric systems with the space



diversity of received signals with the doubled reception. The modulating voltage from equipment for multiplexing or commutation equipment comes the generator of the frequency-modulated oscillations - modulator M, which works at intermediate frequency. In the equipment for tropospheric systems just as in the equipment for radio relay lines, usually is utilized intermediate frequency - 70 MHz. The obtained oscillations are amplified in UFCh and are supplied to the high-frequency mixer G. To the same mixer are supplied the high-frequency oscillations. For obtaining high frequency stability of transmitter in the frequency-modulated generators are applied special measures for the stabilization of medium frequency, and the high-frequency oscillations, necessary for the transformation, are obtained with the aid of frequency multiplication of the oscillations of crystal oscillator K in frequency multiplier UM. In the diagram is utilized the mixing at the high level, however, since for the oscillation of powerful amplifier klystron is required comparatively large power, then the obtained after mixer high-frequency oscillations first are amplified in UVCh, and then through the filter of lateral band F which isolates lower or upper side band, and attenuator AT, which uses for the decoupling between the high-frequency amplifier and with input circuit of power klystron, oscillation they are supplied to the powerful klystron amplifier MU. From the output of the klystron amplifier through the filter of harmonics FG, which shields other radio aids from the interferences from the side of this transmitter, high-frequency energy on the waveguide enters antenna A.

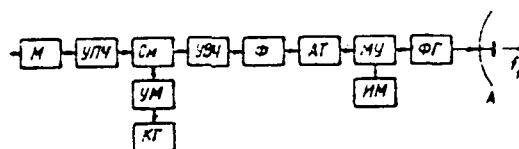


Fig. 5.35. Block diagram of transmitter for the system of the doubled reception with the space separation.

Page 188.

For the tropospheric systems with the frequency diversity of received signals with the doubled reception or for the frequency and space diversity of signals with the quadrupled reception is applied the transmitter, actually, which consists of two identical transmitters, which work at the different frequencies, but which have common modulator. The block diagram of this transmitter for the system of the quadrupled reception is given in Fig. 5.36. For increasing the reliability of transmitter in it are provided for two modulators M, workers and stand-by, and to them switching system PU. Each transmitter works on its antenna. For an improvement in the agreement between the filter of lateral band FF and input circuit of power klystron is connected ferrite gate FV. For decreasing the transient noises, which appear in the long waveguides as a result of the insufficient agreement of the output of power klystron and presence of the waves reflected from the heterogeneities of waveguide itself and from the antenna, at the output of klystron is installed powerful ferrite gate FFV or circulator.

For work in multibarrelled tropospheric lines are applied the transmitters, constructed according to the described block diagrams. For increasing the reliability of system can be provided the multiple operation of two modulators without switching system. Sometimes in similar type doubled transmitters are applied not two crystal oscillators, but one common in one half device is utilized after mixer upper sideband, but the secondly - lower lateral. In this case the operating frequencies of two halves transmitter differ to the dual value of intermediate frequency. Crystal oscillator has stand-by assembly and switching system. Both halves transmitter through separation filter work on one antenna feeder - with the angular separation of received signals or to the separate antenna with the space diversity of signals. The transmitter of another shaft works on the second irradiator or on the second antenna, as it was shown earlier.

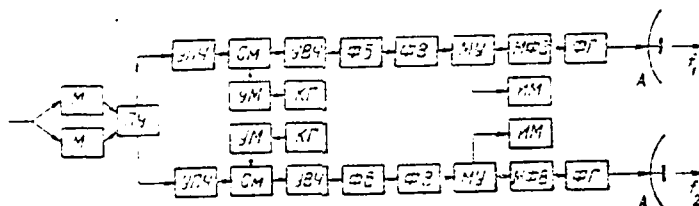


Fig. 5.36. Block diagram of transmitter for the system of the quadrupled reception with the space and frequency separations.

Page 189.

For increasing the reliability of entire system each half transmitter is supplied from two independent electric systems or from two self-contained diesel power plants.

Multicavity span amplifier klystron consists of following basic parts: cathode leg, resonator assembly, collector and separate focusing system [5.18]. In the cathode leg are placed the cathode and heater to it. Resonator node consists of several cylindrical coaxial ducts or rectangular resonators. The center conductor of coaxial integral cavities or special capacitive cylinders in the vacuum construction of klystron with the outer ducts serve as span tube for the escaping from the cathode electrons. Each duct gapped in the center conductor, through which occurs interaction of the high-frequency fields of resonators with the electron beam. Beam is

shaped with the aid of the magnetic field, created by the focusing system, and the electric field, which exists between the cathode and the collector. Resonator node has special channels for the cooling by its water. Collector serves for the creation in the klystron of electric field and for the collection of the electrons, which passed resonator systems. Collector is the copper core, placed on by span tube, cone is also cooled by water.

Klystrons have the great amplification when all ducts are inclined for one frequency; for obtaining the wide passband is conducted mutual staggering or introduction to them of supplementary attenuation, which, of course, decreases the output high-frequency power. Fig. 5.37 gives the photograph of powerful amplifier, in which is well visible the klystron of the KU-308 in the focusing magnetic system. Klystron works with the forced water cooling of collector and resonators. For the cooling it is required by 20 l of water per minute at a pressure of 1.2 atm. For the focusing is utilized one focusing coil with the uniform entire winding along the length resonator node.

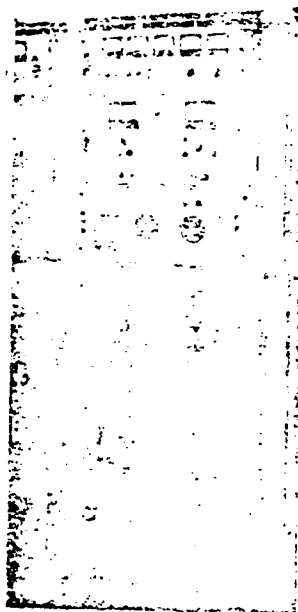


Fig. 5.37. Powerful klystron amplifier.

Page 190.

Accelerating voltage on the collector - 9 kV, amplification factors - 40 dB. A four-resonator klystron of the type of the KU-301 in output high-frequency power 10 kW is considerably more according to the dimensions. Klystron has the magnetic focusing, which consists of five coils, established evenly along the resonator node of klystron. Fig. 5.38 gives the diagram of powerful amplifier stage on the klystron. For the incandescence is utilized alternating current. In

the device the feeds of klystron are provided continuously variable control of filament voltage and, if it is necessary, the stabilization of incandescence, and also the inclusion of getter in the klystrons of large power. The device of feed is insulated from the ground. Voltage and current of heater are monitored by measuring meters. The focusing system of klystron, which consists of one or several coils, is supplied from the special device of feed. For the inspection of the power output of transmitter in the output coaxial <sup>trans</sup> or waveguide is provided for the power-level indicator, which consists of the calibrated directional coupler ~~W~~ and the meter of small power ~~IM~~ with the thermistor or detector cap.



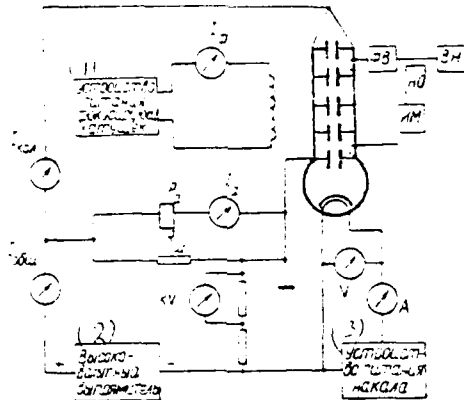


Fig. 5.38. Diagram of stage on the powerful amplifier klystron.

Key: (1). Device of the feed of focusing coils. (2). High-voltage rectifier. (3). Devices of feed of incandescence.

#### §5.8. Low-noise high-frequency amplifiers.

For sensitization of receiver devices of tropospheric radio relay lines are applied the parametric amplifiers, which possess a small inherent noise level. The theory parametric amplifiers detailed, there are methods of their calculation [5.19-5.21]. Will be here examined only the two types of the amplifiers, which found practical use.

The fundamental element of parametric amplifier is the parametric diode, which possesses the property of nonlinear capacitance and which changes its reactance due to the external energy sources. Since purely reactive elements do not possess inherent noise, then parametric amplifiers can provide very low inherent noise levels. For the accumulation of energy is utilized capacitance of p-n junction, a change in capacitance value is realized due to the supply from pump oscillator of the alternating voltage whose frequency higher than frequency of the amplified signal.

In the equipment for tropospheric radio relay lines are used two types of the parametric amplifiers: two-circuit amplifier-converter and two-circuit regenerative amplifier with circulator. The schematic of two-circuit parametric amplifier represents two parallel oscillatory circuits, one of which is tuned to a frequency of signal  $f_s$  and by the second - for difference frequency  $f_p - f_s$ . Parametric diode seemingly is coupling element between these two resonant circuits. To the diode to these or with another method are supplied the oscillations from pumping generator. In the parametric amplifier-converter is utilized the energy of difference frequency, which can be much more than the energy, given up by the source of signal. In the parametric regenerative amplifier with the circulator output energy is removed not at the difference frequency, but at the

signal frequency. The block diagram of amplifier-converter is given in Fig. 5.39a. Energy from the source of signal  $P_{\text{с.с.}}$  is supplied to the signal duct SK, and then through the filter PS to the parametric diode, to which through the filter PN are supplied the oscillations from the generator GN. The ringing of the intensive energy it is realized from the duct BK, inclined to the difference frequency and connected to parametric diode through the filter FR. In filters PS, PN and FR the resistances are equal to zero respectively for the signal frequency, pumpings and difference frequencies, and for other frequencies are equal to infinity.

Parametric amplifier can be characterized by three fundamental indices: by factor of amplification  $M$ , passband  $\Delta f$  and by factor of noise  $n$ .

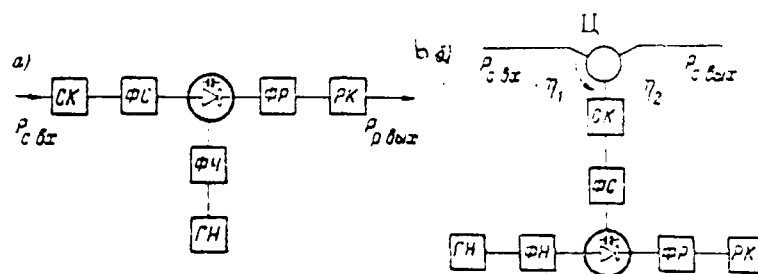


Fig. 5.39. Block diagram of parametric amplifier-converter (a) and regenerative amplifier with the circulator (b).

Page 192.

Power gain for the parametric amplifier-converter with a sufficient degree of accuracy can be expressed by formula [5.21]

$$M_{np} = \frac{P_{p \omega x}}{P_{c \omega x}} = \frac{f_p}{f_c} \frac{4\beta g_r g_n}{(1-\beta)^2 g_c g_p},$$

where  $f_c$  - difference frequency,

$f_p$  - signal frequency,

$g_r$  - the conductivity of the source of signal,

$g_c$  - the conductivity of signal duct

$g_n$  - load admittance,

$g_p$  - the conductivity of differential duct

$\beta$  - the coefficient of regeneration.

The coefficient of regeneration is determined by the expression

$$\beta = \frac{\pi^2 f_c / p \Delta c^2}{g_p g_c},$$

where  $\Delta$  - divergence of the capacitance of parametric diode from mean value.

The bandwidth, determined at the level 0.7:

$$\Delta f = \frac{\Delta c}{4 C_0} V \bar{f_p f_c} (1 - \beta),$$

where  $C_0$  - mean value of the capacitance of parametric diode.

Factor of the noise of the amplifier of the converter

$$n_{np} = \frac{g_c}{g_r} \left( 1 + \frac{1}{\beta} \frac{f_c}{f_p} \right),$$

If losses in the ducts are small, then these expressions can be simplified:

$$M_{np} = \frac{f_p}{f_c} \frac{4\beta}{(1-\beta)^2}$$

$$n_{np} = 1 + \frac{f_c}{f_p} \frac{1}{\beta}.$$

The block diagram of two-circuit parametric regenerative amplifier with the circulator is given in Fig. 5.39b. To the input of ferrite circulator Ts is supplied the energy of signal  $P_{\text{свх}}$ , which through the appropriate arm of circulator falls to the signal duct

SK. The intensive energy at the signal frequency through the second arm of circulator is supplied into the load. Power gain for this amplifier will be

$$M_u = \frac{\left[ \beta - \left( 1 - 2 \frac{g_c}{g_c} \right) \right]^2}{(1 - \beta)^2} \eta_1 \eta_2,$$

where  $\eta_1$  - efficiency of circulator from the source of signal to the amplifier,  $\eta_2$  - efficiency of circulator from the amplifier of load.

Page 193.

With small its own losses in signal duct

$$M_u = \left( \frac{1 + \beta}{1 - \beta} \right)^2 \eta_1 \eta_2$$

and with the values  $\beta$ , the close ones to the unit,

$$M_u = \frac{4 \eta_1 \eta_2}{(1 - \beta)^2}.$$

The factor of the noise of amplifier with the circulator will be

$$n_u = \frac{1}{\eta_1} \left( 1 + \frac{f_c}{f_p} \beta \right).$$

Parametric amplifier-convertors are applied in the range 500-2000 MHz, while parametric amplifiers with the circulator - in the range 500-5000 MHz. This is explained by properties of the existing parametric diodes and by working conditions for their in different diagrams. From the comparison of the given above expressions it is evident that with the equal losses in the ducts amplifier-converter has the amplification  $\frac{f_o}{f_c}$  once more than an amplifier with the circulator, and consequently, it is more stable

in the work, since the same amplification can be obtained at the smaller value of the coefficient of regeneration. from the theory and experimental investigations it is known that the stable work of amplifiers is provided with the coefficients of regeneration 0.6-0.8. Amplification are 10-20 dB, passband - from several megahertz to several ten megahertz, coefficient of noise -  $1.2-2$ .

For pump oscillators are utilized reflex klystrons and magnetrons. For the effective work of parametric diode to it it is necessary to feed from the generator of pumping the power of 10-100 mW, but, taking into account that in the real constructions pump oscillator frequently works in the conditions of poor agreement and can be utilized simultaneously for several amplifiers, the is desirable application of pump oscillators of larger power (100-1000 mW) for guaranteeing good decouplings between different nodes of parametric amplifiers in the overall structure of receiver. In the amplifier-converter the oscillations of difference frequency can be converted into the oscillations of intermediate frequency in usual mixer, to which are supplied simultaneously the oscillations from the high-frequency heterodyne.

Page 194.

Upon the appearance of amplifiers with the noise factor;

differing little from the unit, was introduced a somewhat different value for measuring the sensitivity - sum temperature  $T$ , connected with the noise factor with following expression [5.21] ]:

$$T = T_0(n-1).$$

where  $T_0$  - absolute temperature ( $\sim 300^\circ\text{K}$ ). In the amplifier-converter, operating in the range 500-2000 MHz, for the pumping usually are utilized the generators with the frequency on the order of 10,000 MHz. Mixers at such frequencies have a factor of noise on the order of 10-12 units, i.e., noise temperature on the order of 3000°K, and this means that this mixer to its own temperature of parametric amplifier will add certain value. The noise temperature of receiver is equal to

$$T_{\text{np}} = T_{\text{ny}} + \frac{T_{\text{cm}}}{M_{\text{ny}}}.$$

For decreasing the sum temperature are applied two-stage parametric amplifiers. If in this diagram the first amplifier has the same noise temperature and the same amplification, then the common temperature of receiving device will be substantially less and virtually is determined by the noise temperature of the first stage.

For the same reasons at the more high frequencies is expedient the use of two-stage parametric amplifiers, since one stage of regenerative amplifier, which works directly to the mixer, has sufficiently large noise temperature. In the two-stage amplifier it is possible to obtain at these frequencies the noise temperature on the order of 300°K with the bandwidth in several ten megahertz. As



pump oscillator for both stages it is possible to utilize one common generator on the klystron, which gives oscillations at frequency on the order of 20000 MHz.

#### §5.9. IF amplifiers, modulators and demodulators.

In the equipment for tropospheric radio relay lines, as in the equipment for lines of sight, are applied three types of IF amplifiers in accordance with their purpose: 1) the preamplifier with a small inherent noise level, included after parametric amplifier and mixer of receiver and the ensuring smallest factor of the noise and the preliminary amplification; 2) the fundamental amplifier, included after the preamplifier before the demodulator and which ensures the fundamental amplification of signal, and also necessary frequency characteristic, bandwidth and automatic gain control for the conditions of the linear addition; 3) the powerful IF amplifier, used in the transmitter and the ensuring necessary signal level on the mixer of transmitter. It should be noted that in the ratio of some characteristics UPCh as, for example, the nonuniformities of the band of group time lag, to the amplifiers are made somewhat weaker requirements in comparison with apparatus of the systems of direct visibility.

In accordance with the recommendations of MKKB [MKKP- International Radio Consultative Committee] accepted the parameters of systems are normalized to the length of line into 2500/km, and in the tropospheric systems up to this distance falls 5-10 times less than stations and the capacity of tropospheric lines is usually less than the passage ability of lines of sight. On the other hand, received signals on the tropospheric lines much less; therefore work virtually occurs near the threshold values of signal. Intermediate frequency for all amplifiers of usually 70 MHz. the factor of amplification of preliminary and powerful amplifiers - 10-20 dB, fundamental amplifiers - 80-100 dB [5.2; 5.3; 5.22].

For obtaining the frequency-modulated oscillations in transmitting devices of tropospheric radio-relay lines widest use received the valve-reactor modulators and the modulators, in which frequency modulation is obtained due to a change in the capacity of the semiconductor diode, entering the duct of the generator. These modulators are simple in the tuning and the operation, they are stable from its parameters, they provide a sufficient linearity of modulation characteristic, necessary for the transmission of a relatively small number of telephone channels, and the necessary deviation of frequency for the transmission of the signals of

television image.

For obtaining the large deviation of frequency during small nonlinear distortions are applied the special schematics of the frequency-modulated generators with the reactive tube [5.2]. The tendency to obtain the large deviation of frequency and small noises of nonlinear junctions leads to the need of using the tubes with the large transconductance, and this is the reason for an increase in the instability of average oscillator frequency due to sensitivity of tube to changes in the value of the feeding voltages and ambient temperature.

Recently begin to be widely applied the generators of the frequency-modulated oscillations with the semiconductor diode-varicaps which carry the character of the capacitive reactance, which depends on the value of bias voltage [5.1]. These generators are free from the deficiencies indicated, inherent in devices with the reactance tubes. Semiconductor diodes are applied at frequencies to several hundred megahertz. For obtaining the frequency-modulated oscillations the diode is connected in parallel to the duct of generator or parallel to its part.

The measure for the evaluation of the nonlinearity of the modulation characteristic of generator is the uniformity of the slope

of this characteristic. For decreasing nonlinear distortions into the oscillator circuit is introduced the two-circuit body-fixed system.

By the selection of the parameters of this system into the duct of the generator is introduced this impedance, that the differential characteristic would be symmetrical and it would have minimum nonlinear distortions.

Page 196.

Fig. 5.40 gives the schematic of this generator, while in Fig. 5.41 - the characteristic of slope without the duct and with connected compensating circuit.

The decrease of nonlinear distortions it is possible to obtain with parallel connection of two diodes, which work during different displacement, i.e., those having different dependence of capacitance on the voltage. Displacement is selected in such a way as to ensure the mutual compensation for characteristics expand the limits of a change in frequency [5.1].

The demodulators, used in the equipment for tropospheric lines, consist their three basic parts: limiter, FM discriminator and output assembly. Limiter serves for the elimination of parasitic amplitude

modulation. In the FM discriminator occurs the isolation of useful communication output node provides the agreement of the output of the FM discriminator with the group of the video amplifiers. For obtaining the effective limitation are applied multistage limiters on the special diodes which have fast time constant and low internal resistance [5.3].

During the limitation at the output of the cascades of limiter appear the harmonics of the signal of the intermediate frequency which cause in the FM discriminator the appearance of supplementary nonlinear distortions. These harmonics are filtered out in the special stage with a good filter, which has flat passband in the band of operating frequencies. Widest application in the equipment for radio relay lines found the FM discriminators with two detuned circuits [5.3].

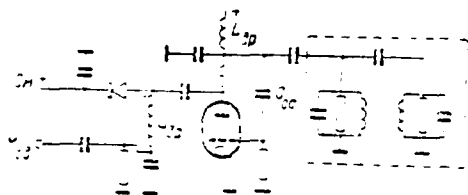


Fig. 5.40.

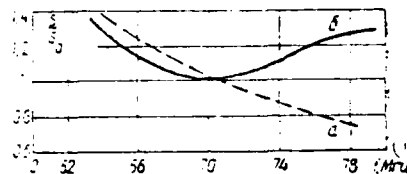


Fig. 5.41.

Fig. 5.40. Oscillator circuit of frequency-modulated oscillations on diode with compensating circuit.

Fig. 5.41. Change in slope of modulation characteristic of generator with diode: a) without compensating circuit, b) with compensating circuit.

Key: (1). MHz.

#### §5.10. Frequency fixing, crystal oscillators, multipliers, mixers.

In the equipment for tropospheric lines for the frequency conversion are applied the heterodynes of high stability. High stability is necessary so that the signal would remain in the center of the passband of the receiver: filters, amplifiers, detector, etc.

For example, for the transmission of 60 telephone channels the circuit of intermediate frequency must have width of band 5-6 MHz, if in it is not provided the correction of phase responses. With the use of correction the band of circuit can be narrowed to 2-3 MHz, and during the setting up of threshold device it can be led to 0.5-0.6 MHz. If we assume that the absolute instability of the frequencies of transmitter and heterodyne of receiver can compose 10% of the bandwidth, i.e., 50-500 kHz, then relative unstably of frequency will compose  $10^{-4}$ - $10^{-5}$  for the range 500-5000 MHz. The necessary value of the high frequency with this stability can be obtained by the method of repeated frequency multiplication of crystal oscillator. During the development of this multiplier should be avoided the appearance of frequencies, which coincide with the intermediate frequency or close to it, since they can cause interferences within the equipment for station itself. Crystal oscillator must be assembled on the special quartz with a small temperature dependence and included in the thermostat. To a considerable degree the instability of transmitter is determined by the instability of the medium frequency of the frequency-modulated generator, which for the generator with the reactance tube at the frequency of 70 MHz, can be 100-200 kHz, and for the generator with the diode - 20-50 kHz. In the transmitters, constructed according to the block diagram with the

powerful mixing, this value of absolute instability is transferred to the high frequency and can substantially make the common instability worse of device. For obtaining the oscillations of this oscillator frequency in the practical diagrams it works on third or higher mechanical crystal harmonics.

Fig. 5.42 gives the schematic of crystal oscillator on the transistors. The first transistor works as amplifier with the grounded base and the duct in the circuit of collector the second - the emitter follower - it serves for agreeing of loads and fulfilling of the balance of phases. All elements of generator consist into the thermostat, for the control of temperature of which is utilized bridge circuit with the thermistor.

For the receiving-transmitting devices of tropospheric radio relay lines is required frequency multiplication 10-100 times.



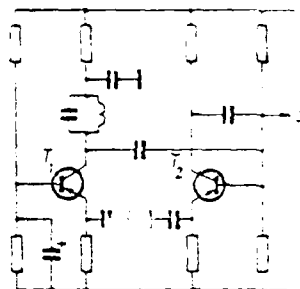


Fig. 5.42. Schematic of crystal oscillator.

Page 198.

Frequency multipliers for the receiving mixer where is required the power of oscillations 10-100 mV, are constructed according to this principle: first obtain the necessary power of oscillations at frequencies of order hundred or several hundred megahertz in the stages with the usual tubes and on the ducts with the concentrated constants, applying stages with duplication or trebling of frequency. High-frequency stage is done on the special high-frequency triode with the coaxial and waveguide circuits. In the transmitters, where the displacement is conducted at the high level and from the multiplier is required the power in several watts, the stages of multiplication are collected on the more high-power tubes, moreover are applied several high-frequency stages of duplication. for obtaining the large power stages of multiplication they can be

combined with amplifier stages.

Recently wide distribution acquires the method of frequency multiplication of oscillations with the use of nonlinear capacitance of semiconductor diodes - varactors [5.24]. The major advantage of such multipliers - high efficiency, which reaches to 500/o. Each stage of this multiplier consists of the duct inclined for the fundamental frequency, varactor itself and duct inclined for the double frequency or the frequency, several times large. There are two types of the stages: the series diagram in which the nonlinear capacitance and ducts are connected in series (Fig. 5.43a), and the parallel diagram (Fig. 5.43b), in which the varactor is connected by one lead in parallel to two ducts. The second diagram has a number of structural advantages especially at the high frequency.

As the only energy source for this multiplier serves the generator of input oscillations.

In the equipment for tropospheric lines are utilized three types of the mixers: 1) the low-noise mixers with a small the high-frequency signal level: 2) mixers for the second frequency conversion even 3) powerful mixers. Mixers with a small level of useful signal are established or directly after the two-circuit parametric amplifier with the circulator (in this case they operate

DCC = 80025111

PAGE

422

at the frequency of arriving signal and are converted high-frequency oscillations into the oscillations of intermediate frequency), or enter into the schematic of the parametric amplifier or converter but in which they serve for the transformation of the fluctuations of the difference frequency of higher than signal frequency, into the oscillations of intermediate frequency.

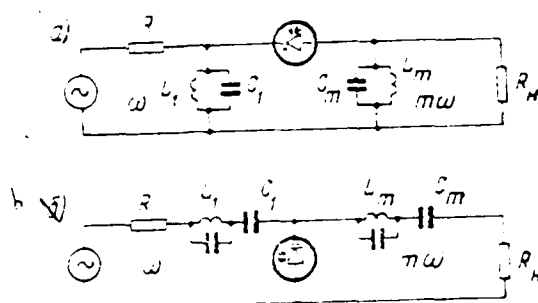


Fig. 5.43. The diagrams of multipliers on the varactors: a) are consecutive, b) parallel.

Page 199.

These mixers are fulfilled in the form of coaxial or waveguide constructions on special mixer diodes and possess low factor of the noise and by low losses during the transformation.

Mixer for the second frequency conversion is applied in the systems of frequency control with an accuracy to phase and in the synchronizing units of add system. These mixers work at the level on the order of 0.1-1 V, they are fulfilled on the tubes or the transistors; sometimes they are collected on the balancing network for the suppression of the second harmonic, which in the broadband system it is difficult to suppress by the use of some filters. Powerful mixers are installed in the transmitters, constructed

according to the diagram of powerful mixing, they are fulfilled on the tubes and on the diode mixers and they can be designed in the form of coaxial and waveguide constructions. The diode mixers have a factor of the noise of 10-20 units. The mixers must have good agreement, otherwise with the work with the parametric amplifiers this can lead to the distortion of the form of frequency characteristic and the appearance of supplementary transient noises in the channels. Usually for eliminating this phenomenon, and also for preventing the incidence of the noises of mixer into the amplifier and their amplification, between parametric amplifier and mixer is installed ferrite gate. In the equipment are applied the mixers on one diode and balancing networks on two diodes. The latter give the possibility somewhat improve noise factor due to certain compensation for the noises of heterodyne with the balance of diodes.

#### §5.11. Devices for decreasing the threshold level $C_{th}$ of receiver.

In the receiver  $C_{th}$  of signals occurs the phenomenon of "threshold  $C_{th}$ " which appear as a sharp increase in the noises at the output of the FM discriminator with the decrease of signal-to-noise ratio at its input of lower than the specific level. Graphically the dependence of relation signal/noise at the output of the FM discriminator on the signal-to-noise ratio at its input is shown in Fig. 5.44. Curve 1 corresponds to usual  $C_{th}$  of receiver. To point A

the relation noise/signal at the output linearly depends on signal-to-noise ratio at the input (for example, with the decrease of signal at the input of receiver two times noise at the output of the FM discriminator it grows also two times). In the signal-to-noise ratio at the input of the FM discriminator below 8-12 dB this dependence is disturbed and curve at first slowly, and then steeply changes its slope. This region on curve 1 lies more left point A.

Page 200.

The threshold point A usually defines as the point at which the relation noise/signal at the output of the FM discriminator differs from the linear dependence signal/noise at its input on 1 dB [5.25]. It should be noted that curve 1 completely does not reflect the phenomenon of threshold and is not considered its subjective perception. Thus, with the work of receiver in the threshold region at the output of the FM discriminator not only is perceived an increase in the noise, but also noises themselves acquire by different character instead of the flat ones since they become pulse. This sharply increases their interference with multichannel telephony and it is not completely commensurated with the increase in the mean power of signal, which can be obtained with measurement. Analogously is received deterioration in the quality of television image. In this case appear the black and lemon spots, which flicker on entire screen

[5.26]. To this one should add that together with a total increase in the noise and a change in its spectral composition at the output of the FM discriminator is observed also the noise suppression of useful signal [5.27], which even more aggravates the threshold effect ChM of receiver. Thus, the decrease of signal of lower than the threshold level leads to complete break in the communication. Therefore a decrease in the threshold level ChM of receiver has fundamental importance for the tropospheric lines of communications, since signal on such lines has deep fadings.

The power of noises, led to the input ChM of receiver, and consequently and threshold level depend on the band of circuit PCh of receiver. Therefore the simplest method of decreasing the threshold level ChM of receiver is the decrease of this band. However, take to the specific value.

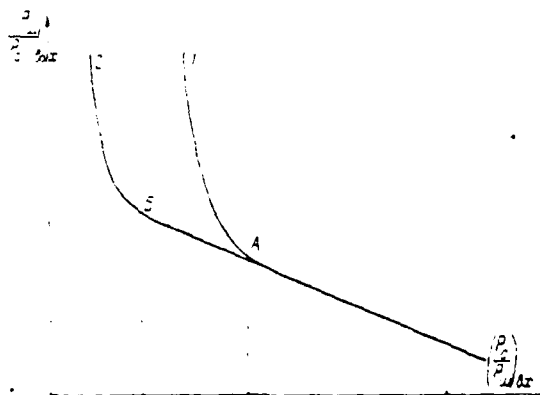


Fig. 5.44. Dependence  $\left(\frac{P_u}{P_c}\right)_{\max}$  on  $\left(\frac{P_c}{P_u}\right)_{\max}$  for ChM.

Page 201.

At present is already developed a large quantity of devices for lowering in the threshold level ChM of receiver [5.25]; it is possible to divide them into two basic groups:

1. The so-called "servo systems", namely: device with the feedback in the frequency (OSCh), the servo filter, which tracks heterodyne, regenerative frequency divider. In these devices the band on PCh is considerably narrowed in comparison with the passband usual ChM of receiver. In accordance with the aid of feedback here decrease deviation the frequencies of useful signal and, therefore, the width of its spectrum. As a result in this system decreases the power of noises without the power loss of signal and thereby is decreased the



threshold level of receiver.

2. In this group of devices is utilized increase in energy of useful signal due to local oscillator. In this case together with the frequency detection is applied phase, and for decreasing the distortions of the communication adopted which in this case appear, is introduced negative feedback in the frequency.

Block diagram ChM of receiver with the feedback in the frequency is depicted in Fig. 5.45. In contrast to conventional superheterodyne ChM of receiver, here heterodyne not with the fixed tuning, but has frequency modulator. In this case the frequency of heterodyne changes according to the same law, as the communication adopted. For this voltage from the output of frequency detector of receiver it is supplied to the frequency shift key of heterodyne. The sign of this voltage is selected in such a way that the instantaneous frequency of heterodyne would be cophasal with the instantaneous frequency of the communication adopted. In this case the instantaneous frequency of heterodyne begins to follow the instantaneous frequency of input signal. As a result of interaction two ChM of signals in the mixer is formed the signal of intermediate frequency with the deviation, equal to a difference in the deviations of these signals. Such by shape, the value of the resulting deviation in the intermediate frequency depends on the deviation of the frequency of heterodyne which, in turn, it depends on amount of feedback.

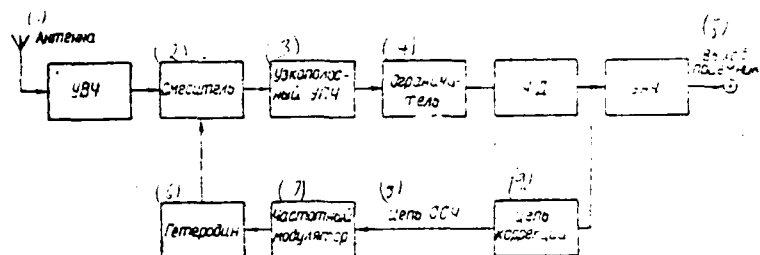


Fig. 5.45. Block diagram ChM of receiver with the feedback in the frequency.

Key: (1). Antenna. (2). Mixer. (3). Narrow-band UPCh. (4). Limiter. (5). Output of receiver. (6). Heterodyne. (7). Frequency shift key. (8). Circuit OSCh. (9). Circuit of correction.

Page 202.

As is known, minus band of frequencies, occupied by ChM by signal on PCh, composes  $2F$ , where  $F$  - the highest frequency of the modulating signal. This occurs with a small index of modulation, virtually with  $m \leq 0.5$ . The frequency band at the input of receiver with the large index of modulation is determined approximately by expression [5.25]

$$\Delta f \approx 2(m-1)F.$$

From this expression it is evident that the maximum amount of feedback, which can be introduced in ChM receiver, is equal to  $2m$ . In

this case the index of modulation in the intermediate frequency will fall to 0.5. Then band of the transmission of narrow-band UPCh can be brought to  $2F$ , i.e., to decrease in  $(n+1)$  once. In so many once it is possible to lower the threshold of power. This is explained by two fundamental reasons [5.28].

1. It is known that negative feedback (CSCh) always expands equivalent band of direct circuit. This occurs also in the system CSCh, which leads to the expansion of the equivalent band of narrow-band UPCh and, therefore, to the loss of gain in the threshold level.

2. On ChM heterodyne of receiver together with NCh with signal is supplied noise from output of frequency detector. This noise, interacting with the input noise, forms the supplementary components which increase the total power of noise at the input of the FM discriminator. An increase in the power of noise under the action of feedback causes the so-called "inherent" threshold of system CSCh. The onset of its own threshold limits the maximum depth of inverse binder. Therefore in practice in the receiver with CSCh amount of feedback is taken less than value  $2n$ . Threshold curve for ChM of receiver with OSCh is given in Fig. 5.44 (curve 2). During the comparison of this curve with the threshold curve for usual ChM of receiver (curve 1) it follows that the receiver with CSCh has smaller

threshold level (point B on curve 2) and respectively gain on the threshold level composes the difference between the signal-to-noise ratios at points A and B. although receiver with OSCh has the best threshold level, nevertheless in the section 4-5 occurs the linear build-up of noise at its output. Therefore in the systems with OSCh for obtaining the high signal-to-noise ratios near the threshold is applied the large deviation of frequency, than in the usual systems. The gain on the threshold level, provided by system OSCh, is 5-6 dB with the amount of feedback 12 dB. From the comparison of these curves it also follows that in the region higher than threshold the receiver with OSCh has no advantages. Let us recall that with the signals of higher than the threshold the noise at the output ChM of receiver is determined by normal band NCh of circuit.

ChM receiver with servo filter (Fig. 5.46) differs from receiver with OSCh only in terms of the place of the correction of the frequency shift key.

Page 203.

In this case under the action of the modulating voltage is reconstructed the narrow-band filter, which follows the instantaneous frequency in the circuit of broadband UPCh, the passband of which is selected different doubled ambrcider to the modulating frequency.

Thus, according to the result of work this diagram is analogous CSCh. However, with the practical fulfillment the servo filter has a number of advantages in comparison with CSCh. First, since the value of intermediate frequency and deviation at input and output of filter are changed, then it can be connected in already finished ChM receiver. In - the second, the servo filter is less inclined to the self-excitation. Therefore the correction of loop of feedback considerably is facilitated [5.25]. To deficiencies in the servo filter should be carried the essential nonlinear distortions of the modulating signal; however, with the reception of TV signals this is not decisive. The gain on the threshold level, given by receiver with the servo filter, is virtually equal to the gain of receiver with CSCh.

ChM receiver with the "servo heterodyne" [5.29]. In the communicating systems, which use remote tropospheric propagation, as a rule, is utilized the diverse reception. In this case the device for an improvement in the threshold level must be connected to add system, i.e., feedback loop must not be embraced stages after the block of adding the signals. Furthermore, device must not be sensitive to fading of input signal. The requirements indicated completely satisfies device for an improvement in the threshold level - "servo heterodyne" (Fig. 5.47) whose use is especially expedient in the system of the diverse reception during the addition of signal to

the FM discriminator. This device is switched on between broadband UPCh and FM discriminator of receiver and consists of three mixers, narrow-band UPCh and reference quartz oscillator. The frequency of received signal at the output of fundamental UPCh of receiver is equal to  $f_n$ . The frequency of reference quartz oscillator is equal to  $f_n$ . The "servo heterodyne" is regenerative device and in the process of work signal frequency at its output is equal to frequency at the input, i.e., is equal to  $f_n$ .

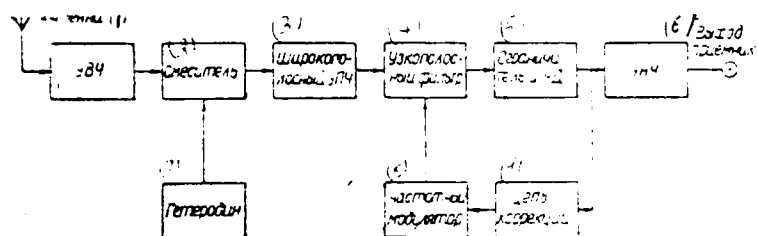


Fig. 5.46. Block diagram ChM of receiver with the servo filter.

Key: (1). Antenna. (2). Mixer. (3). Broadband U.F.C. (4). Narrow-band filter. (5). Limiter and ChL. (6). Output of receiver. (7). Heterodyne. (8). Frequency shift key. (9). Target of correction.

Page 204.

The part of the energy of output signal is supplied to the third mixer where as a result of interaction with the signal of reference quartz oscillator is formed signal with sum frequency  $f_{\Sigma} = f_{\Pi} + f_{\text{KB}}$ . This signal enters simultaneously the first and to the second mixers. In the first mixer after interaction with the input signal is formed difference frequency  $f_{\text{KB}} = f_{\Sigma} - f_{\Pi}$ . The secondly - as a result of the subtraction of frequencies  $f_{\Sigma}$  and  $f_{\text{KB}}$  again is formed the signal with initial frequency  $f_{\Pi} = f_{\Sigma} - f_{\text{KB}}$ .

Let us assume now that the frequency of input signal changes and

comprises, for example  $f_n - \Delta f$ . Then signal frequency at the output is also equal to  $f_n - \Delta f$ . On output of the third mixer the signal frequency equal to  $f_n - \Delta f$ . But in this case is formed signal with difference frequency  $f_{ns} = (f_n - \Delta f) - (f_n + \Delta f)$  and in the second mixer - signal with difference frequency  $(f_n - \Delta f) - f_{ns} = f_n + \Delta f$ . From the given example it is evident that with any changes in the frequency of input signal at the output of the first mixer, i.e., in narrow-band UPCh there is always a signal with constant frequency  $f_{ns}$  to the equal frequency of reference oscillator. This, first of all, provides adjustment-free work of device which gives the possibility to obtain in its narrow-band part signal with the constant and high-stability frequency.

In the process of frequency modulation, i.e., with a rapid change in the frequency, occurs the similar pattern, i.e., in the first mixer are deducted the deviations of signals  $f_n$  and  $f_{ns}$  and the secondly, where is restored frequency drift of input signal, is restored initial deviation. However, with a rapid change of the frequency in the first mixer nevertheless it does not occur the complete subtraction of deviations. The fact is that in the direct circuit of device always occurs signal lag (in essence this time lag is determined by narrow-band UPCh).



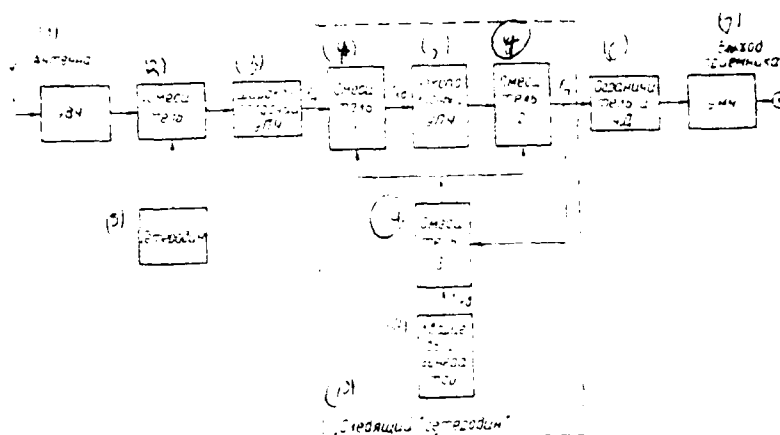


Fig. 5.47. Block diagram ChB of receiver with the servo heterodyne.

Key: (1). Antenna. (2). Mixer. (3). Wideband UPCh. (4). Mixer. (5). Narrow-band UPCh. (6). Limiter and UD. (7). Output of receiver. (8). Heterodyne. (9). Quartz generator. (10). Servo "heterodyne".

Page 205.

Therefore delays the phase of modulation of substances signal with frequency  $f_r$  at the input of the first mixer relative to of modulation in the input signal. As a result in the first mixer the deviation decreases although very strongly, not to zero. In this case the deviation decreases the greater, the lower the modulating frequency, since for the smaller frequencies occurs smaller phase shift. In the second mixer for all modulating frequencies the initial

deviation is restored.

From the description of the operating principle it is evident that the "servo heterodyne" is device with two-loop feedback in the frequency, moreover in the external loop (to the first mixer) is realized negative feedback, and in the internal loop (to the second mixer) - positive. As a result it is obtained, that entire device relative to input and output not at all included by connection with any sign. This makes the "servo heterodyne" free from the deficiencies of OSCh and the analogous devices i.e., here is not required the correction of feedback loops, is not expanded the equivalent band of narrow-band UFCh, and therefore it is possible to completely realize gain in the threshold level. Furthermore, here it does not appear its own threshold of feedback, and therefore it is possible to ensure the significant decrease of the deviation of the frequency of received signal. This device with the identical success works both with the reception of TV signals and signals multichannel telephony.

First type threshold devices include also regenerative divider [5.25]. However, as a result of the more complicated design it did not have extensive application in ChM receivers.

ChM receiver with the regeneration of carrier. As has already

been indicated above, for decreasing the threshold level in the second group of devices is utilized the energy of local oscillator. In this case the voltage from it is introduced into the circuit of intermediate frequency to the limiter, and its frequency and phase are adjusted slightly with the aid of the system of phase automatic frequency control (PAFCh) to the coincidence with the carrier of received signal. Block diagram ChM of receiver with the cophasal regeneration of carrier is shown in Fig. 5.48.

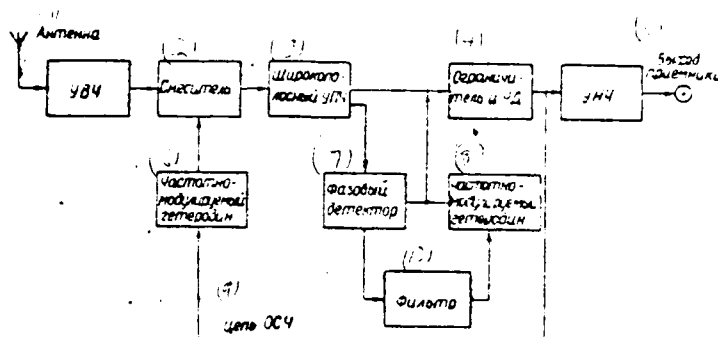


Fig. 5.48. Block diagram ChM of receiver with the regeneration of carrier.

Key: (1). Antenna. (2). Mixer. (3). Broadband UCh. (4). Limiter and ChD. (5). Output of receiver. (6). Frequency-modulated heterodyne. (7). Phase discriminator. (8). Frequency-modulated heterodyne. (9). Circuit OSCh. (10). Filter.

Page 206.

As it is noted in work [5.25], for the undistorted reception ChM of signal with the aid of this device it is necessary to satisfy two conditions: 1) the index of modulation must be considerably less than the unit and 2) voltage from the reference oscillator is considerably more than the carrier of the communication adopted. For satisfaction of the first condition is applied the described above feedback in the frequency. As is known, any synchronous detection, i.e., detection

with the use of reference voltage, is without threshold. However, in this case reference-voltage source is subjected to external effect, since system FAPCh cannot work in any signal-to-noise ratio at its input. This leads to the disturbance of the inphase state of voltages and, consequently, also to the disturbance of the process of the isolation of useful signal. Therefore gain on the threshold level in this system is limited practically by the value of 10-13 dB. Another version of the described height system is depicted in Fig. 5.49. Here for the detection ChM of signal is utilized system FAPCh. Moreover voltage from the reference oscillator is introduced cophasally, but orthogonally with carrying ChM of signal. For decreasing the index of modulation, and also decrease of parasitic amplitude modulation is introduced the circuit CSCh.

To the advantages of synchronous phase detection should be carried also the absence of the overshoots of noise with the work in the threshold region, i.e., the character of shim at the output of the phase discriminator does not change in any signal-to-noise ratios at its input.

From the short description of systems for an improvement in the threshold level it is possible to draw the conclusion that the most adequate threshold device for the use on tropospheric RRL is the "servo heterodyne", which provides the greatest gain on the threshold level, it is insensitive to the instability of the frequency of input signal and changes in its level, furthermore, it can be used in the system of the addition of signals in the intermediate frequency.

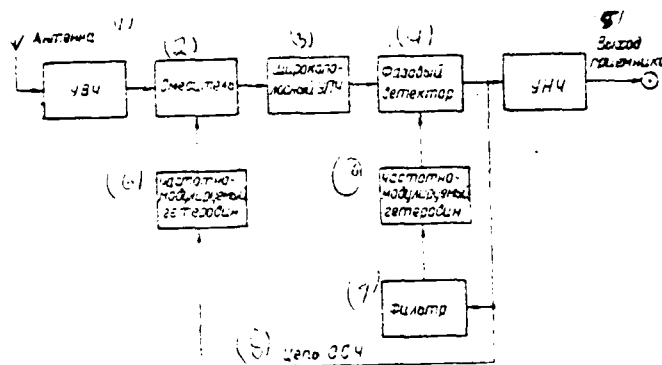


Fig. 5.49. a block-diagram ChM of receiver with the phase detection.

Key: (1). Antenna. (2). Mixer. (3). Broadband UPCh. (4). Phase discriminator. (5). Output of receiver. (6). frequency modulated heterodyne. (7). Filter. (8). Circuit CSCh.

Page 207.

## §5.12. Construction of group circuit.

TRL allow multiplexing high-frequency shaft with the aid of the standard multichannel equipment with frequency channel separation. In accordance with this the group circuit of system must pass the frequency band for 12 channels 12-60 kHz; for 24 channels - 12-108 kHz; for 60 channels - 12-252 kHz and for 120 channels - 12-552 kHz or 60-552 kHz. Since link between operators or the tropospheric lines

is organized in the same fundamental telephone shaft, then in the band of frequencies of the group circuit of system is provided for place for distribution of official channels. For increasing the effectiveness of link between operators it is possible to create several official channels the bands of frequencies of which are placed above and below the band, occupied by telephone channels.

In the equipment T&I independent of apparatus of multiplexing is realized the continuous inspection of fundamental qualitative indices of channels, namely: the control of overall line attenuation of group circuit and noise level in the channels. For the checking in the group circuit are created the monitoring channels bands of frequencies of which are placed above and below band edges, occupied by telephone channels.

The version of the distribution of the band of frequencies in the group circuit of the system of the tropospheric communication, which works with the standard equipment for multiplexing K-60 to 60 telephone channels is given in Fig. 5.50. The block diagram of the construction of group circuit is in connection with this case given in Fig. 5.51. the transmitting part of the group circuit begins from the line transformer LT for the transition from the balanced cable to the asymmetric diagram.

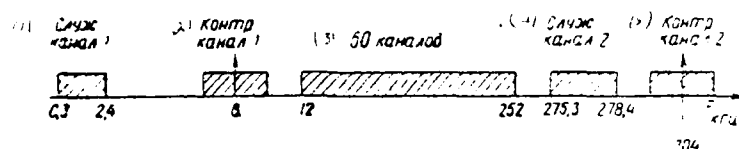


Fig. 5.50. Distribution of the frequency bands in group channel.

Key: (1). Service channel 1. (2). Cont. channel 1. (3). 60 channels.  
(4). Service channel 2. (5). Cont. channel 2.

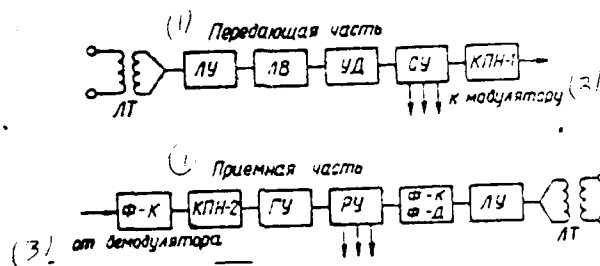


Fig. 5.51. Block diagram of construction of group circuit.

Key: (1). Transmitting part. (2). to modulator. (3). from demodulator.

Page 208.

For the matched connection and the decoupling of the circuits of equipment for multiplexing, generators of pilot frequencies and equipment of official channels serves the matching device SU. In TRI



in accordance with the recommendations of MKKR are applied the predistortions of group signal, which makes it possible to significantly lower the noise level in the upper channels due to the equalization of noises along the channels. In the group circuit on the side of transmission this is accomplished by the pre-distorting duct or by the duct of preliminary slope KPN-1, and on the side of the reception equalization of signal it is conducted by the restoring duct KPN-2.

If equipment for multiplexing is located at a great distance from the station of radio relay line, then on the input of group circuit is installed linear group amplifier LG with the linear equalizer LV for the equalization of the frequency characteristics of coupling cables and the variable extender UE for guaranteeing the nominal level at the input of the modulator of transmitter. In the group circuit on the side of reception are connected following elements: K filter (F-K), which locks currents of lower official channel, restoring duct KPN-2, group amplifier GU, distributor RU for the branching of upper official channel and monitoring channels. At the output of the group circuit before the equipment for multiplexing are switched on the filters F-K and F-U, the locking currents of monitoring channels and upper official channel, after filter can be established the linear amplifier LU and balancing transformer.

At the transit exchanges where is necessary the isolation of the part of the channels, into the diagram of group circuit additionally are introduced the filters and differential systems. Group amplifiers differ little from the amplifiers, used in the usual radio relay equipment and in the equipment for multiplexing. Are utilized the amplifiers, assembled both on the tubes and on the transistors. Group amplifier must provide the amplification of the signals of group frequencies to the assigned value, which corresponds to coupling levels with the equipment for multiplexing, and also compensate losses in the elements of group channel and the coupling lines. Amplifier must provide identical amplification in the band of frequencies of the group circuit with the output stability of overall line attenuation and minimum nonlinear distortions. For fulfilling of these requirements in the group amplifiers is applied negative feedback. The ducts of predistortions KPN-1 and KNP 2 are fulfilled in accordance with the recommendations of MKKR. In Fig. 5.52 are given their frequency characteristics. Ducts are designed so that on the thermal noises they give gain for the upper channel in 4 dB.

In the systems of the tropospheric lines of communications lower official channel usually is intended for the communication between the adjacent stations.

Page 209.

High-frequency official channel in the group spectrum occupies the band of higher than the service band of channels, and on the quality it is considerably higher than the low-frequency official channel and therefore it is utilized for the communication along the entire line. The formation of this channel is realized somewhat by a simpler method than channeling in the equipment for multiplexing. For the transmission of signals in the upper official channel is utilized the method of the amplitude modulation of carrier high-frequency oscillations with the isolation of one lateral frequency band. Single-band transmission is realized by a method of two-phase modulation [5.30] of the carrying oscillations in the so-called phase-difference diagram in Fig. 5.53a.

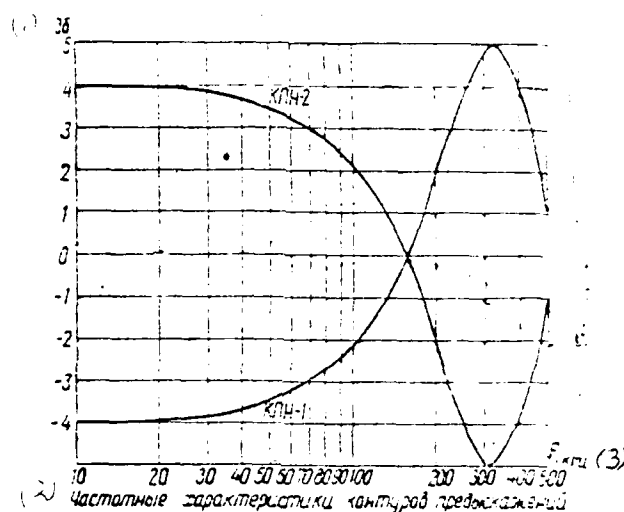


Fig. 5.52. Frequency characteristics of the ducts of predistortions.

Key: (1). dB. (2). Frequency characteristics of ducts of predistortions. (3)  $K_{PH-2}$ .

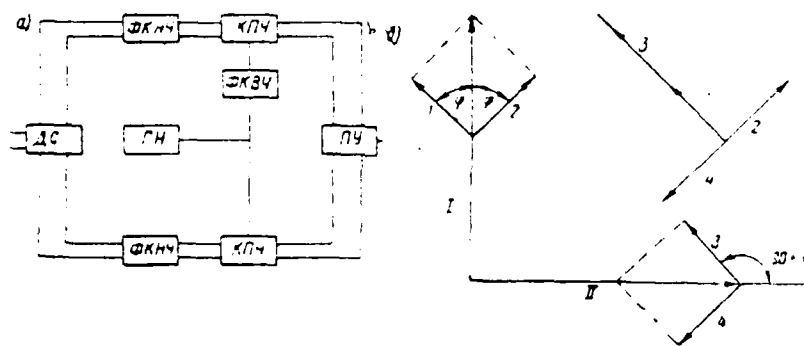


Fig. 5.53. Block diagram (a) and vector diagram (b) of phase-difference modulation.

Page 210.

Diagram consists of two branches, united with the aid of the adapters into one system which fulfills two functions: 1) converts audio signals into the signals of high frequency on the side of transmission and, on the contrary, the signals of high frequency - into the signals of low frequency on the side of reception; 2) isolate one sideband, suppressing in this case the second sideband, which is formed in the process of conversion, and the carrier frequency.

Diagram works as follows. The phase-shifting circuits of low frequency PKNCh provide shift by  $90^\circ$  for any frequency in the band of operating frequencies at output of one relative to the output of another. Two circular frequency converters KFCCh utilize a voltage from one source of the carrying oscillations, but with phase shift on  $90^\circ$ . The rotation of phase is realized in one of the branches with the aid of the phase circuit of high frequency PKVCh. To the low-frequency input of diagram is supplied the signal of tone frequency, which in the differential system DS is divided into two equal in magnitude parts. In each branch the signal obtains phase

shift and undergoes high-frequency conversion. As a result at the output of each branch are obtained two side frequencies, arranged symmetrically relative to the carrier frequency. Outputs of both branches are united with the aid of the adapter PU, forming the twin-lead high-frequency output of diagram. At the output of phase-difference diagram side frequencies of both branches are summarized. In this case as a result of phase shifts in the branches of diagram by  $90^\circ$  in the low and high current frequencies the passed side frequencies coincide in the phase and add up, whereas the currents of the delayed side frequencies, shifted relative to each other on  $180^\circ$ , are eliminated. Fig. 5.53k gives the vector performance record of phase-difference diagram. Vectors I and II depict the oscillations of the carrier frequency: 1.2, and 3.4 - vectors of side frequencies. At the output of diagram the vectors of side frequencies add up in accordance with the vector diagram. Vectors 1 and 3 add up, and 2 and 4 whose phases differ by  $180^\circ$ , are eliminated. The carrier frequency in the phase-difference diagram is suppressed. Degree of the suppression of lateral ones - 2.5 Np in the circular frequency converter. Analogously phase-difference diagram works on the side of reception, in this case in the diagram is conducted rephasing of one of the branches on  $180^\circ$ .

For supplying the signals of upper official channel into the group circuit to the diagram it is added by UVCh, voltage from output

of which is supplied to the matching device, and then to the modulator. On the side of reception between the output of group amplifier and the phase-difference diagram also is switched on the high-frequency amplifier.

For the inspection of fundamental qualitative indices of the communication channels: overall line attenuation of group circuit and noise level in the channels in the the group circuit-provides for two monitoring channels on the edges of the line spectrum of frequencies.

Page 211.

From of the transmitting part into the line are supplied with fixed level the currents of pilot frequencies. At receiving end in the group circuit are installed the special receivers of the monitoring channels in which is made level measurement of the currents of pilot frequencies, for the control of the stability of the amplification of group circuit and level measurement of the psychometric power of thermal and transient noises, led to the point with the zero relative level. Monitoring channel (Fig. 5.54) from the line spectrum of frequencies is isolated with the aid of input band-pass filter PF and it is amplified by high-frequency amplifier UVCh. Filter and amplifier are tuned respectively for the frequency of upper or lower monitoring channel. Pilot frequency is detected by detector DKCh and

on the constant component of detector according to the instrument IKCh they judge the stability of overall line attenuation. To the output of amplifier for the isolation of noise is connected the detector DSh with the low-pass filter FNCh. Receiver circuit of monitoring channels in the part of the isolation of noises is constructed according to the usual principle of the reception of the amplitude-modulated signals. Width of band of check receiver is equivalent to the band of telephone channel. Noises after filter are amplified by low-frequency amplifier UNCh, are detected D and they are measured by instrument RSh. Monitoring channels are utilized also for determining the transient noises in the group circuit of line independent of equipment for multiplexing [5.4]. For this real multichannel signal is replaced by test signal with the uniform spectrum - "white noise". The frequency spectrum of test signal is equal to the frequency spectrum multichannel communication. Energy of white noise directly does not fall into the monitoring channels, since they are located above and below this spectrum, into the channels fall the products, which appear as a result of the nonlinearity of the characteristic of circuit. The power level of test signal must exceed the measuring level of one channel for 24 channels on 4.5 dB, for 60 channels - on 6.1 dB, for 120 channels - on 7.3 dB.

For the creation of test signal in the equipment is provided for the generator of "white noise" with the filters, which cut from the uniform noise spectrum of the regions, which correspond to the line spectrum of different seal systems.



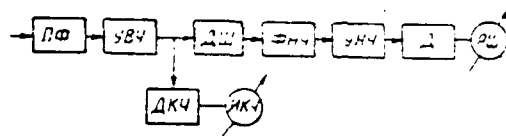


Fig. 5.54. Block diagram of the receiver of monitoring channels.

Page 212.

### §5.13. Equipment of electric power supply.

In the absence of external reliable electric systems it is necessary to resort to the creation of self-contained power plants for each point. All the equipment is distributed in such a way that the half high-frequency shaft, or as is accepted to speak - one subassembly, works from one electric power source, the second subassembly - from the second source. During the malfunction of one source the efficiency of station is retained, but qualitative indices deteriorate - instead of the quadrupled reception there remains only doubled. Table 5.1 gives the diagrams of the possible combinations of different electric power sources with the equipment for the transit exchange of tropospheric radio relay line to different number of shafts and different power of transmitters. In this diagram DGA-20M - diesel-generator installation with the flywheel to power 20 kVA, DGA-48 and DGA-75 - installation on 48 kVA and 75 kVA. DG - slow

diesel generator.

At the stations find wide application the automated diesel-generator installations and converters with the inertial flywheel with the remote control. With the emergency into the work is started another installation and is given signal about the need for repair personnel's call. Operation of station with the impaired indices occurs for a period of time, necessary for starting emergency service.

Receiver for the quadrupled reception requires for the feed the power of the order of several kilowatts. Much energy departs to the feed of television equipment, apparatus for multiplexing or isolation, monitoring and measuring equipment, for the cooling, heating, ventilation, and also to the personal needs of personnel, who operates station and, etc. The power, necessary for the feed of one station, can oscillate from 60 to 200 kW.

Page 213.

Table 5.1.

	блочная схема установки	(2) краткая характеристика
1	<p>I сеть — П/КОМ</p> <p>II сеть — П/КОМ</p>	<p>6 число стволов 1-2</p> <p>мощность пер-ка 1-10 кВт (4-8 шт.)</p> <p>30-200 кВт</p>
2	<p>ДГА-20м</p> <p>сеть</p>	<p>1 ствол</p> <p>мощность пер-ка 1 кВт (4 шт.)</p> <p>40 кВт</p>
3	<p>ДГА-48</p> <p>раб. — П/КОМ</p> <p>рез. — П/КОМ</p> <p>раб. — П/КОМ</p> <p>рез. — П/КОМ</p>	<p>1 ствол</p> <p>мощность пер-ка 3 кВт (4 шт.)</p> <p>96 кВт</p>
4	<p>ДГА-75</p> <p>раб. — П/КОМ I ствол</p> <p>рез. — П/КОМ I ствол</p> <p>раб. — П/КОМ I ствол</p> <p>рез. — П/КОМ II ствол</p>	<p>2 ствола</p> <p>мощность пер-ка 3 кВт (8 шт.)</p> <p>150 кВт</p>
5	<p>ДГА-75</p> <p>раб. — П/КОМ</p> <p>рез. — П/КОМ</p> <p>раб. — П/КОМ</p> <p>рез. — П/КОМ</p>	<p>1 ствол</p> <p>мощность пер-ка 10 кВт (4 шт.)</p> <p>150 кВт</p>
6	<p>ДГА-20м</p> <p>ДГ</p>	<p>1 ствол</p> <p>мощность пер-ка 1 кВт (4 шт.)</p> <p>30 кВт</p>

Key: (1). Block diagram of installation. (2). Short characteristic. (3). network. (4). switch/commutator. (5). Number of shafts - 1-2; power of transmitter. (6). kw. (7). pcs. (8). shaft; power of transmitter. (9). Main. (10). Backup. (11). shaft.

Page 214.

§5.14. Fundamental given and block diagram of six-ten-channel tropospheric radio relay equipment.

As an example of the construction of the system of tropospheric radio relay communication let us examine fundamental data and block diagram of one of the types of Soviet equipment.

Operational frequencies band - 800-1000 MHz. Capacity of high-frequency shaft - 60 telephone channels. For the repeated reception is utilized the system of the quadrupled reception with the diversity of signals in the space and in the frequency. System of addition - combined: the doubled reception with the addition in the intermediate frequency and the quadrupled reception with the addition in the group frequency. System is relied on the fulfillment of the recommendations of MKKR to qualitative indices of telephone channels for the line with a length of 2500 km. For organizing the link

between operators in the equipment are provided two official channels. Antenna is made in the form of the segment of the paraboloid of revolution, irradiated from the point of focus by single horn feed.

Antenna gain in the free space: 44 dB for the mirror with dimensions of 20x20 m, 48 dB for the mirror with dimensions of 30x30 m. Power of transmitter - 3 kW.

Noise temperature of receiver with the parametric amplifier at the input - 300°K.

Modulation - is frequency.

Effective value of the deviation of frequency on the measuring level of one channel - 100 kHz.

Bandwidth of the frequencies of the receiver and transmitter - 6 MHz.

Is utilized crystal control.

Equipment for multiplexing - K-60. Band of frequencies of the group circuit - 12-252 kHz.

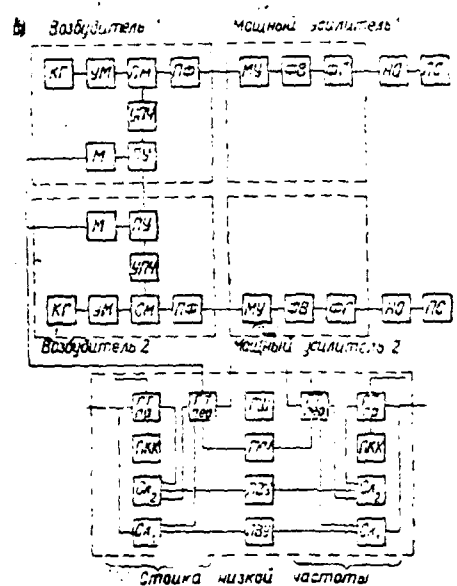
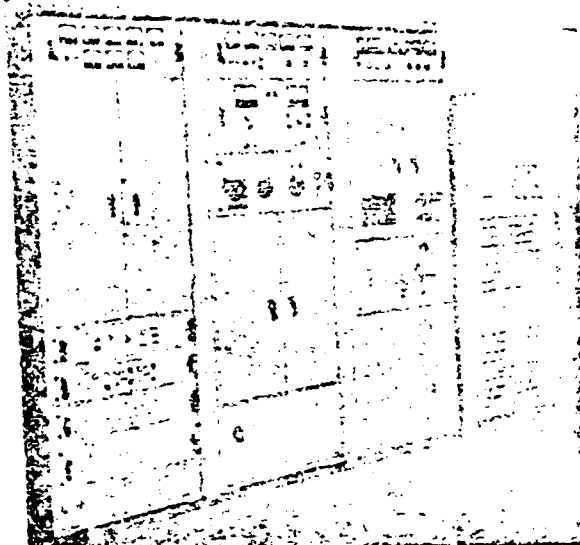
Input and output resistance of group circuit - 135 ohms.  
Measuring level of one channel - 0.55 Np.

The feed of equipment is conducted from the automated diesel-generator installations of the type DGA-48.

Fig. 5.55 gives general view and block diagram of transmitter. For the connection of the transmitting and receivers with the equipment for multiplexing and for the introduction to the group circuit of official channels and pilot frequencies in the assembly of equipment is provided the special stand of low frequency. The signals multichannel communication from equipment for multiplexing come, the strut of low frequency to the elements of the group circuit of transmission  $PT_{\text{low}}$  of the corresponding direction. In the group circuit of transmission, as it was shown earlier, are installed the matching extenders, the circuits of predistortions, etc. From the strut of low signal frequency multichannel communication, united with the signals of official channels and pilot frequencies, are supplied on modulator M of two drivers which with the work are connected with one of the modulators, by the second it is stand-by. Switching is realized by switching system FU. The frequency-modulated oscillations from switching systems are supplied on UFCh, and then to the mixers

OM, which come the oscillations from multipliers MG, excitable from the crystal oscillators KG. After band-pass filter FF the high-frequency oscillations are supplied to the input of powerful amplifier MU. On the given block diagram are given only the fundamental nodes of equipment. After powerful amplifier klystron is installed ferrite gate FV, filter of harmonics FG and directional coupler NO. To the directional coupler is connected the monitor for checking the parameters of transmitter. High-frequency energy from the output of transmitter on the waveguide is supplied to the horn antenna feeder. Each transmitter works on its antenna.

a)



Key: (1). Driver. (2). Powerful amplifier. (3). Strut of low frequency.



Page 216.

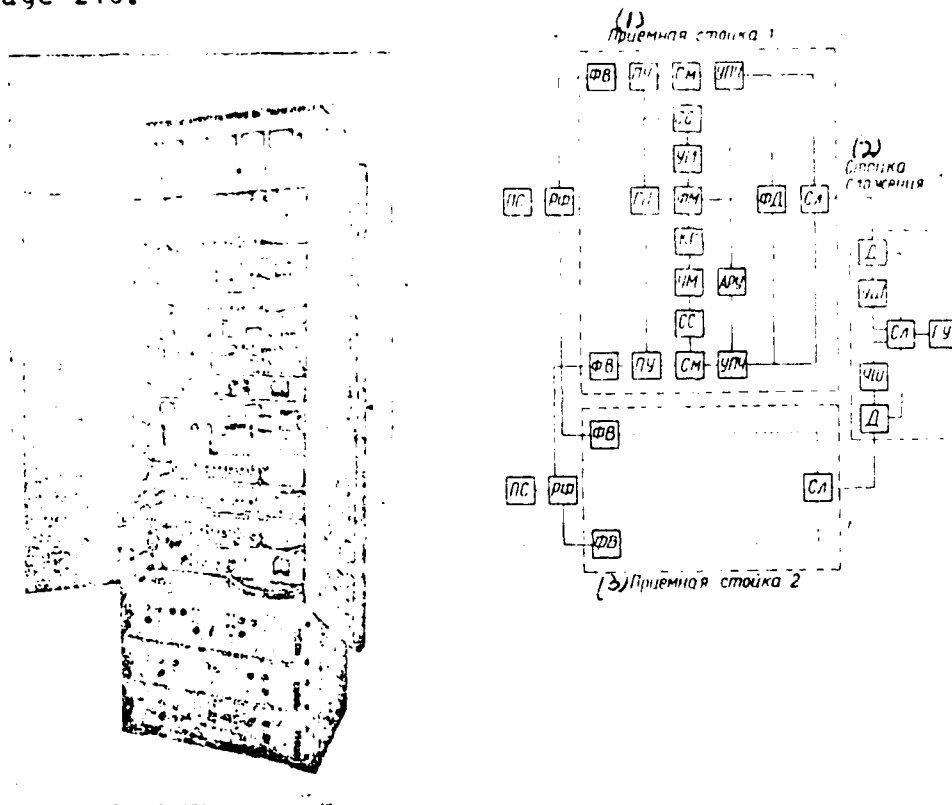


Fig. 5.56. Receiving strut and system block diagram of quadrupled reception.

Key: (1). Receiving stand. (2). Stand of addition. (3). Receiving stand.

Page 217.

The separation of transmission and reception is realized by the use of different polarization in the antenna feeder. Waveguides from the transmitter and the receiver are connected to the common irradiator through the polarizational selector PS. The system of the quadrupled reception consists their three struts: two struts of the doubled reception (Fig. 5.56) with the addition of the signals in the intermediate frequency and of the strut of addition for quadrupling in the low frequency of the in pairs folded signals. In each receiving strut both input parts are inclined for one operating frequency. From one receiving antenna the signals accepted are supplied through separation filter RF, which divides the signals of two frequencies, to two receivers, located in different stands; from another antenna - to two another receivers. High-frequency oscillations from separation filters through the ferrite gate FV are supplied to the parametric amplifier-converter FU, where they are amplified, and also they are converted into the oscillations of intermediate frequency. For both parametric amplifiers of one strut is utilized the common generator of pumping GF. The conditions of linear addition in each strut is provided by parallel automatic gain control - ARU. For the tuning of the phases of the added up vibrations is utilized the phase discriminator FD, connected with the outputs both UPCh, and the phase modulator FM, connected between the crystal oscillator KG and one of the multipliers UM. Folded in the stages of addition ~~6~~ signals from the struts of the doubled

reception are supplied to two demodulators D of the stand of addition, in which the addition is realized in the low frequency in the stage, which consists of two cathode followers with the total load. Control of the arms of cathode follower is realized by amplifiers of noise USt. The folded in the low signal frequency through the group amplifier GU are supplied the group circuit of reception  $\Gamma_V$  of the strut of low frequency, and then enter the terminal equipment for multiplexing.

The isolation of monitoring channels is conducted in the receivers of the monitoring channels of the strut of the low frequency, in which also are isolated official channels and are installed the talk-call equipment EVU.

For the inspection of qualitative indices of receiver there is a special meter panel, which imitates transmitter and which consists of the mixer, the heterodyne, the frequency shift key and other accessories. Signals from this strut can be mixed into the receiving circuit through the directional coupler to separation filter or after it.

Page 218.

## REFERENCES

- 5.1. С. Енедзава и Н. Танака. Связь на сверхвысоких частотах. «Связь», 1967.
- 5.2. С. В. Бородин, В. П. Минашин, А. В. Соколов. Радиорелейная связь. Связьиздат, 1960.
- 5.3. И. А. Гусятинский, Г. В. Рыжков, А. С. Немировский. Радиорелейные линии связи «Связь», 1965.
- 5.4. К. Фатма, Ф. Маня. Частотная модуляция в радиорелейных линиях. «Советское радио», 1964.
- 5.5. М. И. Кривошеев. Основы телевизионных и мерений. «Связь», 1964.
- 5.6. Г. З. Айзенберг. Антенны ультракоротких волн. Связьиздат, 1957.
- 5.7. S. P. Morgan. IEEE Trans on Antennas and Propagation, 1964, v. AP-12, № 6, pp. 605.
- 5.8. Сканнирующие антенные системы. Под ред. Г. Т. Маркова и А. Ф. Чаломкина. «Советское радио», 1966.
- 5.9. А. М. Моделль. Фильтры сеч в радиорелейных системах. «Связь», 1967.
- 5.10. А. Л. Микаэлян. Теория и применение ферритов на сверхвысоких частотах. Госэнергоиздат, 1963.
- 5.11. L'onde Electrique, 1960, v. 40, № 394.
- 5.12. А. В. Соколов, И. С. Печерский. Авторское свидетельство № 154962. Панорамное устройство для двохвостного приема, 1962.
- 5.13. В. В. Шахматова, А. А. Ляховкин. Фазовая подстройка частоты. «Связь», 1966.
- 5.14. А. Д. Артым. Некоторые вопросы теории и проектирования систем с фазовой подстройкой. Радиотехника, 1958, т. 13, № 8.
- 5.15. Philips Telecommunication Review, 1962, v. 23, № 4.
- 5.16. И. А. Гусятинский, Л. Я. Кантор, Ю. М. Марголин, И. С. Черняк, В. П. Лушин. Авторское свидетельство № 187097. Пресобразователи частоты, 1965.
- 5.17. Л. Я. Кантор. Методы повышения помехозащищенности приема ЧМ сигналов. «Связь», 1967.
- 5.18. Ю. А. Кацман. Вопросы теории многорезонаторных хлистронов. Связьиздат, 1965.
- 5.19. Л. А. Блекуэлл, К. Л. Консбу. Параметрические усилители на подпрозрачных диодах. «Мир», 1964.
- 5.20. М. С. Шутанко. Малошумящие усилители сеч. Воениздат, 1966.
- 5.21. А. П. Белоусов. Параметрические усилители с диодным конденсатором. Оборонгиз, 1964.
- 5.22. S. M. Verhagen. Minimum noise-setting of transistors. Proc. IEEE, 1966, v. 54, № 1.
- 5.23. Г. Карпатьян. Частотная модуляция. Издательство академии Румынской Народной Республики, 1961.
- 5.24. И. Э. Рыжков. Умножители и делители частоты. «Связь», 1966.
- 5.25. В. Л. Бажов. Порог при частотной модуляции и методы его снижения. «Электросвязь», 1964, № 12.
- 5.26. Р. Трофимов, Б. Дитман. Практическое выполнение и характеристики дедемодулятора ЧМ демодулятора со сжатием частоты. «ТЭРИ», дек. 1962, № 1.
- 5.27. А. С. Немировский. Помехоустойчивость радиосвязи. «Энергия», 1967.
- 5.28. Л. Я. Кантор. О воздействии флуктуационных помех на следящий прием. «Электросвязь», 1965, № 4.
- 5.29. Ю. М. Марголин, Ю. И. Марголин. Авторское свидетельство № 154962, от 10.X.1963 г. Французский патент № 1470773. Приемник с частотной подстройкой. 1963.
- 5.30. И. А. Черняк. Однополосная модуляция с помощью. «Связь», 1969.
- 5.31. Справочник по электросвязи. Электроустановки.

Page 219.

Chapter 6.

CALCULATION OF LINES DTR DURING THE TRANSMISSION MULTICHANNEL  
TELEPHONY AND BINARY INFORMATION.

§6.1. Introduction. Norms to the channel for the lines DTR.

The communication channel must ensure the transmission of communications from the transmitter to the recipient with the assigned magnitude of reliability and distortions. The reliability of the communication channel quantitatively can be determined by the ratio of the time of the exact work of communication  $t_n$  to entire operating time of line  $T_n$ :

$$H = \frac{t_n}{T_n} = \frac{T_n - t_d}{T_n}, \quad (6.1)$$

where  $t_n$  - total time of the breaks of communication independent of reasons, its caused. On usual type radio relay lines reliability in essence it is determined by breakdowns of equipment on the points for line and with the appropriate redundancy it can be made as to close one as desired to the unit. On the radio relay lines of DTR the

breaks in the transmission of information are possible even during the ideal functioning of equipment. These breaks depend on the random fluctuations of signal level at the point of reception as a result of the rapid and slow fadings. With the drop in the signal at the input of receiver in lower than certain value  $u_{\text{nop}}$  in the communicating system will begin the threshold of the isolation of communication and the transmission of information will be discontinued. Since the probability of this event even during the use of the diverse reception is not equal to zero, on the lines of DTR the reliability of connection in principle cannot be equal to unit. The calculation of the reliability of the channel of communication of DTR, determined by radiowave propagation, is performed in §6.2. The calculation of equipment reliability here is not examined, since it in no way differs from the appropriate calculations of any radio-electronic equipment<sup>1</sup>.

FOOTNOTE <sup>1</sup>. The calculation of equipment reliability is in detail described in [6.1]. ENDFOOTNOTE.

Page 220.

The second most important parameter of channel is the value of distortions which is determined by the transmission characteristics of the communication channel and by the ratio of signal to the

output of hypothetical standard circuit can be exceeded not more than into 0.05% of time. With a sufficient degree of accuracy we will consider that  $P_{\text{un}} \gg 1,000,000$  pb appear at the output of one section of line of DTR only if the value of signals at the inputs of all diverse receivers of one station falls below the threshold of improvement in ChM, which is impossible, since the probability of the simultaneous drop in the signals of lower than the threshold in two different sections of line is vanishingly small. Under these conditions the probability of the drop in all diverse signals of lower than the threshold of ChM in one section of line must not be more

$$\left( \frac{t_n}{t_n} \right)_{\text{yn}} \leq \frac{0.05\%}{m} \quad (6.2)$$

the time of unfavorable month. Consequently, the reliability of the operation of section must be equal to

$$H_{\text{yn}} = \left[ 100 - \frac{0.05}{m} \right] \%.$$

Such high requirements for the reliability are one of causes of use on the lines of DTR of the quadrupled reception.

Let us determine the reserve of the energy potential of line, necessary for the satisfaction of requirements for the reliability, i.e. let us determine the value of the required excess median value of signal for the used above the threshold value of signal.

Page 223.

The power of signal at the input of receiver  $P_{\text{свх}}$  is equal to:

$$P_{\text{свх}} = \frac{P_{\text{пт}} G_{\Sigma}}{A_{\Sigma}}, \quad (6.3)$$

where  $G_{\Sigma} = \frac{G_{\text{пт}} G_{\text{пр}}}{\epsilon_{\text{yc}}}$ ,  $\epsilon_{\text{yc}}$  - losses of antenna gain,  $P_{\text{пт}}$  - power at the output of transmitter,

$G_{\Sigma}$  - the amplification of two antennas taking into account the losses,

$A_{\Sigma}$  - total attenuation between the output of transmitter and the input of the receiver:

$$A_{\Sigma} = A_{\phi} A_{\text{св пр}} \overline{A} A_{\text{м}} A_{\text{р}}. \quad (6.4)$$

In formula (6.4):

$A_{\phi}$  - loss in the receiving and transmitting feeders,

$A_{\text{св пр}}$  - free-space attenuation:

$$A_{\text{св пр}} = \left( \frac{4\pi d}{\lambda} \right)^2,$$

$\overline{A} = \sqrt{2}$  - the rms value of the attenuation factor of signal relative to the field of free space in the worse month,

$A_{\text{м}}$  - the weakening, caused by slow fadings,

$A_{\text{р}}$  - the weakening, caused by rapid fadings.



interference at the output of channel. During the transmission of telephone conversations the fundamental electrical characteristics of channel which are normalized by the recommendations of MKKR and MKKT, they are defined by both the terminal equipment for multiplexing (channel-forming equipment) and by circuit of radio relay line, switching on equipment for terminal and transit exchanges. For ChM and frequency division multiplex of channels (the most widely used method of transmission in the lines of DTR) the separate characteristics of telephone channel are determined only by equipment for multiplexing (amplitude and frequency characteristics, nonlinearity, change of the group time in the band of telephone channel, disagreement of frequencies, etc.). These characteristics subsequently are not examined.

Interest are of the electrical characteristics which influences the circuit of lines of DTR. They include the stability of overall line attenuation, thermal and transient noises.

The recommendations of MKKR and MKKT relate to the hypothetical standard circuit with a length of 2500 km, which has the specific number of transformations of signal. For the line of DTR hypothetical standard circuit takes the form Fig. 6.1 [6.2]. It switches on 3 assemblies of individual converters (channel modulators and demodulators), 6 assemblies of the converters of primary groups

(modulators and demodulators of 12-channel groups) and 9 assemblies of the converters of secondary groups (modulators and demodulators of 60-channel groups). In this case, in contrast to usual RRL, it is not marked off in the identical sections, since the length of the sections of lines of DTE in depending on specific conditions varies from 100 to 400 km and more. Based on this, MRRF recommends to consider that at the average length of one section, equal to  $L$ , the standard circuit has  $2500/L$  sections.

Since on the lines of DTE of propagation condition it is considerably more complicated than to their ordinary RRL, the fulfillment of the norms of MRRF to the noises in the communication channels for the lines of DTE involves considerable difficulties and can lead to the sharp rise in price of communicating system.

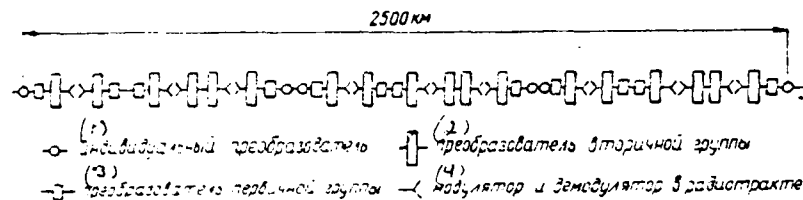


Fig. 6.1. Hypothetical standard circuit for the telephone line of LTR with the frequency division multiplex.

Key: (1). individual converter. (2). converter of secondary group. (3). converter of primary group. (4). modulator and demodulator in radio channel.

Page 221.

Taking into account this, MKEB recommended [6.3] for the tropospheric lines, usually run in the almost inaccessible and sparsely populated areas, of the following amounts of power capacity of noises at the output of the hypothetical standard circuit with a length of 2500 km (in telephone channel, at the point of zero relative level):

1) the average-minute psychometric power of noise must not exceed <sup>25,000</sup>~~2500~~ pW during more than 20% of time of any month;

2) the average-minute psychometric power of noise must not

exceed 63000 pW during more than 0.50/o of time of any month;

3) the unweighted power of noise (with the time of integration 5 ms) can exceed 1,000,000 pW not more than 0.05c/c of time of most unfavorable month.

It is necessary to keep in mind that these recommendations consider only the radio channel of the line; the noises of equipment for frequency division multiplex are not taken into consideration and must comprise not more than 2500 pW in any hctt. The oscillations of overall line attenuation (or amplification) must not exceed  $\pm 0.2$  Np. In §4.3 it is shown that in the circuit of lines of DTR this norm is made. During the transmission of binary information in the channel of communication of line of DTS fundamental characteristic is the magnitude of losses of authenticity. Numerically it is determined by the relation of a number of incorrectly taken pulses for a total number of pulse transmissions.

The calculation of the line of communications in depending on need can it is reduced either to the determination of such parameters of equipment which on the given one to route will accomplish of the recommendations of MKKE and MKKTI to the communication channel or to the determination of such intervals between the adjacent relay stations in which the equipment with the assigned parameters will

accomplish of these norms. Usually the calculation of line begins from the selection of the energy parameters of equipment (power of transmitter, the coefficient of receiver noise, amplification and antenna radiation pattern), on the basis of the technical capabilities of contemporary technology and economic considerations on the value of fundamental initial costs of line and expenditures on the operation. Further is selected the approximate length of section, on the basis of the need for the fulfillment of norm to the reliability of communication, and then they perform the calculation of noises in telephone channel at the output of one section and entire line. Not all sections of line are identical, since they depend on specific conditions (area relief, joining to the populated areas, etc.). For the more precision determination of the noise level at the output of line in this case one should find them on the output of each section, and then summarize. Are usually during the layout assigned the locations of terminal and transit exchanges with the isolation of the part (or of all) channels. The arrangement of intermediate points is conducted on the base of the technical considerations of the guarantee of stable and qualitative communications and convenience in the operation of line. In this case it is necessary to keep in mind which level in correspondent's direction is desirable to have covered.

Page 222.

Closing the level in all by 10' corresponds to a three hundred kilometer route to an increase in effective length of section on 30 km. Consequently, points of line it is desirable to place at the points of dominating feature. (This it is checked with the tracing of the profile of route).

If the line of communications does not satisfy the recommendations of MKKF because of any section, either they divide by two or place intermediate points more evenly. The more evenly distributed the sections of line, the better will be noise distribution at the output of line.

§6.2. Calculation of the reliability of line ITF during the transmission of telephone signals.

As a result of rapid and slow fadings at the separate moments of time the signal falls below any, preassigned value. Let us accept the following assumptions: the line of communications, which consists of  $n$  sections, is considered cut-of-order, if the power of noises in the channel at the output of line exceeds 1,000,000 pW.

According to the norms (see §6.1) this value of noises at the

From formula (6.4) it is evident that signal fading at the point of reception are determined by the product of rapid and slow fadings. Since these fadings are not dependent <sup>1</sup>, the integral distribution of product will be equal

$$W(0 < z \leq Z) = \int_0^z \int_0^{\infty} W(x) W_N\left(\frac{z}{x}\right) \frac{dx dz}{|x|}, \quad (6.5)$$

where to  $W(x)$  - the probability density of slow fadings, determined by the normal logarithmic law

$$W(x) = \frac{1}{\sqrt{2\pi} \sigma_M x} e^{-\frac{(\ln x - \ln x_{med})^2}{2\sigma_M^2}}, \quad (6.6)$$

$W_N\left(\frac{z}{x}\right)$  - the probability density of rapid fadings with the  $N$ -fold diverse reception (see Chapter 2).

FOOTNOTE <sup>1</sup>. In work [6.4] it is shown that as a result of a large difference in the quasi periods of fluctuations the requirement of independence is not compulsory. ENFOOTNOTE.

Analytical computation according to formula (6.5) impractically already with the single receiver. Therefore in [6.5] was produced the graphical integration for the doubled and quadrupled receptions upon the dispersion of slow fadings  $\sigma_M = 6$  dB, and also with the quadrupled reception for  $\sigma_M = 5$  and 4 dB. The results of numerical integration are given in Fig. 6.2, from which it is evident that the transition from doubled to the quadrupled reception improves more

than by an order the probability of a drop in the signals of lower than the threshold of ChM. From the curves of Fig. 6.2 is easy to find the required excess of the median value of the signal above threshold  $\Delta_{0.5}$ .

Page 224.

For example, for the hypothetical standard circuit, which consists of  $n=10$  sections on 250 kHz each, value  $\left(\frac{t_n}{T_n}\right)_{y_{0.5}} = \frac{0.65\%}{10} = 0.005\%$  ( $5 \cdot 10^{-5}$ ) and the required excess with the quadrupled reception will be  $\Delta_{0.5} = 17$  dB ( $\Delta=50$  times).

Thus, it is possible to record

$$P_{cax} = P_{nop} \Delta, \quad (6.7)$$

where  $P_{nop}$  - the threshold value of the power of signal at the input of receiver. It is known that the threshold value of signal ten times exemplarily exceeds the power of the inherent noise of the receiver

$$P_{nop} \approx 10 P_{\Delta ax} = 10 n k T \Delta f_{\Delta}, \quad (6.8)$$

where the coefficient of receiver noise;  $kT=4 \cdot 10^{-21}$  W/Hz;  $\Delta f_{\Delta}$  - the noise bandwidth of receiver.



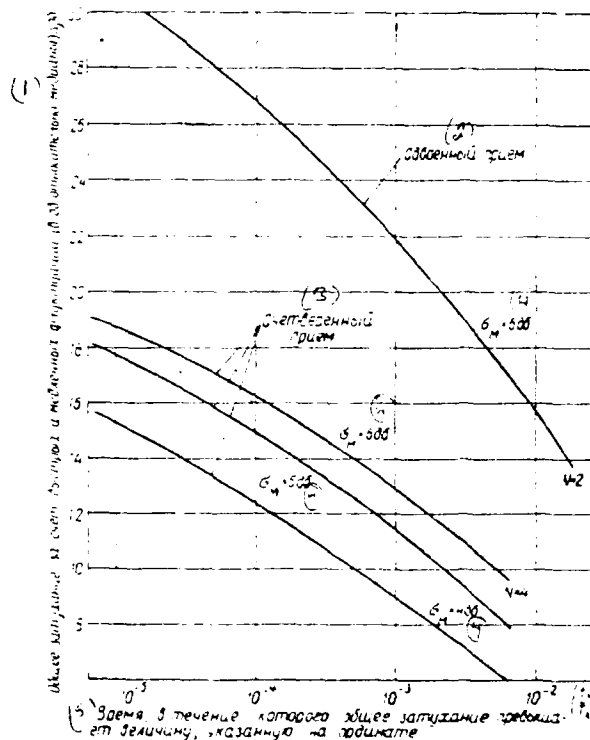


Fig. 6.2. Integral law of the distribution of power of signal taking into account the rapid and slow fading.

Key: (1). Total attenuation due to the rapid and slow fluctuations (in dB relative to median)  $\Delta$ , dB. (2). Doubled reception. (3). Quadrupled reception. (4). dB. (5). Time during which total attenuation exceeds value, indicated on ordinate.

F/0 17/20

**UNCLASSIFIED**

FTD-ID(RS)T-0251-80

NL

6 of 6

AG-

A063445

END

DATE \_\_\_\_\_

FILMED

5-80

DTIC

Page 225.

Usually value  $\Delta f_m$  to 10-20 c/c exceeds the passband of circuit of UPCh  $\Delta f$ , determined from the condition of the undistorted reception of ChM signal with the assigned upper modulating frequency and the deviation<sup>1</sup>.

FOOTNOTE 1. The value of the necessary passband  $\Delta f$  for multichannel ChM systems is determined in [6.6]. ENDFOOTNOTE.

Substituting in (6.7) values  $P_{\text{top}}$  from (6.8) and  $P_{\text{c ax}}$  from (6.3), it is possible taking into account (6.4) to record for the energy potential

$$\frac{P_{\text{пд}} G_{\Sigma}}{n} = 10 \kappa T \Delta f_m A_{\Phi} A_{\text{св пр}} \bar{A} \Delta. \quad (6.9)$$

After replacing the included in formula (6.9) values with the fundamental parameters of equipment and circuit, we will obtain the expression

$$\frac{P_{\text{пд}} G_{\text{пд}} G_{\text{пр}}}{n} = 9,5 \cdot 10^{-12} \frac{d_{(\text{см})}^2 \Delta f_{\text{гнч}} \delta_{\text{yc}} A_{\Phi} \bar{A} \Delta}{\lambda^2 (\text{см})}. \quad (6.9a)$$

This expression makes it possible to select energy the potential of line on the criterion of the reliability of operation. For an increase in the reliability of the work of line or length of interval (with the preservation of reliability) it is possible to utilize one of the methods of an improvement in the threshold properties of ChM receivers.

Frequently is necessary to solve the somewhat different problem:

the energy potential of equipment and the length of the section of line are assigned, necessary determine will be reliable telephone communication. For the solution of this problem from (6.9a) one should determine the value of the obtained reserve of the median signal above the threshold of the receiver

$$\Delta_0 = 0,1 \cdot 10^{12} \frac{P_{\text{пз}} G_{\text{пз}} G_{\text{пр}} \lambda_{\text{сш}}^2}{n d_{\text{сш}}^2 \Delta f_{\text{гпч}} \delta_{\text{yc}} A_{\Phi} A} \quad (6.10)$$

and then compare  $\Delta_0$  with the value of the required reserve  $\Delta$ , determined from the graph of Fig. 6.2 for  $\frac{0,05}{m}$  the time. If value  $\Delta_0 \gg \Delta$ , then the section of line provides the assigned reliability of operation, but if  $\Delta_0 < \Delta$ , then section does not possess the assigned reliability and it is necessary either to change route or to increase the energy potential of line, for example, applying large-size antennas.

§6.3. Calculation of the total power of noises at the output of one section of line DTR.

In Chapter 4 are examined and substantiated the methods of calculation of thermal noises  $P_r$  and transient noises of multiple-pronged origin  $P_n$  at the output of one section of line of DTR. Let us examine the calculation of the total power of noises in the channel at the output of one section of line of DTR:

$$P = P_r + P_n + P_{\text{ант}}, \quad (6.11)$$

where  $P_{\text{ana}}$  - a constant value of the transient interferences, which appear in the equipment and the feeder lines (usually  $P_{\text{ana}}$  must not exceed 10-15% of total power of noises at the output of section).

Page 226.

The probability density of the power of slow changes in the thermal noises at the output of section has normally logarithmic law of the distribution

$$W(P_r) = \frac{1}{\sqrt{2\pi}\beta P_r} e^{-\frac{(\ln P_r - \ln \bar{P}_r)^2}{2\beta^2}}, \quad (6.12)$$

since, in the first place, the same law have the slow fluctuations of signal at the input of receiver and, in the second place, in the subthreshold region the noises at the output of the FM discriminator are inversely proportional to signal at the input of the receiver;

$$\beta = \frac{\sigma_{\ln(P_r)}}{4.34} \quad (6.13)$$

- the standard deviation of value  $\ln P_r$ . The parameters of the law of probability distribution for the power of thermal noises are such:

the median value

$$P_{r\text{med}} = e^{\ln \bar{P}_r}, \quad (6.14)$$

the average/mean value

$$\bar{P}_r = \int_0^\infty P_r W(P_r) dP_r = e^{\ln \bar{P}_r + \frac{\beta^2}{2}} = P_{r\text{med}} \cdot e^{\frac{\beta^2}{2}}, \quad (6.15)$$

the dispersion

$$D(P_r) = \int_0^\infty (P_r - \bar{P}_r)^2 W(P_r) dP_r = P_{r\text{med}}^2 e^{\beta^2} (e^{\beta^2} - 1). \quad (6.16)$$

Let us find the probability density of slow changes in the power of transient noises. formula for calculating the transient interferences is derived in Chapter 4 (see 4.50). The slowly changing value is here an equivalent radius of Earth  $a_e$ .

Page 227.

It is possible to record

$$P_n = \frac{l}{a_e^4}, \quad (6.17)$$

where

$$a_e = \frac{a_0}{1 + \frac{a_0}{2} g}, \quad (6.18)$$

$a_0$  - real radius of the Earth, equal to 6370 km,

$g$  - refractivity gradient, which is determining the slow fluctuations of the power of transient interferences. It is experimentally shown that  $g$  is subordinated to the normal law of distribution [6.9],

$l$  - the coefficient, determined from formula (4.50):

$$l = \frac{2 \Delta F_n \kappa_n^2}{\Delta F} (2\pi \Delta f)^2 (2\pi F_n)^2 y_2(z) \frac{z_0^4 \Delta^2}{c^4} \bar{p}_2^2.$$

Knowing the law of distribution  $g$ , it is simple to find the law of distribution  $P_n$ :

$$W(P_n) = \frac{1}{4 \sqrt{2\pi} \sqrt{P_n^3} \delta} \left\{ e^{-\frac{(\sqrt[4]{P_n} - \sqrt[4]{\bar{P}_n})^2}{2\delta^2}} + e^{-\frac{(\sqrt[4]{P_n} + \sqrt[4]{\bar{P}_n})^2}{2\delta^2}} \right\}. \quad (6.19)$$

Here

$$\tilde{P}_n = \frac{l}{a_0^2} \left( 1 + \frac{a_0}{2} \bar{g} \right)^4, \quad (6.20)$$

$\bar{g}$  - mean value of the slow fluctuations of the refractivity gradient,

$$\delta = \frac{\sqrt{T}}{2} \delta_g, \quad (6.21)$$

$\delta_g$  - the dispersion of the slow fluctuations  $g$ . The parameters of law (6.19) are such:

the mean value

$$\bar{P}_n = \tilde{P}_n [1 + 6q + 3q^2], \quad (6.22)$$

the dispersion

$$D\{P_n\} = \tilde{P}_n^2 8(8q + 21q^2 + 48q^3 + 12q^4), \quad (6.23)$$

where

$$q = \left[ \frac{\frac{a_0}{2} \delta_g}{1 + \frac{a_0}{2} \bar{g}} \right]^2. \quad (6.24)$$

Thus, for the determination of the slow fluctuations of the total power of noises at the output of cre section it is necessary to find the law of the distribution of sum (6.11), in which distribution  $P_r$  is determined by formula (6.12),  $P_n$  - by formula (6.19), and  $P_{ann}$  - constantly. In this case it is necessary to keep in mind that slow

fluctuations  $P_{Ti}$  and  $P_{ni}$  are dependent.

Page 228.

In [6.7] on the basis of experimental investigations it is shown that the correlation coefficient between slow changes in the transient noises and thermal noises  $R-\rho=0.7$ . This, apparently it is explained by the fact that also on the fluctuation of the power of thermal noises is substantial the effect of the fluctuation of value  $g$ . Taking this into account the parameters of the law of the distribution of the total power of noises at the output of section will be equal to:

the mean value

$$\bar{P} = \bar{P}_T + \bar{P}_n + P_{ann}, \quad (6.25)$$

the dispersion

$$D\{P\} = D\{P_T\} + D\{P_n\} + 2\rho \sqrt{D\{P_T\} D\{P_n\}}. \quad (6.26)$$

The analytical determination of the form of the law of distribution  $P$  runs into the insurmountable mathematical difficulties. However, numerical integration shows that the obtained law of distribution with the error, which does not exceed 1.5 dB, can be approximated by normally logarithmic distribution with the parameters, determined by formulas (6.25) and (6.26):

$$W(P) = \frac{1}{\sqrt{2\pi} P \lambda} e^{-\frac{(\ln P - \ln \bar{P})^2}{2\lambda^2}}. \quad (6.27)$$



Here the parameter  $\lambda$ , which is determining the rms value of value  $\ln P$ , we find through the formula

$$\lambda^2 = \ln \left[ 1 + \frac{D(P)}{\bar{P}^2} \right]. \quad (6.28)$$

The parameters of the law of distribution (6.27) are determined from the formulas, analogous (6.14)-(6.16).

The laws of the distribution of the slow fluctuations of thermal, transient and total noises at the output of one section at different values  $\sigma_n$  are given in Fig. 6.3. All values are calibrated relative to the mean power coefficient of thermal noises. In this case:

The mean value of the total power of noises there will be equally

$$\frac{\bar{P}}{\bar{P}_T} = 1 + x + \frac{P_{\text{ann}}}{\bar{P}_T}, \quad (6.29)$$

the dispersion

$$\frac{D(P)}{\bar{P}_T^2} = [V \overline{e^{x^2} - 1} + x a_1]^2 - 0,6 x a_1 V \overline{e^{x^2} - 1}, \quad (6.30)$$

where

$$x = \frac{\bar{P}_n}{\bar{P}_T}, \quad (6.31)$$

$$a_1 = \frac{V \overline{6(8q + 21q^2 + 48q^3 + 12q^4)}}{1 + 6q + 3q^2}. \quad (6.32)$$

Page 229.

For the plotting of curves of the normally logarithmic law of distribution it is necessary to know:

the median power coefficient of the total noises

$$\frac{P_{med}}{\bar{P}_T} = \frac{(\bar{P}_T + \bar{P}_n)}{\bar{P}_T} e^{-\frac{\lambda^2}{2}}, \quad (6.33)$$

the root-mean-square power coefficient of total noises in the decibels

$$\sigma_2 = 4.34 \lambda, \text{ dB.} \quad (6.34)$$

Adding to the plotted curve in each percentage of time the constant value of the power of the noises of the nonlinear transitions of equipment, that compose  $150/c (\bar{P}_T + \bar{P}_n)$ , we obtain the curves of the law of the distribution of power of total noises at the output of one section.

#### §6.4. Calculation of power of noises at the output of line of DTR.

The parameters of equipment and line of DTR must be selected so that would satisfy the requirements, presented in §6.1 with the minimum economic expenditures. Fulfilling these requirements - very complicated technical problem, therefore, in particular, is importantly correct to distribute the contribution of all elements of the circuit of line of DTR to the noises at the output of line. In Chapter 4 was examined the selection of the optimum deviation of frequency taking into account the minimization of the total power of the thermal and transient noises of multiple-pronged origin.

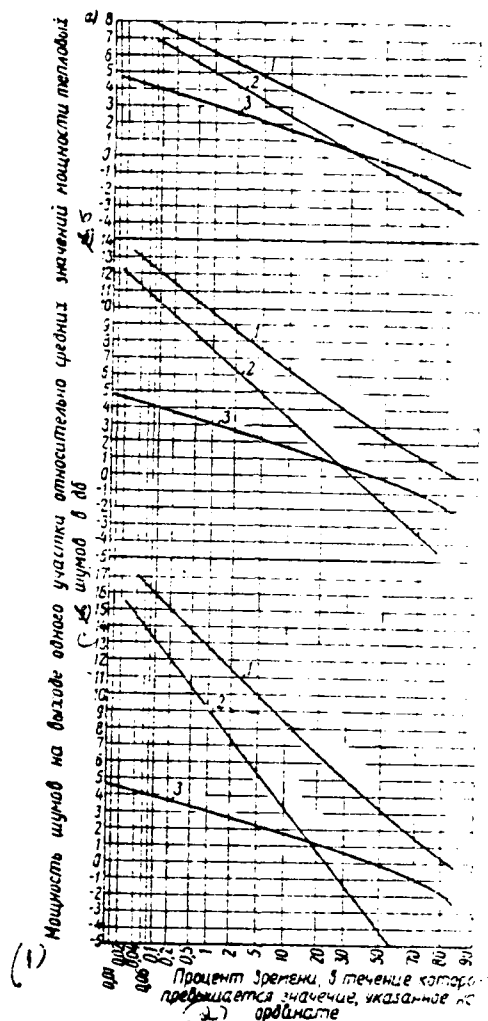


Fig. 6.3. Integral law of the distribution of power of thermal (2), transient (3), total (1) noises at the output of one section: a) at the length of section  $d=625$  km; б)  $d=500$  km and в)  $d=312.5$  km.

Key: (1). Power of noises at the output of one section relative to the mean power coefficients of thermal noises in dB. (2). Percentage of time, during which is exceeded value, indicated on the ordinate.

DOC = 60025113

486

Page 230.

Let us here examine, in the first place, what portion of the power of noises should be led all elements of equipment circuit and, in the second place,

→ let us design the distribution of power of noises for the output of hypothetical

standard circuit.

The transient noises, which appear in the equipment and the feeder lines, are designed from the formulas and the graphs given, for example, in [6.8] for the usual radio relay lines. In this case it is necessary to keep in mind: 1) at each station line of LTR is conducted demodulation; therefore all stations have the modems; 2) the large power output of transmitters does not make it possible to satisfy feeder lines with the traveling-wave ratios [KBV] close to KBV of the usual radio relay lines; 3) the interferences, determined by the inadequacy of limiter, can be very essential as a result of large parasitic AM, caused multi-beam character of the signal in the place of reception.

The fundamental contribution to the total power of noises at the output of line belongs undoubtedly to thermal noises and transient interferences of multiple-pulsed origin. In their portion should be carried 85-90% of all noises, i.e. 21-22.5 thousand pW at the point of zero relative level. This value can be exceeded not more than 20% of time. Remaining of 2.5-4.0 thousand pW should be tentatively distributed as follows:

- 1) 1000-1500 pW (about 40%) led the noises, caused by reflections in the feeder circuits;

2) 400-800 pW (15-20c/o) - the elements of group circuit and the modems;

3) 600-1000 pW (20-25c/o) - to the interferences, determined by the inadequacy of the limiter; and

4) 500-800 pW (~20c/o) - to elements of VCh circuit.

Let us find the distribution of the total power of thermal noises and noises of the nonlinear transitions of multiple-pronged origin at the output of line of LTF. Let the line have  $n$  sections (for the hypothetical standard circuit  $n=8-10$ ). Then the total power of the noises

$$P_{\Sigma} = \sum_{i=1}^n P_i = \sum_{i=1}^n P_{ti} + \sum_{i=1}^n P_{ni} + \sum_{i=1}^n P_{sni}. \quad (6.35)$$

The distribution  $P_{\Sigma}$  can be found with the aid of its expansion in a series in the orthonormalized functions with weight  $W_0(u)$ , which are the standard law of the distribution:

$$W(u) = W_0(u) [c_0 p_0(u) + c_1 p_1(u) + \dots]. \quad (6.36)$$

Page 231.

Here

$u = \frac{P_z - \bar{P}_z}{\sqrt{D\{P_z\}}}$  - the standardized value;

$$c_n = \sum_{k=0}^n d_{nk} \frac{\mu_k}{\frac{k}{2}};$$

$\mu_k$  - central distributions which can be determined through the central moments of the distribution of power of the total noises of one section, since changes in the power of noises in the sections of line of DTR are not correlated;

$p_n = \sum_{k=0}^n d_{nk} u^k$  - orthonormalized polynomials of the  $n$  degree;

$d_{nk}$  - coefficients, determined with orthonormal of the system of exponential functions  $(1, u, u^2, u^3, \dots)$ .

In our case is more expedient to accept for the standard law of distribution normally logarithmic law with standard deviation

$$\lambda^2 = \ln \left[ \frac{D(P_z)}{\bar{P}_z^2} + 1 \right];$$

$$W_0(u) = \frac{\sqrt{e^{\lambda^2} - 1}}{\sqrt{2\pi\lambda} [u \sqrt{e^{\lambda^2} - 1} + 1]} e^{-\frac{(\ln [u \sqrt{e^{\lambda^2} - 1} + 1] + \frac{\lambda^2}{2})^2}{2\lambda^2}}. \quad (6.37)$$

For low rms values  $\sigma_{u_i}$  and large number of sections for the standard law of distribution it is better to take normal. The made calculations showed that the new law of distribution approaches

standard with accuracy  $\leq 0.02\%$ . Then at the output of line the power of the total noises of ILET [Institute of Metallurgy in. A. A. Baykov] the integral law of the distribution of the form

$$W(P_z \geq \mathcal{P}) = \frac{1}{2} \left[ 1 - \Phi \left( \frac{\ln \frac{\mathcal{P}}{P_z} + \frac{\lambda^2}{2}}{\lambda} \right) \right]. \quad (6.38)$$

Here  $\mathcal{P}$  - power of noises, exceeded in the assigned percentage of time. The laws of the distribution of power of noises for the hypothetical standard circuit with a length of 2500 km, calibrated relative to the mean power of thermal noises at the output of one section, are given in Fig. 6.4.



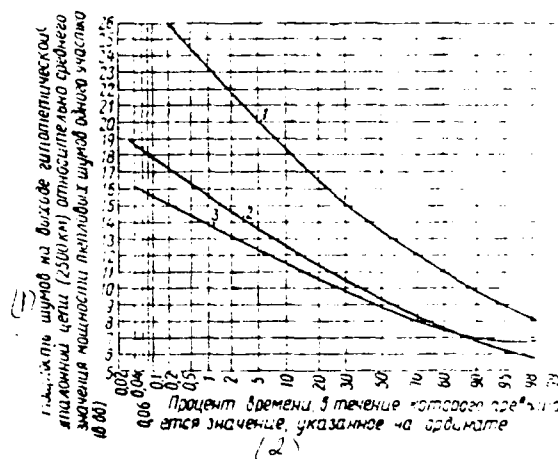


Fig. 6.4. Integral law of the distribution of power of noises at the output of line of DTR.

Key: (1). Power of noises at the output of hypothetical standard circuit (2500 km) relative to the mean power coefficient of the thermal noises of one section (in dB). (2). Percentage of time, during which is exceeded value indicated on ordinate.

Page 232.

Curve 1 corresponds to 6 sections on 312.5 km each ( $\sigma_n = 6$  dB), curve 2-5 to sections on 500 km ( $\sigma_n = 4$  dB) and curve 3-4 to sections on 625 km ( $\sigma_n = 2.5$  dB). On of the curves of Fig. 6.4 it is possible to determine the excess of the power of total noises in telephone channel at the output of the hypothetical standard circuit above the

mean value of thermal noises at the output of one section of line, which corresponds to the calibrated by MKK percentages of time and (20o/o and 0.5o/o). In this case the mean power of thermal noises at the output of one section must be designed according to formula (4.13). Virtually, as has already been spoken above, the sections of line were nonidentical, and therefore more accurately the output power of noises can be determined by its addition in the individual sections.

§6.5. Calculation of the loss of authenticity and reliability during the transmission of binary information along telephone channel of line DTR.

The transmission of digital information along telephone channels is conducted with the aid of the secondary multiplexing of channels by telegraph signals. For this are utilized the special data-transmission systems. The operating principle of such systems is based on the different methods of keying the digital pulses. In this case most frequently are utilized as most shielded from noise, the frequency shift keying and the phase-difference manipulation of different multiplicity (predominantly one- and twofold). Calculation methods examined below are set forth in connection with these methods of data transmission.

During the transmission of digital information along telephone channel with ChM the short duration failures of pulses under the action of thermal noises in the channel occur when signal at the input of receiver falls below the threshold of improvement of ChM. Therefore during the analysis of the loss of authenticity necessary the account of threshold. This means that it is necessary to have the analytical expression of the dependence of signal-to-noise ratio at the output of the FM discriminator in channel  $n_{\text{out}}$  on the signal-to-noise ratio at the input of ChM-receiver  $n_{\text{in}}$ . This dependence is obtained in [6.13], but there its recording is given in the form of formula for the power of noise in telephone channel at the output of the FM discriminator.

Page 233.

Here "threshold" dependence  $n_{\text{out}}$  is given taking into account the fact that by telephone channel are transmitted the digital pulses of the assigned level:

$$f_{n_{\text{out}}} = \frac{\Delta f_{\text{эф}}^2 \cdot P_{\text{сигнал}} \cdot b_{\text{эф}} \cdot 2\pi}{\Delta f_{\text{эф}} \sqrt{\pi} \Delta F_{\text{к}} \left[ 1,85 e^{-n_{\text{in}}} + 2 \left( \frac{F_{\text{к}}}{\Delta f_{\text{эф}}} \right)^2 \left( \frac{1 - e^{-n_{\text{in}}}}{n_{\text{in}}} - e^{-n_{\text{in}}} \right) e^{-\left( \frac{F_{\text{к}}}{\Delta f_{\text{эф}}} \right)^2} \right]}, \quad (6.39)$$

where  $\Delta f_{\text{эф}}$  - effective deviation of frequency to the channel,  $\Delta f_{\text{эф}} \sqrt{\pi}$  - width of band of energy noise spectrum at the input of receiver,  $\Delta F_{\text{к}}$  - width of band of telephone channel,  $P_{\text{сигнал}}$  - the level of useful signal

in the channel,  $b_{up}$  - the coefficient of predistortions in the channel.

Calculation is carried out on the assumption that the information by the channel is transmitted by the frequency or twofold phase-difference manipulation (this, however, it does not decrease the generality of the calculation method).

For these cases work [6.10] gives the dependence of the probability of the error on the signal-to-noise ratio in the channel

$$P_{om}(n_{sux}) = \frac{1}{2} e^{-\frac{n_{sux}}{2}}. \quad (6.40)$$

The corresponding relationship for single FRM takes the form

$$P_{om}(n_{sux}) = \frac{1}{2} e^{-n_{sux}}. \quad (6.40a)$$

Utilizing formula (6.39), it is possible to record (6.40) in the form

$$P_{om}(n_{sx}) = \frac{1}{2} \exp \times \left[ -\frac{1}{2} \frac{\Delta f_{\Phi}^2 P_{sux} \kappa b_{\pi p} 2\pi}{\Delta f_{\Phi} V \pi \Delta F_{\kappa} \left[ 1.85 e^{-n_{sx}} + 2 \left( \frac{F_{\kappa}}{\Delta f_{\Phi}} \right)^2 e^{-\left( \frac{F_{\kappa}}{\Delta f_{\Phi}} \right)^2} \left( \frac{1 - e^{-n_{sx}}}{n_{sx}} - e^{-n_{sx}} \right) \right]} \right] \quad (6.41)$$

Taking into account the rapid Rayleigh fading and dispersed reception with the optimum  $M$ -fold addition the density of distribution of the probabilities of value  $n_{sx}$  is calculated from the formula

$$w_N(n_{sx}) = \frac{n_{sx}^{N-1} e^{-\frac{n_{sx}}{n_0}}}{(N-1)! n_0^N}, \quad (6.42)$$

where  $n_0$  - mean (on the rapid fading) signal-to-noise ratio at the input of one receiver. Let us find mean value  $P_{out, N}$  taking into account distribution (6.48):

$$\begin{aligned} \bar{P}_{out, N} &= \frac{1}{2} \int_0^\infty \exp \times \\ &\times \left[ -\frac{1}{2} \frac{\Delta f_{\Phi}^2 P_{out, N} b_{np} 2\pi}{\Delta f_s \sqrt{\pi} \Delta F_k \left[ 1.85 e^{-n_{ax}} + 2 \left( \frac{F_k}{\Delta f_s} \right)^2 e^{-\left( \frac{F_k}{\Delta f_s} \right)^2} \left( \frac{1 - e^{-n_{ax}}}{n_{ax}} - e^{-n_{ax}} \right) \right]} \right] \times \\ &\times \frac{n_{ax}^{N-1} e^{-\frac{n_{ax}}{n_0}} d n_{ax}}{(N-1)! n_0^N}. \end{aligned} \quad (6.43)$$

Page 234.

For quadrupled reception, most widely used on the lines ETR, we obtain

$$\begin{aligned} P_{out} &= \frac{1}{12 n_0^4} \int_0^\infty \exp \times \\ &\times \left[ -\frac{1}{2} \frac{\Delta f_{\Phi}^2 P_{out, N} b_{np} 2\pi}{\Delta f_s \sqrt{\pi} \Delta F_k \left[ 1.85 e^{-n_{ax}} + 2 \left( \frac{F_k}{\Delta f_s} \right)^2 e^{-\left( \frac{F_k}{\Delta f_s} \right)^2} \left( \frac{1 - e^{-n_{ax}}}{n_{ax}} - e^{-n_{ax}} \right) \right]} \right] \times \\ &\times n_{ax}^3 e^{-\frac{n_{ax}}{n_0}} d n_{ax}. \end{aligned} \quad (6.44)$$

Expression (6.44) can be substantially simplified. For this let us note the following. In (6.44) there is the expression for the energy noise spectrum in the channel at the output of the FM discriminator

$$\frac{G(F_k)}{\pi \Delta f_s \sqrt{\pi}} = 1.85 e^{-n_{ax}} + 2 \left( \frac{F_k}{\Delta f_s} \right)^2 e^{-\left( \frac{F_k}{\Delta f_s} \right)^2} \left( \frac{1 - e^{-n_{ax}}}{n_{ax}} - e^{-n_{ax}} \right). \quad (6.45)$$

Formula (6.45) is more precisely formulating expression for  $\frac{G(F_K)}{2\pi\Delta f_b \sqrt{\pi}}$ , obtained in [6.13], and it is derived in [6.15]. First, from (6.45) it follows that in the region of the signal/noise ratio  $n < 10$  the first term much more than the second. This observation is correct with occurring on the real lines of ratio  $\frac{F_K}{\Delta f_b} < 1$ . In the second place, it is known that on the lines of ETR with the work of higher than the threshold of ChE ( $n > 10$ ) the signal-to-noise ratio  $n_{sx}$  in the channels is very great, and the probability of error is negligibly small. Therefore virtually always in formula (6.45) the second term can be disregarded, i.e.

$$\frac{G(F_K)}{2\pi\Delta f_b \sqrt{\pi}} \approx 1.85 e^{-n_{sx}}. \quad (6.46)$$

In the third, formula (6.44) value  $P_{\text{BMTK}}$  is also function  $n_{sx}$ . In [6.11] it is shown that

$$P_{\text{BMTK}}(n_{sx}) = P_{\text{BMTK пер}} (1 - e^{-n_{sx}})^3, \quad (6.47)$$

where  $P_{\text{BMTK пер}}$  - transmitted level of useful signal.

Let us further note that for the low values of the losses of authenticity, usually necessary for the satisfactory quality of the transmission of binary information ( $P_{\text{om}} \leq 10^{-3}$ ), is made the following equality:

$$e^{-\frac{n_{sx}}{n_0}} \approx 1. \quad (6.48)$$

Page 235.

The error in this simplification does not exceed 30-40%/c. This value of error can be considered completely acceptable, since the calculation of the loss of authenticity is utilized below during the analysis of the reliability of the transmission of digital information along the tropospheric channel. In this case it is shown that the computation of reliability is connected with the determination of certain value of value  $r_0$  which with the error in calculation of the loss of authenticity, equal to 40%/c is estimated with the error in all of 10%/c. This accuracy is commensurated with the accuracy of the experimental estimate of  $r_0$ .

After substituting in (6.44) value  $\frac{G(F_K)}{2\pi\Delta f_b V \pi}$  from (6.46) and  $P_{\text{авт}}$  from (6.47) and after considering (6.48), we will obtain

$$\bar{P}_{\text{авт}} = \frac{1}{12n_0^4} \int_0^\infty \exp\left[-\frac{1}{2} r (1 - e^{-n_{\text{ав}}})^2 e^{n_{\text{ав}}}\right] n_{\text{ав}}^3 dn_{\text{ав}}, \quad (6.49)$$

where

$$r = \frac{\Delta f_{\text{эф}}^2 P_{\text{авт}} \text{ на } b_{\text{нр}} 2\pi}{\Delta f_b V \pi \Delta F_{\text{г}} 1,85}. \quad (6.50)$$

Let us note that expression (6.49) is function  $n_0$ ; therefore with given one  $\bar{P}_{\text{авт}}$  it is possible to determine the appropriate value of  $n_0$  according to the formula:

$$n_0 = \sqrt[4]{\frac{I(r)}{12\bar{P}_{\text{авт}}}}. \quad (6.51)$$

where

$$I(r) = \int_0^{\infty} \exp \left[ -\frac{1}{2} r (1 - e^{-n})^2 e^n \right] n^3 dn. \quad (6.52)$$

Taking into account relationship (6.40a), we find that single FRM  $n_0$  is found from the equality:

$$n_0 = \sqrt[4]{\frac{I(2r)}{12 \bar{P}_{om}}}. \quad (6.51a)$$

Fig. 6.5 depicts the curve of values  $I(r)$ , obtained as a result of numerical integration.

Let us calculate for an example from formulas (6.51) and (6.51a) value  $n_0$  when  $\bar{P}_{om} = 10^{-4}$ ;  $\Delta f_{\text{до}} = 100$  kHz;  $P_{\text{max}} = 0.135$  mW;  $b_{\text{до}} = 2.5$ ;  $\Delta f_{\text{н}} \sqrt{\pi} = 7.5$  MHz;  $\Delta f_{\text{н}} = 3.1$  kHz. In this case we obtain  $r = 0.46$ . We respectively find that  $I(0.46) = 5$  and  $I(0.92) = 1.5$ . Hence with  $I(0.46)$  we obtain  $n_0 = 12$  and with  $I(0.92) = 1.5$  have  $n_0 = 10$ .

Page 236.

Let us use the now presented method of calculation of the losses of authenticity to the analysis of the reliability of the transmission of digital information along the tropospheric channel. Let us define reliability as probability that with the work during the performance of duration  $t$  the transmitter will be realized with



the loss of authenticity, not worse than assigned magnitude  $P_{\text{сш крит}}$ . Let us note that the mean on the rapid fading signal-to-noise ratio at the output of receiver  $r_c$  slowly fades according to the normally logarithmic law and is stationary process. Distribution  $W(y)$  of process  $y$  is written in the form:

$$W(y) = \frac{1}{\sqrt{2\pi}} e^{-\frac{y^2}{2\sigma^2}}, \quad (6.53)$$

where

$$y = 10 \lg \frac{\pi_0 \text{ мед}}{\pi_0}, \quad (6.54)$$

$\pi_0 \text{ мед}$  - the median value  $\pi_0$ , connected with  $\pi_c$  by formula (6.15),  $\sigma$  - standard deviation of value  $y$ .

For assigned magnitude  $\overline{P}_{\text{сш крит}}$  according to formula (6.51) it is necessary to calculate appropriate value  $\pi_0 \text{ крит}$ . Then in our determination reliability proves to be equal to the probability of the fact that with the performance of the work of duration  $t$  is fulfilled the inequality

$$\pi_0 > \pi_0 \text{ крит} \quad (6.55)$$

according to (6.54)

$$y < y_{\text{крит}} = 10 \lg \frac{\pi_0 \text{ мед}}{\pi_0 \text{ крит}}. \quad (6.56)$$

Thus, the determination of reliability can be reduced to the problem about the overshoots of stationary random process. In this case the reliability will be equal to the probability of the fact that during the transmission of information during the performance of duration  $t$  the stationary process  $y$  will not have overshoots for

DOC = 90025113

PAGE 500

level <sup>us</sup> input. It will interest the solution for one special case, when overshoots for this level are the rare and independent events. In work [6.12] it is given the solution for this case.

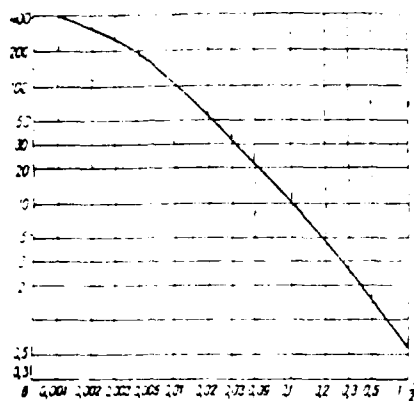


Fig. 6.5. Value of integral.

$$\int_0^{\infty} \exp \left[ -\frac{r}{2} \left( 1 - e^{-a x} \right)^2 e^{a x} \right] \times \\ \times a_{ax}^2 da_{ax}$$

Page 237.

In this case it is noted that the overshoots can be considered rare and independent variables, if an average number of overshoots for time  $t$  is sufficiently small (this is equivalent so that the reliability is close to 1). For the interesting case the probability of the absence of overshoots is determined from formula [6.16]

$$P = \exp \left\{ -\frac{t}{2\pi} \sqrt{-\frac{R''(\tau)}{R(\tau)}} \Big|_{\tau=0} e^{-\frac{R(0)}{2\pi^2}} \right\}. \quad (6.57)$$

where  $R(\tau)$  - the correlation function of process of  $y$ ,  $R''(\tau)$  - second derivative  $y$ . On the basis of experimental investigations it

is obtained that the autocorrelation function of slow fluctuations can be approximated by the following expression:

$$R(\tau) = \frac{1}{3} e^{-\frac{\tau}{30}} \left[ \cos \frac{2\pi\tau}{24} + \frac{24}{2\pi 30} \sin \frac{2\pi\tau}{24} \right] + \frac{2}{3} e^{-\tau} \left[ \cos \frac{2\pi\tau}{24} + \frac{24}{2\pi} \sin \frac{2\pi\tau}{24} \right]. \quad (6.58)$$

Fig. 6.6 gives experimental (2) and approximating (1) curves. After substituting  $R(\tau)$  and its second derivative into formula (6.57), we will obtain that for one section the reliability is equal to

$$P_1 = \exp \left\{ -0.131 e^{-\frac{\tau_{\text{KPH}}^2}{2\pi^2}} \right\}. \quad (6.59)$$

For  $n$  sections

$$P_n = \exp \left\{ -0.131 n e^{-\frac{\tau_{\text{KPH}}^2}{2\pi^2}} \right\}, \quad (6.60)$$

since slow signal fading in the adjacent sections of RRL are independent.

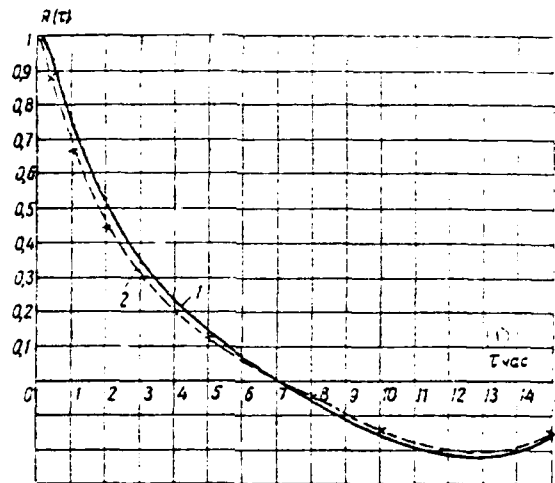


Fig. 6.6. Coefficient of correlation of slow input signal fading.

Key: (1). hour.

Page 238.

Let us produce now according to formula (6.57) the calculation of reliability during the transmission of information with the loss of authenticity not more than  $10^{-4}$ , during the performance of the duration of 11 h when  $\rho_{\text{крит}} = 12$  and  $\rho_{\text{крит}} = 10$  (obtained under conditions of the preceding example) on the section of line DTR. It is assumed that the median value of signal-to-noise ratio  $\rho_{\text{ср}} = 250$  and  $\sigma = 6$  dB. We find that with  $\rho_{\text{крит}} = 12$ ,  $\rho_{\text{крит}} = 18.5$  dB with  $\rho_{\text{крит}} = 10$ ,  $\rho_{\text{крит}} = 20$  dB. According to formula

(6.65) we obtain when  $n_{\text{обл}} = 12$   $P_1 = 0.990$  and when  $n_{\text{обл}} = 11$   $P_1 = 0.994$

## REFERENCES

61. И. Битовский. Надежность. Теория и практика. «Мир», 1965.
62. Документы X Пленарной ассамблеи МККР (Женева, 1963), Том IV, Рек. рекомендация 386.
63. Т. Дже. Рекомендация 397.
64. Лекции по теории систем связи. Под ред. Е. Дж. Багдади. Перевод с англ. «Мир», 1964.
65. А. С. Немировский. К расчету устойчивости многолучевых каналов с учетом быстрых и медленных замираний. Сб. трудов НИИР, вып. I (29), 1963.
66. С. В. Бородин. О необходимой полосе пропускания высокочастотного тракта многоканальных радиорелейных систем. «Электросвязь», 1962, № 7.
67. А. С. Немировский. Экспериментальное определение корреляции медленных изменений тепловых и переходных помех на тропосферных линиях. «Электросвязь», № 5, 1964.
68. И. А. Гусятинский, Е. В. Рыжкова, А. С. Немировский. Радиорелейные линии связи. «Связь», 1965.
69. Коллектив авторов «Дальнее тропосферное распространение ухв» под ред. В. А. Звонковского и др. «Советское радио», 1965.
70. Н. Т. Петровская. Передача бинарной информации в каналах с фазовым искажением. «Советское радио», 1965.
71. М. С. Немировский. Помехоустойчивость радиосвязи «Энергия», 1966.
72. А. А. Савельчиков. Прикладные методы теории случайных функций. «Связь», 1966.
73. Э. Я. Рыжский. О пороговом уровне ЧМ приемника «Электросвязь», № 4, 1963.
74. Лекции по теории систем связи под ред. Е. Дж. Багдади. «Мир», 1964.
75. Э. Я. Рыжский. К вопросу о пороговом уровне ЧМ приемника (в печати).
76. Э. Я. Рыжский. Метод расчета потери достоверности при передаче цифровой информации по каналам тропосферных радиорелейных линий. «Электросвязь», № 5, 1965.

Page 239.

Chapter 7.

Prospects for the development of tropospheric radio relay lines.

§7.1. Introduction.

The first tropospheric radio relay line was constructed in the USA into 1955 and operated in the range of the frequencies of 500-700 MHz with the distance between the adjacent stations approximately 250 km. During the subsequent years was outlined the transition to the more high frequencies (to 5000-6000 MHz). The range of communication as a result of the larger attenuation during the radiowave propagation in this case decreases; however, grows the capacity of communicating system and decrease the distortions of the transmitted information. For the increase the reliability began to utilize the quadrupled reception with the space and frequency diversities, and also reception of higher multiplicity with the angular diversity. Appeared the mobile systems of military radio communication. Is

conducted intense work on the use of lines DTF for the communication of Earth-aircraft and Earth-ship. The development of radio engineering and electronics allowed in recent years to construct the line of tropospheric communications at frequencies of 500-1000 MHz, with the distance between the adjacent stations to 800, and in the separate ones, the favorable ones according to the conditions for radiowave propagation the cases, and to 1000 km. For this it was necessary to create radio transmitting equipment in power to 100 kW, antenna systems whose area approaches 2000 square meters receivers with noise temperature of 70-150°K and special devices which improve threshold properties ChM. Usually width of band of the transmitted signals on the lines of hyperdistant tropospheric propagation (STR) does not exceed 100-200 MHz. This makes it possible to transmit by them 12-24 telephone channels.

Further possible aspect of the use of lines STR is compiling the single-channel lines of distant communication service with the low energy parameters. Calculations show that such lines can be very economical.

Page 240.

Together with an increase in the length of the sections of line the development of the communicating systems, which use DTR, follows



the path of expanding the band of the transmitted signals. This is achieved, in particular, by the use of the narrow-beam antennas; although increases in the energy parameters of equipment barely occurs, since grow the losses of antenna gain, the narrow beam of electromagnetic energy provides small time lags between the separate components of the multiple-pronged signal in the place of reception and, because of this, small distortions. The expansion of transmission band made it possible to transmit along the lines DTR the TV signals along with sonic tracking. There are reports about the use on the lines DTR of impulse coding modulation. For expanding the band of frequencies and decrease of distortions during the use of remote tropospheric propagation of VHF find a use the newest methods of fight with the multi-beam character by the method of using the signals with the wide base<sup>1</sup>.

FOOTNOTE <sup>1</sup>. By signals with the wide base or the composite signals are called such signals which have the product of the frequency band to the duration of one baud much more than 1. ENDFOOTNOTE.

#### §7.2. Hyperdistant tropospheric radio relay lines.

The studies of the propagation of the waves of decimeter range showed the possibility of an increase in the distance between the relay stations of tropospheric lines to 800-1000 km. In this case the

space of scattering is located in the stratosphere. The mechanism of radiowave propagation up to such distances is still insufficiently studied; however, experiments showed that amplitude distribution of signal with the rapid fading also obeys the law of Rayleigh, the distribution of signal with the slow fading is subordinated to normally logarithmic law; however, the dispersion of distribution decreases to 2-2.5 dB. This means that the range of the slow fluctuations of signal is considerably less than on the usual lines ETR; seasonal behavior of attenuation factor also is considerably less than on the usual lines DTR. It turned out that the routes, which pass above sea, are considerably better according to propagation conditions than the route of the same length above the dry land (signal is higher by 10-20 dB). Lines STR approach in the distance between the adjacent sections lines of ionospheric scattering; however, as a result of the considerably larger broad-band character a channel-kilometer of line of hyperdistant tropospheric propagation costs approximately 10 times less than on the lines of ionospheric scattering.

Calculations for the lines STR show that with the reliability of communication, equal to 99.950/c, it is possible to obtain the power of noises in the channel, which does not emerge beyond the limits of the norms of MKKR (with the use of companders, which give 8-10 dB of gain in the average-minute power of noises in telephone channel

[7.1)]<sup>2</sup>.

FOOTNOTE <sup>2</sup>. Companders are switched on in the 4-wire circuit of telephone channel and consist of the compressors, which lower the dynamic range of signal by the transmission, and the expanders, which restore it at the reception. ENDFOOTNOTE.

Page 241.

Further increase in the reliability of line can be obtained by the use of tracking in the frequency. The experiments, described in [7.2], [7.3], showed that with the scanning within the band of frequencies of 150 MHz always can be found the frequency on which path loss will be minimum. Moreover this optimum frequency smoothly is moved within the range 150 MHz, without leaving it. Line STR must have for the tracking a feedback loop, according to which to the transmitting lead is supplied the information about the state of circuit. In accordance with this information, the frequency of transmitter smoothly changes, remaining always at the maximum of the transmission factor of the troposphere. Receiver continuously is adjusted slightly. Gain from the use of this system of tracking is equal to 9-10 dB. However, its use is hindered by the need of using the very broad band.

An increase in the time lag between the components of multiple-pronged signal with STE sharply increases multiplicative interferences and, therefore, besides deterioration in power engineering of reception is caused an increase in the transient interferences with multichannel telephony. During the transmission of digital information the "memory" of channel limits the speed of transmission, since appear the intersymbolic distortions. However, the capacity of multiple-pronged channel falls insignificantly (to 17c/o); moreover, it can be restored by the optimum methods of the transmission of information. All existing methods of fight with the multiplicative interference can be, in the principle, they are divided into the following groups:

1. The method of accumulation, with which are formed several spears of the received signal, differently affected by multiplicative interference. These copies are combined.

2. Method of adaptive reception by which is made continuous or periodic measurement of characteristics of medium of propagation. data of these measurements are utilized for optimization of the selection of signals in the transmission by a method of using of informational feedback and optimum processing of signals at the reception.

3. Method of using of ascending codes and feedback after solutions (postdecision feedback).

The use of one or the other method is determined, on one hand, by the characteristics of the communication channel, and another - by the transmitted information and by the permissible distortions. On multichannel tropospheric RFL widest use found the first method, in detail described in chapter 2. Let us examine here other possible methods in connection with the channel of hyperdistant tropospheric propagation.

Let us recall that the multiple-pronged communication channel can be represented linear filter with the variable parameters, among which necessary for further examination they are: maximum time jitter of delay  $\tau_H$  (width of the multi-beam character or the "memory" of channel), the Doppler expansion of spectrum  $f_D$  (rate of fading).

Page 242.

These parameters are statistical,  $\frac{1}{\tau_H}$  can serve as the measure for the correlation of signal fading at the fixed moment of time  $t_0$  at the different frequencies, and  $\frac{1}{f_D}$  - by measure for the correlation of signal fading in the time at the fixed frequency. Product  $\tau_H f_D$  for the channel DTR much less than 1.

During the transmission of digital information instead of the methods of diversity, presented in chapter 2, are applied the methods, based on the possibility of the separation of the beams in the place of reception. It should be noted that the representation of received signal in the form of the final sum of beams with amplitudes of  $U_i$ , by phases  $\varphi_i$  and by delays  $\tau_i$  will completely agree with the physical nature of propagation only on the short waves. In the channel DTR it is not represented possible to isolate one powerful beam; however, nevertheless the representation of signal in the form of the final sum of beams is competent. If, for example, the band of transmitted signal  $\Delta f_c$  can be represented the superposition of beams with the delays relative to each other, equal to  $\frac{1}{2\Delta f_c}$  (according to Kotelnikov); then a number of divided beams is equal to  $2\Delta f_c$ . Utilizing signals with the wide base and correlation reception or reception to the matched filter, it is possible to divide beams in the time of arrival. In this case the time lag in each beam will considerably less  $\tau_R$  and, consequently decrease signal distortion and multiplicative interferences. In this case in depending on the methods of reception is possible either the isolation of one strongest beam or the use of several beams by a method of coherent reception and addition of all beams on the basis of the voltage.

The separability of beams is connected with the presence in of widebase signal of the very rapidly dropped autocorrelation function. If the width of the peak of the autocorrelation function of the specially designed signal is lower than the minimum time lag between the beams and if any method at the point of reception was determined most strong beam (or the group of beams), then simple autocorrelation receiver will suppress all remaining beams both advancing and delaying, in accordance with the values of autocorrelation function for the time, equal to delay factor of these beams.

The isolation of the most powerful beam, and also all others, can be realized by a method of the synchronization of local signals by each of the beams. After the separation of beams it is possible to utilize entire energy, after forming them. Main disadvantages in such systems are the considerable complication of receiving equipment and the expansion of the occupied frequency band.

Page 243.

According to the method of the reception of signals with the wide base are distinguished correlation reception with the aid of multichannel correlator with the delay line with outlets [7.4] [7.5] and reception to matched filters [7.6]. In the first case as the reference broadband signal is utilized a binary pseudorandom sequence

of the type of a  $M$ -sequence with the subsequent filtration. Is possible the use also of other pseudorandom sequences (multiphase codes of Frank, etc.). Their fundamental properties - uniformity of the spectrum in the broad band, distinct maximum of autocorrelation function and small peak factor. Transition to a  $M$ -position coding makes it possible in the same band to increase the speed of transmission to  $\log_2 M$  times in comparison with the binary coding. In this case the equipment becomes complicated ( $\sim M$  once). As the reference signals can be used different  $M$ -sequences, and also multifrequency and multiphase manipulations. For the transmission of analog information can be used relatively narrow-band frequency modulation [7.7]. With this CPM signal in the transmission (then at the reception) it is multiplied with the reference pseudorandom signal. However, transmission with the aid of KIM and  $\Delta$ -modulation is considered as the more effective [7.8] [7.9].

As a serious problem is considered synchronization both clock and intraband. Although broadband signals themselves possess the good time resolution, the realization of these properties for the resolution of multi-beam character requires the corresponding to accuracy synchronization. There are also great difficulties during the actual realization of the broadband line of delay and search circuit with the netting.



With the reception to the matched filters usually is utilized intra-pulse linear frequency modulation, for example, with the aid of the dispersive ultrasonic delay line. Utilizing linear ChM with the opposite slope, it is possible to transmit binary signals. At the reception the matched filter is analogous to transmission delay line.

Systems with widebase signals solve multi-beam character on the base of the analysis of the pulse reaction of the communication channel, i.e., is utilized the equivalent model of channel, based on the selective values of its pulse reaction. However, it is possible to utilize the equivalent model of channel, based on the selective values of the transfer function of the channel (in that case it is convenient to speak not about the multi-beam character, but about the selective fadings). Forging in the transmission the multifrequency signal, comprised of the cuts of sinusoids, and measuring at the reception of amplitude and phase of these frequencies, and then coherently storing them, we will obtain the optimum system, which generates at the reception adaptation or measurement and account of objective parameters. For characteristic measurement of the circuit of propagation can be utilized either special signals, as for instance, in the system with test pulse [7.10], or informational signals. As the test pulse it is convenient to utilize a pulse with <sup>on</sup> IFM [7.11].

Page 244.

As a whole optimum receiver rates the state of channel and optimizes its characteristics (reference signals). This optimization possible to produce not only at receiving end, but also on that transmitting, utilizing a return duct. Or many lines of communications to organize similar channel is simple. Analyzing the received signal, it is possible, for example, it is simple to change the power of transmitter into the cycle with the fading.

Above has already been indicated that in the feedback, periodically by investigating large frequency band and by selecting optimum transmitting frequency, it is possible to obtain considerable gain. This gain depends on the band, occupied by informational signal, and on the accuracy of the resolution of the signal of sounding in the frequency. This method is equivalent to diversity in the frequency with the automatic selection; however, the order of diversity is defined by both the interval of correlation by frequency and by accuracy of resolution or by number of the frequencies being investigated in the measuring signal (one should, true, note that during the automatic selection with an increase in the order of diversity the gain increases slowly, and furthermore, with an increase in the band of informational communication gain from the work at the optimum frequency rapidly falls). fundamental difficulty

- to ensure sweeping this large frequency band. In the sections STR with the large time lag of beams  $\tau$ , probably, it will prove to be sufficient to investigate the communication channel in the band of frequencies of 20 MHz. In this case is possible the simultaneous transmission of measuring and informational signals, moreover for the transmission of information it is possible to utilize analogous methods of modulation, for example, frequency, and as the reference noise-like signal with the uniform spectrum in the band 20 MHz [7.12]. In the process of work at receiving end at of processing measuring signal is evaluated the state of channel in entire range and is selected the optimum frequency whose value is coded and is transmitted by the channel of feedback. In the principle, the resolution of measuring signal can be made very large; however, the gain of this method wholly depends on the statistical properties of channel STR.

In the systems by the return duct of communications it is possible to change not only the frequency of transmitter, but also deviation (in the case ChM), number of channels, power of transmitter or everything simultaneously. Fundamental peculiarity - possibility of the transmission of analog information, in contrast to the previous systems, which transmit only digital information.

Use of discreteness and quantization of analog information,

i.e., transition and to digital information, gives the possibility to match the speed of transmission of information with the passband of circuit during the use of usual narrow-band methods of modulation. This is possible, for example, by the method of splitting of channel with the high rate to n of parallel channels (with their diversity in the time and the frequency) with the speed of transmission, to n of times of less. Are possible use and multiposition codings.

Page 245.

To promisingly utilize multichannel system where in the sub-channels are utilized the multiposition codes. In this case the equipment possesses large flexibility, since under the pccr conditions for propagation it is easy to increase the order of the diverse reception due to a decrease in the velocity of transmission [7.13].

Work on the introduction of the enumerated above methods of fight with the multi-beam character into the practice of lines STR is very intensely conducted both to the USSR and abroad.

#### §7.3. Transmission of TV signals along the lines DTR.

Energy calculations show that the transmission of the signals of television is possible up to the distance between the adjacent

stations 200-240 km with the antennas with amplification  $G_A = 50$  by dB, on the power of transmitter  $P_{\text{out}} = 3-10$  kW and to the noise temperature of receiver of 300-400°K. First experiments in the transmission of television on the tropospheric radio channel were conducted in 1953-1955. However, the operating television lines DTF to 1966 it is counted unit, and they all are located in the areas of good conditions for radiowave propagation (above sea and in the areas with the warm, humid climate). This, apparently, it is explained by the difficulties, which appear as a result of transmitter distortions of television along the multiple-pronged channel. The presence of rapid and slow fadings leads with CHM to changes in the noise level in the television channel. The use of the diverse reception and the high energy potential of television lines DTF considerably decrease the effect of fadings on the image. The multiple-pronged structure of signal leads to the distortions of the form of TV signal. Here should be distinguished, in the first place, the distortions of the signals of the synchronizations, which call the disruptions of synchronization in the rows (but sometimes also on the frames). For dealing with this phenomenon must be used special equipment for the regeneration of the signals of synchronization, which: a) restores the timing pulses, which are changed in the value and which have distorted front; b) restores the extinguishing pulses, moreover it provides their independent adjustment; c) produces the joining of videosignal on level of "black", removing low-frequency distortions

and alternating-current hum. Secondly, as a result of the echo signals on the image accepted appear the edging also of plastic. For eliminating this phenomenon on the lines DTF can be applied special correctors with the automatic correction. Automatic tuning in them must it is conducted with the aid of the signals of the experimental row, transmitted simultaneously with signal and that intended for operational quality control of the interurban telecasts (for more detail see [7.14]).

Page 246.

And finally thirdly, for dealing with the fluctuations of overall line attenuation in the channel of tropospheric line in the television equipment must be provided the device of the stabilization of the level of TV signal.

The transmission of the sonic tracking of television by the methods, used on the usual lines RRL- ChE at the sub-carrier frequency, is very difficult as a result of the presence of selective fadings and need in this case of the considerable expansion of the band of circuit. Therefore on the tropospheric television lines it is expedient to utilize a time-division multiplex of the line synchronizing and extinguishing pulses by the signals of sonic tracking [7.15]. Supplying in the interval of back stroke two

modulated pulses, it is possible to ensure the transmission of sonic tracking with the band to 12 kHz.

#### REFERENCES

71. A. G. Нечирковский. Подавление шумов слоговым комбинатором. «Электроника», № 8, 1964.
72. W. Lundblad. «Experimental sweep-frequency troposcatter link». IRE Trans. on Information and Probability, v. AP-8, 1960, № 4, pp. 423-427.
73. Le. T. T. T. «Тропосферная связь за пределами горизонта на ультравысоких частотах». Перевод: ВНИИИИИ. П4107. «Revista de Informacion Electronica», 1964, p. 31, pp. 170-186.
74. Kasowski, S. «A Rake System for Lunar Relay Communications». IEEE International Convention Record, Part 3, 1963, p. 197.
75. D. Bitzer, D. Chester. «A Rake System for Troposcatter». IEEE Trans. Comm. Techn. Comp-14, 1960, № 4, p. 489.
76. S. S. S. «A Matched Filter Communication System for Multipath Channels». IRE Trans. on Inform. Theory, IT-5, 1960, № 3, pp. 367-372.
77. J. S. S. «A Comparison of Pseudo-Noise and Conventional Modulation for Multiple Access Satellite Communications». IBM Journal, 1965, № 1, p. 211.
78. S. S. S. «Deterministic for Long Troposcatter Links». IEEE International Convention Record, 1961, Part 1, p. 62.
79. W. S. Patterson. «Troposcatter for Tactical Communications». IEEE Trans. on Electron. v. MIL-9, № 2, 1963, p. 137.
80. A. G. Нечирковский. Отличительные методы передачи сигналов по тропосфере. «Связь», 1967.
81. A. G. Нечирковский. «Повышенная помехоустойчивость в каналах с тропосферной связью». «Радиотехника», № 12, № 12, 1964.
82. J. P. Kruttenholz. «A Simultaneous Information Transfer and Channel Sampling Modulation Technique for Wideband Channels». IEEE Trans. Comm. Techn. Vol. Com-13, 1965, № 2, pp. 162-164.
83. Л. С. Лу. «Поча West Europe» как средство связи. ТННВР, № 5, 1964.
84. С. П. Коробков, А. З. Коррекция произвольных линейных искажений в тропосферной связи. «Связь», 1965.
85. К. П. Копеев, С. И. Зубарева Ю. Б. Передача сигналов видео и звука на сверхвысоких частотах. «Техника телевидения», 1964 г., вып. 2.